On cluster algebras and topological string theory

Proefschrift

ter verkrijging van
de graad van doctor aan de Universiteit Leiden,
op gezag van rector magnificus prof.dr.ir. H. Bijl,
volgens besluit van het college voor promoties
te verdedigen op donderdag 15 september 2022
klokke 11.15 uur

door

Mykola Semenyakin

geboren te Kryviy Rih (Oekraïne)
in 1995

Promotores:	Prof.dr. C.W.J. Beenakker
	Prof.dr. A.V. Marshakov
Promotiecommissie:	Prof.dr. A. Grassi
	(CERN and University of Geneva, Switzerland)
	Prof.dr. N. Nekrasov (University of Stony Brook, USA)
	Prof.dr. M. Shapiro
	(Michigan State University, East Lansing, USA)
	Prof.dr. J. Aarts
	Prof.dr. K.E. Schalm
	Dr. V. Cheianov

Casimir PhD Series Delft-Leiden 2022-24
ISBN 978-90-8593-534-6
An electronic version of this thesis can be found
at `https://openaccess.leidenuniv.nl`

Front cover: a boy is trying to assemble a three-dimensional box-counting with dimers, looking at the cluster quiver for assembly instructions. Illustration by Yevheniia Cheipesh.

To my teachers
Моїм вчителям
Моим учителям

Contents

Chapter 1

Introduction

Here we are going to briefly explain the structure of the puzzle shown on Fig. 1.1. Then we will get a little bit more into motivation of it and discuss what is done so far and our proposal on how it could be solved.

1.1 Preface

Starting from Newton polygon, which is convex polygon with integral coordinates of vertices, one can construct two seemingly unrelated objects. Either go down to toric diagram, encoding some toric $3d$ Calabi-Yau manifold, partition function of topological strings on which can be computed using topological vertices, and which sometimes coincides with the partition function of instantons of $5d$ $N = 1$ gauge theory. We will call "Fourier" transform of it to be dual partition function. Or go to the right of the figure, constructing bipartite graph on torus, which encodes cluster integrable system, whose spectral curve have the same Newton polygon. One can deautonomize this system in a canonical way, loosing involutive and preserved hamiltonians, but getting bilinear q-difference equations on A-cluster variables, for any element of cluster mapping class group of the quiver. It was checked in some examples [14], [16], [15] (all of which were of field-theoretic type), that the string-theoretic partition functions mentioned above are satisfy equations coming from cluster algebras. And despite of the simplicity of formulation, there is no proof for the general Newton polygon yet. In this thesis we make several steps toward the proof of this proposal in the full generality.

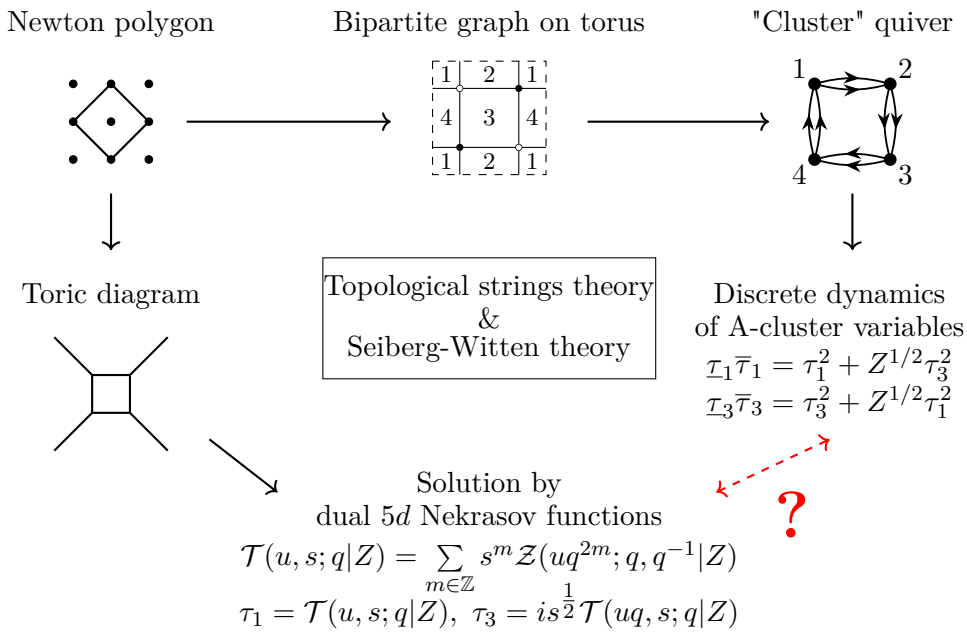

Figure 1.1. The long way between the q-difference equations and their solutions

1.2 String theory and theory of integrable systems

Throughout its history a string theory grew in a tight connection with the most advanced mathematical developments. One of the brightest directions of this collaboration originates in the late 80th, when it appeared that in the many settings of string theory the most natural language for its description is the one of classical and quantum integrable systems. Since that times variety of new examples in this direction was found, and this interplay generated large number of brilliant novel results.

The special role in strings theory/integrable systems relations is played by the instanton counting. One can take as a starting point of this part of story an exact description of low-energy physics of $4d$ $\mathcal{N} = 2$ supersymmetric gauge theories found by N.Seiberg and E.Witten [172]. Applying holomorphicity of the prepotential of the abelian theory, describing low-energetic theory on Coulomb branch, and symmetry of the theory under electro-magnetic dualities, they computed the spectrum of stable

low-energy states of $SU(2)$ theory in terms of the families of complex curves with meromorphic differentials on them. Shortly, it appeared that the results gave birth to the entirely new branch of stings theory. First of all, it were generalized to other gauge groups, theories with matter and quiver gauge theories. The provided description were even powerful enough to study spectrums of non-Lagrangian superconformal theories [1]. Another direction of studies, important in the following, were detailed consideration of the so-called "wall crossing" phenomenon [45, 46]: how the spectrum of stable (or BPS-protected) particles discontinuously jumps at the phase transitions of the theory, which occur at the walls of marginal stability on the moduli space of vacua. The considerations of compactifications of exact solution of $4d$ theory to $3d$ [173] latter played an important role in this story. Also the exact solution gave a powerful boost to the study of engineering of gauge theories using geometry and branes in strings theory and M-theory [167, 178].

Almost since its appearence the Seiber-Witten theory found its mathematical counterpat in the theory of integrable systems [72]. Prciselly the same families of comples curves which was applied in Seiberg-Witten theory, served as a main tools for the separation of variables in integrable systems of particles, and exact solutions of those in terms of θ-functions. The analogues of Seiberg-Witten theories for 5d $\mathcal{N} = 1$ theories compatified on circle [164] and 6d $(2, 0)$-theories compactified on torus [165] immediately found their descriptions in trigonometric (or "relativistic") [143] and elliptic [133] integrable systems. The theory of integrable systems also played a central role in the counting of BPS states. In [121] Kontsevich and Soibelman from geometric perspective derived an explicit formula matching certain symplectomorphism of algebraic torus with any phase of $4d$ $\mathcal{N} = 2$ theory. This symplectomorphisms capture all the information about the BPS spectrums of the phases, and the requirement of their equality in different phases (wall crossing invariance) allows to compute the entire spectrum of BPS particles of the theory, with almost no a priori knowledges about it. The physical explanation of this formula was given in the series of papers starting from [78, 79]. The authors utilized the hyperkähler structure of the moduli space of vacuas of $4d$ theories compactified to $3d$, and reformulated the wall-crossing invariance as a requirement of the smoothness of the metric on this space. The nonperturbative definition of this metric was given via identification of the moduli space of vacua with the moduli space of Higgs bundles. Consider-

ation of complex structures, approximating the particular degenerate one, in which Higgs bundles degenerate to Hitchin systems (the class of which includes the integrable systems of particles mentioned above), allowed to rederive the Kontsevich-Soibelman wall-crossing formula identifying symplectomorphisms of the torus with the cluster transformations of Fock-Goncharov $\mathcal{X}$-cluster coordinates on the moduli spaces of decorated local systems [47].

The new stage of development of the correpondence started when the exact computation of instantonic partition function was done by N.Nekrasov [141] using localization and regularization of divergencies by so-called Omega background $\Omega_{\epsilon_1,\epsilon_2}$. The beauty and non-triviality of the formula gave rise to many nice advances. The AGT correspondence [5] have identified the partition functions of instantons with the main ingredient of correlation functions in conformal field theory - conformal blocks, thus opening a novel direction for collaboration between representations theory and strings theory. Tuning Omega background to $\epsilon_1 \to 0$, the authors of [145] explored Bethe/Gauge correspondence, relating instanton counting with the quantization of underlying integrable systems. In the another limit of $\epsilon_1 = -\epsilon_2$ the integrable systems are "deautonomized" becoming isomonodromic problems of Painlevé type, and instanton partition functions solve them by "Kyiv formula" of [68].

Another brilliant check of Nekrasov's formula was re-derivation of its 5d version in $\epsilon_1 = -\epsilon_2$ limit using all-genus topological sting amplitudes [97] on 3d toric Calabi-Yau manifolds. By any Newton polygon one can construct family of $3d$ toric Calabi-Yau manifolds (see e.g. [7]), and compactification of M-theory on those (or dual (p, q) branes web) defines $5d$ $\mathcal{N} = 1$ gauge theory [6]. In the cases when the gauge theory posses Lagrangian description, so that the partition function of instantons in Ω-background can be computed, it can be reproduced by the computation of the partition function of topological string on corresponding manifold [96], [97], [40]. The computation of the partition function exploited there was based on the "topological vertex" technique [7]: the Calabi-Yau manifolds under consideration are toric, so they can be cutted into $\mathbb{C}^3$ pieces, glued one with another by transition maps. The geometry can be read off from the "toric diagram", which is dual as a graph to the triangulated Newton polygon, as on Fig. 1.1. Roughly speaking[1], to compute the partition function by this picture one associates with each junction of three

[1] Up to subtleties with the "framing" and choosing of Kähler parameters

line segments the topological vertex function

$$V_{\mu,\nu,\lambda}(q) = \sum_{\pi_{\lambda,\mu,\nu}} q^{|\pi|}, \tag{1.1}$$

which counts $3d$ Young diagrams with $2d$ Young diagrams λ, μ, ν as asymptotics weighted by the number of boxes in them, and summation over $2d$ Young diagrams weighted by Q_i's to the power of the number of $2d$ boxes to each compact line segment. The parameters Q_i are called Kähler parameters, and can be treated as exponentiated lengths of the segment on picture, so the parallel segments bounded by the same parallel lines should have equal Kähler parameters. For the example on Fig. 1.1 following this rules one gets

$$Z_{\text{boxes}}(q, Q_B, Q_F) = \tag{1.2}$$

$$= \sum_{\lambda,\mu,\nu,\rho} (Q_B)^{|\lambda|+|\nu|} (Q_F)^{|\mu|+|\rho|} V_{\mu,\nu,\emptyset}(q) V_{\nu,\rho,\emptyset}(q) V_{\rho,\lambda,\emptyset}(q) V_{\lambda,\mu,\emptyset}(q),$$

where the empty diagrams are associated with non-compact line segments. Taking summations over μ and ρ, this becomes a partition function of $SU(2)$ theory with no matter multiplets. As an analog of AGT correspondence for topological strings, can be viewed result of [2], where the refinement of topological vertex to $\epsilon_1 \neq \epsilon_2$ is shown to be intertwining operator of quantum toroidal algebra $U_{q,t}(\ddot{\mathfrak{gl}}_1)$.

The another integrable structure in topological string theory is Topological String/Spectral Theory correspondence [129]. It conjectures, that the determinants of quantum Hamiltonians of integrable systems with single Hamiltonians are equal to topological strings partition function. The exact quantization conditions for the integrable system can be derived from this [64]. One can view such kind of formulas as an example of well-known Ordinary Differential Equations/Integrable Models correspondence. The formula might be generalized to the partition functions for the systems with the several hamiltonians, utilizing spectral curve of $5d$ theory [143], which is zero locus of Laurent polynomial with the same Newton polygon as those which were used to build the toric Calabi-Yau manifold, and which defines its mirror-dual Calabi-Yau manifold. Topological strings/spectral theory correspondence then states that the partition function of topological strings is equal to Fredholm determinant of infinite-dimensional linear operator, quantizing the spectral curve of the system.

Non-autonomous equations and partition functions. Conjecture that the instanton partition functions solve Painlevé equations was proposed for the first time in [68]. The motivation for the solution came there from a relation between the theory of isomonodromic deformations and the theory of holonomic fields [169]. The claim was that the τ-function of Painlevé VI equation, which encodes isomonodromic deformations of rank two Fuchsian system with four punctures on $\mathbb{C}P^1$, is equal to the chiral correlating function of four generic primary operators in $c = 1$ conformal field theory. Using AGT correspondence [5] this function was written there as Fourier transformation of $4d$ $\mathcal{N} = 2$ $SU(2)$ gauge theory with $N_f = 4$ flavours. The correspondence was immediately generalized by the same authors to the partition functions of theories with $N_f = 0, 1, 2, 3$ as solutions to Painlevé III and V equations in [69]. It was promoted to higher rank [61], [77], [74], [70], with Virasoro algebra being replaced by W_N algebra. In gauge theoretic terms it was shown that the partition function of $SU(N)$ theory with the linear quiver of length n solves isomonodromic equations for the Fuchsian system of rank N with 2 full and $n-2$ semi-degenerate punctures [74]. Important observation was that all of the conformal field theories involved in the correspondence were free-fermionic, so the τ-functions were shown to be free-fermionic then [100], [77], [74].

Natural deformation of the approach of [68] was to solve q-difference Painlevé equations with the partition functions of $5d$ $\mathcal{N} = 1$ supersymmetric theories. The first example of this kind was the solution of q-Painlevé III equation with the partition functions of $5d$ $SU(2)$ gauge theory without matter in [24]. This is a example which we considered above. Being modified by simple "perturbative" factor and "Fourier" transformed, as in definition of $\mathcal{T}$ on Fig. 1.1, bottom, formula (1.2) becomes a general solution of q-Painlevé III equation shown on Fig. 1.1, right, where $\overline{\tau} = \tau(u, s; q|qZ)$, $\underline{\tau} = \tau(u, s; q|q^{-1}Z)$. More general case of q-Painlevé VI and theories with $N_f = 4$ flavours was considered in [102]. In [16] it was suggested that there should be similar formulas for the solutions of all q-Painleve equations, which might be classified using the Newton polygons[2] with one internal point [156], [14]. Since not all of the Newton polygons of this type might be brought into correspondence to some Lagrangian gauge theory with the well-defined partition function of instantons, it was

[2]The Newton polygons are just convex polygons on integral plane $\mathbb{Z}^2$, which will play important role in the following.

suggested there to use in this case a grand canonical partition function of topological string instead.

1.3 From quantum to classical spin chains

We will start with brief overview of the generalities of R-matrix formalism for the quantum XXZ-like spin chain, following [111], [148], and then turn to the details of their classical limit, presenting explicit formulas for the rank 2 and 3 cases.

1.3.1 Quantum XXZ spin chain

Quantum $\mathfrak{gl}_M$ spin chain of XXZ type can be defined using quantum monodromy matrix $T(u)$, satisfying so-called RTT-relations:

$$R(u,v)\cdot(T(u)\otimes\mathbf{1})\cdot(\mathbf{1}\otimes T(v)) = (\mathbf{1}\otimes T(v))\cdot(T(u)\otimes\mathbf{1})\cdot R(u,v). \quad (1.3)$$

Here $T(u) = \sum_{i,j=1}^{M} E_{ij}\otimes T_{ij}(u)$ (two-sided formal series in spectral parameter u, as we consider double of RTT algebra) acts in the product of 'auxiliary' space $V = \mathbb{C}^M$ ($E_{ij}\in \mathrm{End}(V)$ – standard matrix units), and 'quantum' Hilbert space of the chain $\mathcal{H}$, $T_{ij}(u)\in\mathrm{End}(\mathcal{H})$. The trigonometric R-matrix, $R\in\mathrm{End}(V\otimes V)$, is given by:

$$R(u,v) = \sum_{i=1}^{M} E_{ii}\otimes E_{ii} + \frac{\sqrt{u/v}-\sqrt{v/u}}{q\sqrt{u/v}-q^{-1}\sqrt{v/u}}\sum_{i\neq j} E_{ii}\otimes E_{jj} + \quad (1.4)$$

$$+\frac{q-q^{-1}}{q\sqrt{u/v}-q^{-1}\sqrt{v/u}}\sum_{i\neq j}(u/v)^{-\frac{1}{2}s_{ij}}E_{ij}\otimes E_{ji}$$

with the sign-factors

$$s_{ij} = \begin{cases} +1, & i>j \\ -1, & i<j \\ 0, & i=j \end{cases} \quad (1.5)$$

The integrals of motion of the chain come from the coefficients of expansion of the transfer matrix $\mathcal{T}(u) = \mathrm{tr}_V\ T(u) = \sum_{k\in\mathbb{Z}} u^k H_k$. Their commutativity immediately follows from the RTT-relations 1.3:

$$0 = [\mathcal{T}(u),\mathcal{T}(v)] = \sum_{m,n=-\infty}^{+\infty} u^m v^n [H_m, H_n] \ \Rightarrow\ [H_m,H_n]=0. \quad (1.6)$$

For the higher-rank case $M > 2$ this does not provide the complete set of commuting Hamiltonians, one has to add higher transfer matrices, or take the coefficients of the so-called quantum spectral curve equation

$$S(\lambda, \mu) = \det_q \left(T(\mu) - \lambda \cdot \mathbf{1}\right) = \sum_{i,j} H_{ij} \lambda^i \mu^j \tag{1.7}$$

with the quantum determinant is defined by

$$\det_q F(u) = \sum_{\sigma} (-1)^{\text{sign}(\sigma)} F_{1,\sigma(1)}(u) F_{2,\sigma(2)}(uq) ... F_{M,\sigma(M)}(uq^M) \tag{1.8}$$

The center of the RTT algebra 1.3 ($[T_{ij}(u), C_k] = 0 \ \ \forall i, j$) is generated by quantum determinant of T-operator: $\det_q T(u) = \sum C_k u^k$.

A seminal statement, proven in [35], claims that the algebra defined by (1.3) is isomorphic to the quantum affine algebra $U_q(\widehat{\mathfrak{gl}}_M)$. More precisely, there is an isomorphism between the algebra, generated by modes of the currents

$$L^{\pm}(z) = \sum_{k=0}^{+\infty} \sum_{i,j=1}^{M} E_{ij} \otimes L^{\pm}_{i,j}[\pm k] z^{\mp k}. \tag{1.9}$$

satisfying the RTT-relations 1.3

$$R(u,v) \cdot (L^{\pm}(u) \otimes \mathbf{1}) \cdot (\mathbf{1} \otimes L^{\pm}(v)) = (\mathbf{1} \otimes L^{\pm}(v)) \cdot (L^{\pm}(u) \otimes \mathbf{1}) \cdot R(u,v) \tag{1.10}$$

together with

$$R(uq^{\frac{c}{2}}, vq^{-\frac{c}{2}}) \cdot (L^+(u) \otimes \mathbf{1}) \cdot (\mathbf{1} \otimes L^-(v)) = \tag{1.11}$$

$$= (\mathbf{1} \otimes L^-(v)) \cdot (L^+(u) \otimes \mathbf{1}) \cdot R(uq^{-\frac{c}{2}}, vq^{\frac{c}{2}}) \tag{1.12}$$

$$L^+_{j,i}[0] = L^-_{i,j}[0] = 0, \quad L^+_{k,k}[0] L^-_{k,k}[0] = 1, \ \ 1 \le i < j \le M, \ \ 1 \le k \le M \tag{1.13}$$

and quantum affine algebra $U_q(\widehat{\mathfrak{gl}}_M)$ with the central extension c. Hence, different integrable systems, constructed from trigonometric RTT-relations can be identified with different representations of $U_q(\widehat{\mathfrak{gl}}_M)$.

Among these are spin chains on N sites, exploiting the co-product property that if $T_1(u)$ and $T_2(v)$ both satisfy RTT-relations, and act in different quantum spaces, then so does $T = T_1(u) T_2(v)$, where the product is taken over the common auxiliary space. To construct a chain of length

N, one has to associate an L-operator in some representation π_k of the $U_q(\widehat{\mathfrak{gl}}_M)$ with each site of the chain, and construct quantum monodromy matrix, taking product in the common auxiliary space

$$T(u) = L^{(N)}(u/u_N) \ ... \ L^{(1)}(u/u_1)Q \tag{1.14}$$

where $u_k \in \mathbb{C}$ are so-called inhomogeneities, $L^{(k)}(u) = \pi_k(L^+)(u)$ and $Q \in \mathrm{End}(V)$ – a 'twist' matrix, having trivial quantum space. Such approach allows to construct many non-trivial integrable systems by assigning to each site a simple representation of $U_q(\widehat{\mathfrak{gl}}_M)$. Conventional way to do so in case of zero central charge, is to apply first evaluation homomorphism $\mathcal{E}v_z : U_q(\widehat{\mathfrak{gl}}_M) \to U_q(\mathfrak{gl}_M)$

$$\begin{aligned}
&\mathcal{E}v_z(L^+_{i,j}[0]) = L^+_{i,j} \ , && i \le j, \\
&\mathcal{E}v_z(L^+_{i,j}[0]) = 0 \ , && i \ge j, \\
&\mathcal{E}v_z(L^-_{i,j}[0]) = 0 \ , && i \le j, \\
&\mathcal{E}v_z(L^-_{i,j}[0]) = L^-_{i,j} \ , && i \ge j, \\
&\mathcal{E}v_z(L^\pm_{i,j}[\pm k]) = z^{\pm k} L^+_{i,j} \ , && i \le j, \quad k > 0 \\
&\mathcal{E}v_z(L^\pm_{i,j}[\pm k]) = z^{\pm k} L^-_{i,j} \ , && i \ge j, \quad k > 0, \\
&\mathcal{E}v_z(L^+_{i,j}[0]) = L^+_{i,j} \ , && i \le j, \\
&\mathcal{E}v_z(L^+_{i,j}[0]) = 0 \ , && i \ge j, \\
&\mathcal{E}v_z(L^-_{i,j}[0]) = 0 \ , && i \le j, \\
&\mathcal{E}v_z(L^-_{i,j}[0]) = L^-_{i,j} \ , && i \ge j, \\
&\mathcal{E}v_z(L^\pm_{i,j}[\pm k]) = z^{\pm k} L^+_{i,j} \ , && i \le j, \quad k > 0, \\
&\mathcal{E}v_z(L^\pm_{i,j}[\pm k]) = z^{\pm k} L^-_{i,j} \ , && i \ge j, \quad k > 0, \\
&L^+_{ii} L^-_{ii} = 1.
\end{aligned} \tag{1.15}$$

Positive and negative currents could be collected to:

$$\begin{aligned}
&\mathcal{E}v_z(L^+(u)) = \frac{1}{\sqrt{u/z}-\sqrt{z/u}}\left(\sqrt{\frac{u}{z}}L^+ + \sqrt{\frac{z}{u}}L^-\right) = L_{\text{ev}}(u/z)\\
&\mathcal{E}v_z(L^-(u)) = -\frac{1}{\sqrt{u/z}-\sqrt{z/u}}\left(\sqrt{\frac{u}{z}}L^+ + \sqrt{\frac{z}{u}}L^-\right) = -L_{\text{ev}}(u/z)\\
&L^{\pm} = \sum_{i,j=1}^{M} E_{ij}\otimes L^{\pm}_{ij}.
\end{aligned} \tag{1.16}$$

Homomorphism $\mathcal{E}v_z$ is well defined only for positive or negative subalgebra at once as geometrical progression for $L^+(u)$ converges if $u/v<1$ and for $L^-(u)$ if $u/v>1$. But luckily we need only positive part for our purposes. Note also that L^+ as a matrix is upper triangular, while L^- - lower triangular. If we substitute L_{ev} into RTT relation we can decompose it by degrees of spectral parameters, and get for $L^{\pm}$

$$R^+\cdot(L^{\pm}\otimes\mathbf{1})\cdot(\mathbf{1}\otimes L^{\pm}) = (\mathbf{1}\otimes L^{\pm})\cdot(L^{\pm}\otimes\mathbf{1})\cdot R^+ \tag{1.17}$$

$$R^+\cdot(L^{+}\otimes\mathbf{1})\cdot(\mathbf{1}\otimes L^{-}) = (\mathbf{1}\otimes L^{-})\cdot(L^{+}\otimes\mathbf{1})\cdot R^+ \tag{1.18}$$

where we used that $R(u,v)$ can be represented as

$$\left(q\sqrt{u/v}-q^{-1}\sqrt{v/u}\right)\cdot R(u,v) = \sqrt{\frac{u}{v}}R^+ + \sqrt{\frac{v}{u}}R^- \tag{1.19}$$

with

$$R^+ = q\sum_{i=1}^{M}E_{ii}\otimes E_{ii} + \sum_{i\neq j}E_{ii}\otimes E_{jj} + (q-q^{-1})\sum_{i<j}E_{ij}\otimes E_{ji} \tag{1.20}$$

$$R^- = q^{-1}\sum_{i=1}^{M}E_{ii}\otimes E_{ii} + \sum_{i\neq j}E_{ii}\otimes E_{jj} - (q-q^{-1})\sum_{i>j}E_{ij}\otimes E_{ji} \tag{1.21}$$

and relations

$$PR^{\pm}P = \left(R^{\mp}\right)^{-1}, \quad R^+ - R^- = (q-q^{-1})P \tag{1.22}$$

where $P=\sum_{i,j}E_{ij}\otimes E_{ji}$ - permutation matrix. The situation here is similar to the one, which was in the affine context: RTT algebra, now

without spectral parameters, generated by matrix elements of $L^{\pm}$ satisfying (1.17)-(1.18) is isomorphic to the quantum group $U_q(\mathfrak{gl}_M)$ in the Drinfeld-Jimbo definitions, if we put

$$L^{+}_{i,j} = \begin{cases} (q-q^{-1})e_{ji}q^{h_j} & i<j \\ q^{h_i} & i=j \\ 0 & i>j \end{cases}, \quad L^{-}_{i,j} = \begin{cases} 0 & i<j \\ q^{-h_i} & i=j \\ (q^{-1}-q)q^{-h_i}e_{ji} & i>j \end{cases} \tag{1.23}$$

where $e_{i,j}$ - generators of $U_q(\mathfrak{gl}_M)$, corresponding to the roots, h_k - to the Cartan sub-algebra [158, 35]. Generators, corresponding to the simple roots $e_i = e_{i,i+1}$, $f_i = e_{i+1,i}$ satisfy relations which are deformation of the usual $\mathfrak{gl}_M$ relations

$$q^{h_a}e_b = q^{\delta_{ab}-\delta_{a,b+1}}e_b q^{h_a}, \quad q^{h_a}f_b = q^{\delta_{a,b+1}-\delta_{ab}}f_b q^{h_a} \tag{1.24}$$

$$[e_a, f_b] = \delta_{ab}\frac{q^{h_a}q^{-h_{a+1}} - q^{-h_a}q^{h_{a+1}}}{q-q^{-1}}, \quad q^{h_a}q^{h_b} = q^{h_b}q^{h_a} \tag{1.25}$$

and q-deformed Serre relations

$$f_a^2 f_{a-1} - (q+q^{-1})f_a f_{a-1} f_a + f_{a-1}f_a^2 = 0, \tag{1.26}$$

$$f_{a-1}^2 f_a - (q+q^{-1})f_{a-1} f_a f_{a-1} + f_a f_{a-1}^2 = 0 \tag{1.27}$$

$$e_a^2 e_{a-1} - (q+q^{-1})e_a e_{a-1} e_a + e_{a-1}e_a^2 = 0, \tag{1.28}$$

$$e_{a-1}^2 e_a - (q+q^{-1})e_{a-1} e_a e_{a-1} + e_a e_{a-1}^2 = 0. \tag{1.29}$$

Non-simple roots could be expressed using recurrence relation

$$e_{a,c} = e_{a,b}e_{b,c} - qe_{b,c}e_{a,b}\,, \quad e_{c,a} = e_{c,b}e_{b,a} - q^{-1}e_{b,a}e_{c,b}\,, \quad a<b<c. \tag{1.30}$$

Algebra $U_q(\mathfrak{gl}_M)$ plays here role of deformation of the usual algebra of spin variables. So considering any representation of $U_q(\mathfrak{gl}_M)$, we construct L-operators satisfying RTT relation, and consequently - integrable spin chain of XXZ type.

1.3.2 Classical XXZ spin chain

Classical limit of the quantum spin chain appears when we replace algebra of quantum operators in the limit $\hbar \to 0$ by some commutative Poisson

algebra of classical dynamical variables. Poisson bracket is coming from the usual prescription

$$\{A, B\} = \lim_{\hbar \to 0} \ \frac{\kappa}{\hbar}[\hat{A}, \hat{B}]. \tag{1.31}$$

Quantum parameter can be introduced as $q = e^{\hbar}$. Additional parameter $\kappa \in \mathbb{C}^{\times}$ provides us with the family of non-isomorphic Poisson algebras. Classical r-matrix appears as a first order of the expansion $R(u, v, e^{\hbar}) \to \mathbf{1} \otimes \mathbf{1} + \hbar\, r(u, v) + O(\hbar^2)$, and looks

$$r(u,v) = -\frac{\sqrt{u/v} + \sqrt{v/u}}{\sqrt{u/v} - \sqrt{v/u}} \sum_{i \neq j} E_{ii} \otimes E_{jj} + \tag{1.32}$$

$$+ \frac{2}{\sqrt{u/v} - \sqrt{v/u}} \sum_{i \neq j} (u/v)^{-\frac{1}{2} s_{ij}} E_{ij} \otimes E_{ji}$$

Note that we don't assume any dependence of u and v on $\hbar$. This gives for the RLL relation

$$\{L(u) \otimes L(v)\} = \kappa [L(u) \otimes L(v), r(u/v)], \tag{1.33}$$

$$\{L(u) \otimes L(v)\} = \sum_{ijkl} \{L_{ij}(u) \otimes L_{kl}(v)\} \ E_{ij} \otimes E_{kl} \tag{1.34}$$

with the classical L-operator

$$L_{\mathrm{cl}+}(u) = \lim_{\hbar \to 0} \ L_{\mathrm{ev}}(u, q = e^{\hbar}) = \tag{1.35}$$

$$= \frac{1}{u^{\frac{1}{2}} - u^{-\frac{1}{2}}} \left(\sum_{i=1}^{M} \left(u^{\frac{1}{2}} e^{S_i^0} + u^{-\frac{1}{2}} e^{-S_i^0} \right) E_{ii} + \right.$$

$$\left. + 2u^{\frac{1}{2}} \sum_{i<j} S_{ji} e^{S_j^0} E_{ij} - 2u^{-\frac{1}{2}} \sum_{i>j} S_{ji} e^{-S_i^0} E_{ij} \right)$$

For classical limit of $U_q(\mathfrak{gl}_M)$, we assume

$$h_i = S_i^0/\hbar, \qquad e_{ij} = S_{ij}/\hbar, \tag{1.36}$$

$$e_i = e_{i,i+1} = S_i^+/\hbar, \ \ f_i = e_{i+1,i} = S_i^-/\hbar.$$

Their Poisson brackets and classical limit of Serre relations are

$$\{S_a^0, S_b^\pm\} = \pm\kappa(\delta_{ab} - \delta_{a,b+1})S_b^\pm, \quad \{S_a^+, S_b^-\} = \kappa\delta_{ab}\sinh(S_a^0 - S_{a+1}^0), \tag{1.37}$$

$$\{S_a^0, S_b^0\} = 0, \tag{1.38}$$

$$\{S_a^+, \{S_a^+, S_{a-1}^+\}\} = \kappa(S_a^+)^2 S_{a-1}^+, \quad \{S_{a-1}^+, \{S_{a-1}^+, S_a^+\}\} = \kappa(S_{a-1}^+)^2 S_a^+ \tag{1.39}$$

$$\{S_a^-, \{S_a^-, S_{a-1}^-\}\} = \kappa(S_a^-)^2 S_{a-1}^-, \quad \{S_{a-1}^-, \{S_{a-1}^-, S_a^-\}\} = \kappa(S_{a-1}^-)^2 S_a^-. \tag{1.40}$$

Generators, corresponding to non-simple roots are coming from

$$\kappa^{-1}\{S_{ab}, S_{bc}\} = S_{ac} + S_{ab}S_{bc}, \quad a < b < c \tag{1.41}$$

$$\kappa^{-1}\{S_{ab}, S_{bc}\} = S_{ac} - S_{ab}S_{bc}, \quad a > b > c \tag{1.42}$$

Different Poisson algebra appears, if we put $q = e^{-\hbar}$. R-matrix is tending to $R(u,v) \to \mathbf{1}\otimes\mathbf{1} - \hbar\, r(u,v) + O(\hbar^2)$ with the same r-matrix. Classical RLL equation changes sign to

$$\{L(u)\otimes L(v)\} = \kappa[r(u/v), L(u)\otimes L(v)]. \tag{1.43}$$

L-operator, represented through the classical $U_q(\mathfrak{gl}_M)$ generators becomes

$$L_{\mathrm{cl}-}(u) = \lim_{\hbar\to 0}\ L_{\mathrm{ev}}(u, q = e^{-\hbar}) = \tag{1.44}$$

$$= \frac{1}{u^{\frac{1}{2}} - u^{-\frac{1}{2}}}\left(\sum_{i=1}^{M}\left(u^{\frac{1}{2}}e^{-S_i^0} + u^{-\frac{1}{2}}e^{S_i^0}\right)E_{ii} - \right.$$

$$\left. -2u^{\frac{1}{2}}\sum_{i<j} S_{ji}e^{-S_j^0}E_{ij} + 2u^{-\frac{1}{2}}\sum_{i>j} S_{ji}e^{S_i^0}E_{ij}\right)$$

It is different from the $L_{\mathrm{cl}+}(u)$ only by the change of signs near generators

$$L_{\mathrm{cl}+}(u; S_{ij}, S_i^0) = L_{\mathrm{cl}-}(u; -S_{ij}, -S_i^0). \tag{1.45}$$

Together, this results in that the only relations which change are

$$\kappa^{-1}\{S_{ab}, S_{bc}\} = S_{ac} - S_{ab}S_{bc}, \quad a < b < c \tag{1.46}$$

$$\kappa^{-1}\{S_{ab}, S_{bc}\} = S_{ac} + S_{ab}S_{bc}, \quad a > b > c \tag{1.47}$$

The general recipe to turn expressions from one algebra to another is to invert sign at all the simple generators, and at all the brackets. As a product of L-operators in both cases $q = e^{\pm\hbar}$ satisfies classical RTT equation, we can construct classical monodromy matrix

$$T(u) = L^{(N)}(u/u_N) \ ... \ L^{(1)}(u/u_1)Q. \tag{1.48}$$

Commuting Hamiltonians of the classical XXZ spin chain are coefficients of the classical spectral curve

$$S(\lambda, \mu) = \det\left(T(\mu) - \lambda\right) = \det T(\mu) + ... + (-\lambda)^{n-1}\mathrm{Tr}\, T(\mu) + (-\lambda)^n \tag{1.49}$$

where the Casimir functions are generated by $\det T(\mu)$.

Example. Classical limit of $U_q(\mathfrak{gl}_2)$

Algebra $U_q(\mathfrak{gl}_2)$ has rank 2 and has 4 generators - $S_1^0,\ S_2^0,\ S_{12} = S_1^+,\ S_{21} = S_1^-$. Poisson brackets in the both cases $q = e^{\pm\hbar}$ are similar

$$\{S_1^0, S_2^0\} = 0, \quad \{S_1^0, S_1^\pm\} = \pm\kappa S_1^\pm, \quad \{S_2^0, S_1^\pm\} = \mp\kappa S_1^\pm, \tag{1.50}$$

$$\{S_1^+, S_1^-\} = \kappa \sinh(S_1^0 - S_2^0) \tag{1.51}$$

Lax operators are

$$L_{\mathrm{cl}\pm}(u) = \frac{1}{u^{\frac{1}{2}} - u^{-\frac{1}{2}}} \begin{pmatrix} u^{\frac{1}{2}} e^{\pm S_1^0} + u^{-\frac{1}{2}} e^{\mp S_1^0} & \pm 2u^{\frac{1}{2}} S_1^- e^{\pm S_2^0} \\ \mp 2u^{-\frac{1}{2}} S_1^+ e^{\mp S_2^0} & u^{\frac{1}{2}} e^{\pm S_2^0} + u^{-\frac{1}{2}} e^{\mp S_2^0} \end{pmatrix}. \tag{1.52}$$

Casimirs are generated by

$$\det L_{\mathrm{cl}\pm}(u) = \frac{1}{(u^{\frac{1}{2}} - u^{-\frac{1}{2}})^2} \Big(u e^{\pm S^0} + u^{-1} e^{\mp S^0} + \tag{1.53}$$

$$+ 2(\cosh(S_1^0 - S_2^0) + 2S_1^+ S_1^-) \Big)$$

So there are two independent Casimirs - total projection of the spin $S^0 = S_1^0 + S_2^0$ and 'square' of the spin (or quadratic Casimir) $C_2 = \cosh(S_1^0 - S_2^0) + 2S_1^+ S_1^-$. If their values are fixed, the resulting symplectic leaf is 2-dimensional. Coordinates $S_1^0 - S_2^0$ and S_1^+ / S_1^- could be chosen on it, for

example. Form usual for $\mathfrak{sl}_2$ chain appears if we transform Lax operator by

$$u \mapsto u\, e^{\mp(S_1^0+S_2^0)}, \quad L(u) \mapsto (u^{\frac{1}{2}} - u^{-\frac{1}{2}}) \begin{pmatrix} u^{-1/2} & 0 \\ 0 & 1 \end{pmatrix} \cdot L(u) \cdot \begin{pmatrix} u^{1/2} & 0 \\ 0 & 1 \end{pmatrix} \tag{1.54}$$

Introducing variables

$$\tilde{S}^0 = \frac{1}{2}\left(S_1^0 - S_2^0\right), \quad \tilde{S}^+ = S_1^+ e^{\pm\tilde{S}^0}, \quad \tilde{S}^- = S_1^- e^{\mp\tilde{S}^0} \tag{1.55}$$

Lax operators becomes

$$L_{\mathrm{cl}\pm}(u) = \begin{pmatrix} u^{\frac{1}{2}} e^{\pm\tilde{S}^0} + u^{-\frac{1}{2}} e^{\mp\tilde{S}^0} & \pm 2\tilde{S}^- \\ \mp 2\tilde{S}^+ & u^{\frac{1}{2}} e^{\mp\tilde{S}^0} + u^{-\frac{1}{2}} e^{\pm\tilde{S}^0} \end{pmatrix}. \tag{1.56}$$

New variables satisfy almost the same relations

$$\{\tilde{S}^0, \tilde{S}^\pm\} = \pm\kappa\tilde{S}^0, \quad \{\tilde{S}^+, \tilde{S}^-\} = \kappa \sinh(2\tilde{S}^0). \tag{1.57}$$

Note that only in 2×2 case it is possible to eliminate spectral parameter from the off-diagonal elements of matrix.

Example. Classical limit of $U_q(\mathfrak{gl}_3)$

Algebra $U_q(\mathfrak{gl}_3)$ has rank 3 and 9 generators. In the classical limit, generators corresponding to the simple positive roots are $S_{12} = S_1^+,\ S_{23} = S_2^+$. If $q = e^\hbar$, only non-simple positive root S_{13} can be defined using relation

$$\kappa^{-1}\{S_1^+, S_2^+\} = S_1^+ S_2^+ + S_{13}. \tag{1.58}$$

Substituting this into Serre relations

$$\{S_1^+, \{S_1^+, S_2^+\}\} = \kappa^2 (S_1^+)^2 S_2^+, \quad \{S_2^+, \{S_2^+, S_1^+\}\} = \kappa^2 (S_2^+)^2 S_1^+ \tag{1.59}$$

we can get two remaining brackets

$$\{S_1^+, S_{13}\} = -\kappa S_1^+ S_{13}, \quad \{S_2^+, S_{13}\} = \kappa S_2^+ S_{13} \tag{1.60}$$

Analogously, $S_{21} = S_1^-,\ S_{32} = S_2^-,\ S_{31}$ are negative generators, with the brackets

$$\kappa^{-1}\{S_1^-, S_2^-\} = S_1^- S_2^- - S_{31} \tag{1.61}$$

$$\{S_1^-, S_{31}\} = -\kappa\, S_1^- S_{31}, \quad \{S_2^-, S_{31}\} = \kappa\, S_2^- S_{31} \tag{1.62}$$

Cartan part has got three commuting generators $S_1^0,\ S_2^0,\ S_3^0$. Their Poisson brackets with other generators are

$$\begin{aligned} &\{S_1^0, S_1^\pm\} = \pm\kappa\, S_1^\pm, \quad \{S_2^0, S_1^\pm\} = \mp\kappa\, S_1^\pm, \quad \{S_3^0, S_1^\pm\} = 0 \\ &\{S_1^0, S_2^\pm\} = 0, \qquad\quad \{S_2^0, S_2^\pm\} = \pm\kappa\, S_2^\pm, \quad \{S_3^0, S_2^\pm\} = \mp\kappa\, S_2^\pm \\ &\{S_1^0, S_3^\pm\} = \mp\kappa\, S_3^\pm, \quad \{S_2^0, S_3^\pm\} = 0, \qquad\quad \{S_3^0, S_3^\pm\} = \pm\kappa\, S_3^\pm \end{aligned} \tag{1.63}$$

Or generally

$$\{S_k^0, S_{ij}\} = \kappa\,(\delta_{ik} - \delta_{jk}) S_{ij} \tag{1.64}$$

For the Poisson brackets between positive and negative simple roots we have got

$$\{S_1^+, S_1^-\} = \kappa\, \sinh\left(S_1^0 - S_2^0\right),\ \{S_2^+, S_2^-\} = \kappa\, \sinh\left(S_2^0 - S_3^0\right), \tag{1.65}$$

$$\{S_3^+, S_3^-\} = \kappa\, \sinh\left(S_3^0 - S_1^0\right) \tag{1.66}$$

$$\{S_1^\pm, S_2^\mp\} = 0, \quad \{S_2^\pm, S_3^\mp\} = 0, \quad \{S_3^\pm, S_1^\mp\} = 0 \tag{1.67}$$

Finally, for non-simple roots using Jacobi identity

$$\{S_{13}, S_1^-\} = -\kappa\, S_2^+ e^{S_1^0 - S_2^0}, \quad \{S_{13}, S_2^-\} = \kappa\, S_1^+ e^{S_3^0 - S_2^0} \tag{1.68}$$

$$\{S_{31}, S_1^+\} = -\kappa\, S_2^- e^{S_1^0 - S_2^0}, \quad \{S_{31}, S_2^+\} = \kappa\, S_1^- e^{S_3^0 - S_2^0} \tag{1.69}$$

$$\{S_{13}, S_{31}\} = \kappa\, \sinh(S_1^0 - S_3^0) \tag{1.70}$$

In agreement with the general prescription, the relations, which are being changing, if we choose $q = e^{-\hbar}$, are

$$\kappa^{-1}\{S_1^+, S_2^+\} = -S_1^+ S_2^+ + S_{13}, \quad \{S_1^+, S_{13}\} = \kappa\, S_1^+ S_{13}, \tag{1.71}$$

$$\{S_2^+, S_{13}\} = -\kappa\, S_2^+ S_{13} \tag{1.72}$$

$$\kappa^{-1}\{S_1^-, S_2^-\} = -S_1^- S_2^- - S_{31}, \quad \{S_1^-, S_{31}\} = \kappa\, S_1^- S_{31}, \tag{1.73}$$

$$\{S_2^-, S_{31}\} = -\kappa\, S_2^- S_{31} \tag{1.74}$$

$$\{S_{13}, S_1^-\} = -\kappa\, S_2^+ e^{-S_1^0 + S_2^0}, \quad \{S_{13}, S_2^-\} = \kappa\, S_1^+ e^{-S_3^0 + S_2^0} \tag{1.75}$$

$$\{S_{31}, S_1^+\} = -\kappa\, S_2^- e^{-S_1^0 + S_2^0}, \quad \{S_{31}, S_2^+\} = \kappa\, S_1^- e^{-S_3^0 + S_2^0} \tag{1.76}$$

The Lax operator is

$$L_{\mathrm{cl}+}(u) = \frac{1}{u^{\frac{1}{2}} - u^{-\frac{1}{2}}} \cdot \tag{1.77}$$

$$\cdot \begin{pmatrix} u^{\frac{1}{2}} e^{S_1^0} + u^{-\frac{1}{2}} e^{-S_1^0} & 2u^{\frac{1}{2}} S_1^- e^{S_2^0} & 2u^{\frac{1}{2}} S_{31}^- e^{S_3^0} \\ -2u^{-\frac{1}{2}} S_1^+ e^{-S_2^0} & u^{\frac{1}{2}} e^{S_2^0} + u^{-\frac{1}{2}} e^{-S_2^0} & 2u^{\frac{1}{2}} S_2^- e^{S_3^0} \\ -2u^{-\frac{1}{2}} S_{13}^+ e^{-S_3^0} & -2u^{-\frac{1}{2}} S_2^+ e^{-S_3^0} & u^{\frac{1}{2}} e^{S_3^0} + u^{-\frac{1}{2}} e^{-S_3^0} \end{pmatrix}$$

which gives generating function of the Casimirs:

$$C(u) = \det L_{\mathrm{cl}+}(u) = \frac{1}{(u^{\frac{1}{2}} - u^{-\frac{1}{2}})^3} \cdot$$

$$\cdot \left(u^{3/2} e^{-S^0} + u^{1/2} e^{-S^0} C_3^+ + u^{-1/2} e^{S^0} C_3^- + u^{-3/2} e^{S^0} \right)$$

where

$$S^0 = S_1^0 + S_2^0 + S_3^0 \tag{1.78}$$

$$C_3^+ = e^{2S_1^0} + e^{2S_2^0} + e^{2S_3^0} + 4e^{S_1^0 + S_2^0} S_{12} S_{21} + 4e^{S_1^0 + S_3^0} S_{13} S_{31} + \tag{1.79}$$

$$+ 4e^{S_2^0 + S_3^0} S_{23} S_{32} + 8e^{S_1^0 + S_3^0} S_{32} S_{21} S_{13}$$

$$C_3^- = e^{-2S_3^0} + e^{-2S_2^0} + e^{-2S_1^0} + 4e^{-S_1^0 - S_2^0} S_{12} S_{21} + 4e^{-S_1^0 - S_3^0} S_{13} S_{31} + \tag{1.80}$$

$$+ 4e^{-S_2^0 - S_3^0} S_{23} S_{32} - 8e^{-S_1^0 - S_3^0} S_{12} S_{23} S_{31}$$

note that if we pass from $L_{\mathrm{cl}+}$ to $L_{\mathrm{cl}-}$, Casimirs would change $S^0 \to -S^0$, $C_3^{\pm} \to C_3^{\mp}$.

1.4 Cluster integrable system

The notion of cluster algebras appeared from the solution [60], [157] of the total positivity problem of *"How to parametrize all matrices whose minors are strictly positive?"*. The main component of the solution was the certain anzatses for the factorization of matrices, which might be usefully encoded into planar bicoloured graphs with oriented paths on the graphs corresponding to the monomials in parametrization. The weights in the anzatses served as prototypes for $\mathcal{X}$-cluster variables, the minors in the matrices gave birth to A-cluster variables, and transformations, identifying equivalent anzatses, became mutations of cluster seeds. The formal definition of cluster algebra was given first in [58]. It appeared

soon, that the cluster algebras admit good Poisson structures [81], [83] which are nicely quantizable [27], [48], and provide a convenient language for parametrization of the spaces of local systems on surfaces [47], for theory of stability conditions in algebraic geometry [121] and theory of integrable systems [82], [71], [55].

Here we remind some basics of the cluster classical integrable systems, which have two equivalent constructions:

- A combinatorial way [71] assigns to a convex Newton polygon a bipartite graph Γ on torus $\mathbb{T}^2$. The cluster variables $\{x_i\}$ are then just monodromies of $\mathbb{C}^\times$-valued connection around the faces of Γ. The spectral curve of integrable system is given by dimer's partition function on $\Gamma \subset \mathbb{T}^2$.

- A group theory construction exploits the Poisson submanifolds or double Bruhat cells, parameterized by cyclically irreducible words in $(W \times W)^\sharp$ (the co-extended double affine Weyl group of $\widehat{PGL}(N)$) [55]. The structure of cluster Poisson variety is coming from restriction of standard trigonometric r-matrix bracket [49], while the integrals of motion are given by Ad-invariant functions on the Poisson submanifold.

1.4.1 $\mathcal{X}$-cluster variety

$\mathcal{X}$-cluster variety is defined by the set of split toric charts $(\mathbb{C}^\times)^d$ assigned with $d \times d$ integer-valued and skew-symmetric *exchange matrix* ε. Such a pair is called *seed* or *cluster seed*. Coordinate functions $x_i \in \mathbb{C}^\times$ on these charts are Poisson variables with the logarithmically constant Poisson bracket

$$\{x_i, x_j\} = \varepsilon_{ij} x_i x_j. \tag{1.81}$$

The matrix ε can be encoded by *quiver* $\mathcal{Q}$ – an oriented graph, whose vertices are labeled by cluster variables, and number of arrows from vertex i to j is equal[3] to ε_{ij}. Generally the Poisson bracket 1.81 has Casimir functions $Z(x)$, $\{Z, x_i\} = 0$ for any x_i, the number of independent Casimir functions coincides with the dimension of kernel of ε.

[3]The arrows from any vertex to itself are forbidden and any two opposite arrows should be annihilated.

$$\varepsilon = \begin{pmatrix} 0 & 2 & 0 & -2 \\ -2 & 0 & 2 & 0 \\ 0 & -2 & 0 & 2 \\ 2 & 0 & -2 & 0 \end{pmatrix}$$

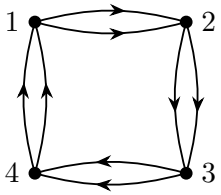

Figure 1.2. An example of skew-symmetric matrix ε (two-particle Toda chain) and corresponding quiver. Poisson bracket has two Casimir functions $\mathcal{Z} = x_1 x_3$ and $q = x_1 x_2 x_3 x_4$.

The cluster seeds are glued together by special coordinate birational transformations – *mutations* $\mu_k : (\{x_i\}, \varepsilon) \to (\{x'_i\}, \varepsilon')$, assigned to each vertex of the quiver $\mathcal{Q}$ or variable x_k:

$$x_i \mapsto x'_i = \begin{cases} x_i^{-1} & , \quad i = k \\ x_i \left(1 + x_k^{\operatorname{sgn} \varepsilon_{ik}}\right)^{\varepsilon_{ik}} & , \quad i \neq k \end{cases} \tag{1.82}$$

$$\varepsilon_{ij} \mapsto \varepsilon'_{ij} = \begin{cases} -\varepsilon_{ij} & , \quad i = k \text{ or } j = k, \\ \varepsilon_{ij} + \dfrac{\varepsilon_{ik}|\varepsilon_{kj}| + \varepsilon_{kj}|\varepsilon_{ik}|}{2} & , \quad \text{otherwise} \end{cases} . \tag{1.83}$$

The transformation of exchange matrix can be easily reformulated as transformation of corresponding quiver. Mutations are the Poisson maps, i.e.

$$\{x'_i, x'_j\} = \varepsilon'_{ij} x'_i x'_j, \tag{1.84}$$

Collection of seeds glued by mutations is called $\mathcal{X}$*-cluster variety.*

Denote by $\mathcal{G}_{\mathcal{Q}}$ the stabilizer of the quiver $\mathcal{Q}$ – the group consisting of composition of mutations and permutations of the vertices, which maps quiver $\mathcal{Q}$ to itself: such transformations nevertheless generate non-trivial maps of the cluster variables $\{x_i\}$. This group is called the *mapping class group* of $\mathcal{X}$-cluster variety.

1.4.2 From bipartite graph to cluster integrable system

$\mathcal{X}$-cluster variety from bipartite graph. For a bipartite graph $\Gamma \hookrightarrow \mathbb{T}^2$ embedded in torus (without self-intersections) the vertices are divided into black and white subsets $B, W \subset C_0(\Gamma)$ so that the black vertices are connected only with the white ones and visa versa. We chose orientation

of edges from black to white, and assume that graph is connected and all 2-valent vertices are contracted.

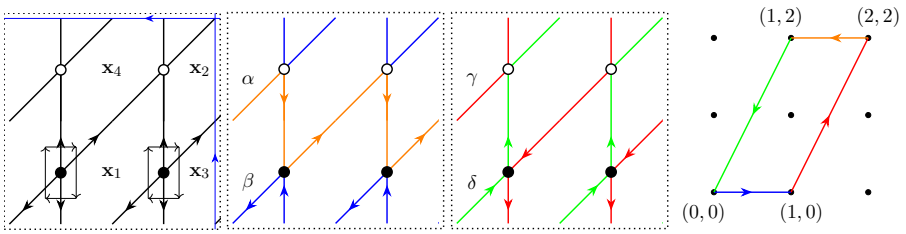

Figure 1.3. Left: Bipartite graph for the two-particle Toda chain, small arrows give the Poisson structure from figure 1.2. Center: zig-zag paths $\alpha, \beta, \gamma, \delta$. Right: Newton polygon obtained from zig-zags as elements $\mathrm{H}_1(\mathbb{T}^2, \mathbb{Z})$. Numbers are labeling degrees of (λ, μ) in spectral curve (1.93).

The coordinates $X = \{x_\gamma \in \mathbb{C}^\times \,|\, \gamma \in \mathrm{H}_1(\Gamma, \mathbb{Z})\}$ of GK integrable system are multiplicative functions on $\mathrm{H}_1(\Gamma, \mathbb{Z})$, considered as an Abelian group, i.e. $x_{\gamma_1} x_{\gamma_2} = x_{\gamma_1+\gamma_2}$. Any element $\gamma \in \mathrm{H}_1(\Gamma, \mathbb{Z})$ can be decomposed as

$$\gamma = n_A \gamma_A + n_B \gamma_B + \sum_i k_i f_i, \quad n_A, n_B, k_i \in \mathbb{Z} \tag{1.85}$$

where γ_A, γ_B form a basis in $\mathrm{H}_1(\mathbb{T}^2, \mathbb{Z})$, while $\mathsf{F} = \{f_i\} = \{\partial B_i\}$ is the set of faces or boundaries of the disks $\mathbb{T}^2 \setminus \Gamma = \sqcup_i B_i$ with the orientation induced from surface, generating $\mathrm{H}_1(\Gamma, \mathbb{Z})/\mathrm{H}_1(\mathbb{T}^2, \mathbb{Z})$ modulo single relation $\sum_k f_k = 0$. Therefore, there is an exact sequence

$$0 \to \mathbb{Z} \to \mathsf{F} \to \mathrm{H}_1(\Gamma, \mathbb{Z}) \to \mathrm{H}_1(\mathbb{T}^2, \mathbb{Z}) \to 0 \tag{1.86}$$

The set of face variables $\{x_f | f \in \mathsf{F}\}$ are coordinates on the toric chart on X_G, these are the X-cluster variables, transforming rationally under the cluster mutations or 'spider moves' of bipartite graph. Relation $\sum_k f_k = 0$ can be relaxed, this results in *deautonomization* $q = \prod_i x_{f_i} \neq 1$ of cluster integrable system and leads to non-trivial q-dynamics.

Exchange matrix of the cluster seed is given by intersection form on the dual surface $\hat{S}$, obtained from Γ by gluing disks, which become faces of $\hat{S}$, to zig-zag paths Z [4], and forgetting structure of the torus. Embedding $\hat{\pi}$:

[4] Zig-zags could be easily found, as they are presented by paths on Γ, which turn maximally right at each black vertex, and turn maximally left at each white one. In the central and right pictures from figure 1.3 the zig-zag paths for Toda chain on two sites are drawn.

$\Gamma \hookrightarrow \hat{S}$ allows to consider any cycle $\gamma \in \mathrm{H}_1(\Gamma, \mathbb{Z})$ as an element of $\mathrm{H}_1(\hat{S}, \mathbb{Z})$, which is equipped with non-degenerate skew-symmetric intersection form $\langle \cdot, \cdot \rangle : \mathrm{H}_1(\hat{S}, \mathbb{Z}) \times \mathrm{H}_1(\hat{S}, \mathbb{Z}) \to \mathbb{Z}$, which defines the Poisson bracket on X by

$$\{x_\gamma, x_{\gamma'}\} = \langle \hat{\pi}\gamma, \hat{\pi}\gamma' \rangle \, x_\gamma x_{\gamma'}. \tag{1.87}$$

Intersection form computed on faces F give exchange matrix of cluster seed $\varepsilon_{ij} = \langle f_i, f_j \rangle$. Effective way of writing this matrix is the following: for each black vertex, draw arrows in the clockwise direction between each pair of consecutive faces, which have this vertex as a corner. Then matrix element ε_{ij} is equal to the alternated number of arrows from f_i to f_j, see figure 1.3.

Classes of zig zag paths in $\mathrm{H}_1(\mathbb{T}^2, \mathbb{Z})$ are in one to one correspondence with the boundary intervals of Newton polygon $\overline{\Delta}$, and this correspondence is the simple way to build Δ by bipartite graph. They are trivial in $\mathrm{H}_1(\hat{S}, \mathbb{Z})$ so that the variables x_ζ, corresponding to the zig-zag paths $\zeta \in \mathrm{H}_1(\Gamma, \mathbb{Z})$ are Casimir functions of the bracket (1.87), i.e.

$$\{x_\zeta, x_\gamma\} = 0, \qquad \zeta \in \mathsf{Z}, \ \forall \gamma \in H_1(\Gamma, \mathbb{Z}). \tag{1.88}$$

Zig-zag variables x_{z_i} always present non-trivial elements from $\mathrm{H}_1(\mathbb{T}^2, \mathbb{Z})$, so single zig-zag itself cannot be expressed via the cluster variables. On the central and right pictures from figure 1.3 zig-zag paths for the Toda chain on two sites are drawn. Casimir Z from the example from previous sub-section in terms of it is given by $\mathcal{Z} = x_\alpha x_\beta$.

Spectral curve. Now, we are ready to construct Hamiltonians of integrable system, which is given by dimer partition function on it.

Perfect matching on bipartite graph Γ is such configuration of edges $D \subset C_1(\Gamma)$ that each vertex has one adjacent edge from D. Such configurations has specific property that $\partial D = W - B$. Fixing any $D_0 \subset C_1(\Gamma)$ we can put an element $D - D_0 \in C_1(\Gamma)$, which is closed, into correspondence to any perfect matching. Any $D - D_0$ under decomposition (1.85) can be presented as

$$D - D_0 = n_A(D - D_0)\gamma_A + n_B(D - D_0)\gamma_B + \sum_i k_i(D - D_0) f_i \tag{1.89}$$

Denoting variables $x_i = x_{f_i}, \ \lambda = x_{\gamma_A}, \ \mu = x_{\gamma_B}$ *dimer partition function*

of bipartite graph Γ could be defined as

$$\mathcal{Z}_{\Gamma,D_0}(\lambda,\mu)=\sum_{D}\lambda^{n_A(D-D_0)}\mu^{n_B(D-D_0)}\prod_i x_i^{k_i(D-D_0)} \tag{1.90}$$

Equation $Z_\Gamma(\lambda,\mu)=0$ with $\lambda,\mu\in\mathbb{C}^\times$ defines curve $C\subset\mathbb{C}^\times\times\mathbb{C}^\times$. The curve C is spectral curve of integrable system. Collecting terms corresponding to the same degrees of spectral parameters

$$\mathcal{Z}_{\Gamma,D_0}(\lambda,\mu)=\sum_{(i,j)\in N}\lambda^i\mu^j\mathcal{H}_{ij},\quad N\subset\mathbb{Z}^2 \tag{1.91}$$

we get Hamiltonians $\mathcal{H}_{ij}$ of the Goncharov-Kenyon integrable system with the Newton polygon Δ. Change of the base configuration D_0 just multiplies partition function by monomial

$$\mathcal{Z}_{D_0'}=x_{D_0-D_0'}\mathcal{Z}_{D_0},\quad x_{D_0-D_0'}=\lambda^{n_A(D_0-D_0')}\mu^{n_B(D_0-D_0')}\prod_i x_i^{k_i(D_0-D_0')}. \tag{1.92}$$

In [71] authors proved for the special choose of D_0 that the model is integrable - i.e. that $\{\mathcal{H}_{ij},\mathcal{H}_{kl}\}=0$, and the number of independent Hamiltonians is half of the dimension of phase space. Hamiltonians which correspond to the boundary integral points of N are Casimirs of Poisson bracket, and have to be fixed, to get symplectic leaf with non-degenerate Poisson bracket. Boundary intervals of ∂N are in one to one correspondence with zig-zag paths. Vector presenting boundary interval coincides with the class of corresponding zig-zag in $\mathrm{H}_1(\mathbb{T}^2,\mathbb{Z})$. Choice of D_0 proposed in [71] are so that $\mathcal{H}_{ij}=1$ for one corner of Newton polygon.

Important detail which remained out of the scope yet is that we have to choose concrete representative in $\mathrm{H}_1(\Gamma,\mathbb{Z})$ for cycles γ_A and γ_B. Usually, spectral parameters are expected to commute with all dynamical variables of the system, so γ_A and γ_B have to be chosen as an integral combinations of zig-zag paths. However, it is not always possible – even for the simplest example of bipartite graph from figure 1.3, zig-zags are $(1,0),(1,2),(-1,0),(-1,-2)$-cycles, and subgroup generated by them in $\mathrm{H}_1(\mathbb{T}^2,\mathbb{Z})$ has index two. Generally, this order is $d=|\mathrm{H}_1(\mathbb{T}^2,\mathbb{Z})/\mathsf{Z}|$, so by choosing spectral parameters expressed via zig-zags, we get Hamiltonians depending on fractional powers of cluster variables $x_i^{1/d}$. Convenient choosing of spectral parameters normalization is so that three Hamiltonians in three corners of Newton polygon become equal to unit.

On right panel of figure 1.4 perfect matchings for bipartite graph from figure 1.3 are drawn. Selecting third matching in the first row as a D_0, and spectral parameters by $\lambda = x_{\gamma_A},\ \mu = x_{\gamma_B}$ with $\gamma_A = \beta,\ \gamma_B = -\frac{1}{2}(\beta+\delta)$, one gets spectral curve

$$\mathcal{Z} = 1 + \lambda + \lambda\mu^2 + \lambda^2\mu^2\mathcal{Z}^{-1} + \lambda\mu\left(\sqrt{x_1x_4} + Z^{-1}\sqrt{\frac{x_1}{x_4}} + \sqrt{\frac{x_4}{x_1}} + \frac{1}{\sqrt{x_1x_4}}\right). \tag{1.93}$$

Coefficient at $\lambda\mu$ is precisely Hamiltonian of closed relativistic Toda chain on two sites. Newton polygon of this curve coincides with the one obtained from zig-zags and drawn on the right panel of figure 1.3.

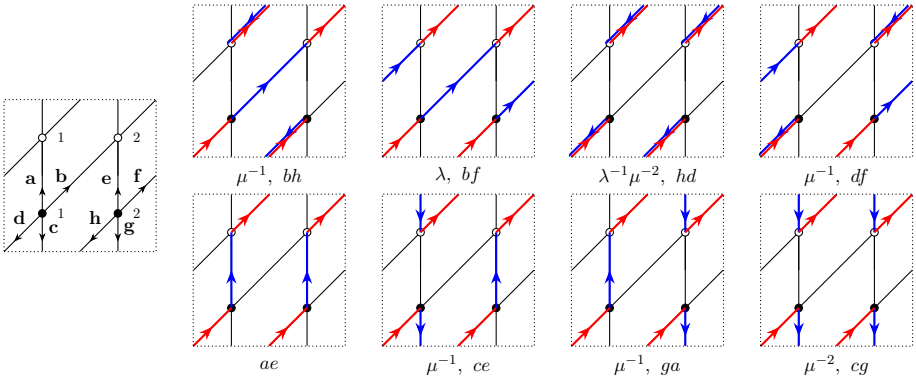

Figure 1.4. Left: bipartite graph with the edge weights. Small integers are to enumerate black and white vertices. Right: Perfect matchings for bipartite graph from figure 1.3 are in blue. Red color indicates reference matching D_0. Weights of the corresponding contributions to determinant of Kasteleyn operator are written below.

Kasteleyn operator. Dimer partition function can be computed using the *Kasteleyn operator*. To define it, first, consider discrete linear bundle with connection a on bipartite graph Γ. In trivialization this means that we associate 1-d vector space $\mathbb{C}$ with each vertex of Γ, and discrete monodromy $a_e \in \mathbb{C}^\times$ with each edge e oriented from black to white. For the edge with the opposite orientation set $a_{-e} = a_e^{-1}$. This definition can be extended to any $\gamma \in C_1(\Gamma, \mathbb{Z})$ by $a_{\gamma_1+\gamma_2} = a_{\gamma_1}a_{\gamma_2}$. Dynamical variables x_γ used above, could be naturally associated with monodromies taken over cycles, i.e. $x_\gamma = a_\gamma$ if $\partial\gamma = 0$. It is problematic to introduce Poisson

structure for variables a_e, as they are not 'gauge invariant'. We can perform gauge transformation $e^{i\phi_k}$ at each vertex k, which results in change $a_{e_{ij}} \to a_{e_{ij}} e^{i(\phi_i - \phi_j)}$ of edge variables[5]. However monodromies x_γ are well defined, so their bracket is given by (1.87).

Second ingredient in this construction is discrete spin structure - multiplicative map $K_e : C_1(\Gamma) \to \{\pm 1\}$, which assigns ± 1 to each edge e in such a way that for any face B_i

$$K_{\partial B_i} = (-1)^{l(B_i)/2+1} \tag{1.94}$$

where $l(B_i)$ - number of edges, adjacent to B_i.

Finally, the third ingredient is choosing of two oriented cycles h_A and h_B on $\mathbb{T}^2$, which cross edges of Γ transversally, and as elements of $\mathrm{H}_1(\mathbb{T}^2, \mathbb{Z})$ they present $[h_A] = \gamma_B$ and $[h_B] = \gamma_A$ (indices A and B are indeed interchanged). We denote by $\langle e, h_{A,B} \rangle$ intersection index of edge e with cycle $h_{A,B}$. It is $+1$ if edge cross cycle from the left to the right, if you look along cycle. Bringing all ingredients together, Kasteleyn operator $\mathfrak{D} : \mathbb{C}^{|B|} \to \mathbb{C}^{|W|}$ of graph Γ is a $|B|$ by $|W|$ (which are equal) matrix

$$\mathfrak{D} = \sum_{i=1}^{|B|} \sum_{j=1}^{|W|} \mathfrak{D}_{ij} E_{ij}, \quad \mathfrak{D}_{ij}(\lambda, \mu) = a_{e_{ij}} K_{e_{ij}} \lambda^{\langle e_{ij}, h_A \rangle} \mu^{\langle e_{ij}, h_B \rangle} \tag{1.95}$$

where we assume that $a_{e_{ij}}$ is zero, if there are no edges between vertices i and j. Note that as an operator acting $\mathbb{C}^{|B|} \to \mathbb{C}^{|W|}$, it acts from the right on row vectors. It could be shown that

$$\det \mathfrak{D}(\tilde{\lambda}, \tilde{\mu}) = \sum_D (-1)^{s([D])} \tilde{\lambda}^{\langle D, h_A \rangle} \tilde{\mu}^{\langle D, h_B \rangle} a_D \tag{1.96}$$

where summation goes over all perfect matchings, sign $(-1)^s$ will depend only on the resulting class in homology of perfect matching after normalization. Parameters $\tilde{\lambda}$ and $\tilde{\mu}$ are different from λ and μ used above. They do not indicate belonging of contribution to any particular homology class, as D are not closed. To make it so, we have to subtract some 'reference configuration' D_0, and choose pair of elements $\zeta_A, \zeta_B \in \mathrm{H}_1(\mathbb{T}^2, \mathbb{Z})$, presenting A and B cycles on $\mathbb{T}^2$. Precise relation between determinant of

[5] Actually, Poisson structure could be introduced even for non-closed loops. Interested reader can find one in Appendix of [71].

Kasteleyn operator and dimer partition function is

$$\mathcal{Z}'_{\Gamma,D_0}(\lambda,\mu) = \sum_{(i,j)\in N} (-1)^{s(i,j)} \lambda^i \mu^j \mathcal{H}_{ij} = \tag{1.97}$$

$$= \left. \frac{\det \mathfrak{D}(\tilde{\lambda},\tilde{\mu})}{a_{D_0} \tilde{\lambda}^{\langle D_0, h_A\rangle} \tilde{\mu}^{\langle D_0, h_B\rangle}} \right|_{\tilde{\lambda}\to\lambda/a_{\zeta_A}, \tilde{\mu}\to\mu/a_{\zeta_B}}$$

For our example, cycles h_A and h_B are shown in figure 1.3, left. Weights of perfect matchings are written under the pictures in figure 1.4. It can be easily seen that sum over them could be computed by

$$\det \mathfrak{D}(\lambda,\mu) = \det \begin{pmatrix} a+\mu^{-1}\,c & -b-\lambda^{-1}\mu^{-1}\,d \\ \lambda\,f+\mu^{-1}\,h & e+\mu^{-1}\,g \end{pmatrix} = \tag{1.98}$$

$$= \mu^{-1}\,bh + \lambda\,bf + \lambda^{-1}\mu^{-2}\,hd + \mu^{-1}\,df + ae + \mu^{-1}\,ce + \mu^{-1}\,ag + \mu^{-2}\,cg$$

Dividing it by $a_{D_0} = \lambda^{-1}\mu^{-2}hd$ and rescaling $\lambda \to \lambda/x_\beta,\ \mu \to \mu/x_{-\frac{1}{2}(\beta+\delta)}$ with $x_\beta = \dfrac{cg}{hd},\ x_\delta = \dfrac{dh}{ae}$, one immediately gets spectral curve (1.93).

Spider moves. There is a special class of mutations for the quivers constructed from bipartite graph called *spider moves* [71]. If mutation is performed at four-valent vertex corresponding to four-gonal face of bipartite graph, one can change bipartite graph as shown in figure 1.5, left, and redefine weights on the edges in such a way that dimer partition function remains unchanged. Cluster variables expressed by edges are changing as they should under corresponding mutations (see figure 1.5, right, for the change of quiver).

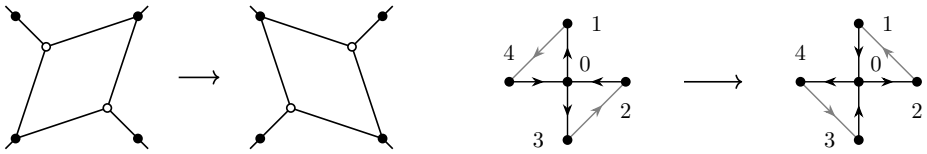

Figure 1.5. Left: Transformation of bipartite graph under spider move. Right: mutation of quiver under spider-move. We draw only the edges, connecting $1, 2, 3, 4$ with 0, affected by the mutation.

1.4.3 Cluster algebras

Dual description to $\mathcal{X}$-cluster language is A-cluster language [59]. To define A-cluster algebra, starting from the quiver Q, we associate with each vertex $i \in \mathcal{Q}$ of quiver a pair of variables $(\tau_i, \mathbf{y}_i)$, $\mathbf{y}$-variables are often called the *coefficients*, and τ-variables usually refereed as *cluster variables* [6]. The coefficients take values in *tropical semi-field*

$$\mathbb{P} = \mathrm{Trop}(\mathbf{u}_1, ..., \mathbf{u}_r) = \langle \mathbf{u}_1^{n_1} ... \mathbf{u}_r^{n_r} \,|\, n_\alpha \in \mathbb{Q} \rangle \tag{1.99}$$

– a set equipped with the pair of operations:

$$\begin{aligned} \mathbf{u}_1^{n_1} ... \, \mathbf{u}_r^{n_r} \odot \mathbf{u}_1^{m_1} ... \, \mathbf{u}_r^{m_r} &= \mathbf{u}_1^{n_1+m_1} ... \, \mathbf{u}_r^{n_r+m_r} \\ \mathbf{u}_1^{n_1} ... \, \mathbf{u}_r^{n_r} \oplus \mathbf{u}_1^{m_1} ... \, \mathbf{u}_r^{m_r} &= \mathbf{u}_1^{\min(n_1,m_1)} ... \, \mathbf{u}_r^{\min(n_r,m_r)} \end{aligned} \tag{1.100}$$

It can be easily seen that with respect to $\odot$ element $1 = \mathbf{u}_1^0 ... \, \mathbf{u}_r^0$ is unit, and each element $\mathbf{y} = \mathbf{u}_1^{n_1} ... \, \mathbf{u}_r^{n_r}$ has inverse $\mathbf{u}^{-1} = \mathbf{u}_1^{-n_1} ... \, \mathbf{u}_r^{-n_r}$. Both operations are commutative, we also have distributivity $a \odot (b \oplus c) = a \odot b \oplus a \odot c$. It is convenient for our purposes to allow fractional powers of $\mathbf{u}$, so that elements $\mathbf{u}_1, ..., \mathbf{u}_r$ generate whole $\mathbb{P}$. Field $\mathcal{F}$ of rational functions in $\{\tau_i\}_{i\in\mathcal{Q}}$ with coefficients in $\mathbb{P}$ is called *ambient field*. *Cluster seed* is a set $(\mathcal{Q}, \{\tau_i, \mathbf{y}_i\}_{i\in\mathcal{Q}})$. Mutation μ_k transforms seed into some other seed $(\mathcal{Q}', \{\tau_i', \mathbf{y}_i'\}_{i\in\mathcal{Q}'})$ with $\mathcal{Q}'$ related to $\mathcal{Q}$ by the rules (1.83), while new cluster variables $\tau_i' \in \mathcal{F}$ and coefficients $\mathbf{y}_i' \in \mathbb{P}$ are defined by

$$\mathbf{y}_i' = \begin{cases} \mathbf{y}_i^{-1} & , \quad i = k \\ \mathbf{y}_i \left(1 \oplus \mathbf{y}_k^{\mathrm{sgn}\, \varepsilon_{ik}}\right)^{\varepsilon_{ik}} & , \quad i \neq k \end{cases} \tag{1.101}$$

$$\tau_k' = \frac{\mathbf{y}_k \prod_{i=1}^{|\mathcal{Q}|} \tau_i^{[\varepsilon_{ik}]_+} + \prod_{i=1}^{|\mathcal{Q}|} \tau_i^{[-\varepsilon_{ik}]_+}}{(1 \oplus \mathbf{y}_k)\tau_k}, \quad \tau_i' = \tau_i \text{ if } i \neq k \tag{1.102}$$

where $[a]_+ = \max(0, a)$. Alternative point of view on coefficients is to consider generators of $\mathbb{P}$ as *frozen variables*, placed in additional vertices of quiver, where mutations are forbidden. If coefficients are expressed through the generators $\{\mathbf{u}_\alpha\}$ by $\mathbf{y}_i = \mathbf{u}_1^{n_{1,i}} ... \, \mathbf{u}_r^{n_{r,i}}$ for some fixed seed, we

[6] In contrast to original papers, see e.g. [59], we denote them as τ-variables, since they satisfy some bilinear relations, as shown in Sect. 2.4.3.

introduce another matrix b which contains exchange matrix ε as a block

$$b = \begin{pmatrix} \boxed{\varepsilon} \\ \boxed{N} \end{pmatrix}, \text{ where } N = \begin{pmatrix} n_{1,1} & n_{1,2} & \dots & n_{1,|\mathcal{Q}|} \\ n_{2,1} & n_{2,2} & \dots & n_{2,|\mathcal{Q}|} \\ \dots & \dots & \dots & \dots \\ n_{r,1} & n_{r,2} & \dots & n_{r,|\mathcal{Q}|} \end{pmatrix}. \tag{1.103}$$

This can be viewed as an addition of r vertices with the variables $\tau_{|\mathcal{Q}|+1} = \mathbf{u}_1, \dots, \tau_{|\mathcal{Q}|+r} = \mathbf{u}_r$ to the quiver, and connection of each vertex containing $\tau_{|\mathcal{Q}|+\alpha}$ with the vertices containing τ_i, $i < |\mathcal{Q}|$ by $n_{\alpha,i}$ arrows. We will denote extended quiver by $\hat{\mathcal{Q}}$ so that $|\hat{\mathcal{Q}}| = |\mathcal{Q}| + r$. Mutation rules for τ variables get unified form

$$\tau'_k = \frac{\prod_{i=1}^{|\hat{\mathcal{Q}}|} \tau_i^{[b_{ik}]_+} + \prod_{i=1}^{|\hat{\mathcal{Q}}|} \tau_i^{[-b_{ik}]_+}}{\tau_k}, \quad \tau'_i = \tau_i \text{ if } i \neq k, \tag{1.104}$$

while mutation rules for coefficients are no longer needed - they transformations are taken into account by transformations of extended quiver with frozen variables. The map from A-cluster variables to X-cluster variables is given by

$$x_i = \prod_{k=1}^{|\hat{\mathcal{Q}}|} \tau_k^{b_{ki}}, \quad 1 \leq i \leq |\mathcal{Q}|. \tag{1.105}$$

Under this map the frozen variables (i.e. coefficients) parameterize the Casimir functions of Poisson algebra $\{\mathcal{Z}, \cdot\} = 0$, which are monomials $\mathcal{Z} = \prod_i x_i^{c_i}$ in X-variables, defined by the property that $\sum_i \varepsilon_{ij} c_j = 0$. If one takes all unit coefficients, the Casimirs

$$\mathcal{Z} = \prod_{i=1}^{|\mathcal{Q}|} x_i^{c_i} = \prod_{i=1}^{|\mathcal{Q}|} \prod_{k=1}^{|\mathcal{Q}|} \tau_k^{\varepsilon_{ki} c_i} = \prod_{k=1}^{|\mathcal{Q}|} \tau_k^{\sum_i \varepsilon_{ki} c_i} = 1, \tag{1.106}$$

become trivial. Mutation rules (1.104) and (1.82) are consistent with (1.105).

In the example of relativistic affine Toda chain with two particles (or on two sites) one gets two Casimir functions Z and q. Extended exchange matrix, chosen following [14], is drawn at figure 1.6.

The coefficients can be read from the matrix b (two lowest rows)

$$\mathbf{y}_1 = (\tau_5 \tau_6)^2, \quad \mathbf{y}_2 = \tau_6^{-2}, \quad \mathbf{y}_3 = (\tau_5 \tau_6)^2, \quad \mathbf{y}_4 = \tau_6^{-2} \tag{1.107}$$

$$b = \begin{pmatrix} 0 & 2 & 0 & -2 \\ -2 & 0 & 2 & 0 \\ 0 & -2 & 0 & 2 \\ 2 & 0 & -2 & 0 \\ 2 & 0 & 2 & 0 \\ 2 & -2 & 2 & -2 \end{pmatrix}$$

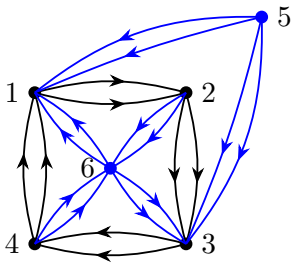

Figure 1.6. Left: extended exchange matrix b for $\widehat{SL_2}$ Toda chain. Right: extended quiver with frozen vertices shown by blue.

Introducing (cf. with figure 1.2) $\tau_5 = q^{\frac{1}{4}}$, $\tau_6 = \mathcal{Z}^{\frac{1}{4}}$, one can write dynamics of cluster variables under q-Painlevé flow $T = s_{1,2}s_{3,4}\mu_1\mu_3$, $T\tau_i = \overline{\tau}_i = \tau_i(qZ)$, as

$$\overline{(\tau_1, \tau_2, \tau_3, \tau_4)} = \left(\tau_2, \frac{\tau_2^2 + q^{\frac{1}{2}}\mathcal{Z}^{\frac{1}{2}}\tau_4^2}{\tau_1}, \tau_4, \frac{\tau_4^2 + q^{\frac{1}{2}}\mathcal{Z}^{\frac{1}{2}}\tau_2^2}{\tau_3}\right). \tag{1.108}$$

Eliminating τ_2 and τ_4, one turns it into bilinear form of q-Painlevé $A_7^{(1)'}$ equation

$$\overline{\tau}_1\underline{\tau}_1 = \tau_1^2 + \mathcal{Z}^{\frac{1}{2}}\tau_3^2, \quad \overline{\tau}_3\underline{\tau}_3 = \tau_3^2 + \mathcal{Z}^{\frac{1}{2}}\tau_1^2. \tag{1.109}$$

1.4.4 Dimer models and box-counting

The important equivalence of counting of paths and counting of dimers on graphs was observed in the context of cluster integrable systems in [71],[55]. The statistical models of random dimer configurations are well-studied [105], [118], and are free fermionic, and all correlators and partition function of the model might have been written using the minors of Kasteleyn operator, which is basically just the weighted adjacency matrix of the underlying graph. The spectral curve, which is generating function of Hamiltonians of the cluster integrable system was written in [71] in the form (1.97). It was also shown there, how to construct cluster integrable system with the arbitrary Newton polygon of the spectral curve. The coordinates on phase space of cluster integrable system are $\mathcal{X}$-cluster coordinates x_f, which can be conveniently interpreted as monodromies of discrete $\mathbb{R}_{>0}$ connection around the faces f of the graph. They are naturally constrained by the condition $\prod_f x_f = 1$ because of the triviality of

bundle. In [14] it was shown, that relaxation of the condition to $q \neq 1$ breaks classical integrability of the model, but "deautonomize" dynamics generated by the elements of cluster mapping class group. It was also shown there, that A-cluster variables provide bilinear form for this dynamics, and for the cases of Newton polygons with one internal point, the corresponding dynamical systems are all q-Painlevé equations except two.

Another appearance of parameter q was in the incarnation of dimer model as a model of statistical physics. The dimer models have nice alternative interpretation as an ensembles of stepped surfaces built from the "boxes" having shapes of the faces of graph, which are stacked one on another. The statistical weights of boxes are equal to weights of faces, and for large periodic graph with fixed boundary conditions the flux through the fundamental domain q controls average volume under the surface. The explicit computations of correlating functions for general q were done in [149], [150] for hexagonal lattice using the free-fermionic vertex operators, with various boundary conditions. In this case it was just explicitly the problem of the counting of boxes, staying along the wall of the room of complex shape. In the limit $q = e^{-\varepsilon} \to 1$ the "typical" surface acquires infinite volume $\sim \varepsilon^{-3}$. The "limit shape" problem of finding its shape were solved first using variational methods in [30] for hexagonal lattice, and then in [116] for the general graph and boundary conditions. From the point of view of counting of instantons, the $\varepsilon \to 0$ corresponds to Seiberg-Witten limit [144], where the partition function is dominated by single term, with the free-energy density being equal to Seiberg-Witten prepotential of 5d gauge theory [143].

Extensive number of attempts were made to connect topological string theory, counting of dimers and cluster algebras in the context of so-called "crystal melting" models, see e.g. [151], [101], [94], [135], [36], [179], [154], [139], [29], [8], [180]. The dimer models on bipartite graphs on torus also appeared in string theory in the context of "brane tiling" [88], [51], [93], [50] constructions of $4d$ $\mathcal{N} = 1$ theories. Closest to the exposition of this Chapter consideration were presented in [89], [92], [91], where the determinant of tight binding Hamiltonian of particle in magnetic field where attempted to be related to the partition function of topological string at $|q| = 1$, and in [114] where both the ideas of "transverse magnetic flux" and of tropicalization were used. Also similar 2d lattice operators in the context of the theory of integrable systems were considered e.g. in [106], [177]. However, there is yet no consistent proof of the conjecture on

how the partition functions of topological string should appear from the counting of dimers on the lattices, built by appropriate Newton polygon.

1.5 This thesis

Bellow, I briefly highlight the main results presented in the thesis.

1.5.1 Chapter 2

In this Chapter we discuss relation between the cluster integrable systems and spin chains in the context of their correspondence with 5d supersymmetric gauge theories. We show that $\mathfrak{gl}_N$ XXZ-type spin chain on M sites is isomorphic to a cluster integrable system with $N \times M$ rectangular Newton polygon and $N \times M$ fundamental domain of a 'fence net' bipartite graph. The Casimir functions of the Poisson bracket, labeled by the zig-zag paths on the graph, correspond to the inhomogeneities, on-site Casimirs and twists of the chain, supplemented by total spin. The symmetricity of cluster formulation implies natural spectral duality, relating $\mathfrak{gl}_N$-chain on M sites with the $\mathfrak{gl}_M$-chain on N sites. For these systems we construct explicitly a subgroup of the cluster mapping class group $\mathcal{G}_{\mathcal{Q}}$ and show that it acts by permutations of zig-zags and, as a consequence, by permutations of twists and inhomogeneities. Finally, we derive Hirota bilinear equations, describing dynamics of the tau-functions or A-cluster variables under the action of some generators of $\mathcal{G}_{\mathcal{Q}}$.

1.5.2 Chapter 3

Here we notice a remarkable connection between the Bazhanov-Sergeev solution of Zamolodchikov tetrahedron equation and certain well-known cluster algebra expression. The tetrahedron transformation is then identified with a sequence of four mutations. As an application of the new formalism, we show how to construct an integrable system with the spectral curve with arbitrary symmetric Newton polygon. Finally, we embed this integrable system into the double Bruhat cell of a Poisson-Lie group, show how triangular decomposition can be used to extend our approach to the general non-symmetric Newton polygons, and prove the Lemma which classifies conjugacy classes in double affine Weyl groups of A-type by decorated Newton polygons.

1.5.3 Chapter 4

Important illustration to the principle *"partition functions in string theory are τ-functions of integrable equations"* is the fact that the (dual) partition functions of $4d$ $\mathcal{N} = 2$ gauge theories solve Painlevé equations. In this Chapter we show a road to self-consistent proof of the recently suggested generalization of this correspondence: partition functions of topological strings on local Calabi-Yau manifolds solve q-difference equations of non-autonomous dynamics of the "cluster-algebraic"integrable systems.

We explain in details the "solutions" side of the proposal. In the simplest non-trivial example we show how $3d$ box-counting of topological string partition function appears from the counting of dimers on bipartite graph with the discrete gauge field of "flux" q. This is a new form of topological string/spectral theory type correspondence, since the partition function of dimers can be computed as determinant of the linear q-difference Kasteleyn operator. As a by-product using WKB method in the "melting" $q \to 1$ limit we an integral formula for Seiberg-Witten prepotential of the corresponding $5d$ gauge theory. The "equations" side of the correspondence remains the intriguing topic for the further studies.

1.5.4 Chapter 5

The topic of research presented in this Chapter is disjoint from the topics of others, and is related to hydrodynamic of electronic currents in graphene.

Strong interaction among charge carriers can make them move like viscous fluid. In this Chapter we explore alternating current (AC) effects in viscous electronics. In the Ohmic case, incompressible current distribution in a sample adjusts fast to a time-dependent voltage on the electrodes, while in the viscous case, momentum diffusion makes for retardation and for the possibility of propagating slow shear waves. We focus on specific geometries that showcase interesting aspects of such waves: current parallel to a one-dimensional defect and current applied across a long strip. We find that the phase velocity of the wave propagating along the strip respectively increases/decreases with the frequency for no-slip/no-stress boundary conditions. This is so because when the frequency or strip width goes to zero (alternatively, viscosity go to infinity), the wavelength of the current pattern tends to infinity in the no-stress case and to a finite value in a general case. We also show that for DC current across a strip

with no-stress boundary, there only one pair of vortices, while there is an infinite vortex chain for all other types of boundary conditions.

Chapter 2

Cluster integrable systems and spin chains

2.1 Introduction

In the seminal paper [172] Seiberg and Witten found 'exact solution' to 4d $\mathcal{N} = 2$ super-symmetric gauge theory in the strong coupling regime. More strictly, the IR effective couplings were constructed geometrically, from the period integrals on a complex curve, whose moduli are determined by the condensates and bare couplings of the UV gauge theory. Shortly after, it has been also realized [72] that natural language for the Seiberg-Witten theory is given by classical integrable systems. In such context the pure supersymmetric gauge theories (with only $\mathcal{N} = 2$ vector supermultiplets) correspond to the Toda chains, while integrable systems for the gauge theories with fundamental matter multiplets are usually identified with classical spin chains of XXX-type.

The next important step was proposed in [164], where this picture has been lifted to $5d$. Then it has been shown that transition from $4d$ to $5d$ (actually – four plus one compact dimensions) results in 'relativization' of the integrable systems [143] (in the sense of Ruijsenaars [159]). In the simplest case of $SU(2)$ pure Yang-Mills theory, or affine Toda chain with two particles, instead of the Hamiltonian

$$H_{4d} = p^2 + e^q + Ze^{-q}, \tag{2.1}$$

corresponding to $4d$ theory, one has to consider

$$H_{5d} = e^p + e^{-p} + e^q + Ze^{-q}, \tag{2.2}$$

or the Hamiltonian of relativistic Toda chain, which describes effective theory for $5d$ pure $SU(2)$ Yang-Mills [1]. It has been also shown that $5d$ theories with fundamental matter correspond to XXZ-type spin chains (see e.g. [133] and references therein).

Relativistic Toda chains lead to natural relation of this story with the integrable systems on the Poisson submanifolds in Lie groups, or more generally to the *cluster* integrable systems – recently discovered class of integrable systems of relativistic type [71, 128, 55]. Direct relation between cluster integrable systems and $5d$ gauge theories has been proposed in [14]. It was shown there that for the case of Newton polygons with single internal point, dynamics of discrete flow is governed by q-Painlevé equations and their bilinear form is solved by Nekrasov $5d$ dual partition functions (for other examples of $5d$ gauge theories the same phenomenon was considered in [102, 16, 15])[2].

Cluster integrable systems Any convex polygon Δ with vertices in $\mathbb{Z}^2 \subset \mathbb{R}^2$ can be considered as a Newton polygon of polynomial $f_\Delta(\lambda, \mu)$, and equation

$$f_\Delta(\lambda, \mu) = \sum_{(a,b)\in\Delta} \lambda^a \mu^b f_{a,b} = 0. \tag{2.3}$$

defines a plane (noncompact) spectral curve in $\mathbb{C}^\times \times \mathbb{C}^\times$. The genus g of this curve is equal to the number of integral points strictly inside the polygon Δ.

According to [71],[55] a convex Newton polygon Δ, modulo action of $SA(2,\mathbb{Z}) = SL(2,\mathbb{Z}) \ltimes \mathbb{Z}^2$, defines a cluster integrable system, i.e. an integrable system on X-cluster Poisson variety $\mathcal{X}$ of dimension $\dim_{\mathcal{X}} = 2S$, where S is area of the polygon Δ. The Poisson structure can be encoded by quiver $\mathcal{Q}$ with $2S$ vertices. Let ϵ_{ij} be the number of arrows from i-th to j-th vertex ($\epsilon_{ji} = -\epsilon_{ij}$) of $\mathcal{Q}$, then logarithmically constant Poisson bracket has the form

$$\{x_i, x_j\} = \varepsilon_{ij} x_i x_j, \qquad \{x_i\} \in \left(\mathbb{C}^\times\right)^{2S}. \tag{2.4}$$

[1] The slightly misleading term 'relativistic' appears here due to formal similarity of momentum dependence to the rapidities of a massive relativistic particle in $1+1$ dimensions.

[2] Other relations between $5d$ supersymmetric gauge theories and cluster integrable systems (involving exact spectrum of quantized cluster integrable systems, BPS counting and toric Calabi-Yau quantization) were discussed in [52], [62], [151] correspondingly. They seem to be related to our case and we are going to return to these issues elsewhere.

The product of all cluster variables $\prod_i x_i$ is a Casimir for the Poisson bracket ((2.4)). Setting it to be

$$q = \prod_i x_i = 1 \tag{2.5}$$

and fixing values of other Casimirs, corresponding to the boundary points of Newton polygon $I \in \bar{\Delta}$ (their total number is $B-3$, since equation (2.3) is defined modulo multiplicative renormalization of spectral parameters λ, μ and $f_\Delta(\lambda, \mu)$ itself), one obtains symplectic leaf.

The properly normalized coefficients, corresponding to the internal points, are integrals of motion in involution

$$\{f_{a,b}(x), f_{c,d}(x)\} = 0, \qquad (a,b),(c,d) \in \Delta \tag{2.6}$$

w.r.t. the Poisson bracket (2.4). By Pick theorem one has

$$2S - 1 = (B-3) + 2g \tag{2.7}$$

where g is the number of internal points (or genus of the curve (2.3)), or the number of independent integrals of motion. So the number of independent integrals of motion is half of the dimension of symplectic leaf, and the system is integrable. One of distinguished features of the cluster integrable systems is that their integrals of motion are the Laurent polynomials of (generally – fractional powers) in the cluster variables.

There are several different ways to get explicit form of the spectral curve equation (2.3):

- Compute the dimer partition function (with signs) for a bipartite graph on a torus. One possible form of it is a characteristic equation

  $$\det \mathfrak{D}(\lambda, \mu) = 0 \tag{2.8}$$

  for the Kasteleyn-Dirac operator on a bipartite graph $\Gamma \subset \mathbb{T}^2$, depending on two 'quasimomenta' $\lambda, \mu \in \mathbb{C}^\times$;

- Alternatively, one can get the same equation (2.3) as a Lax-type equation of a spectral curve, with the Lax operator coming from affine Lie group construction, identifying cluster variety with a Poisson submanifold in the co-extended affine group.

Short exposition of the first construction of cluster integrable system, relevant for this chapter, is contained Section 1.4.

Classical integrable chains Integrability of classical $\mathfrak{gl}_M$ chains of XXZ type is based on the that their $M \times M$ Lax matrices satisfy the following classical RLL relation

$$\{L(\lambda) \otimes L(\mu)\} = \kappa[r(\lambda/\mu), L(\lambda) \otimes L(\mu)] \tag{2.9}$$

with the classical (trigonometric) r-matrix [3]

$$r(\lambda) = -\frac{\lambda^{1/2} + \lambda^{-1/2}}{\lambda^{1/2} - \lambda^{-1/2}} \sum_{i \neq j} E_{ii} \otimes E_{jj} + \frac{2}{\lambda^{1/2} - \lambda^{-1/2}} \sum_{i \neq j} \lambda^{-\frac{1}{2} s_{ij}} E_{ij} \otimes E_{ji}. \tag{2.10}$$

A classical chain of trigonometric type can be defined by the monodromy operator

$$T(\mu) = L_N(\mu/\mu_N) \dots L_1(\mu/\mu_1) \in \mathrm{End}(\mathbb{C}^M) \tag{2.11}$$

where M is called 'rank' of the chain. Integrability is guaranteed by classical RTT-relation

$$\{T(\lambda) \otimes T(\mu)\} = \kappa[r(\lambda/\mu), T(\lambda) \otimes T(\mu)] \tag{2.12}$$

for the monodromy operator that follows from (2.9), and gives rise to the integrals of motion, which can be extracted from the spectral curve equation (2.3) given explicitly by the formula

$$f_\Delta(\lambda, \mu) = \det\left(\lambda Q - T(\mu)\right) = 0. \tag{2.13}$$

where Q - diagonal twist matrix with the constant entities. Relativistic Toda system can be considered as certain degenerate case of generic XXZ chain of rank $M = 2$ (of length N for N particles).

Examples of Newton polygons In what follows we mostly consider cluster integrable systems, corresponding to the Newton polygons of the following types:

- Quadrangles with four boundary points, where all internal points are located along the same straight line, as on Fig. 2.1, left. This is the case of relativistic Toda chains, studied in [14]. The corresponding gauge theory is 5d $\mathcal{N} = 1$ Yang-Mills theory with $SU(N)$

[3] See details of derivation of Lax matrix from quantum algebra and notations in Section 1.3.

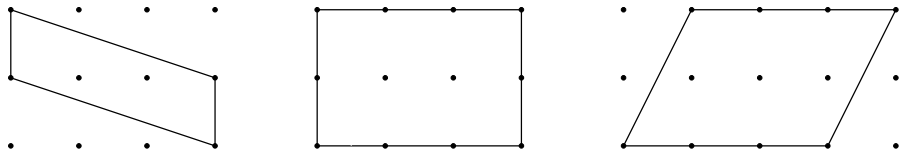

Figure 2.1. From left to right Newton polygons for: Toda chain on three sites, $\mathfrak{gl}_2$ XXZ spin chain on three sites, $\mathfrak{gl}_2$ spin chain on three sites with cyclic twist matrix.

gauge group (for $N-1$ internal points) without matter multiplets, possibly with the Chern-Simons term of level $|k| \leq N$ – in such case quadrangle is not a parallelogram.

- "Big" rectangles (modulo $SA(2,\mathbb{Z})$ transform). For the $N \times M$ rectangle (see Fig. 2.1, center) this can be alternatively described as a $\mathfrak{gl}_N$ spin chain on M sites (cf. with [21]), or vice versa. The corresponding 5d gauge theories are given by linear quivers theories with the $SU(N)$ gauge group at each of $M-1$ nodes: see Fig. 2.2.

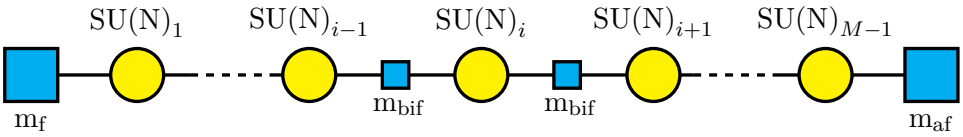

Figure 2.2. Linear quiver which defines multiplets for $\mathcal{N}=1$ gauge theory. Circles are for gauge vector multiplets, boxes are for hypermultiplets.

- "Twisted rectangles", or just the parallelograms, which are not $SA(2,\mathbb{Z})$-equivalent to the previous class (see Fig. 2.1, right), they can be alternatively formulated as spin chains with nontrivial twists. Gauge theory counterpart for this class of polygons is not yet known, except for the twisted $\mathfrak{gl}_N$ chain on one site, leading back to the basic class of Toda chains.

For all these families the spectral curve of an integrable system, determined by equation (2.3) is endowed with a pair of meromorphic differentials $\left(\frac{d\lambda}{\lambda}, \frac{d\mu}{\mu}\right)$ with the fixed $2\pi i\mathbb{Z}$-valued periods. One can also use this

pair to introduce (the $SL(2,\mathbb{Z})$-invariant for our family) 2-form $\frac{d\lambda}{\lambda} \wedge \frac{d\mu}{\mu}$ on $\mathbb{C}^\times \times \mathbb{C}^\times$, whose 'pre-symplectic' form is the SW differential.

Structure of the Chapter The main aim is to extend the correspondence between 5d theories and cluster integrable systems to wider class of models. We find isomorphism between the classes of $\mathfrak{gl}_N$ XXZ-like spin chains on M sites, corresponding to $5d$ $SU(N)$ linear quiver gauge theories (see Fig. 2.2) [21], and cluster integrable systems with $N \times M$ rectangular Newton polygons.

We start from the brief overview of classical XXZ spin chains. We illustrate with the simple example of relativistic Toda chain, how Lax operators naturally arise from the Dirac-Kasteleyn operator of cluster integrable system. Then we do this for the general case of XXZ spin chain of arbitrary length and rank. Spectral (or fiber-base) duality arises as an obvious consequence of the structure of considered bipartite graph. Spin chains with additional cyclic permutation twist matrix arise in the cluster context naturally as well.

Then we explain structure of large subgroup of cluster mapping class group $\mathcal{G}_\mathcal{Q}$. We show that in case of general rank and length of chain it contains subgroup (2.87) which act in autonomous $q = 1$ limit by permutations of inhomogeneities and diagonal twist parameters of spin chain. We also discuss issue of deautonomization and propose a way to define action of $\mathcal{G}_\mathcal{Q}$ on zig-zags in $q \neq 1$ case. Then we derive bilinear equations for the action of generators of $\mathcal{G}_\mathcal{Q}$ on A-cluster variables.

2.2 Spin chains

2.2.1 Relativistic Toda chain

Let us start with the case of relativistic Toda chain, which is known to be related to Seiberg-Witten theory in $5d$ without matter [143]. Relativistic Toda chains arise naturally on Lie groups [56], and therefore have cluster description. A typical bipartite graph of affine relativistic Toda is shown in Fig. 2.3. For the Toda system with N particles it has $2N$ vertices, $4N$ edges and $2N$ faces. Corresponding Newton polygon is shown in Fig. 2.1, left.

The cluster Poisson bracket (2.4) for the Toda face variables is

$$\{x_i^\times, x_j^\times\} = \{x_i^+, x_j^+\} = 0, \tag{2.14}$$

$$\{x_i^\times, x_j^+\} = (\delta_{i,j+1} + \delta_{i+1,j} - 2\delta_{i,j}) x_i^\times x_j^+, \quad i,j \in \mathbb{Z}/N\mathbb{Z}$$

where in the non-vanishing r.h.s. one can immediately recognize the Cartan matrix of $\widehat{sl_N}$. This Poisson bracket has obviously two Casimir functions, which can be chosen, say, as[4]

$$q = \prod_j (x_j^\times x_j^+), \qquad \varkappa_1/\varkappa_2 = \prod_j x_j^+. \tag{2.15}$$

However, in what follows we are going to use the edge variables (see Section 1.4 for details), which do not have any canonical Poisson bracket, e.g. since they are not gauge invariant, when treated as elements of $\mathbb{C}^\times$-valued gauge connection on the graph. Hence, following [128], we fix the gauge and parameterize all edges by $2N$ exponentiated Darboux variables ξ_k, η_k

$$\{\xi_i, \eta_j\} = \delta_{ij}\xi_i\eta_j, \quad \{\xi_i, \varkappa_a\} = \{\eta_i, \varkappa_a\} = 0, \tag{2.16}$$

so that the face variables are expressed, as a products of oriented edge variables (see Fig. 2.3, left) by

$$x_i^\times = \frac{\xi_{i+1}}{\xi_i}(\varkappa_2/\varkappa_1)^{\delta_{iN}}, \;\; x_i^+ = \frac{\eta_i}{\eta_{i+1}}(\varkappa_1/\varkappa_2)^{\delta_{iN}}. \tag{2.17}$$

In terms of the edge variables (2.16) the monodromies over zig-zag paths (see Fig. 2.3, middle, right) can be expressed as follows

$$\alpha = \zeta/\varkappa_1, \quad \beta = \varkappa_2/\zeta, \quad \gamma = \varkappa_1\zeta, \quad \delta = 1/\varkappa_2\zeta, \quad \zeta = \prod_{k=1}^N \sqrt{\frac{\xi_k}{\eta_k}} \tag{2.18}$$

In the autonomous limit $q = 1$, there is a single independent Casimir – diagonal twist of monodromy operator $\varkappa_1/\varkappa_2$ or coupling of the affine Toda chain. Reduction from four zig-zags $\alpha, \beta, \gamma, \delta$ to single Casimir $\varkappa_1/\varkappa_2$ is a reminiscence of the freedom $\lambda \to a\lambda$, $\mu \to b\mu$ and the fact that $\alpha\beta\gamma\delta = 1$.

The Dirac-Kasteleyn operator here can be read of the left picture at Fig. 2.3, and is given by $N \times N$ matrix[5]:

$$\mathfrak{D}(\lambda,\mu) = \sum_{i=1}^N \Big((\xi_i + \mu^{-1}\eta_i)E_{ii} - \varkappa_1^{\delta_{iN}}\sqrt{\xi_i\eta_i}E_{i,i+1} + \varkappa_2^{-\delta_{iN}}\mu^{-1}\sqrt{\xi_i\eta_i}E_{i+1,i}\Big) \tag{2.19}$$

[4]Only the ratio of $\varkappa$'s is actually independent Casimir, but we introduce both of them for convenience in what follows.

[5]The spectral parameters or quasimomenta λ and μ appear due to intersection of the edge with the blue and purple cycles in $\mathrm{H}_1(\mathbb{T}^2, \mathbb{Z})$, and minuses arise due to discrete spin structure.

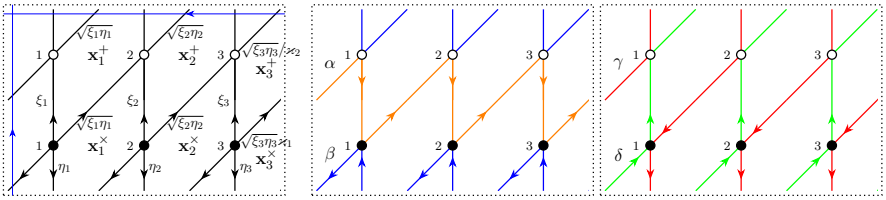

Figure 2.3. Left: Bipartite graph for the Toda chain. Center, right: zig-zag paths $\alpha, \beta, \gamma, \delta$.

where we have additionally defined

$$E_{N,N+1} = \lambda E_{N,1}, \quad E_{N+1,N} = \lambda^{-1} E_{1,N} \tag{2.20}$$

and it almost coincides here [39] with the standard $N \times N$ formalism for the spectral curve of relativistic Toda chain

$$\det \mathfrak{D}(\lambda, \mu) = 0 \;\Leftrightarrow\; \exists\; \mathfrak{D}(\lambda, \mu)\psi = 0 \tag{2.21}$$

with Baker-Akhiezer function $\psi \in \mathbb{C}^N$.

Now, to illustrate what is going to be done for the spin chains, let us rewrite this equation in terms of the well-known 2×2 formalism for Toda chains, but not quite in a standard way. In order to do that, we first add an additional black (white) vertex to each top (bottom) edge in left Fig. 2.3, and draw it in deformed way as in Fig. 2.4. Such operation obviously does not change the set of dimer configurations, and new dimer partition function differs from the old one only by total nonvanishing factor.

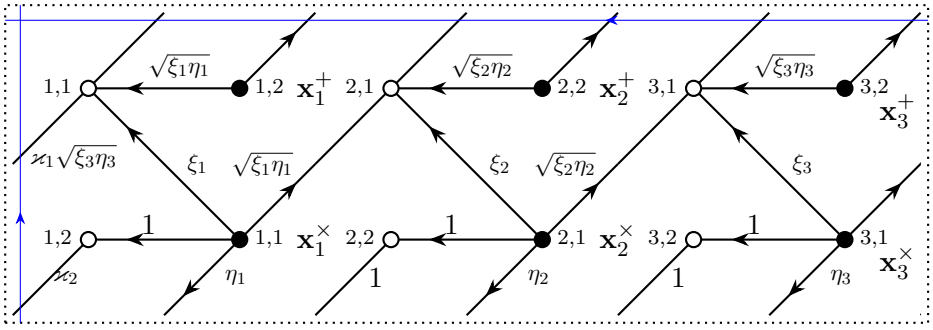

Figure 2.4. Extended and deformed bipartite graph for the Toda chain.

The Dirac-Kasteleyn matrix, read from the Fig. 2.4, can be written in the block form

$$\mathfrak{D}(\lambda,\mu)=\sum_{i=1}^{N}\Big(E_{ii}\otimes A_i+E_{i,i+1}\otimes C_iQ^{\delta_{i,N}}\Big)= \tag{2.22}$$

$$=\sum_{i=1}^{N}\Big((\xi_i+\mu^{-1}\eta_i)E_{ii}\otimes E_{11}+E_{ii}\otimes E_{12}+\sqrt{\xi_i\eta_i}E_{ii}\otimes E_{21}-$$

$$-\varkappa_1^{\delta_{i,N}}\sqrt{\xi_i\eta_i}E_{i,i+1}\otimes E_{11}-\mu\varkappa_2^{\delta_{i,N}}E_{i,i+1}\otimes E_{22}\Big)$$

with

$$A_i=\begin{pmatrix}\xi_i+\mu^{-1}\eta_i & 1\\ \sqrt{\xi_i\eta_i} & 0\end{pmatrix},\quad C_i=\begin{pmatrix}-\sqrt{\xi_i\eta_i} & 0\\ 0 & -\mu\end{pmatrix},\quad Q=\begin{pmatrix}\varkappa_1 & 0\\ 0 & \varkappa_2\end{pmatrix}. \tag{2.23}$$

The first factor in the tensor product corresponds to the number of the particle (or of the 'site'), arising naturally in the framework of 2×2 formalism for Toda systems and spin chains below, while the second – to position of a vertex inside the 'site'. For the 'extended' (compare to (2.19)) operator (2.22) one gets the same equation (2.21), but now with $\psi\in\mathbb{C}^{2N}$, which can be written as:

$$\psi=\sum_{i=1}^{N}e_i\otimes\begin{pmatrix}\psi_{i,1}\\ \psi_{i,2}\end{pmatrix}=\sum_{i=1}^{N}e_i\otimes\psi_i. \tag{2.24}$$

For the coefficients of this expansion (2.21) gives

$$\begin{cases}\psi_{k+1}=L_k(\mu)\psi_k\\ \psi_{N+1}=\lambda Q\psi_1\end{cases} \tag{2.25}$$

or the system of finite-difference equations on Baker-Akhiezer functions with the quasi-periodic boundary conditions, where the 2×2 Lax matrix

$$L_i(\mu)=-C_i^{-1}(\mu)A_i(\mu)=\mu^{-\frac{1}{2}}\begin{pmatrix}\mu^{\frac{1}{2}}\sqrt{\dfrac{\xi_i}{\eta_i}}+\mu^{-\frac{1}{2}}\sqrt{\dfrac{\eta_i}{\xi_i}} & \dfrac{\mu^{\frac{1}{2}}}{\sqrt{\eta_i\xi_i}}\\ \mu^{-\frac{1}{2}}\sqrt{\xi_i\eta_i} & 0\end{pmatrix} \tag{2.26}$$

is equivalent to the standard Lax matrix for relativistic Toda chain (see e.g. [128]) up to conjugation by permutation matrix, and redefinition of the variables

$$\xi \mapsto \eta, \quad \eta \mapsto \xi^{-1}, \quad \mu \mapsto \mu^{-1}. \tag{2.27}$$

This Lax operator satisfies classical RLL relation

$$\{L_i(\lambda) \otimes L_j(\mu)\} = \delta_{ij}[r(\lambda/\mu), L_i(\lambda) \otimes L_j(\mu)] \tag{2.28}$$

with the classical (trigonometric) r-matrix (2.10) [6]. Compatibility condition of (2.25) gives spectral curve equation in the form

$$\det\left(\lambda Q - L_N(\mu)...L_1(\mu)\right) = 0 \tag{2.29}$$

where $Q = \mathrm{diag}\,(\varkappa_1, \varkappa_2)$ is extra twist matrix[7], and inhomogeneities $\{\mu_i\}$, which appear in the case of generic XXZ chain, are absorbed here into redefinition of dynamical variables.

2.2.2 Spin chains of XXZ type

Let us now apply the same arguments, which we used for the Toda chain, to the following class of chains: the rank M chains on N cites of XXZ-type, which means that the Poisson structure (2.28) is defined by trigonometric r-matrix. Such systems naturally arise in $q \to 1$ limit of $U_q(\mathfrak{gl}_M)$, see Appendix 1.3. We claim that such classical spin chain can be alternatively described as cluster integrable systems, constructed from 'big rectangles' of the size $N \times M$.

For a cluster integrable system with such Newton polygon (see Fig. 2.5, left) one gets a bipartite graph, drawn at Fig. 2.6. According to [71] this graph is drawn on torus $\mathbb{T}^2$, i.e. left side is glued with the right side, and top - with the bottom, we will call such graphs as $N \times M$ 'fence nets'.

The cluster coordinates $x^{\times}_{ia}, x^{+}_{ia}$, now associated with the faces of graph at Fig. 2.6, satisfy the following Poisson bracket relations

$$\{x^{\times}_{ia}, x^{+}_{jb}\} = (-\delta_{ij}\delta_{ab} + \delta_{i,j+1}\delta_{ab} + \delta_{ij}\delta_{a+1,b} - \delta_{i,j+1}\delta_{a+1,b})x^{\times}_{ia}x^{+}_{jb}, \tag{2.30}$$

$$\{x^{\times}_{ia}, x^{\times}_{jb}\} = \{x^{+}_{ia}, x^{+}_{jb}\} = 0, \qquad i,j \in \mathbb{Z}/N\mathbb{Z}, \qquad a,b \in \mathbb{Z}/M\mathbb{Z}$$

[6] Up to numeric rescaling, see Section 1.3 for discussion.

[7] Note that constant diagonal matrices Q satisfy $[r, Q \otimes Q] = 0$, and therefore can be also used in construction of monodromy operators.

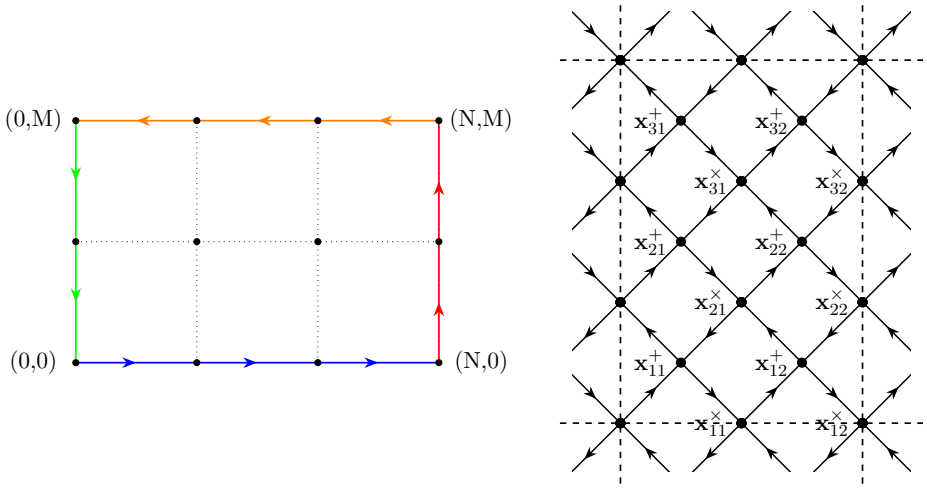

Figure 2.5. Left: Newton polygon for $(N, M) = (3, 2)$. Zig-zags from Fig. 2.6 as elements of torus first homology group are drawn by colored arrows. Right: Poisson quiver. It is drawn on the torus, so vertices lying on left-right and up-down sides have to be identified.

with two kinds of indices living 'on circles': i, j enumerating rows of bipartite graph and a, b enumerating columns. Corresponding quiver is drawn at Fig. 2.5, right. As in Toda case, 'fixing' a gauge, we pass now to the edge variables

$$x^\times_{ia} = \frac{\eta^2_{ia}}{\xi^2_{ia}}, \quad x^+_{ia} = \frac{\xi_{ia}\xi_{i+1,a-1}}{\eta_{i+1,a}\eta_{i,a-1}}(\sigma_{i+1}/\sigma_i)^{\delta_{a,1}}(\varkappa_{a-1}/\varkappa_a)^{\delta_{i,N}}. \tag{2.31}$$

with the Poisson bracket

$$\{\xi_{ia}, \eta_{jb}\} = \frac{1}{2}\delta_{ij}\delta_{ab}\xi_{ia}\eta_{jb}, \qquad i, j \in \mathbb{Z}/N\mathbb{Z}, \qquad a, b \in \mathbb{Z}/M\mathbb{Z} \tag{2.32}$$

Extra parameters in (2.31) are the Casimir functions of the bracket (2.30), together with

$$\zeta^h_i = \prod_{b=1}^{M} \frac{\xi_{ib}}{\eta_{ib}}, \quad \zeta^v_a = \prod_{j=1}^{N} \frac{\xi_{ja}}{\eta_{ja}}, \quad \{x^\times, \zeta^{h,v}\} = \{x^+, \zeta^{h,v}\} = 0. \tag{2.33}$$

It is useful to re-express them via the zig-zag variables (see the zig-zag paths on Fig. 2.6, middle and right)

$$\alpha_i = \sigma_i/\zeta^h_i, \quad \beta_i = 1/\zeta^h_i\sigma_i, \quad i = 1, \dots, N \tag{2.34}$$

$$\gamma_a = \zeta_a^v/\varkappa_a, \quad \delta_a = \zeta_a^v \varkappa_a, \quad a = 1, \dots, M \tag{2.35}$$

These formulas relate convenient generators of the center of cluster Poisson algebra with inhomogeneities $\{\mu_k = 1/\sigma_k \zeta_k^h = \beta_k\}$, twists $\{\kappa_a\}$, 'on-site' Casimirs $\zeta_i^h = (\alpha_i \beta_i)^{\frac{1}{2}}$ and 'projections of spins'[8] $\zeta_a^v = (\gamma_a \delta_a)^{\frac{1}{2}}$ of the chain.

Our main statement here is that the classical spin variables (for definition see Section 1.3) associated with single site of the chain could also be expressed via the edge variables ξ, η by

$$e^{S_a^0} = z_a^2, \quad S_{ab} = \frac{1}{2} z_b^{-2}(z_a^2 + z_a^{-2}) \frac{\tau_a}{\tau_b}, \; a < b, \quad S_{ab} = -\frac{1}{2} z_a^2 (z_a^2 + z_a^{-2}) \frac{\tau_a}{\tau_b}, \; a > b, \tag{2.36}$$

where[9]

$$z_a = \sqrt{\xi_a/\eta_a}, \quad \tau_a = \sqrt{\xi_a \eta_a} \prod_{b=1}^{M} z_b^{\operatorname{sgn}(b-a)} \tag{2.37}$$

and the 'site index' $i = 1, \dots, N$ is omitted here. Spin-variables cannot be directly expressed through the cluster variables in a natural way, but rather as a product of edge variables over some non-closed paths. However it is possible to express cluster variables via the spin variables on two adjacent sites by

$$x_{i,a}^{\times} = e^{-2(S_a^0)_i}, \tag{2.38}$$

$$x_{i,a}^{+} = -\frac{e^{(S_a^0)_{i+1} + (S_{a-1}^0)_i} (S_{a-1}^+)_{i+1} (S_{a-1}^-)_i}{\cosh (S_{a-1}^0)_{i+1} \cosh (S_a^0)_i} \left(\frac{\sigma_{i+1}}{\sigma_i}\right)^{\delta_{a,1}} \left(\frac{\varkappa_{a-1}}{\varkappa_a}\right)^{\delta_{i,N}} \tag{2.39}$$

where index outside brackets of spin variables enumerates number of site.

The spectral curve again can be given by determinant of the Dirac-Kasteleyn operator, which is the weighted adjacency matrix of the bipartite graph. For generic (N, M) system it has the form:

$$\begin{aligned} \mathfrak{D}(\lambda, \mu) = \sum_{i=1}^{N} \sum_{a=1}^{M} \xi_{ia} (E_{i,i} \otimes E_{a,a} - \varkappa_a^{\delta_{i,1}} \sigma_i^{\delta_{M,a}} E_{i,i-1} \otimes E_{a+1,a}) + \\ + \eta_{ia} (\varkappa_a^{\delta_{1,i}} E_{i,i-1} \otimes E_{a,a} + \sigma_i^{\delta_{M,a}} E_{i,i} \otimes E_{a+1,a}) \end{aligned} \tag{2.40}$$

[8] Notice that spin's projections are not originally the Casimir functions for spin's brackets, but rather 'trivial' integrals of motion – like the total momentum of particles in Toda chains.

[9] This is basically standard bosonization formulas for the spin variables, cf. for example with [23],[134].

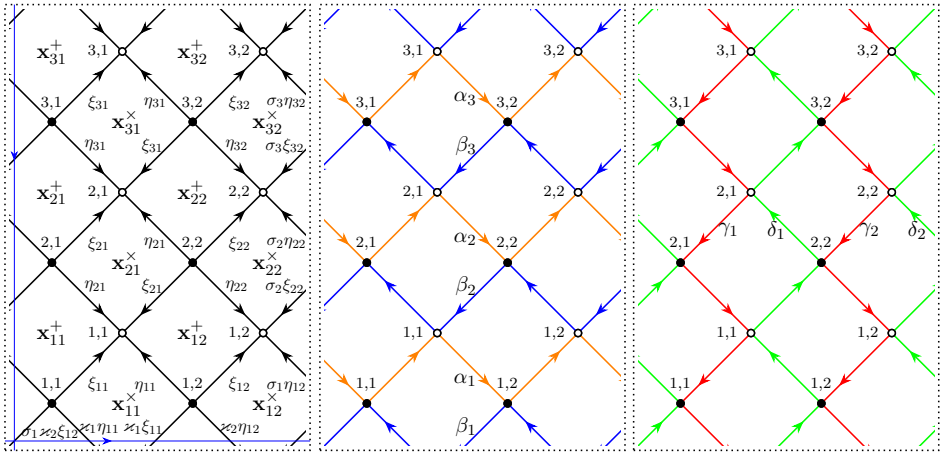

Figure 2.6. Left: bipartite graphs with labeled edges and faces: each edge, crossing purple cycle has to be multiplied by μ, each edge, crossing blue cycle – by λ. Center: horizontal zig-zag paths. Right: vertical zig-zag paths.

where the summand $E_{ij} \otimes E_{ab}$ is corresponding to the edge between black and white vertices[10] $(i, a) \to (j, b)$, and those matrices E_{ij} which get out of fundamental domain are promoted to the elements of the 'loop algebra', with the 'loop' parameters (λ, μ):

$$E_{1,0} \equiv \lambda E_{1,N}, \qquad \mathrm{E}_{M+1,M} \equiv \mu E_{1,M}. \tag{2.41}$$

Remark 2.2.1. The operator (2.40) as an element of $\mathrm{End}(\mathbb{C}^N)[[\lambda^{-1}]] \otimes \mathrm{End}(\mathbb{C}^M)[[\mu^{-1}]]$ can be naturally embedded into tensor product of evaluation representations of the loop algebras $\widetilde{\mathfrak{gl}}_N \otimes \widetilde{\mathfrak{gl}}_M$, i.e.

$$\begin{aligned}\mathfrak{D}(\lambda,\mu) = \sum_{i=1}^{N}\sum_{a=1}^{M} \xi_{ia}(h_i \otimes h_a - \varkappa_a^{\delta_{i,1}}\sigma_i^{\delta_{M,a}} f_{i-1} \otimes f_a) + \\ + \eta_{ia}(\varkappa_a^{\delta_{1,i}} f_{i-1} \otimes h_a + \sigma_i^{\delta_{M,a}} h_i \otimes f_a)\end{aligned} \tag{2.42}$$

[10] Signs '−' in $\mathfrak{D}$ arise in a standard way [71] due to choice of Kasteleyn marking or discrete spin structure on $\mathbb{T}^2$.

for two evaluation representations $\widetilde{\mathfrak{gl}}_K \to \mathrm{End}(\mathbb{C}^K)[[\zeta]]$:

$$\begin{aligned} &e_i = E_{i,i+1}, \quad 1 \le i \le K-1, \quad e_0 = e_K = \zeta E_{K,1} \\ &f_i = E_{i+1,i}, \quad 1 \le i \le K-1, \quad f_0 = f_K = \zeta^{-1} E_{1,K} \\ &h_i = E_{ii}, \qquad 1 \le i \le K. \end{aligned} \tag{2.43}$$

Let us now, breaking $M \leftrightarrow N$ symmetry, collect the terms, corresponding to E_{ii} and $E_{i,i-1}$ in the first tensor factor, i.e. rewrite (2.40) as:

$$\mathfrak{D}(\lambda,\mu) = \sum_{i=1}^{N} E_{i,i} \otimes A_i + E_{i,i-1} \otimes C_i (Q)^{\delta_{1,i}} \tag{2.44}$$

with

$$A_i = \sum_{b=1}^{M} \left(\xi_{ib} E_{b,b} + \eta_{ib} \sigma_i^{\delta_{M,b}} E_{b+1,b} \right), \quad C_i = \sum_{b=1}^{M} \left(\eta_{ib} E_{b,b} - \xi_{ib} \sigma_i^{\delta_{M,b}} E_{b+1,b} \right), \tag{2.45}$$

$$Q = \sum_{b=1}^{M} \varkappa_b E_{bb}$$

From the spectral curve equation $\det \mathfrak{D}(\lambda,\mu) = 0$ one finds for

$$\psi = \sum_{i=1}^{N} \psi_i e_i = \sum_{i=1}^{N} \sum_{a=1}^{M} \psi_{ia} e_i \otimes e_a \in \mathbb{C}^{MN} : \ \mathfrak{D}(\lambda,\mu)\psi = 0. \tag{2.46}$$

that

$$A_i \psi_i + C_i (Q)^{\delta_{i,1}} \psi_{i-1} = 0, \quad i = 1, \dots, N, \quad \psi_0 \equiv \lambda \psi_N. \tag{2.47}$$

Solving these equations recursively for the vectors $\psi_i = \sum\limits_{a=1}^{M} \psi_{ia} e_a$, one finally gets

$$\left(\lambda Q - (-1)^N C_1^{-1} A_1 ... C_N^{-1} A_N \right) \psi_N = 0 \tag{2.48}$$

with consistency condition

$$\det \left(\lambda\, Q - L_1 \left(\sigma_1 \zeta_1^h \mu \right) ... L_N \left(\sigma_N \zeta_N^h \mu \right) \right) = 0 \tag{2.49}$$

of the form (2.13), with the Lax matrices

$$L_i \left(\sigma_i \zeta_i^h \mu \right) = -C_i^{-1} A_i, \qquad i = 1, \dots, N. \tag{2.50}$$

Hence, the spectral curve $\det \mathfrak{D}(\lambda,\mu) = 0$ is represented in the form (2.11), common for the classical integrable chains with inhomogeneities $\mu_i = 1/\sigma_i\zeta_i^h = \beta_i$ and twist $Q = \sum_a \varkappa_a E_{aa} = \sum_a \sqrt{\delta_a/\gamma_a}E_{aa}$. There are also two sets of Casimirs related to spin variables: total projections of spin $\zeta_a^v = \prod_i e^{S^0_{ia}}$ and single non-trivial on-site Casimirs ζ_i^h. The Lax operators (2.50) on different sites satisfy classical RLL-relations

$$\{L_i(\mu) \otimes L_j(\mu')\} = \frac{1}{2}\delta_{ij}[r(\mu/\mu'), L_i(\mu)\otimes L_j(\mu')] \tag{2.51}$$

which coincide with (1.43) arising from the classical limit of $U_q(\mathfrak{gl}_M)$ with $q = e^{-\hbar}$ and $\kappa = \frac{1}{2}$ in (1.31), see Section 2.6 for details. In such way one gets explicit formulas (with the sign-factors (1.5)

$$(L_i)_{ab}(\mu) = \frac{1}{\mu^{\frac{1}{2}} - \mu^{-\frac{1}{2}}} \begin{cases} a = b, & \mu^{\frac{1}{2}} z_{ia}^{-2} + \mu^{-\frac{1}{2}} z_{ia}^2 \\ a \neq b, & \mu^{-\frac{s_{ab}}{2}}(z_{ib}^2 + z_{ib}^{-2})\dfrac{\tau_{ib}}{\tau_{ia}} \end{cases}, \tag{2.52}$$

for the Lax operators (2.50) on the sites $i \in 1, ..., N$ in terms of variables introduced in (2.37).

Comparing L-operator (2.52) with (1.44) one comes to the formulas (2.36), expressing the 'spin operators' on each site in terms of the edge variables. Expressions (2.36) satisfy all the relations of the classical limit of $U_q(\mathfrak{gl}_M)$ with $\kappa = \frac{1}{2}$. Note that this Lax operator is belonging to the lowest rank Kirillov orbit.

Remark 2.2.2. An equivalent construction of the cluster integrable systems is based on the Poisson submanifolds or double Bruhat cells in $\widehat{\mathrm{PGL}}$, endowed with the usual r-matrix Poisson structure [49, 55]. For the family of systems we consider here, given by the $SA(2,\mathbb{Z})$-orbit of rectangular $N \times M$ Newton polygons, one gets in such way a double Bruhat cell of $\widehat{\mathrm{PGL}}(N+M)$, given by the word

$$u = (s_M \bar{s}_M \, ... \, s_1 \bar{s}_1 \Lambda)^N \tag{2.53}$$

in the co-extended double Weyl group $\widetilde{W}(A_K^{(1)} \times A_K^{(1)})$ (here with $K = N + M$) with the generators $s_i, s_{\bar{i}}, \Lambda$ satisfying relations

$$\begin{array}{l} s_i^2 = 1, \quad (s_i s_{i+1})^3 = 1, \quad s_i s_j = s_j s_i, \quad \text{for} \quad |i-j| > 1 \\ \bar{s}_i^2 = 1, \quad (\bar{s}_i \bar{s}_{i+1})^3 = 1, \quad \bar{s}_i \bar{s}_j = \bar{s}_j \bar{s}_i, \quad \text{for} \quad |i-j| > 1 \qquad i,j = 1,\dots,K \\ \Lambda^K = 1, \quad \Lambda s_{i+1} = s_i \Lambda, \quad \Lambda \bar{s}_{i+1} = \bar{s}_i \Lambda \end{array} \tag{2.54}$$

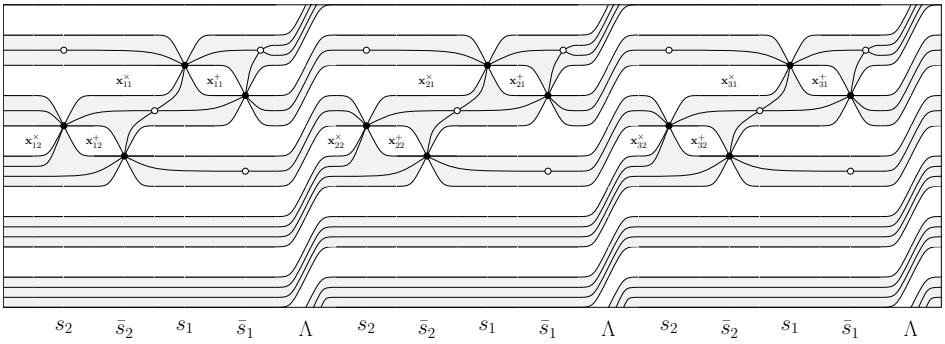

Figure 2.7. Thurston diagram in the $(3,2)$ case, which appears from $u = (s_2\bar{s}_2s_1\bar{s}_1\Lambda)^3$.

We are not going to repeat here all steps of the construction in detail, and just present the main ingredient – the Thurston diagram for (2.53), drawn for $(N,M) = (3,2)$ at Fig. 2.7. The corresponding bipartite graph (see Fig. 2.7) differs from the discussed above 'fence-net' by additional horizontal twist of the cylinder by 2π, which does not affect an integrable system, since it corresponds to the $SL(2,\mathbb{Z})$ transformation of the spectral parameters $(\lambda,\mu) \to (\lambda,\mu\lambda^{-1})$.

Example. SU(2) theory with $N_f = 4$ The most well-known case of the system we consider here corresponds to the five-dimensional supersymmetric gauge theory with the $SU(2)$ gauge group and $N_f = 4$ fundamental multiplets. The corresponding Newton polygon is a square with sides of length $N = M = 2$ (see Fig. 2.8), and as a spin chain this is just common XXZ-model on two sites with the Lax operator[11] (see e.g. [133])

$$L(\mu) = \begin{pmatrix} \mu e^{S^0} - \mu^{-1}e^{-S^0} & 2S^- \\ 2S^+ & \mu e^{-S^0} - \mu^{-1}e^{S^0} \end{pmatrix}, \qquad Q = \begin{pmatrix} \varkappa & 0 \\ 0 & \varkappa^{-1} \end{pmatrix}. \tag{2.55}$$

Spectral curve for the system is given by

$$\det\left(L\left(\mu/\mu_1\right)L\left(\mu/\mu_2\right)Q - \lambda\right) = 0. \tag{2.56}$$

[11] This form is slightly different from (1.52) arising from the classical limit of $U_q(\mathfrak{gl}_2)$. However, in 2×2 case these two forms are equivalent.

The Poisson brackets of spin operators are given by classical trigonometric r-matrix and written as:

$$\{S^0,\ S^{\pm}\} = \pm\, S^{\pm},\ \ \{S^+,\ S^-\} = \sinh\, 2S^0 \tag{2.57}$$

for the S-variables on the same site, and zero for the variables on the different sites. Such bracket has one natural Casimir function

$$K = -\zeta^h - (\zeta^h)^{-1} = \frac{1}{2}\cosh 2S^0 + S^+S^-. \tag{2.58}$$

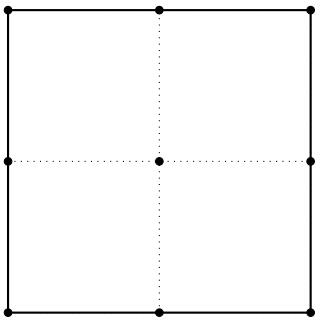

Figure 2.8. Newton polygon for $(N, M) = (2, 2)$.

As a cluster integrable system it lives on X-variety with the quiver corresponding to $A_3^{(1)}$-type system from figure 2 in [14], and its deautonomization leads to the Painlevé VI equation, solvable by conformal blocks, or equivalently topological strings amplitudes [102]. We derive Lax operator for this system from Kasteleyn operator in details in the next example, which is simply generalization of this example to three sites.

Example. SU(3) theory with $N_f = 6$. This case is corresponding to the word $u = (2\bar{2}1\bar{1}\Lambda)^3$ in double Weyl group of $\widehat{\mathrm{PGL}}(5)$. Bipartite graph

is drawn on Fig. 2.6. Kasteleyn operator is 6×6 matrix

$$\mathfrak{D} = \begin{array}{c|cccccc} bw & 11 & 12 & 21 & 22 & 31 & 32 \\ \hline 11 & \xi_{11} & \mu\sigma_1\eta_{12} & 0 & 0 & \lambda\varkappa_1\eta_{11} & -\lambda\mu\varkappa_2\sigma_1\xi_{12} \\ 12 & \eta_{11} & \xi_{12} & 0 & 0 & -\lambda\varkappa_1\xi_{11} & \lambda\varkappa_2\eta_{12} \\ 21 & \eta_{21} & -\mu\sigma_2\xi_{22} & \xi_{21} & \mu\sigma_2\eta_{22} & 0 & 0 \\ 22 & -\xi_{21} & \eta_{22} & \eta_{21} & \xi_{22} & 0 & 0 \\ 31 & 0 & 0 & \eta_{31} & -\mu\sigma_2\xi_{32} & \xi_{31} & \mu\sigma_2\eta_{32} \\ 32 & 0 & 0 & -\xi_{31} & \eta_{32} & \eta_{31} & \xi_{32} \end{array} = \tag{2.59}$$

$$= \begin{pmatrix} A_1 & 0 & \lambda C_1 Q \\ C_2 & A_2 & 0 \\ 0 & C_3 & A_3 \end{pmatrix}.$$

Spectral curve is given by condition

$$\det \mathfrak{D}(\lambda,\mu) = 0 \quad \Leftrightarrow \quad \exists\, \psi = \begin{pmatrix} \psi_1 \\ \psi_2 \\ \psi_3 \end{pmatrix} : \tag{2.60}$$

$$\mathfrak{D}(\lambda,\mu)\psi = 0 \qquad \Leftrightarrow \quad \begin{cases} \lambda Q\psi_3 = L_1(\sigma_1\zeta_1^h\mu)\psi_1 \\ \psi_1 = L_2(\sigma_2\zeta_2^h\mu)\psi_2 \\ \psi_2 = L_3(\sigma_3\zeta_3^h\mu)\psi_3 \end{cases}$$

$$L_i(\mu) = \frac{1}{\mu^{\frac{1}{2}} - \mu^{-\frac{1}{2}}} \begin{pmatrix} \mu^{-\frac{1}{2}}\dfrac{\xi_{i1}}{\eta_{i1}} + \mu^{\frac{1}{2}}\dfrac{\eta_{i1}}{\xi_{i1}} & \mu^{\frac{1}{2}}\dfrac{\eta_{i2}}{\xi_{i1}}\left(\dfrac{\xi_{i2}}{\eta_{i2}} + \dfrac{\eta_{i2}}{\xi_{i2}}\right) \\ \mu^{-\frac{1}{2}}\dfrac{\xi_{i1}}{\eta_{i2}}\left(\dfrac{\xi_{i1}}{\eta_{i1}} + \dfrac{\eta_{i1}}{\xi_{i1}}\right) & \mu^{-\frac{1}{2}}\dfrac{\xi_{i2}}{\eta_{i2}} + \mu^{\frac{1}{2}}\dfrac{\eta_{i2}}{\xi_{i2}} \end{pmatrix} \tag{2.61}$$

$$\zeta_i^h = \frac{\xi_{i1}\xi_{i2}}{\eta_{i1}\eta_{i2}}, \quad Q = \begin{pmatrix} \varkappa_1 & 0 \\ 0 & \varkappa_2 \end{pmatrix}$$

which could be rewritten using monodromy operator

$$\begin{gathered}\left(\lambda Q - T_3^{2\times 2}(\mu)\right)\psi_3 = 0 \quad \Leftrightarrow \quad \det\left(\lambda Q - T_3^{2\times 2}(\mu)\right) = 0, \\ T_3^{2\times 2}(\mu) = L_1(\sigma_1\zeta_1^h\mu)L_2(\sigma_2\zeta_2^h\mu)L_3(\sigma_3\zeta_3^h\mu).\end{gathered} \tag{2.62}$$

Lax operator (2.61) is of $\mathfrak{gl}_2$ type, so can be mapped to (1.52). To transform it in $\mathfrak{sl}_2$ form (2.55) we have to apply transformations like (1.54)

$$\mu \mapsto -\mu\,\frac{\xi_1\xi_2}{\eta_1\eta_2}, \tag{2.63}$$

$$L(\mu) \mapsto \left(\sqrt{\frac{\xi_1\xi_2}{\eta_1\eta_2}}\mu^{\frac{1}{2}} - \sqrt{\frac{\eta_1\eta_2}{\xi_1\xi_2}}\mu^{-\frac{1}{2}}\right)\begin{pmatrix}\mu^{-1/2} & 0\\ 0 & 1\end{pmatrix}\cdot L(\mu)\cdot\begin{pmatrix}\mu^{1/2} & 0\\ 0 & 1\end{pmatrix}$$

so it becomes

$$L(\mu) = \begin{pmatrix} \mu^{\frac{1}{2}}\sqrt{\frac{\eta_1\xi_2}{\xi_1\eta_2}} - \mu^{-\frac{1}{2}}\sqrt{\frac{\xi_1\eta_2}{\eta_1\xi_2}} & \sqrt{\frac{\xi_2\eta_2}{\xi_1\eta_1}}\left(\frac{\xi_2}{\eta_2}+\frac{\eta_2}{\xi_2}\right) \\ -\sqrt{\frac{\xi_1\eta_1}{\xi_2\eta_2}}\left(\frac{\xi_1}{\eta_1}+\frac{\eta_1}{\xi_1}\right) & \mu^{\frac{1}{2}}\sqrt{\frac{\xi_1\eta_2}{\eta_1\xi_2}} - \mu^{-\frac{1}{2}}\sqrt{\frac{\eta_1\xi_2}{\xi_1\eta_2}} \end{pmatrix}. \tag{2.64}$$

Defining classical $\mathfrak{sl}_2$ spin variables by

$$S^- = \frac{1}{2}\sqrt{\frac{\xi_2\eta_2}{\xi_1\eta_1}}\left(\frac{\xi_2}{\eta_2}+\frac{\eta_2}{\xi_2}\right), \quad S^+ = -\frac{1}{2}\sqrt{\frac{\xi_1\eta_1}{\eta_2\xi_2}}\left(\frac{\xi_1}{\eta_1}+\frac{\eta_1}{\xi_1}\right), \quad e^{S^0} = \sqrt{\frac{\xi_1\eta_2}{\eta_1\xi_2}} \tag{2.65}$$

we see that Lax operator (2.64) coincides with the (2.55) up to replacement $\mu^{1/2} \to \mu$ and $S^0 \mapsto -S^0$. The latter is a consequence of the fact that (2.64) is coming from $q = e^{-\hbar}$ prescription, but (2.55) - from the usual $q = e^{\hbar}$. Poisson brackets of spin variables coming from edge variables bracket $\{\xi_i, \eta_j\} = \frac{1}{2}\delta_{ij}\xi_i\eta_j$ are

$$\{S^0,\ S^\pm\} = \pm\frac{1}{2}\,S^\pm, \ \ \{S^+,\ S^-\} = \frac{1}{2}\sinh 2S^0 \tag{2.66}$$

which differs from (2.57) by factor 1/2, appearing from $\kappa = \frac{1}{2}$ in the prescription for the classical limit of commutators (1.31). For details see Section 1.3. Spectral curve (2.56) could be obtained from (2.49) by transformation $\lambda \mapsto \lambda(\varkappa_1\varkappa_2)^{-\frac{1}{2}}$ with identification of parameters $\varkappa = (\varkappa_1/\varkappa_2)^{\frac{1}{2}}$, $\mu_i = (\varkappa_1\varkappa_2)^{\frac{1}{2}}(\sigma_i\zeta_i^h)^{-1}$.

2.3 Dualities and twists

2.3.1 Spectral duality

For some integrable chains special kind of duality could be observed both on the classical and on the quantum level: namely system with N-dimensional auxiliary space on M sites share Hamiltonians with some other system with M-dimensional auxiliary space on N sites. Under duality spectral parameter which monodromy operator depends on, and spectral parameter of characteristic equation exchange, so this duality is often called spectral duality (however, sometimes referred as 'level-rank' or 'fiber-base' duality, see [134] and references therein).

In the case of our interest, system doesn't change its type: XXZ classical spin chain of $\mathfrak{gl}_M$ type on N sites is dual to the XXZ chain of the $\mathfrak{gl}_N$ type on M sites [134], [23]. Looking at $M \times N$ fence-net bipartite graph, it becomes obvious: graph keeps its structure under 90-degree rotation. On the level of Kasteleyn operator, this corresponds to exchange of factors in tensor product, and using different expressions for spin variables.

SU(2) theory with $N_f = 4$ and one bi-fundamental multiplet. We start discussion of spectral duality in our context from simplest non-trivial example. Let us consider $\mathfrak{gl}_3$ spin chain on two sites, which is dual to $\mathfrak{gl}_2$ chain on three sites, considered in Section 2.2.2. To derive dual Lax operators, we should permute some rows and columns of Kasteleyn operator (2.59), which is exchanging of factors in tensor product $\mathrm{End}(\mathbb{C}^2 \otimes \mathbb{C}^3) = \mathrm{End}(\mathbb{C}^3 \otimes \mathbb{C}^2)$:

$$\mathfrak{D} = \begin{array}{c|cccccc} & 11 & 21 & 31 & 12 & 22 & 32 \\ \hline 11 & \xi_{11} & 0 & \lambda\varkappa_1\eta_{11} & \mu\sigma_1\eta_{12} & 0 & -\lambda\mu\varkappa_2\sigma_1\xi_{12} \\ 21 & \eta_{21} & \xi_{21} & 0 & -\mu\sigma_2\xi_{22} & \mu\sigma_2\eta_{22} & 0 \\ 31 & 0 & \eta_{31} & \xi_{31} & 0 & -\mu\sigma_3\xi_{32} & \mu\sigma_3\eta_{32} \\ 12 & \eta_{11} & 0 & -\lambda\varkappa_1\xi_{11} & \xi_{12} & 0 & \lambda\varkappa_2\eta_{12} \\ 22 & -\xi_{21} & \eta_{21} & 0 & \eta_{22} & \xi_{22} & 0 \\ 32 & 0 & -\xi_{31} & \eta_{31} & 0 & \eta_{32} & \xi_{32} \end{array} = \tag{2.67}$$

$$= \begin{pmatrix} \tilde{A}_1 & \mu\tilde{Q}\tilde{C}_2 \\ \tilde{C}_1 & \tilde{A}_2 \end{pmatrix}$$

Spectral curve is given by condition

$$\det \mathfrak{D}(\lambda,\mu) = 0 \quad \Leftrightarrow \quad \exists\, \tilde{\psi} = \begin{pmatrix} \tilde{\psi}_1 & \tilde{\psi}_2 \end{pmatrix} : \tag{2.68}$$

$$\tilde{\psi}\mathfrak{D}(\lambda,\mu) = 0 \qquad \Leftrightarrow \quad \begin{cases} \tilde{\psi}_2 = \tilde{\psi}_1 \tilde{L}_1(\varkappa_1 \zeta_1^v \lambda) \\ \mu\tilde{\psi}_1\tilde{Q} = \tilde{\psi}_2 \tilde{L}_2(\varkappa_2\zeta_2^v\lambda) \end{cases}$$

$$\tilde{L}_k(\lambda) = \frac{1}{\lambda^{\frac{1}{2}} - \lambda^{-\frac{1}{2}}} \cdot \tag{2.69}$$

$$\cdot \begin{pmatrix} \lambda^{-\frac{1}{2}}\frac{\xi_{1k}}{\eta_{1k}} + \lambda^{\frac{1}{2}}\frac{\eta_{1k}}{\xi_{1k}} & \lambda^{\frac{1}{2}}\frac{\eta_{1k}}{\xi_{2k}}\left(\frac{\xi_{1k}}{\eta_{1k}} + \frac{\eta_{1k}}{\xi_{1k}}\right) & \lambda^{\frac{1}{2}}\frac{\eta_{1k}\eta_{2k}}{\xi_{2k}\xi_{3k}}\left(\frac{\xi_{1k}}{\eta_{1k}} + \frac{\eta_{1k}}{\xi_{1k}}\right) \\ \lambda^{-\frac{1}{2}}\frac{\xi_{2k}}{\eta_{1k}}\left(\frac{\xi_{2k}}{\eta_{2k}} + \frac{\eta_{2k}}{\xi_{2k}}\right) & \lambda^{-\frac{1}{2}}\frac{\xi_{2k}}{\eta_{2k}} + \lambda^{\frac{1}{2}}\frac{\eta_{2k}}{\xi_{2k}} & \lambda^{\frac{1}{2}}\frac{\eta_{2k}}{\xi_{3k}}\left(\frac{\xi_{2k}}{\eta_{2k}} + \frac{\eta_{2k}}{\xi_{2k}}\right) \\ \lambda^{-\frac{1}{2}}\frac{\xi_{2k}\xi_{3k}}{\eta_{1k}\eta_{2k}}\left(\frac{\xi_{3k}}{\eta_{3k}} + \frac{\eta_{3k}}{\xi_{3k}}\right) & \lambda^{-\frac{1}{2}}\frac{\xi_{3k}}{\eta_{2k}}\left(\frac{\xi_{3k}}{\eta_{3k}} + \frac{\eta_{3k}}{\xi_{3k}}\right) & \lambda^{-\frac{1}{2}}\frac{\xi_{3k}}{\eta_{3k}} + \lambda^{\frac{1}{2}}\frac{\eta_{3k}}{\xi_{3k}} \end{pmatrix}$$

$$\zeta_k^v = \frac{\xi_{1k}\xi_{2k}\eta_{3k}}{\eta_{1k}\eta_{2k}\eta_{3k}}, \quad \tilde{Q} = \begin{pmatrix} \sigma_1 & 0 & 0 \\ 0 & \sigma_2 & 0 \\ 0 & 0 & \sigma_3 \end{pmatrix} \tag{2.70}$$

which could be rewritten using monodromy operator

$$\tilde{\psi}_1\left(\mu\tilde{Q} - \tilde{T}_2^{3\times 3}(\lambda)\right) = 0 \quad \Leftrightarrow \quad \det\left(\mu\tilde{Q} - \tilde{T}_2^{3\times 3}(\lambda)\right) = 0, \tag{2.71}$$

$$\tilde{T}_2^{3\times 3}(\lambda) = \tilde{L}_1(\varkappa_1\zeta_1^v\lambda)\tilde{L}_2(\varkappa_2\zeta_2^v\lambda).$$

It is indeed spectral dual to the curve (2.62). One can check by direct calculation that

$$\begin{aligned} &(1-\varkappa_1\zeta_1^v\lambda)(1-\varkappa_2\zeta_2^v\lambda)\det\left(\mu\tilde{Q} - \tilde{T}_2^{3\times 3}(\lambda)\right) = \\ &= (1-\sigma_1\zeta_1^h\mu)(1-\sigma_2\zeta_2^h\mu)(1-\sigma_3\zeta_3^h\mu)\det\left(\lambda Q - T_3^{2\times 2}(\mu)\right). \end{aligned} \tag{2.72}$$

General case. If the order of factors in tensor product in (2.44) had been chosen in the other way, we would get M matrices A_k and C_k of size $N \times N$:

$$\mathfrak{D}(\lambda,\mu) = \sum_{m=1}^{M} \tilde{A}_m \otimes E_{m,m} + (\tilde{Q})^{\delta_{M,m}} \tilde{C}_m \otimes E_{m+1,m} \tag{2.73}$$

$$\tilde{A}_m = \sum_{n=1}^{N} \xi_{nm} E_{n,n} + \eta_{nm} \varkappa_m^{\delta_{1,n}} E_{n,n-1},\ \tilde{C}_m = \sum_{n=1}^{N} \eta_{nm} E_{n,n} - \xi_{nm} \varkappa_m^{\delta_{n,1}} E_{n,n-1}, \tag{2.74}$$

$$\tilde{Q} = \sum_{n=1}^{N} \sigma_n E_{nn}.$$

Again, we present spectral curve as condition

$$\exists\, \tilde{\psi} = \sum_{n=1}^{N} \sum_{m=1}^{M} \tilde{\psi}_{nm} e_n \otimes e_m \in \mathbb{C}^{MN} :\ \tilde{\psi}\mathfrak{D}(\lambda,\mu) = 0 \tag{2.75}$$

which gives for the spectral curve

$$\det\left(\tilde{L}_1(\varkappa_1\zeta_1^v\lambda)...\tilde{L}_M(\varkappa_M\zeta_M^v\lambda) - \mu\tilde{Q}\right) = 0, \quad \tilde{L}_k(\varkappa_k\zeta_k^v\lambda) = -\tilde{A}_k\tilde{C}_k^{-1}. \tag{2.76}$$

Using variables (2.37) we can write dual Lax operator

$$(\tilde{L}_m)_{ij}(\lambda) = \frac{1}{\lambda^{\frac{1}{2}} - \lambda^{-\frac{1}{2}}} \begin{cases} i \neq j, & \lambda^{-\frac{s_{ij}}{2}}(z_{im}^2 + z_{im}^{-2})\dfrac{\tilde{\tau}_{im}}{\tilde{\tau}_{jm}} \\ i = j, & \lambda^{\frac{1}{2}} z_{im}^{-2} + \lambda^{-\frac{1}{2}} z_{im}^2 \end{cases}, \tag{2.77}$$

$$\tilde{\tau}_{nm} = w_{nm} \prod_{i=1}^{N} z_{im}^{-s_{in}}\ .$$

We can relate them to L-operators (2.52) of the same size

$$L(z,w,\mu) = \tilde{L}(z \to z^{-1}, w, \lambda \to \mu^{-1})^{\top}. \tag{2.78}$$

Noting that for the classical r-matrix

$$r(a^{-1})^{\top} = -r(a) \tag{2.79}$$

where transposition is taken in each tensor multiplier, we can deduce from (2.51) that

$$\{\tilde{L}(\lambda) \otimes \tilde{L}(\mu)\} = \frac{1}{2}[\tilde{L}(\lambda) \otimes \tilde{L}(\mu), r(\lambda/\mu)]. \tag{2.80}$$

To obtain explicit relation for the dual spectral curves, we have to come back to the Kasteleyn operator of the system, and consider its determinant. In terms of $M \times M$ blocks A_k, C_k defined by (2.74) spectral curve is given by

$$\det \mathfrak{D}(\lambda,\mu) = \begin{vmatrix} A_1 & 0 & ... & 0 & \lambda C_1 Q \\ C_2 & A_2 & ... & 0 & 0 \\ ... & ... & ... & ... & ... \\ 0 & 0 & ... & A_{N-1} & 0 \\ 0 & 0 & ... & C_N & A_N \end{vmatrix} = \tag{2.81}$$

$$= \prod_i (\det C_i) \cdot \begin{vmatrix} C_1^{-1}A_1 & 0 & ... & 0 & \lambda Q \\ \mathbf{1} & C_2^{-1}A_2 & ... & 0 & 0 \\ ... & ... & ... & ... & ... \\ 0 & 0 & ... & C_{N-1}^{-1}A_{N-1} & 0 \\ 0 & 0 & ... & \mathbf{1} & C_N^{-1}A_N \end{vmatrix} =$$

$$= ... = \prod_i (\det C_i) \cdot \begin{vmatrix} \mathbf{1} & 0 & ... & 0 & \lambda Q \\ \mathbf{1} & \mathbf{1} & ... & 0 & 0 \\ ... & ... & ... & ... & ... \\ 0 & 0 & ... & \mathbf{1} & 0 \\ 0 & 0 & ... & \mathbf{1} & (-1)^N T_N^{M\times M} \end{vmatrix},$$

$$T_N^{M\times M} = L_1 ... L_N, \quad L_k = -C_k^{-1}A_k,$$

and subtracting consequentially lines from first to last

$$\det \mathfrak{D}(\lambda,\mu) = (-1)^{NM} \det (C_1 ... C_N) \det (T_N^{M\times M}(\mu) - \lambda Q). \tag{2.82}$$

Acting in the same way, we get for the dual spectral curve

$$\det \mathfrak{D}(\lambda,\mu) = (-1)^{NM} \det \left(\tilde{C}_1 ... \tilde{C}_M\right) \det (\tilde{T}_M^{N\times N}(\lambda) - \mu \tilde{Q}), \tag{2.83}$$

$$\tilde{T}_M^{N\times N} = \tilde{L}_1 ... \tilde{L}_M, \quad \tilde{L}_k = -\tilde{A}_k \tilde{C}_k^{-1}$$

so, precise relation between curves is

$$\det\,(C_1...C_N)\det\,(T_N^{M\times M}(\mu)-\lambda Q)=\det\,\left(\tilde{C}_1...\tilde{C}_M\right)\det\,(\tilde{T}_M^{N\times N}(\lambda)-\mu\tilde{Q}) \tag{2.84}$$

Note that the relation of pre-factors is Casimir of the bracket

$$\frac{\det\,(C_1...C_N)}{\det\,\left(\tilde{C}_1...\tilde{C}_N\right)}=\frac{\mu^{\frac{N}{2}}}{\lambda^{\frac{M}{2}}}\left(\frac{\sigma_1...\sigma_N}{\varkappa_1...\varkappa_M}\right)^{1/2}\frac{\prod\limits_{n=1}^{N}(\sigma_n\zeta_n^h\mu)^{-1/2}-(\sigma_n\zeta_n^h\mu)^{1/2}}{\prod\limits_{m=1}^{M}(\varkappa_m\zeta_m^v\lambda)^{-1/2}-(\varkappa_m\zeta_m^v\mu)^{1/2}}. \tag{2.85}$$

2.3.2 Twisted chains

A diagonal twist matrix is not the only one, commuting with r-matrices. A cyclic twist

$$Q_\Lambda(\lambda)=\sum_{i=1}^{N}E_{i+1,i}=\sum_{i=1}^{N-1}\mathrm{E}_{i+1,i}+\lambda\mathrm{E}_{1,N} \tag{2.86}$$

also satisfies $[r(\lambda/\mu),Q_\Lambda(\lambda)\otimes Q_\Lambda(\mu)]=0$. In terms of bipartite graphs it corresponds to the twist on a cycle of the torus, where the bipartite graph is drawn on, or the gluing condition for the sides of fundamental domain, see Fig. 2.6. Such twist also changes a Poisson quiver, even though the edge variables are not affected themselves.

The twist of a bipartite graph results further in change of the zig-zag's structure. Several parallel zig-zags now join into 'longer sequences' with non-trivial winding so that rectangle Newton polygon undergoes a 'shear shift' – see examples on Fig. 2.9.

In the context of such transformations one can expect nontrivial consequences for spectral duality. Consider the trivial case of $\mathfrak{gl}_N$ chain on a single site, which is dual to rank 1 chain on N sites, and apply the cyclic twist along the longer side of a bipartite graph. In original picture this is just a multiplication of a single $N\times N$ Lax operator by cyclic permutation matrix. However in the dual setup, this results in passing from trivial $\mathfrak{gl}_1$ chain to the Toda chain on the same number of sites, which can be verified by comparing Fig. 2.9 and Fig. 2.3. After such procedure the number of Casimirs drops by $2N-2$, while number of Hamiltonians jumps from 0 to $N-1$.

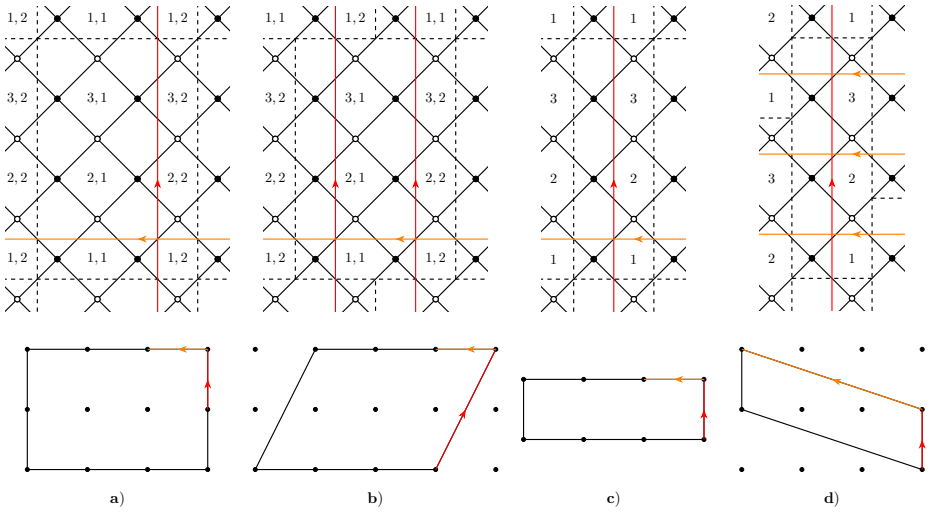

Figure 2.9. Examples of twisted $\mathfrak{gl}_2$ chains. Dashed lines bound fundamental domains. We use different notations for zig-zags here, comparing to the pictures above. Edges crossed by red arrows belong to γ_2 zig-zag, orange arrows are for α_1. a,b) XXZ chain of rank two and its twisted cousin. Note that the twisted twice chain is equivalent up to $\mathrm{SL}(2,\mathbb{Z})$ transformation $\lambda \to \lambda\mu$ to the untwisted chain, as $Q_\Lambda^2 = \mu\,\mathbf{1}$, like in Remark 2.2.2. c,d) Making Toda chain by twisting $\mathfrak{gl}_N$ chain dual to $\mathfrak{gl}_1$ chain.

For supersymmetric theories such transformation turns the theory of a single $\mathrm{SU}(N)$ hypermultiplet with only $\mathrm{SU}(N) \times \mathrm{SU}(N)$ flavor symmetry into pure $\mathrm{SU}(N)$ gauge theory.

2.4 Discrete dynamics

The cluster mapping class group $\mathcal{G}_\mathcal{Q}$ consists of sequences of mutations and permutations of quiver vertices, which maps quiver to itself, but acts in general non-trivially to the cluster variables (see Section 1.4 for details). As a simplification one can restrict the action of $\mathcal{G}_\mathcal{Q}$ to the set of Casimirs of the Poisson bracket. Each monomial Casimir maps to the monomial in Casimir functions. When the necessary for integrability condition $\prod_i x_i = 1$ is relaxed to $\prod_i x_i = q$ (which is called as deautonomization), these flows act on the set of Casimirs, inducing non-trivial $q-$dynamics.

In [14] the cluster mapping class groups for the quivers, corresponding

to Newton polygons with a single internal point, were identified with the symmetry groups of q-Painlevé equations[12]. Passing from X-cluster to A-cluster variety, the q-Painlevé equations acquire bilinear form for the tau-functions, and can be solved via the dual Nekrasov partition functions for 5d supersymmetric SU(2) gauge theories [24, 14, 102, 16], which is a natural '5d uplift' of '4d' isomonodromic/CFT correspondence [68]. In [15] the cluster description was further applied to discrete dynamics of relativistic Toda chains of arbitrary lengths, where the solutions of non-autonomous versions are given by $SU(N)$ partition functions with the $|k| \leq N$ Chern-Simons terms. Recently, cluster realization of generalized q-Painlevé VI system was also observed in [153]. Note that for $q = 1$ case with trivial Casimirs solution of discrete dynamics for arbitrary bipartite graph can be written in terms of θ-functions [44].

Below in this section we discuss the cluster mapping class groups and non-autonomous bilinear equations, arising for generic rectangle Newton polygons. We present their explicit construction in the example, which will illustrate the following results:

Structure of the group $\mathcal{G}_{\mathcal{Q}}$.
For the $SA(2,\mathbb{Z})$-class of $N \times M$ rectangular Newton polygon, the MCG $\mathcal{G}_{\mathcal{Q}}$ always contains a subgroup of the form

$$\widetilde{W}\left(A^{(1)}_{N-1} \times A^{(1)}_{N-1}\right) \times \widetilde{W}\left(A^{(1)}_{M-1} \times A^{(1)}_{M-1}\right) \rtimes \mathbb{Z} \subset \mathcal{G}_{\mathcal{Q}}. \tag{2.87}$$

where $\widetilde{W}\left(A^{(1)}_{N-1} \times A^{(1)}_{N-1}\right)$ is a co-extended double Weyl group (2.54).

The generators of each subgroup are naturally labeled by intervals on sides of a Newton polygon, or subset of 'parallel' zig-zag paths (in the same homology class) on a bipartite graph:

$$\widetilde{W}\left(A^{(1)}_{N-1} \times A^{(1)}_{N-1}\right): \ \{s_{\alpha_i,\alpha_{i+1}}\}, \quad \{s_{\beta_i,\beta_{i+1}}\}, \quad i \in \mathbb{Z}/N\mathbb{Z} \tag{2.88}$$

$$\widetilde{W}\left(A^{(1)}_{M-1} \times A^{(1)}_{M-1}\right): \ \{s_{\gamma_a,\gamma_{a+1}}\}, \quad \{s_{\delta_a,\delta_{a+1}}\}, \quad a \in \mathbb{Z}/M\mathbb{Z} \tag{2.89}$$

where subscripts $\alpha, \beta, \gamma, \delta$ label the corresponding group of paths, see Fig. 2.6 middle and right. The group being extended by the additional generator ρ contains lattice of the rank $2N + 2M - 3$ of $q-$difference flows of integrable system.

[12] Such relation for particular cases was earlier mentioned in [90, 146, 24, 147].

Moreover, in special cases there is an obvious symmetry enhancement: for example, for $N = M$ an additional 'external' generator appears, which rotates the whole picture by $\pi/2$. However, sometimes this enhancement is more essential: if any of the sides is of length 2, two rest Weyl groups can be 'glued' together by additional permutation, so the known subgroup of $\mathcal{G}_{\mathcal{Q}}$ becomes

$$\widetilde{W}\left(A^{(1)}_{2N-1}\right) \times \widetilde{W}\left(A^{(1)}_1 \times A^{(1)}_1\right) \subset \mathcal{G}_{\mathcal{Q}} \tag{2.90}$$

This enhancement is closely related to the fact that spectral curves with the $N \times 2$ rectangular Newton polygon can be mapped to the curves with the triangular Newton polygon with the integer sides $2N \times 2 \times 2$ (see e.g. (3.70) in [62]). If both $N = M = 2$ one finds the extra enhancement from $\widetilde{W}(A^{(1)}_1 \times A^{(1)}_1) \times \widetilde{W}(A^{(1)}_1 \times A^{(1)}_1)$ to $\widetilde{W}(D^{(1)}_5)$, see below.

Action on spin chain Casimirs.
Inhomogeneities, total spins, on-site Casimirs and twists of spin chain are permuted under the action of different components of $\mathcal{G}_{\mathcal{Q}}$.

Inhomogeneities are given by single zig-zags $\mu_i = \beta_{\dot{\imath}}$, while on-site Casimirs are given by products of zig-zags $\zeta^h_i = (\alpha_i\beta_i)^{\frac{1}{2}}$. So the well defined transformation of them, which 'permutes sites' of spin chain are products of primitive permutations

$$\mathrm{s}_{\alpha_i,\alpha_{i+1}}\mathrm{s}_{\beta_i,\beta_{i+1}}: \quad \mu_i \mapsto \mu_{i+1},\ \mu_{i+1} \mapsto \mu_i, \quad \zeta^h_i \mapsto \zeta^h_{i+1},\ \zeta^h_{i+1} \mapsto \zeta^h_i. \tag{2.91}$$

Permutations of twists $\varkappa_a = (\delta_a/\gamma_a)^{\frac{1}{2}}$ and projections of spins $\zeta^v_a = (\gamma_a\delta_a)^{\frac{1}{2}}$ by products

$$\mathrm{s}_{\gamma_a,\gamma_{a+1}}\mathrm{s}_{\delta_a,\delta_{a+1}}: \quad \varkappa_a \mapsto \varkappa_{a+1},\ \varkappa_{a+1} \mapsto \varkappa_a, \quad \zeta^v_a \mapsto \zeta^v_{a+1},\ \zeta^v_{a+1} \mapsto \zeta^v_a. \tag{2.92}$$

can be viewed as an action of the Weyl group by permutations on the maximal torus of Lie group.

Bilinear equations.
Equations defining the action of each single generator of $\mathcal{G}_{\mathcal{Q}}$ on A-cluster variables $(\tau^{\times}_{ij}, \tau^{+}_{ij})$ could be rewritten in the form of bilinear equations. Evolution of coefficients can be encapsulated into the transformations of frozen variables $\{\mathbf{u}_{\alpha_i}, \mathbf{u}_{\beta_i}, \mathbf{u}_{\gamma_a}, \mathbf{u}_{\delta_a}\}$, which are evolving in the same way

as Casimirs in $\mathcal{X}$-variables.

For example τ-variables $\bar{\tau}^{\times}_{k,a}, \bar{\tau}^{+}_{k,a}$ transformed under the action of generator $\mathrm{s}_{\beta_i,\beta_{i+1}}$ satisfy bilinear equations

$$\begin{aligned}
&(\mathbf{u}_{\beta_{i+1}} - q^{\frac{1}{N}}\mathbf{u}_{\beta_i})(\mathbf{u}_\delta \mathbf{u}_{\gamma_a})^{\frac{1}{N}} \tau^{+}_{i-1,a}\tau^{\times}_{i+1,a} = \\
&= \mathbf{u}^{\frac{1}{M}}_{\beta_{i+1}} \bar{\tau}^{+}_{i,a}\tau^{\times}_{i,a} - q^{\frac{1}{NM}}\mathbf{u}^{\frac{1}{M}}_{\beta_i} \bar{\tau}^{\times}_{i,a}\tau^{+}_{i,a} \\
&(\mathbf{u}_{\beta_{i+1}} - q^{\frac{1}{N}}\mathbf{u}_{\beta_i})(\mathbf{u}_\delta / \mathbf{u}_{\delta_a})^{\frac{1}{N}} \tau^{+}_{i-1,a+1}\tau^{\times}_{i+1,a} = \\
&\mathbf{u}^{-\frac{1}{M}}_{\alpha_i} \bar{\tau}^{\times}_{i,a}\tau^{+}_{i,a+1} - q^{\frac{1}{NM}}\mathbf{u}^{-\frac{1}{M}}_{\alpha_i} \bar{\tau}^{+}_{i,a+1}\tau^{\times}_{i,a}
\end{aligned} \tag{2.93}$$

for all $a \in \mathbb{Z}/M\mathbb{Z}$, where $\mathbf{u}_\delta = \prod_a \mathbf{u}_{\delta_a}$. Frozen variables are transforming as

$$\mathrm{s}_{\beta_i,\beta_{i+1}}: \quad \mathbf{u}_{\beta_i} \mapsto q^{-\frac{1}{N}}\mathbf{u}_{\beta_{i+1}}, \ \mathbf{u}_{\beta_{i+1}} \mapsto q^{\frac{1}{N}}\mathbf{u}_{\beta_i}. \tag{2.94}$$

Bilinear equations for the action of generators $\mathrm{s}_{\alpha_i,\alpha_{i+1}}, \mathrm{s}_{\gamma_a,\gamma_{a+1}}, \mathrm{s}_{\delta_a,\delta_{a+1}}$ are similar.

2.4.1 Structure of $\mathcal{G}_{\mathcal{Q}}$

Now we present generators of $\mathcal{G}_{\mathcal{Q}}$ in terms of the quiver mutations[13] $\{\mu^{\times}_{ij}, \mu^{+}_{ij}\}$ (in the vertices, initially assigned with $\{x^{\times}_{ij}, x^{+}_{ij}\}$) and permutations of the vertices $\{s^{\lambda_a,\lambda_b}_{ij,kl}\}$. Consider for simplicity the $(3,2)$-example, which already illustrates how the explicit formulas look like in generic case. Here $2(N+M) = 10$ generators (2.88) can be realized as

$$\begin{aligned}
\mathrm{s}_{\beta_1,\beta_2} &= s^{\lambda_a,\lambda_b}_{12,12}\mu^{+}_{11}\mu^{\times}_{11}\mu^{+}_{12}\mu^{\times}_{12}\mu^{+}_{11}\mu^{\times}_{11} & \mathrm{s}_{\alpha_3,\alpha_1} &= s^{\lambda_a,\lambda_b}_{12,31}\mu^{+}_{32}\mu^{\times}_{11}\mu^{+}_{12}\mu^{\times}_{31}\mu^{+}_{11}\mu^{\times}_{32} \\
\mathrm{s}_{\beta_2,\beta_3} &= s^{\lambda_a,\lambda_b}_{22,22}\mu^{+}_{21}\mu^{\times}_{21}\mu^{+}_{22}\mu^{\times}_{22}\mu^{+}_{21}\mu^{\times}_{21} & \mathrm{s}_{\alpha_1,\alpha_2} &= s^{\lambda_a,\lambda_b}_{22,11}\mu^{+}_{12}\mu^{\times}_{21}\mu^{+}_{22}\mu^{\times}_{11}\mu^{+}_{21}\mu^{\times}_{12} \\
\mathrm{s}_{\beta_3,\beta_1} &= s^{\lambda_a,\lambda_b}_{32,32}\mu^{+}_{31}\mu^{\times}_{31}\mu^{+}_{32}\mu^{\times}_{32}\mu^{+}_{31}\mu^{\times}_{31} & \mathrm{s}_{\alpha_2,\alpha_3} &= s^{\lambda_a,\lambda_b}_{32,21}\mu^{+}_{22}\mu^{\times}_{31}\mu^{+}_{32}\mu^{\times}_{21}\mu^{+}_{31}\mu^{\times}_{22}
\end{aligned} \tag{2.95}$$

and

$$\begin{aligned}
\mathrm{s}_{\delta_2,\delta_1} &= s^{\lambda_a,\lambda_b}_{31,31}\mu^{+}_{21}\mu^{\times}_{21}\mu^{+}_{11}\mu^{\times}_{11}\mu^{\times}_{31}\mu^{+}_{31}\mu^{\times}_{11}\mu^{+}_{11}\mu^{\times}_{21}\mu^{+}_{21} \\
\mathrm{s}_{\gamma_1,\gamma_2} &= s^{\lambda_a,\lambda_b}_{21,12}\mu^{+}_{22}\mu^{\times}_{31}\mu^{+}_{32}\mu^{\times}_{11}\mu^{\times}_{21}\mu^{+}_{12}\mu^{\times}_{11}\mu^{+}_{32}\mu^{\times}_{31}\mu^{+}_{22}
\end{aligned} \tag{2.96}$$

[13] For the definitions on cluster algebras see Section 1.4.

$$\mathrm{s}_{\delta_1,\delta_2} = s^{\lambda_a,\lambda_b}_{32,32}\mu^+_{22}\mu^\times_{22}\mu^+_{12}\mu^\times_{12}\mu^\times_{32}\mu^+_{32}\mu^\times_{12}\mu^+_{12}\mu^\times_{22}\mu^+_{22}$$

$$\mathrm{s}_{\gamma_2,\gamma_1} = s^{\lambda_a,\lambda_b}_{22,11}\mu^+_{21}\mu^\times_{32}\mu^+_{31}\mu^\times_{12}\mu^\times_{22}\mu^+_{11}\mu^\times_{12}\mu^+_{31}\mu^\times_{32}\mu^+_{21}$$

which are sequences of mutations in the vertices along zig-zags in the forward and then backward directions. One can check that each generator here is involution i.e. $\mathrm{s}^2 = 1$, and acts by rational transformation on X-cluster variables: e.g. for $\mathrm{s}_{\beta_2,\beta_3} = s^{\lambda_a,\lambda_b}_{22,22}\mu^+_{21}\mu^\times_{21}\mu^\times_{22}\mu^+_{22}\mu^\times_{21}\mu^+_{21}$ one can explicitly write:

$$x^\times_{31} \mapsto x^\times_{31}\cdot x^+_{22}x^\times_{21}\frac{[x^\times_{22},x^+_{21},x^\times_{21}]}{[x^\times_{21},x^+_{22},x^\times_{22}]},\quad x^\times_{32} \mapsto x^\times_{32}\cdot x^+_{21}x^\times_{22}\frac{[x^\times_{21},x^+_{22},x^\times_{22}]}{[x^\times_{22},x^+_{21},x^\times_{21}]}, \tag{2.97}$$

$$x^+_{21} \mapsto \frac{1}{x^\times_{21}}\cdot\frac{[x^+_{21},x^\times_{21},x^+_{22}]}{[x^+_{22},x^\times_{22},x^+_{21}]},\quad x^+_{22} \mapsto \frac{1}{x^\times_{22}}\cdot\frac{[x^+_{22},x^\times_{22},x^+_{21}]}{[x^+_{21},x^\times_{21},x^+_{22}]},$$

$$x^\times_{21} \mapsto \frac{1}{x^+_{22}}\cdot\frac{[x^\times_{21},x^+_{22},x^\times_{22}]}{[x^\times_{22},x^+_{21},x^\times_{21}]},\quad x^\times_{22} \mapsto \frac{1}{x^+_{21}}\cdot\frac{[x^\times_{22},x^+_{21},x^\times_{21}]}{[x^\times_{21},x^+_{22},x^\times_{22}]},$$

$$x^+_{11} \mapsto x^+_{11}\cdot x^\times_{21}x^+_{21}\frac{[x^+_{22},x^\times_{22},x^+_{21}]}{[x^+_{21},x^\times_{21},x^+_{22}]},\quad x^+_{12} \mapsto x^+_{12}\cdot x^\times_{22}x^+_{22}\frac{[x^+_{21},x^\times_{21},x^+_{22}]}{[x^+_{22},x^\times_{22},x^+_{21}]},$$

while all the other variables remain unchanged. Here we have used the notation

$$[x_1,x_2,..,x_n] = 1 + x_1 + x_1\cdot x_2 + ... + x_1\cdot ...\cdot x_n = \tag{2.98}$$

$$= 1 + x_1(1 + x_2(.... + x_{n-1}(1 + x_n)...)).$$

Notice also that the result of zig-zag mutation sequences actually do not depends on the point of the 'zig-zag strip' one starts with the first mutation and direction of the jumps along/across given zig-zag. Note that the [ ]-function possesses nice 'inversion' property

$$[x_1,...,x_n] = x_1...x_n\cdot[x_n^{-1},...,x_1^{-1}] \tag{2.99}$$

which allows to write equivalently, for example

$$x^\times_{21} \mapsto \frac{1}{x^+_{22}}\cdot\frac{[x^\times_{21},x^+_{22},x^\times_{22}]}{[x^\times_{22},x^+_{21},x^\times_{21}]} = \frac{1}{x^+_{21}}\cdot\frac{[(x^\times_{22})^{-1},(x^+_{22})^{-1},(x^\times_{21})^{-1}]}{[(x^\times_{21})^{-1},(x^+_{21})^{-1},(x^\times_{22})^{-1}]}. \tag{2.100}$$

Each set of permutations $\mathrm{s}_{\zeta_i,\zeta_{i+1}}$ with similar ζ constitute affine Weyl group of $A^{(1)}$-type. The groups for different z are commuting, so they satisfy usual relations

$$\begin{cases} \mathrm{s}^2_{\zeta_i,\zeta_{i+1}} = 1, \\ (\mathrm{s}_{\zeta_i,\zeta_{i+1}}\mathrm{s}_{\zeta_{i+1},\zeta_{i+2}})^3 = 1 \\ \mathrm{s}_{\zeta_i,\zeta_{i+1}}\mathrm{s}_{\zeta_j,\zeta_{j+1}} = \mathrm{s}_{\zeta_j,\zeta_{j+1}}\mathrm{s}_{\zeta_i,\zeta_{i+1}}, \quad |i-j|>1 \end{cases} \tag{2.101}$$

$\zeta = \alpha, \beta$ with $i, j \in \mathbb{Z}/3\mathbb{Z}$

$$\mathrm{s}^2_{\zeta_i,\zeta_{a+1}} = 1$$

$\zeta = \gamma, \delta$ with $i, j \in \mathbb{Z}/2\mathbb{Z}$.

$$\mathrm{s}_{\zeta_i,\zeta_{i+1}}\mathrm{s}_{\zeta'_j,\zeta'_{j+1}} = \mathrm{s}_{\zeta'_j,\zeta'_{j+1}}\mathrm{s}_{\zeta_i,\zeta_{i+1}},$$

$\zeta, \zeta' = \alpha, \beta, \gamma, \delta$ such that $\zeta \neq \zeta'$. There are two more 'external' automorphisms preserving bipartite graph

$$\begin{aligned} \Lambda_h: &\quad x^{\times}_{ia} \mapsto x^{\times}_{i,a-1}, \quad x^{+}_{ia} \mapsto x^{+}_{i,a-1} \\ \Lambda_v: &\quad x^{\times}_{ia} \mapsto x^{\times}_{i-1,a}, \quad x^{+}_{ia} \mapsto x^{+}_{i-1,a} \end{aligned} \tag{2.102}$$

which satisfy obvious relations

$$\Lambda_h\Lambda_v = \Lambda_v\Lambda_h, \quad \Lambda_h^2 = 1, \quad \Lambda_v^3 = 1, \tag{2.103}$$

$$\Lambda_h \mathrm{s}_{\zeta_a,\zeta_{a+1}} = \mathrm{s}_{\zeta_{a-1},\zeta_a}\Lambda_h, \quad \text{for } \zeta = \gamma, \delta, \tag{2.104}$$

$$\Lambda_h \mathrm{s}_{\zeta_i,\zeta_{i+1}} = \mathrm{s}_{\zeta_i,\zeta_{i+1}}\Lambda_h, \quad \text{for } \zeta = \alpha, \beta, \tag{2.105}$$

$$\Lambda_v \mathrm{s}_{\zeta_i,\zeta_{i+1}} = \mathrm{s}_{\zeta_{i-1},\zeta_i}\Lambda_v, \quad \text{for } \zeta = \alpha, \beta \ , \tag{2.106}$$

$$\Lambda_v \mathrm{s}_{\zeta_a,\zeta_{a+1}} = \mathrm{s}_{\zeta_a,\zeta_{a+1}}\Lambda_v, \quad \text{for } \zeta = \gamma, \delta \ , \tag{2.107}$$

and promote affine Weyl groups to extended affine Weyl groups. There is also one more generator of infinite order

$$\rho = s^{\lambda_b\lambda_a}\mu^{\lambda_b}: \quad \mu^{\lambda_b} = \prod_{i,a}\mu_{ia}^{\lambda_b}, \quad s^{\lambda_b\lambda_a}: \quad x^{+}_{ia} \mapsto x^{\times}_{ia}, \quad x^{\times}_{ia} \mapsto x^{+}_{i-1,a+1}, \tag{2.108}$$

satisfying relations

$$\rho\, \mathrm{s}_{\alpha_{i-1},\alpha_i} = \mathrm{s}_{\alpha_i,\alpha_{i+1}}\, \rho, \quad \rho\, \mathrm{s}_{\beta_i,\beta_{i+1}} = \mathrm{s}_{\beta_i,\beta_{i+1}}\, \rho, \tag{2.109}$$

$$\rho\, \mathrm{s}_{\gamma_i,\gamma_{i+1}} = \mathrm{s}_{\gamma_{i-1},\gamma_i}\, \rho, \quad \rho\, \mathrm{s}_{\delta_i,\delta_{i+1}} = \mathrm{s}_{\delta_i,\delta_{i+1}}\, \rho,$$

so the cluster mapping class group contains

$$\widetilde{W}\left(A_2^{(1)} \times A_2^{(1)}\right) \times \widetilde{W}\left(A_1^{(1)} \times A_1^{(1)}\right) \rtimes \mathbb{Z} \subset \mathcal{G}_{\mathcal{Q}}. \tag{2.110}$$

We conjecture that for general rectangular $N \times M$ Newton polygon, cluster mapping class group contains subgroup (2.87). Construction of generators for general N and M is straightforward, by 'jumps over zig-zags' as in example.

In the case $N = M$ there is also an additional 'external' generator $R_{\pi/2}$ of order 4, which rotates bipartite graph by $\pi/2$

$$R_{\pi/2}:\ x^{\times}_{i,a} \mapsto x^{+}_{-a,i}, \quad x^{+}_{i,a} \mapsto x^{\times}_{1-a,i}. \tag{2.111}$$

In the case $N = 2K$ or $M = 2K$ there is another additional 'external' generator, which flips the rectangle.

Discrete flows. The group $\mathcal{G}_{\mathcal{Q}}$ contains lattice L of discrete flows of rank $B - 3$, where $B = 2N + 2M$ is the number of boundary integral points of Newton polygon. It consists of four pairwise commuting lattices contained in two copies of $W(A^{(1)}_{N-1}) = \mathbb{Z}^{N-1} \rtimes W(A_{N-1})$ and two copies of $W(A^{(1)}_{M-1}) = \mathbb{Z}^{M-1} \rtimes W(A_{M-1})$, and generator $(\rho)^{\mathrm{lcm}(N,M)}$ where $\mathrm{lcm}(N, M)$ is the least common multiple of N and M. The lattice is generated by elements $\mathrm{T}_{\zeta_i,\zeta_{i+1}}$ which take pair of adjacent strands, wind them up in opposite directions over cylinder and put on the initial places, if one imagine $W(A^{(1)}_{N-1}), W(A^{(1)}_{M-1})$ as a groups acting by permutations of strands on cylinder. For $(3, 2)$ example β-piece of $\mathcal{G}_{\mathcal{Q}}$ can be presented as $W(A^{(1)}_2) = \mathbb{Z}^2 \rtimes W(A_2)$ with $\mathbb{Z}^2$ and $W(A_2)$ generated by

$$\mathrm{T}_{\beta_1,\beta_2} = \mathrm{s}_{\beta_1,\beta_2}\mathrm{s}_{\beta_2,\beta_3}\mathrm{s}_{\beta_3,\beta_1}\mathrm{s}_{\beta_2,\beta_3}, \quad \mathrm{T}_{\beta_2,\beta_3} = \mathrm{s}_{\beta_2,\beta_3}\mathrm{s}_{\beta_3,\beta_1}\mathrm{s}_{\beta_1,\beta_2}\mathrm{s}_{\beta_3,\beta_1} \tag{2.112}$$

and by

$$\mathrm{s}_{\beta_1,\beta_2}, \mathrm{s}_{\beta_2,\beta_3} \tag{2.113}$$

correspondingly.

One can find a homomorphism of the lattice L of the shifts (2.112) into the group of discrete flows $\mathcal{G}'_\Delta$ (defined as in [55] to be an additive group of integral valued functions on boundary vertices of Newton polygon modulo sub-group A generated by the restrictions from $\mathbb{Z}^2$ to the boundary of Newton polygon of affine functions $f(i,j) = ai + bj + c$). For the case of rectangular Newton polygons one can easily finds that $\mathcal{G}'_\Delta = \mathbb{Z}^{B-3}$. Embedding of L to $\mathcal{G}'_\Delta$ actually comes from consideration of the action of $\mathcal{G}_\mathcal{Q}$ on zig-zags presented in the next section, and results in the image $\mathbb{Z}^{B-3}$. However, the factor is $\mathcal{G}'_\Delta/L = \mathbb{Z}/\mathrm{lcm}(N,M)\mathbb{Z} \oplus \mathbb{Z}/N\mathbb{Z} \oplus \mathbb{Z}/M\mathbb{Z}$. The non-trivial index appears due to the functions on the corners of Newton polygon. It can be also seen that the image of generator $(\rho)^{\mathrm{lcm}(N,M)}$ coincides with the image of generator τ from [55].

2.4.2 Monomial dynamics of Casimirs

According to [71] the lattice of Casimir functions x_γ is generated by zig-zag paths[14]

$$\mathsf{Z} = \{\gamma \in \mathrm{H}_1(\Gamma, \mathbb{Z}) \mid \varepsilon(\gamma, \cdot) = 0\}. \tag{2.114}$$

As the skew-symmetric form ε is intersection form on dual surface, this condition is equivalent to being trivial in dual surface $\hat{S}$ homologies. In order to be expressed in terms of cluster variables $\{x_{ij}^\times, x_{ij}^+\}$ Casimir should be also trivial in torus homologies, i.e. we are interested in subset

$$\mathsf{C} = \{\gamma \in \mathrm{H}_1(\Gamma, \mathbb{Z}) \mid [\gamma] = 0 \in \mathrm{H}_1(\hat{S}, \mathbb{Z}), \quad [\gamma] = 0 \in \mathrm{H}_1(\mathbb{T}^2, \mathbb{Z})\}. \tag{2.115}$$

As zig-zags and faces are drawn on torus $\mathsf{Z}, \mathsf{F} \subset \mathrm{H}_1(\Gamma, \mathbb{Z})$, they are constrained by $\prod_i x_{\zeta_i} = 1$, where the product goes over all zig-zag paths and $\prod_i x_{f_i} = 1$, where the product goes over all faces of bipartite graph on torus. To obtain non-trivial q-dynamic these constraints have to be relaxed to $\prod_i x_{f_i} = q \neq 1$ so that x_γ now is an element of extension $\mathrm{H}_1(\tilde{\Gamma}, \mathbb{Z}) = \mathrm{H}_1(\Gamma, \mathbb{Z}) \oplus \mathbb{Q}^2_{\langle\omega,\hat{\omega}\rangle}$ with the relations $\sum_i f_i = \omega$, $\sum_i \zeta_i = \hat{\omega}$. In multiplicative notations this reads

$$\prod_i x_{f_i} = q, \ \prod_i x_{\zeta_i} = \hat{q} \tag{2.116}$$

where we have additionally defined $q = x_\omega$, $\hat{q} = x_{\hat{\omega}}$. Introduction of $q \neq 1$ can be considered by lifting of bipartite graph to universal cover of $\mathbb{T}^2$ which is $\mathbb{R}^2$.

[14] For details on definitions see Section 1.4.

Any variable x_γ, $\gamma \in \mathsf{C}$ can be expressed via face variables x_{f_i}, which are cluster variables, and can be mutated by usual rules (1.82). However, there is no generic rule for mutation of variable associated with a single zig-zag, except for mutation in four-valent vertex identified with a 'spider move' [71]. We propose here the generic rule for transformation of zig-zags [15] under the action of generators (2.94), namely, for the $N \times M$ rectangle:

$$\begin{aligned}
\mathrm{s}_{\alpha_i,\alpha_{i+1}}: &\quad \alpha_i \mapsto q^{\frac{1}{N}}\alpha_{i+1}, \qquad \alpha_{i+1} \mapsto q^{-\frac{1}{N}}\alpha_i,\\
\mathrm{s}_{\beta_i,\beta_{i+1}}: &\quad \beta_i \mapsto q^{-\frac{1}{N}}\beta_{i+1}, \quad \beta_{i+1} \mapsto q^{\frac{1}{N}}\beta_i,\\
\mathrm{s}_{\gamma_a,\gamma_{a+1}}: &\quad \gamma_a \mapsto q^{\frac{1}{M}}\gamma_{a+1}, \qquad \gamma_{a+1} \mapsto q^{-\frac{1}{M}}\gamma_a,\\
\mathrm{s}_{\delta_a,\delta_{a+1}}: &\quad \delta_a \mapsto q^{-\frac{1}{M}}\delta_{a+1}, \quad \delta_{a+1} \mapsto q^{\frac{1}{M}}\delta_a,
\end{aligned} \tag{2.117}$$

where $i = 1, \dots, N$, $a = 1, \dots, M$. The group $\mathcal{G}_\mathcal{Q}$ acts on the elements of C, embedded in multiplicative lattice generated by zig-zags, precisely as Coxeter groups of A_{K-1}-type act on the root lattices embedded into $\mathbb{Z}^K$ (c.f. [153, 95]).

These rules basically come just from consistency with mutation transformations for the elements of C. There is a two-parametric family of transformations for zig-zag variables

$$\zeta \mapsto \zeta a^{[\zeta]_A} b^{[\zeta]_B}, \text{ if } [\zeta] = ([\zeta]_\mathrm{A}, [\zeta]_\mathrm{B}) - \text{class of } \zeta \text{ in } \mathrm{H}_1(\mathbb{T}^2, \mathbb{Z}) \tag{2.118}$$

which do not affect C, since C consists of the combinations of zig-zags with zero class in torus homology. This ambiguity is fixed using the 'locality assumption' that zig-zags not adjacent to the transformed faces are not changed.

Let us now demonstrate, how formulas (2.117) come for $(N, M) = (3, 2)$ from consistency with transformations of C, where one can introduce the following over-determined set of generators

$$\begin{aligned}
&Z_{\beta_1,\alpha_1} = x^\times_{11}x^\times_{12}, && Z_{\beta_2,\alpha_2} = x^\times_{21}x^\times_{22}, && Z_{\beta_3,\alpha_3} = x^\times_{31}x^\times_{32},\\
&Z_{\alpha_1,\beta_2} = (x^+_{11}x^+_{12})^{-1}, && Z_{\alpha_2,\beta_3} = (x^+_{21}x^+_{22})^{-1}, && Z_{\alpha_3,\beta_1} = (x^+_{31}x^+_{32})^{-1}
\end{aligned} \tag{2.119}$$

[15] We abuse notations, denoting $x_\zeta = \zeta$ for zig-zags.

$$\begin{aligned} Z_{\gamma_1,\delta_1} &= (x^{\times}_{11}x^{\times}_{21}x^{\times}_{31})^{-1}, \quad Z_{\delta_1,\gamma_2} = x^{+}_{12}x^{+}_{22}x^{+}_{32}, \\ Z_{\gamma_2,\delta_2} &= (x^{\times}_{12}x^{\times}_{22}x^{\times}_{32})^{-1}, \quad Z_{\delta_2,\gamma_1} = x^{+}_{11}x^{+}_{21}x^{+}_{31} \end{aligned} \tag{2.120}$$

satisfying

$$\begin{aligned} &Z_{\beta_1,\alpha_1}Z_{\beta_2,\alpha_2}Z_{\beta_3,\alpha_3}Z_{\gamma_1,\delta_1}Z_{\gamma_2,\delta_2} = 1 \\ &Z_{\alpha_1,\beta_2}Z_{\alpha_2,\beta_3}Z_{\alpha_3,\beta_1}Z_{\delta_1,\gamma_2}Z_{\delta_2,\gamma_1} = 1 \\ &Z_{\beta_1,\alpha_1}Z_{\beta_2,\alpha_2}Z_{\beta_3,\alpha_3}(Z_{\alpha_1,\beta_2}Z_{\alpha_2,\beta_3}Z_{\alpha_3,\beta_1})^{-1} = q = 1. \end{aligned} \tag{2.121}$$

so that the number of independent Casimirs is seven. In the autonomous limit, these Casimirs reduce to $Z_{\zeta,\zeta'} = \zeta \cdot \zeta'$, where ζ, ζ' correspond to zig-zags $\{\alpha, \beta, \gamma, \delta\}$, expressed via the edge variables. The transformation, for example, $\mathrm{s}_{\beta_1,\beta_2}$ acts by

$$\begin{aligned} \mathrm{s}_{\beta_1,\beta_2}: \quad & Z_{\beta_1,\alpha_1} \mapsto Z_{\alpha_1,\beta_2}, \quad Z_{\beta_2,\alpha_2} \mapsto \frac{Z_{\beta_2,\alpha_2}Z_{\beta_1,\alpha_1}}{Z_{\alpha_1,\beta_2}}, \quad Z_{\beta_3,\alpha_3} \mapsto Z_{\beta_3,\alpha_3}, \\ & Z_{\alpha_1,\beta_2} \mapsto Z_{\beta_1,\alpha_1}, \quad Z_{\alpha_2,\beta_3} \mapsto Z_{\alpha_2,\beta_3}, \quad Z_{\alpha_3,\beta_1} \mapsto \frac{Z_{\alpha_3,\beta_1}Z_{\alpha_1,\beta_2}}{Z_{\beta_1,\alpha_1}}. \end{aligned} \tag{2.122}$$

and substituting here $Z_{\zeta,\zeta'} = \zeta \cdot \zeta'$ one finds that the action of $\mathrm{s}_{\beta_1,\beta_2}$ reduces just to permutation of β_1 and β_2, the same is true for the other generators $\mathrm{s}_{\zeta_1,\zeta_2}$.

For $q \neq 1$ consider the generators $\mathrm{T}_{\beta_i,\beta_{i+1}}$ (2.112) which act trivially on C at all in the autonomous limit. One gets now

$$\begin{aligned} \mathrm{T}_{\beta_1,\beta_2}: \quad & Z_{\beta_1,\alpha_1} \mapsto q^{-1}Z_{\beta_1,\alpha_1}, \quad Z_{\beta_2,\alpha_2} \mapsto qZ_{\beta_2,\alpha_2} \\ & Z_{\alpha_1,\beta_2} \mapsto qZ_{\alpha_1,\beta_2}, \quad Z_{\alpha_3,\beta_1} \mapsto q^{-1}Z_{\alpha_3,\beta_1} \end{aligned} \tag{2.123}$$

where $q = \prod_{i,j} x^{\times}_{ij}x^{+}_{ij}$. Again, after expressing the Casimirs via zig-zags, the action of $\mathrm{T}_{\beta_1,\beta_2}$ is equivalent to $\beta_1 \mapsto q^{-1}\beta_1,\ \beta_2 \mapsto q\beta_2$. These formulas suggest that at $q \neq 1$ one can express generators of C via zig-zags and q by [16]

$$\begin{aligned} Z_{\beta_1,\alpha_1} &= q^{\frac{1}{6}}\beta_1\alpha_1, \quad Z_{\beta_2,\alpha_2} = q^{\frac{1}{6}}\beta_2\alpha_2, \quad Z_{\beta_3,\alpha_3} = q^{\frac{1}{6}}\beta_3\alpha_3, \\ Z_{\alpha_1,\beta_2} &= q^{-\frac{1}{6}}\alpha_1\beta_2, \quad Z_{\alpha_2,\beta_3} = q^{-\frac{1}{6}}\alpha_2\beta_3, \quad Z_{\alpha_3,\beta_1} = q^{-\frac{1}{6}}\alpha_3\beta_1 \end{aligned} \tag{2.124}$$

[16] The fractional powers of q in these formulas can be restored using the 'magnetic flux' interpretation for $q \neq 1$ in non-autonomous case. This interpretation is also consistent with the fact that zig-zags with the different orientations collect fluxes of different signs.

$$Z_{\gamma_1,\delta_1} = q^{-\frac{1}{4}}\gamma_1\delta_1, \quad Z_{\delta_1,\gamma_2} = q^{\frac{1}{4}}\delta_1\gamma_2, \quad Z_{\gamma_2,\delta_2} = q^{-\frac{1}{4}}\gamma_2\delta_2, \quad Z_{\delta_2,\gamma_1} = q^{\frac{1}{4}}\delta_2\gamma_1 \tag{2.125}$$

which are consistent with constraints (2.121) with $q \neq 1$ if one assumed[17] $\alpha_1\alpha_2\alpha_3\beta_1\beta_2\beta_3\gamma_1\gamma_2\delta_1\delta_2 = \hat{q} = 1$. Comparison of transformation (2.122) with (2.124) and (2.125) leads to the formulas (2.117) for $(N, M) = (3, 2)$. The action of remaining generators is defined by

$$\begin{array}{lllll} \Lambda_h: & \alpha_i \mapsto \alpha_i, & \beta_i \mapsto \beta_i, & \gamma_a \to \gamma_{a+1}, & \delta_a \mapsto \delta_{a+1}, \\ \Lambda_v: & \alpha_i \mapsto \alpha_{i+1}, & \beta_i \to \beta_{i+1}, & \gamma_a \mapsto \gamma_a, & \delta_a \mapsto \delta_a, \\ \rho: & \alpha_i \mapsto q^{-\frac{1}{N}}\alpha_{i-1}, & \beta_i \mapsto \beta_i, & \gamma_a \to q^{\frac{1}{M}}\gamma_{a+1}, & \delta_a \mapsto \delta_a. \end{array} \tag{2.128}$$

Remark 2.4.1. Specialities of $N = 2$ or $M = 2$ case.
It is well known (see e.g. [62], eq.(3.70)) that spectral curves with a Newton polygon being $2 \times N$ rectangle can be mapped to the 'triangle ones' with the catheti of lengths 2 and $2N$ (see Fig. 2.10) just by change of variables. Namely, equation

$$S(\lambda, \mu) = P_N^+(\mu)\lambda^2 + P_N(\mu)\lambda + P_N^-(\mu) = 0 \tag{2.129}$$

under $\lambda \mapsto P_N^-(\mu) \cdot \lambda^{-1}$ than $S(\lambda, \mu) \mapsto \lambda^2 P_N^-(\mu)^{-1} S(\lambda, \mu)$ turns into

$$S(\lambda, \mu) = \lambda^2 + P_N(\mu)\lambda + P_N^+(\mu)P_N^-(\mu) = 0. \tag{2.130}$$

For a corresponding cluster integrable system the Poisson quiver from Fig. 2.5 can be transformed into the form drawn at Fig. 2.11 – more common for 'triangular' polygons [18], studied in detail in [153]. This corre-

[17] One can incorporate $\hat{q} \neq 1$ consistently modifying formulas (2.119) and (2.120) by

$$\begin{gathered} Z_{\beta_1,\alpha_1} = \hat{q}^{\frac{1}{5}} x_{11}^{\times} x_{12}^{\times}, \quad Z_{\beta_2,\alpha_2} = \hat{q}^{\frac{1}{5}} x_{21}^{\times} x_{22}^{\times}, \quad Z_{\beta_3,\alpha_3} = \hat{q}^{\frac{1}{5}} x_{31}^{\times} x_{32}^{\times}, \\ Z_{\alpha_1,\beta_2} = \hat{q}^{\frac{1}{5}} (x_{11}^{+} x_{12}^{+})^{-1}, \quad Z_{\alpha_2,\beta_3} = \hat{q}^{\frac{1}{5}} (x_{21}^{+} x_{22}^{+})^{-1}, \quad Z_{\alpha_3,\beta_1} = \hat{q}^{\frac{1}{5}} (x_{31}^{+} x_{32}^{+})^{-1} \end{gathered} \tag{2.126}$$

$$\begin{gathered} Z_{\gamma_1,\delta_1} = \hat{q}^{\frac{1}{5}} (x_{11}^{\times} x_{21}^{\times} x_{31}^{\times})^{-1}, \quad Z_{\delta_1,\gamma_2} = \hat{q}^{\frac{1}{5}} x_{12}^{+} x_{22}^{+} x_{32}^{+}, \\ Z_{\gamma_2,\delta_2} = \hat{q}^{\frac{1}{5}} (x_{12}^{\times} x_{22}^{\times} x_{32}^{\times})^{-1}, \quad Z_{\delta_2,\gamma_1} = \hat{q}^{\frac{1}{5}} x_{11}^{+} x_{21}^{+} x_{31}^{+} \end{gathered} \tag{2.127}$$

However, as a meaning of this extension is not clear, we will assume $\hat{q} = 1$ in the following.

[18] For generic triangular Newton polygon each node of quiver is connected to six arrows (and corresponding dimer lattice is hexagonal). However, in $2 \times 2N$ case a partial cancelation happens: the arrows directed from $\mathbf{x}_{i1}^{\times}$ to $\mathbf{x}_{i2}^{\times}$ annihilate the arrows from $\mathbf{x}_{i2}^{\times}$ to $\mathbf{x}_{i1}^{\times}$, and the same happens with $\mathbf{x}_{i1}^{+}$ and $\mathbf{x}_{i2}^{+}$, so only four arrows at each node remain.

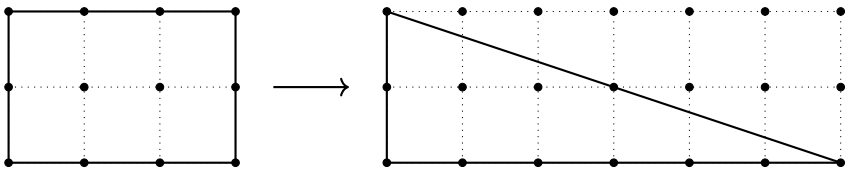

Figure 2.10. Transformation from rectangle to triangle for $(3,2)$ case.

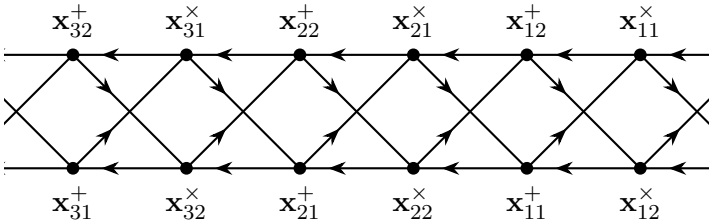

Figure 2.11. Quiver for $(3,2)$ case represented in 'triangular' form.

spondence results in the 'enhancement' of the symmetry group [19]: a pair of commuting Weyl groups $A^{(1)}_{N-1} \times A^{(1)}_{N-1}$ is now embedded into larger group $A^{(1)}_{2N-1}$ with the generators

$$\mathrm{s}_{\alpha_i\beta_{i+1}} = s^{\lambda_b,\lambda_b}_{i1,i2}\ \mu^{\lambda_b}_{i1}\mu^{\lambda_b}_{i2}, \quad \mathrm{s}_{\beta_i\alpha_i} = s^{\lambda_a,\lambda_a}_{i1,i2}\ \mu^{\lambda_a}_{i1}\mu^{\lambda_a}_{i2}, \qquad i = 1,\dots,N \quad (2.131)$$

Embedding $A^{(1)}_{N-1} \times A^{(1)}_{N-1} \to A^{(1)}_{2N-1}$ is provided by

$$\mathrm{s}_{\beta_i,\beta_{i+1}} = \mathrm{s}_{\beta_i\alpha_i}\mathrm{s}_{\alpha_i\beta_{i+1}}\mathrm{s}_{\beta_i\alpha_i}, \quad \mathrm{s}_{\alpha_i,\alpha_{i+1}} = \mathrm{s}_{\alpha_i\beta_{i+1}}\mathrm{s}_{\beta_{i+1}\alpha_{i+1}}\mathrm{s}_{\alpha_i\beta_{i+1}} \qquad (2.132)$$

and commutativity of $\mathrm{s}_{\alpha_i,\alpha_{i+1}}$ and $\mathrm{s}_{\beta_i,\beta_{i+1}}$ just follows form the relations on 'elementary' generators $\mathrm{s}_{\beta_i\alpha_i}$, $\mathrm{s}_{\alpha_i\beta_{i+1}}$. The generators of $A^{(1)}_{2N-1}$ also commute with $\mathrm{s}_{\delta_i,\delta_{i+1}}$, $\mathrm{s}_{\gamma_i,\gamma_{i+1}}$. The generator ρ is also absorbed. Now it is not a primitive one, but can be presented as a composition

$$\rho = \Lambda_h\tilde{\Lambda}_v \prod_{i=1}^{N} \mathrm{s}_{\alpha_i,\beta_{i+1}} \qquad (2.133)$$

[19] We are grateful to Y.Yamada for clarification of this point.

where we used 'root' from Λ_v

$$\tilde{\Lambda}_v : \; x^{\times}_{ia} \mapsto x^{+}_{i-1,a}, \quad x^{+}_{ia} \mapsto x^{\times}_{i,a}, \quad \text{so} \quad \Lambda_v = (\tilde{\Lambda}_v)^2 \tag{2.134}$$

so there are no extra 'dimensions' in the lattice of the flows.

The action of the enhanced group on Casimirs can be constructed in a way similar to generic case. For example, for the generator $\mathrm{s}_{\alpha_1,\beta_2}$ in $(N, M) = (3, 2)$ case from

$$\mathrm{s}_{\alpha_1,\beta_2} : \begin{array}{ll} Z_{\beta_1,\alpha_1} \mapsto \dfrac{Z_{\beta_1,\alpha_1}}{Z_{\alpha_1,\beta_2}} & Z_{\alpha_1,\beta_2} \mapsto \dfrac{1}{Z_{\alpha_1,\beta_2}}, \\ Z_{\beta_2,\alpha_2} \mapsto \dfrac{Z_{\beta_2,\alpha_2}}{Z_{\alpha_1,\beta_2}} & Z_{\gamma_1,\delta_1} \mapsto Z_{\alpha_1,\beta_2} Z_{\gamma_1,\delta_1}, \\ Z_{\delta_1,\gamma_2} \mapsto Z_{\alpha_1,\beta_2} Z_{\delta_1,\gamma_2}, & Z_{\gamma_2,\delta_2} \mapsto Z_{\alpha_1,\beta_2} Z_{\gamma_2,\delta_2}, \\ Z_{\delta_2,\gamma_1} \mapsto Z_{\alpha_1,\beta_2} Z_{\delta_2,\gamma_1} & \end{array} \tag{2.135}$$

one gets for the zig-zags

$$\mathrm{s}_{\alpha_1,\beta_2} : \quad \alpha_1 \mapsto q^{\frac{1}{6}} \beta_2^{-1}, \quad \beta_2 \mapsto q^{\frac{1}{6}} \alpha_1^{-1}, \quad \gamma_a \delta_a \mapsto q^{-\frac{1}{6}} \alpha_1 \beta_2 \gamma_a \delta_a. \tag{2.136}$$

which contains now 'inversion' of zig-zag, since α_i and β_i correspond to the opposite classes in $\mathrm{H}_1(\mathbb{T}^2, \mathbb{Z})$. Generally, for the action of $A_5^{(1)}$ on zig-zags one gets

$$\begin{array}{rl} \mathrm{s}_{\alpha_i\beta_{i+1}} : & \alpha_i \mapsto q^{\frac{1}{6}} \beta_{i+1}^{-1}, \quad \beta_{i+1} \mapsto q^{\frac{1}{6}} \alpha_i^{-1}, \quad \gamma_a \delta_a \mapsto q^{-\frac{1}{6}} \alpha_i \beta_{i+1} \gamma_a \delta_a \\ \mathrm{s}_{\beta_i\alpha_i} : & \alpha_i \mapsto q^{-\frac{1}{6}} \beta_i^{-1}, \quad \beta_i \mapsto q^{-\frac{1}{6}} \alpha_i^{-1}, \quad \gamma_a \delta_a \mapsto q^{\frac{1}{6}} \alpha_i \beta_i \gamma_a \delta_a. \end{array} \tag{2.137}$$

Remark 2.4.2. Further enhancement for $N = M = 2$ 'small square'.
The group $\mathcal{G}_{\mathcal{Q}}$ for this case can be identified with the q-Painlevé VI symmetry group $W(D_5^{(1)})$ (see e.g. [14]). It corresponds naively to the 'double' symmetry enhancement

$$A^{(1)}_{1,\alpha} \times A^{(1)}_{1,\beta} \to A^{(1)}_{3,\alpha,\beta}, \quad A^{(1)}_{1,\gamma} \times A^{(1)}_{1,\delta} \to A^{(1)}_{3,\gamma,\delta}. \tag{2.138}$$

but it turns out moreover that generators of the 'new' extended groups do not commute. For example the generators $\mathrm{s}_{\alpha_1\beta_2}$ and $\mathrm{s}_{\delta_1\gamma_2}$ satisfy

$$(\mathrm{s}_{\alpha_1,\beta_2} \mathrm{s}_{\gamma_1,\delta_1})^3 = 1 \tag{2.139}$$

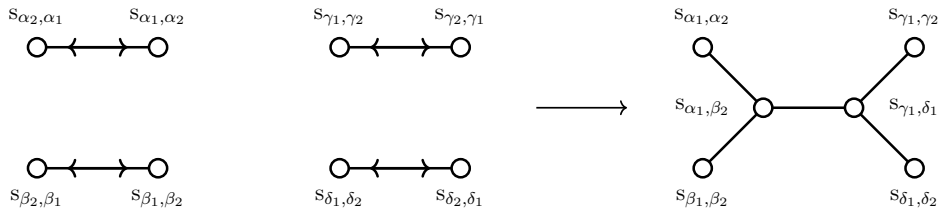

Figure 2.12. Symmetry enhancement from $W\left(A_1^{(1)} \times A_1^{(1)} \times A_1^{(1)} \times A_1^{(1)}\right)$ to $W(D_5^{(1)})$.

and this non-commutativity results in gluing of Dynkin quivers as shown on Fig. 2.12.

Another cluster realization of $W\left(D_5^{(1)}\right)$ has been proposed in [14], given by generators

$$\begin{array}{lll} \mathrm{s}_0 = s_{11,22}^{\lambda_b,\lambda_b}, & \mathrm{s}_1 = s_{12,21}^{\lambda_b,\lambda_b}, & \mathrm{s}_2 = s_{11,12}^{\lambda_b,\lambda_b}\mu_{11}^{\lambda_b}\mu_{12}^{\lambda_b} \\ \mathrm{s}_5 = s_{21,12}^{\lambda_a,\lambda_a}, & \mathrm{s}_4 = s_{11,22}^{\lambda_a,\lambda_a}, & \mathrm{s}_3 = s_{11,21}^{\lambda_a,\lambda_a}\mu_{11}^{\lambda_a}\mu_{21}^{\lambda_a} \end{array} . \tag{2.140}$$

in terms of mutations of the same bipartite graph. In our notation this generators are

$$\begin{array}{lll} \mathrm{s}_0 = \mathrm{s}_{\alpha_1\beta_2}\mathrm{s}_{\delta_1\gamma_1}\mathrm{s}_{\gamma_1\gamma_2}\mathrm{s}_{\delta_1\gamma_1}\mathrm{s}_{\alpha_1\beta_2}, & \mathrm{s}_1 = \mathrm{s}_{\alpha_1\beta_2}\mathrm{s}_{\delta_1\gamma_1}\mathrm{s}_{\delta_1\delta_2}\mathrm{s}_{\delta_1\gamma_1}\mathrm{s}_{\alpha_1\beta_2}, & \mathrm{s}_2 = \mathrm{s}_{\alpha_1\beta_2} \\ \mathrm{s}_5 = \mathrm{s}_{\gamma_1\delta_1}\mathrm{s}_{\alpha_1\beta_2}\mathrm{s}_{\beta_1\beta_2}\mathrm{s}_{\alpha_1\beta_2}\mathrm{s}_{\gamma_1\delta_1}, & \mathrm{s}_4 = \mathrm{s}_{\gamma_1\delta_1}\mathrm{s}_{\alpha_1\beta_2}\mathrm{s}_{\alpha_1\alpha_2}\mathrm{s}_{\alpha_1\beta_2}\mathrm{s}_{\gamma_1\delta_1}, & \mathrm{s}_3 = \mathrm{s}_{\gamma_1\delta_1}. \end{array} \tag{2.141}$$

Two presentations can be mapped one to another by conjugation by $\mathrm{s}_{\alpha_1\beta_2}\mathrm{s}_{\gamma_1\delta_1}\mathrm{s}_{\alpha_1\beta_2}$.

2.4.3 Towards bilinear equations

Let us finally turn to the issue of bilinear equations for the cluster tau-functions or A-cluster variables. We postpone rigorous discussion of this issue for a separate publication, but demonstrate here, how Hirota bilinear equations can arise in the systems, corresponding to rectangle Newton polygons.

The simplest example of bilinear equations is provided by spider moves, or mutations in a four-valent vertex of the Poisson quiver, see also Fig. 1.5

in Appendix for the transformation of corresponding piece of a bipartite graph. Such transformation induce the only change in τ-variables, which (for all unit coefficients)

$$\tau_0 \mapsto \bar{\tau}_0 = \frac{\tau_1\tau_3 + \tau_2\tau_4}{\tau_0} \quad \text{or} \quad \tau_0\bar{\tau}_0 = \tau_1\tau_3 + \tau_2\tau_4. \tag{2.142}$$

obviously leads to bilinear equation. However, there is no *a priori* reason to get bilinear equations from generic action by an element of $\mathcal{G}_{\mathcal{Q}}$. For example, a single mutation in a six-valent vertex rather leads to relation, which symbolically has form

$$\tau\bar{\tau} = \tau^3 + \tau^3 \tag{2.143}$$

instead of bilinear. Sometimes one can get nevertheless a bilinear relation for a sequence of mutations without no *a priori* reason for them to hold, see e.g. Section. 2.8 of [15]. We are going to show in this section that the same happens for the transformations, induced by the zig-zag permutations (e.g. $\{\mathrm{s}_{\beta_i,\beta_{i+1}}\}$ or $\{\mathrm{s}_{\gamma_a,\gamma_{a+1}}\}$), constructing their explicit action on tau-variables.

For A-cluster algebras[20] the role of Casimir functions is played by 'coefficients' [59], taking values in some tropical semi-field $\mathbb{P}$, see also discussion in [15]. For the case of rectangle Newton polygons we label the generators of $\mathbb{P}$ by zig-zags (together with q), i.e.

$$\mathbb{P} = \mathrm{Trop}(q, \{\mathbf{u}_{\alpha_i}, \mathbf{u}_{\beta_i}\}_{i=1,\ldots,N}, \{\mathbf{u}_{\gamma_a}, \mathbf{u}_{\delta_a}\}_{i=1,\ldots,M}). \tag{2.144}$$

so that the coefficients are expressed by

$$\mathbf{y}^{\times}_{ia} = q^{\frac{1}{NM}} \frac{(\mathbf{u}_{\alpha_i}\mathbf{u}_{\beta_i})^{\frac{1}{M}}}{(\mathbf{u}_{\gamma_a}\mathbf{u}_{\delta_a})^{\frac{1}{N}}}, \quad \mathbf{y}^{+}_{ia} = q^{\frac{1}{NM}} \frac{(\mathbf{u}_{\gamma_a}\mathbf{u}_{\delta_{a-1}})^{\frac{1}{N}}}{(\mathbf{u}_{\alpha_i}\mathbf{u}_{\beta_{i+1}})^{\frac{1}{M}}}. \tag{2.145}$$

The action of transformations $\mathrm{s}_{\zeta_i,\zeta_{i+1}}$ on coefficients in this basis is equivalent to the action on generators of $\mathbb{P}$ like in (2.117) on zig-zags, i.e.

$$\begin{aligned}
\mathrm{s}_{\alpha_i,\alpha_{i+1}}: &\quad \mathbf{u}_{\alpha_i} \mapsto q^{\frac{1}{N}}\mathbf{u}_{\alpha_{i+1}}, \quad \mathbf{u}_{\alpha_{i+1}} \mapsto q^{-\frac{1}{N}}\mathbf{u}_{\alpha_i},\\
\mathrm{s}_{\beta_i,\beta_{i+1}}: &\quad \mathbf{u}_{\beta_i} \mapsto q^{-\frac{1}{N}}\mathbf{u}_{\beta_{i+1}}, \quad \mathbf{u}_{\beta_{i+1}} \mapsto q^{\frac{1}{N}}\mathbf{u}_{\beta_i},\\
\mathrm{s}_{\gamma_a,\gamma_{a+1}}: &\quad \mathbf{u}_{\gamma_a} \mapsto q^{\frac{1}{M}}\mathbf{u}_{\gamma_{a+1}}, \quad \mathbf{u}_{\gamma_{a+1}} \mapsto q^{-\frac{1}{M}}\mathbf{u}_{\gamma_a},\\
\mathrm{s}_{\delta_a,\delta_{a+1}}: &\quad \mathbf{u}_{\delta_a} \mapsto q^{-\frac{1}{M}}\mathbf{u}_{\delta_{a+1}}, \quad \mathbf{u}_{\delta_{a+1}} \mapsto q^{\frac{1}{M}}\mathbf{u}_{\delta_a}.
\end{aligned} \tag{2.146}$$

[20] For the definition of A-cluster algebra with coefficients and transition from $\mathcal{X}$ to A-cluster algebra see Section 1.4.3.

Coefficients could be encoded by 'frozen' vertices of quiver. This suggests principle that we assign frozen variables to faces of dual surface, corresponding to zig-zag variables, while mutable variables - to faces of original torus.

Let us now present an example of the action of the generator $\mathrm{s}_{\beta_1,\beta_2}$ on τ-variables in $(N,M)=(3,2)$ case. An explicit computation gives

$$\begin{pmatrix} \frac{\bar\tau^+_{11}}{\tau^+_{11}} \\ \frac{\bar\tau^\times_{11}}{\tau^\times_{11}} \\ \frac{\bar\tau^+_{12}}{\tau^+_{12}} \\ \frac{\bar\tau^\times_{12}}{\tau^\times_{12}} \end{pmatrix} = \begin{pmatrix} \mathbf{u}_{\beta_2}^{\frac12} & q^{\frac{1}{12}}(\mathbf{u}_{\beta_1}\mathbf{u}_{\beta_2})^{\frac12} & q^{\frac{2}{12}}\mathbf{u}_{\beta_1}^{\frac12} & q^{\frac{3}{12}}\mathbf{u}_{\beta_1} \\ q^{\frac{3}{12}}\mathbf{u}_{\beta_1}^{\frac12} & \mathbf{u}_{\beta_2} & q^{\frac{1}{12}}\mathbf{u}_{\beta_2}^{\frac12} & q^{\frac{2}{12}}(\mathbf{u}_{\beta_1}\mathbf{u}_{\beta_2})^{\frac12} \\ q^{\frac{2}{12}}\mathbf{u}_{\beta_1}^{\frac12} & q^{\frac{3}{12}}\mathbf{u}_{\beta_1} & \mathbf{u}_{\beta_2}^{\frac12} & q^{\frac{1}{12}}(\mathbf{u}_{\beta_1}\mathbf{u}_{\beta_2})^{\frac12} \\ q^{\frac{1}{12}}\mathbf{u}_{\beta_2}^{\frac12} & q^{\frac{2}{12}}(\mathbf{u}_{\beta_1}\mathbf{u}_{\beta_2})^{\frac12} & q^{\frac{3}{12}}\mathbf{u}_{\beta_1}^{\frac12} & \mathbf{u}_{\beta_2} \end{pmatrix} \cdot C \cdot \begin{pmatrix} \frac{\tau^+_{31}\tau^\times_{21}}{\tau^+_{11}\tau^\times_{11}} \\ \frac{\tau^+_{32}\tau^\times_{21}}{\tau^+_{12}\tau^\times_{11}} \\ \frac{\tau^+_{32}\tau^\times_{22}}{\tau^+_{12}\tau^\times_{12}} \\ \frac{\tau^+_{31}\tau^\times_{22}}{\tau^+_{11}\tau^\times_{12}} \end{pmatrix} \tag{2.147}$$

where $C=\mathrm{diag}\left((\mathbf{u}_{\gamma_1}\mathbf{u}_\delta)^{\frac13},\mathbf{u}_{\alpha_1}^{\frac12}(\mathbf{u}_\delta/\mathbf{u}_{\delta_1})^{\frac13},(\mathbf{u}_{\gamma_2}\mathbf{u}_\delta)^{\frac13},\mathbf{u}_{\alpha_1}^{\frac12}(\mathbf{u}_\delta/\mathbf{u}_{\delta_2})^{\frac13}\right)$, $\mathbf{u}_\delta=\mathbf{u}_{\delta_1}\mathbf{u}_{\delta_2}$. The main point is that the matrix in the r.h.s. is nicely invertible so that these equations can be rewritten in *bilinear form*

$$\begin{cases} (\mathbf{u}_{\beta_2}-q^{\frac13}\mathbf{u}_{\beta_1})(\mathbf{u}_\delta\mathbf{u}_{\gamma_1})^{\frac13}\tau^+_{31}\tau^\times_{21}=\mathbf{u}_{\beta_2}^{\frac12}\bar\tau^+_{11}\tau^\times_{11}-q^{\frac{1}{12}}\mathbf{u}_{\beta_1}^{\frac12}\bar\tau^\times_{11}\tau^+_{11} \\ (\mathbf{u}_{\beta_2}-q^{\frac13}\mathbf{u}_{\beta_1})(\mathbf{u}_\delta/\mathbf{u}_{\delta_1})^{\frac13}\tau^+_{32}\tau^\times_{21}=\mathbf{u}_{\alpha_1}^{-\frac12}\bar\tau^\times_{11}\tau^+_{12}-q^{\frac{1}{12}}\mathbf{u}_{\alpha_1}^{-\frac12}\bar\tau^+_{12}\tau^\times_{11} \\ (\mathbf{u}_{\beta_2}-q^{\frac13}\mathbf{u}_{\beta_1})(\mathbf{u}_\delta\mathbf{u}_{\gamma_2})^{\frac13}\tau^+_{32}\tau^\times_{22}=\mathbf{u}_{\beta_2}^{\frac12}\bar\tau^+_{12}\tau^\times_{12}-q^{\frac{1}{12}}\mathbf{u}_{\beta_1}^{\frac12}\bar\tau^\times_{12}\tau^+_{12} \\ (\mathbf{u}_{\beta_2}-q^{\frac13}\mathbf{u}_{\beta_1})(\mathbf{u}_\delta/\mathbf{u}_{\delta_2})^{\frac13}\tau^+_{31}\tau^\times_{22}=\mathbf{u}_{\alpha_1}^{-\frac12}\bar\tau^\times_{12}\tau^+_{11}-q^{\frac{1}{12}}\mathbf{u}_{\alpha_1}^{-\frac12}\bar\tau^+_{11}\tau^\times_{12} \end{cases}. \tag{2.148}$$

This is actually a generic phenomenon for the zig-zag generators: the same happens, for example, for the generator $\mathrm{s}_{\delta_1,\delta_2}$ from another component of $\mathcal{G}_\mathcal{Q}$. One gets explicitly for the transformation of A-cluster variables

$$t_1=C_1\cdot C_2\cdot t_2, \tag{2.149}$$

where

$$t_1 = \left(\frac{\bar\tau^+_{32}}{\tau^+_{32}} \quad \frac{\bar\tau^\times_{32}}{\tau^\times_{32}} \quad \frac{\bar\tau^+_{22}}{\tau^+_{22}} \quad \frac{\bar\tau^\times_{22}}{\tau^\times_{22}} \quad \frac{\bar\tau^+_{12}}{\tau^+_{12}} \quad \frac{\bar\tau^\times_{12}}{\tau^\times_{12}} \right)^T$$
$$t_2 = \left(\frac{\tau^+_{31}\tau^\times_{31}}{\tau^+_{32}\tau^\times_{32}} \quad \frac{\tau^+_{21}\tau^\times_{31}}{\tau^+_{22}\tau^\times_{32}} \quad \frac{\tau^+_{21}\tau^\times_{21}}{\tau^+_{22}\tau^\times_{22}} \quad \frac{\tau^+_{11}\tau^\times_{21}}{\tau^+_{12}\tau^\times_{22}} \quad \frac{\tau^+_{11}\tau^\times_{11}}{\tau^+_{12}\tau^\times_{12}} \quad \frac{\tau^+_{31}\tau^\times_{11}}{\tau^+_{32}\tau^\times_{12}} \right)^T \tag{2.150}$$

$$C_1 = \begin{pmatrix}
\mathbf{u}_{\delta_2} & q^{\frac{1}{12}}\mathbf{u}^{\frac{2}{3}}_{\delta_2} & q^{\frac{2}{12}}(\mathbf{u}_{\delta_1}\mathbf{u}^2_{\delta_2})^{\frac{1}{3}} & q^{\frac{3}{12}}(\mathbf{u}_{\delta_1}\mathbf{u}_{\delta_2})^{\frac{1}{3}} & q^{\frac{4}{12}}(\mathbf{u}^2_{\delta_1}\mathbf{u}_{\delta_2})^{\frac{1}{3}} & q^{\frac{5}{12}}\mathbf{u}^{\frac{2}{3}}_{\delta_1} \\
q^{\frac{5}{12}}\mathbf{u}_{\delta_1} & \mathbf{u}^{\frac{2}{3}}_{\delta_2} & q^{\frac{1}{12}}(\mathbf{u}_{\delta_1}\mathbf{u}^2_{\delta_2})^{\frac{1}{3}} & q^{\frac{2}{12}}(\mathbf{u}_{\delta_1}\mathbf{u}_{\delta_2})^{\frac{1}{3}} & q^{\frac{3}{12}}(\mathbf{u}^2_{\delta_1}\mathbf{u}_{\delta_2})^{\frac{1}{3}} & q^{\frac{4}{12}}\mathbf{u}^{\frac{2}{3}}_{\delta_1} \\
q^{\frac{4}{12}}(\mathbf{u}^2_{\delta_1}\mathbf{u}_{\delta_2})^{\frac{1}{3}} & q^{\frac{5}{12}}\mathbf{u}^{\frac{2}{3}}_{\delta_1} & \mathbf{u}_{\delta_2} & q^{\frac{1}{12}}\mathbf{u}^{\frac{2}{3}}_{\delta_2} & q^{\frac{2}{12}}(\mathbf{u}_{\delta_1}\mathbf{u}^2_{\delta_2})^{\frac{1}{3}} & q^{\frac{3}{12}}(\mathbf{u}_{\delta_1}\mathbf{u}^2_{\delta_2})^{\frac{1}{3}} \\
q^{\frac{3}{12}}(\mathbf{u}^2_{\delta_1}\mathbf{u}_{\delta_2})^{\frac{1}{3}} & q^{\frac{4}{12}}\mathbf{u}^{\frac{2}{3}}_{\delta_1} & q^{\frac{5}{12}}\mathbf{u}_{\delta_1} & \mathbf{u}^{\frac{2}{3}}_{\delta_2} & q^{\frac{1}{12}}(\mathbf{u}_{\delta_1}\mathbf{u}^2_{\delta_2})^{\frac{1}{3}} & q^{\frac{2}{12}}(\mathbf{u}_{\delta_1}\mathbf{u}_{\delta_2})^{\frac{1}{3}} \\
q^{\frac{2}{12}}(\mathbf{u}_{\delta_1}\mathbf{u}^2_{\delta_2})^{\frac{1}{3}} & q^{\frac{3}{12}}(\mathbf{u}_{\delta_1}\mathbf{u}_{\delta_2})^{\frac{1}{3}} & q^{\frac{4}{12}}(\mathbf{u}^2_{\delta_1}\mathbf{u}_{\delta_2})^{\frac{1}{3}} & q^{\frac{5}{12}}\mathbf{u}^{\frac{2}{3}}_{\delta_1} & \mathbf{u}_{\delta_2} & q^{\frac{1}{12}}\mathbf{u}^{\frac{2}{3}}_{\delta_2} \\
q^{\frac{1}{12}}(\mathbf{u}_{\delta_1}\mathbf{u}^2_{\delta_2})^{\frac{1}{3}} & q^{\frac{2}{12}}(\mathbf{u}_{\delta_1}\mathbf{u}_{\delta_2})^{\frac{1}{3}} & q^{\frac{3}{12}}(\mathbf{u}^2_{\delta_1}\mathbf{u}_{\delta_2})^{\frac{1}{3}} & q^{\frac{4}{12}}\mathbf{u}^{\frac{2}{3}}_{\delta_1} & q^{\frac{5}{12}}\mathbf{u}_{\delta_1} & \mathbf{u}^{\frac{2}{3}}_{\delta_2}
\end{pmatrix} \tag{2.151}$$

$$C_2 = \operatorname{diag}\left((\mathbf{u}_\alpha/\mathbf{u}_{\alpha_3})^{\frac{1}{2}}\mathbf{u}^{\frac{1}{3}}_{\gamma_2}, (\mathbf{u}_\alpha\mathbf{u}_{\beta_3})^{\frac{1}{2}}, (\mathbf{u}_\alpha/\mathbf{u}_{\alpha_2})^{\frac{1}{2}}\mathbf{u}^{\frac{1}{3}}_{\gamma_2}, (\mathbf{u}_\alpha\mathbf{u}_{\beta_2})^{\frac{1}{2}}, (\mathbf{u}_\alpha/\mathbf{u}_{\alpha_1})^{\frac{1}{2}}\mathbf{u}^{\frac{1}{3}}_{\gamma_2}, (\mathbf{u}_\alpha\mathbf{u}_{\beta_1})^{\frac{1}{2}} \right) \tag{2.152}$$

with $\mathbf{u}_\alpha = \mathbf{u}_{\alpha_1}\mathbf{u}_{\alpha_2}\mathbf{u}_{\alpha_3}$. Again, inverting matrix C_1 we end up with the set of bilinear equations

$$\begin{cases}
(\mathbf{u}_{\delta_2} - q^{\frac{1}{2}}\mathbf{u}_{\delta_1})(\mathbf{u}_\alpha/\mathbf{u}_{\alpha_3})^{\frac{1}{2}}\tau^+_{31}\tau^\times_{31} = \mathbf{u}^{-\frac{1}{3}}_{\gamma_2}\bar\tau^+_{32}\tau^\times_{32} - q^{\frac{1}{12}}\mathbf{u}^{-\frac{1}{3}}_{\gamma_2}\bar\tau^\times_{32}\tau^+_{32} \\
(\mathbf{u}_{\delta_2} - q^{\frac{1}{2}}\mathbf{u}_{\delta_1})(\mathbf{u}_\alpha\mathbf{u}_{\beta_3})^{\frac{1}{2}}\tau^+_{21}\tau^\times_{31} = \mathbf{u}^{\frac{1}{3}}_{\delta_2}\bar\tau^\times_{32}\tau^+_{22} - q^{\frac{1}{12}}\mathbf{u}^{\frac{1}{3}}_{\delta_1}\bar\tau^+_{22}\tau^\times_{32} \\
(\mathbf{u}_{\delta_2} - q^{\frac{1}{2}}\mathbf{u}_{\delta_1})(\mathbf{u}_\alpha/\mathbf{u}_{\alpha_2})^{\frac{1}{2}}\tau^+_{21}\tau^\times_{21} = \mathbf{u}^{-\frac{1}{3}}_{\gamma_2}\bar\tau^+_{22}\tau^\times_{22} - q^{\frac{1}{12}}\mathbf{u}^{-\frac{1}{3}}_{\gamma_2}\bar\tau^\times_{22}\tau^+_{22} \\
(\mathbf{u}_{\delta_2} - q^{\frac{1}{2}}\mathbf{u}_{\delta_1})(\mathbf{u}_\alpha\mathbf{u}_{\beta_2})^{\frac{1}{2}}\tau^+_{11}\tau^\times_{21} = \mathbf{u}^{\frac{1}{3}}_{\delta_2}\bar\tau^\times_{22}\tau^+_{12} - q^{\frac{1}{12}}\mathbf{u}^{\frac{1}{3}}_{\delta_1}\bar\tau^+_{12}\tau^\times_{22} \\
(\mathbf{u}_{\delta_2} - q^{\frac{1}{2}}\mathbf{u}_{\delta_1})(\mathbf{u}_\alpha/\mathbf{u}_{\alpha_1})^{\frac{1}{2}}\tau^+_{11}\tau^\times_{11} = \mathbf{u}^{-\frac{1}{3}}_{\gamma_2}\bar\tau^+_{12}\tau^\times_{12} - q^{\frac{1}{12}}\mathbf{u}^{-\frac{1}{3}}_{\gamma_2}\bar\tau^\times_{12}\tau^+_{12} \\
(\mathbf{u}_{\delta_2} - q^{\frac{1}{2}}\mathbf{u}_{\delta_1})(\mathbf{u}_\alpha\mathbf{u}_{\beta_1})^{\frac{1}{2}}\tau^+_{31}\tau^\times_{11} = \mathbf{u}^{\frac{1}{3}}_{\delta_2}\bar\tau^\times_{12}\tau^+_{32} - q^{\frac{1}{12}}\mathbf{u}^{\frac{1}{3}}_{\delta_1}\bar\tau^+_{32}\tau^\times_{12}
\end{cases} \tag{2.153}$$

It remains yet unclear, how to derive bilinear equations systematically for compositions of elements of $\mathcal{G}_\mathcal{Q}$. We are going to return to this issue together with discussion of their solutions elsewhere.

2.5 Conclusion

In this chapter we have presented extra evidence that cluster integrable systems provide convenient framework for the description of 5d supersymmetric Yang-Mills theory. It has been shown that cluster integrable systems with the Newton polygons $SA(2,\mathbb{Z})$-equivalent to the $N \times M$ rectangles are isomorphic to the XXZ-like spin chains of rank M on N sites (or vice versa) on the 'lowest orbit'. Due to special symmetry of the Kasteleyn operators, defining spectral curves of these systems, it turns to be possible to express the Lax operators of spin chain in terms of the X-cluster variables. Inhomogeneities and twists of the chain can be expressed via (part of) the zig-zag paths on the Goncharov-Kenyon bipartite graphs.

Rectangle Newton polygons generally correspond to linear quiver gauge theories [21] so that inhomogeneities, 'on-site' Casimirs and twists define the fundamental and bi-fundamental masses together with the bare couplings on the Yang-Mills side. The proposed cluster description possesses obvious symmetry between the structure in horizontal and vertical directions so that one gets a natural spectral (or fiber-base or length-rank) duality, interchanging also the rank and length of spin chains. Shear shift of one side of a Newton polygon to the shape of $N \times M$ parallelogram results in the multiplication of the monodromy operator of the spin chain by the cyclic twist matrix.

We have found that the cluster mapping class group $\mathcal{G}_{\mathcal{Q}}$ for the 'spin-chain class' always contains a subgroup isomorphic to

$$\widetilde{W}\left(A^{(1)}_{N-1,\alpha} \times A^{(1)}_{N-1,\beta}\right) \times \widetilde{W}\left(A^{(1)}_{M-1,\gamma} \times A^{(1)}_{M-1,\delta}\right) \rtimes \mathbb{Z} \tag{2.154}$$

whose generators act on zig-zag paths by permutations. Moreover, their action on the A-cluster variables gives rise to the $q-$difference bilinear relations. The symmetry enhancement happens in the case $N = 2$ (or $M = 2$) and results in 'gluing' of two copies of $A^{(1)}_{N-1}$ into $A^{(1)}_{2N-1}$. If both $N = M = 2$ the symmetry $\widetilde{W}\left(A^{(1)}_1 \times A^{(1)}_1\right) \times \widetilde{W}\left(A^{(1)}_1 \times A^{(1)}_1\right) \rtimes \mathbb{Z}$ enhances to the $D^{(1)}_5$ symmetry group of q-PVI equation.

Our first results in this direction actually produce more question than give answers. The following obvious questions (at least!) can be addressed for the further investigations:

- Trivial rank-N spin chain on a single site once twisted becomes spectrally dual to relativistic Toda chain, see Section 2.3.2. Can we similarly identify the spectral duals of the twisted chains of arbitrary

lengths and twists, whose Newton polygons are generic parallelograms – or even extend this to generic four-gons? This question is also very interesting on the gauge-theory side, where by now only the hyperelliptic case of 'generalized Toda' (four boundary points and all internal points are lying on one line – pure $SU(N)$ theory with the CS term) was studied in [15].

- We have derived in Section 2.4.3 the bilinear relations, coming out of the action of a single 'permutation' generator of $\mathcal{G}_{\mathcal{Q}}$ on A-cluster variables, acting by transpositions on zig-zags. Is there any systematic principle to derive bilinear equations for compositions of such transformations?

- In [24], [14], [102], [15], [25] and [136] the solutions for q-difference bilinear equations and their degenerations, arising from certain cluster integrable systems, were found in terms of Fourier-transformed Nekrasov functions for the corresponding 5d gauge theories. As partition functions for the 5d linear quiver gauge theories are well known, a natural further step is to show that they solve the bilinear equations found here (and their hypothetical generalizations!).

2.6 Appendix. Proof of the RLL relation for cluster L-matrices

Here some details of proof of (2.51) are collected. Recall the definitions (2.52) (here and below $i, j = 1, \ldots, M$)

$$L_{ij}(\mu) = \frac{1}{\mu^{\frac{1}{2}} - \mu^{-\frac{1}{2}}} \begin{cases} i = j, & \mu^{\frac{1}{2}} z_i^{-2} + \mu^{-\frac{1}{2}} z_i^2 \\ i \neq j, & \mu^{-\frac{s_{ij}}{2}} (z_j^2 + z_j^{-2}) \dfrac{\tau_j}{\tau_i} \end{cases} , \quad \tau_i = w_i \prod_{k=1}^{M} z_k^{s_{ki}} . \tag{2.155}$$

where the variables z_i, w_i have Poisson brackets

$$\{z_i, w_j\} = \frac{1}{4} \delta_{ij} z_i w_j, \quad \{z_i, z_j\} = \{w_i, w_j\} = 0. \tag{2.156}$$

It is useful to note that

$$\{z_i, \tau_j\} = \frac{1}{4} \delta_{ij} z_i \tau_j, \quad \{\tau_i, \tau_j\} = -\frac{1}{2} s_{ij} \tau_i \tau_j. \tag{2.157}$$

In addition to the sign-factors (1.5) we also introduce [21]

$$s_{ij}^k = \begin{cases} +1, & k \in (ij) \\ -1, & k \in (ji) \\ 0, & k = i, j \end{cases} \tag{2.158}$$

which satisfies

$$s_{ij}^k = -s_{ji}^k, \quad s_{ij}^k = s_{jk}^i, \quad s_{ij}^k = s_{ij} + s_{jk} + s_{ki}. \tag{2.159}$$

From definitions (2.155)

$$z_k^2 = -\frac{L_{kk}(\lambda)\sqrt{\mu} - L_{kk}(\mu)\sqrt{\lambda}}{\sqrt{\lambda/\mu} - \sqrt{\mu/\lambda}}, \quad z_k^{-2} = \frac{L_{kk}(\lambda)/\sqrt{\mu} - L_{kk}(\mu)/\sqrt{\lambda}}{\sqrt{\lambda/\mu} - \sqrt{\mu/\lambda}} \tag{2.160}$$

$$L_{ij}(\lambda)L_{kl}(\mu) = \lambda^{-\frac{1}{2}s_{ij}+\frac{1}{2}s_{kl}}\mu^{\frac{1}{2}s_{ij}-\frac{1}{2}s_{kl}}L_{ij}(\mu)L_{kl}(\lambda), \quad i \neq j, \quad k \neq l.$$

We take an anzatz

$$\tilde{r}(a) = \sum_{k=1}^{M} f_k(a)E_{kk} \otimes E_{kk} + \sum_{m \neq n} g_{mn}(a)E_{mn} \otimes E_{nm} \tag{2.161}$$

and show that one can choose f_k and g_{mn} such that equation

$$\{L(\lambda) \otimes L(\mu)\} = [\tilde{r}(\lambda/\mu), L(\lambda) \otimes L(\mu)] \tag{2.162}$$

holds. By direct computation it can be shown that ($a \neq i \neq j \neq k \neq l$):

	$a.\ \{L(\lambda) \otimes L(\mu)\}$	$b.\ [\tilde{r}(\lambda/\mu), L(\lambda) \otimes L(\mu)]$
1. $E_{ii} \otimes E_{jj}$	0	0
2. $E_{aa} \otimes E_{ij}$	0	$g_{ai}L_{ia}(\lambda)L_{aj}(\mu) - g_{ja}L_{aj}(\lambda)L_{ia}(\mu)$
3. $E_{aa} \otimes E_{aj}$	$AL_{aa}(\lambda)L_{aj}(\mu) - B_{aj}L_{aj}(\lambda)L_{aa}(\mu)$	$f_aL_{aa}(\lambda)L_{aj}(\mu) - g_{ja}L_{aj}(\lambda)L_{aa}(\mu)$
4. $E_{aa} \otimes E_{ia}$	$-AL_{aa}(\lambda)L_{ia}(\mu) + B_{ia}L_{ia}(\lambda)L_{aa}(\mu)$	$-f_aL_{aa}(\lambda)L_{ia}(\mu) + g_{ai}L_{ia}(\lambda)L_{aa}(\mu)$
5. $E_{ij} \otimes E_{ji}$	$B_{ji}(L_{jj}(\lambda)L_{ii}(\mu) - L_{ii}(\lambda)L_{jj}(\mu))$	$g_{ij}L_{jj}(\lambda)L_{ii}(\mu) - g_{ij}L_{ii}(\lambda)L_{jj}(\mu)$
6. $E_{ij} \otimes E_{kl}$	$\frac{1}{2}(s_{ij}^k + s_{ji}^l)L_{ij}(\lambda)L_{kl}(\mu)$	$g_{ik}L_{kj}(\lambda)L_{il}(\mu) - g_{lj}L_{il}(\lambda)L_{kj}(\mu)$
7. $E_{ij} \otimes E_{ia}$	$-\frac{1}{2}s_{ij}^aL_{ij}(\lambda)L_{ia}(\mu)$	$f_iL_{ij}(\lambda)L_{ia}(\mu) - g_{aj}L_{ia}(\lambda)L_{ij}(\mu)$
8. $E_{ij} \otimes E_{aj}$	$\frac{1}{2}s_{ij}^aL_{ij}(\lambda)L_{aj}(\mu)$	$-f_jL_{ij}(\lambda)L_{aj}(\mu) + g_{ia}L_{aj}(\lambda)L_{ij}(\mu)$
9. $E_{ij} \otimes E_{ja}$	$B_{ji}L_{jj}(\lambda)L_{ia}(\mu) - B_{ja}L_{ia}(\lambda)L_{jj}(\mu)$	$g_{ij}L_{jj}(\lambda)L_{ia}(\mu) - g_{aj}L_{ia}(\lambda)L_{jj}(\mu)$
10. $E_{ij} \otimes E_{ai}$	$-B_{ji}L_{ii}(\lambda)L_{aj}(\mu) + B_{ai}L_{aj}(\lambda)L_{ii}(\mu)$	$-g_{ij}L_{ii}(\lambda)L_{aj}(\mu) + g_{ia}L_{aj}(\lambda)L_{ii}(\mu)$

(2.163)

[21] Notation $k \in (ij)$ means that we consider i, j, k on the circle $\mathbb{Z}/M\mathbb{Z}$, with k in the oriented interval from i to j.

with

$$A = A(\sqrt{\lambda/\mu}) = \frac{1}{2}\frac{\sqrt{\lambda/\mu}+\sqrt{\mu/\lambda}}{\sqrt{\lambda/\mu}-\sqrt{\mu/\lambda}}, \quad B_{ij} = B_{ij}(\sqrt{\lambda/\mu}) = \frac{(\lambda/\mu)^{\frac{1}{2}s_{ij}}}{\sqrt{\lambda/\mu}-\sqrt{\mu/\lambda}}. \tag{2.164}$$

Computations in 1,2,7,8.a) are straightforward. In 3, 4, 5.a) relation (2.160) has to be used. 9,10.a) can be obtained by application of (2.160) and (2.159):

$$\{L_{ij}(\lambda), L_{ja}(\mu)\} = \tag{2.165}$$

$$= -\frac{1}{2}\lambda^{-\frac{1}{2}s_{ij}}\mu^{-\frac{1}{2}s_{ja}}\frac{\tau_a}{\tau_i}(s^a_{ij}(z_j^2+z_j^{-2})(z_a^2+z_a^{-2}) + (z_j^2-z_j^{-2})(z_a^2+z_a^{-2})) =$$

$$= -\frac{1}{2}\lambda^{-\frac{1}{2}s_{ij}}\mu^{-\frac{1}{2}s_{ja}}(z_a^2+z_a^{-2})\frac{\tau_a}{\tau_i}((s^a_{ij}+1)z_j^2 + (s^a_{ij}-1)z_j^{-2})) =$$

$$= -s^a_{ij}\lambda^{-\frac{1}{2}s_{ij}}\mu^{-\frac{1}{2}s_{ja}}(z_a^2+z_a^{-2})\frac{\tau_a}{\tau_i}z_j^{2s^a_{ij}} =$$

$$= \frac{\lambda^{-\frac{1}{2}s_{ij}+\frac{1}{2}s_{ia}}\mu^{-\frac{1}{2}s_{ja}}}{\sqrt{\lambda/\mu}-\sqrt{\mu/\lambda}}L_{ia}(\lambda)\left[L_{jj}(\lambda)\mu^{\frac{1}{2}s^a_{ij}} - L_{jj}(\mu)\lambda^{\frac{1}{2}s^a_{ij}}\right] =$$

$$= \frac{(\lambda/\mu)^{\frac{1}{2}s_{ji}}L_{jj}(\lambda)L_{ia}(\mu) - (\lambda/\mu)^{\frac{1}{2}s_{ja}}L_{ia}(\lambda)L_{jj}(\mu)}{\sqrt{\lambda/\mu}-\sqrt{\mu/\lambda}}$$

Looking at the table (2.163) we can suggest that the last two columns are equal, if we put

$$f_i = A(\sqrt{\lambda/\mu}), \;\; g_{ij} = B_{ji}(\sqrt{\lambda/\mu}) \tag{2.166}$$

For 1-5 and 9-10 it is obvious. For 6, 7, 8 it is easier to move from the right to the left. For 6, using (2.159):

$$g_{ik}L_{kj}(\lambda)L_{il}(\mu) - g_{lj}L_{il}(\lambda)L_{kj}(\mu) = \tag{2.167}$$

$$= \frac{\lambda^{-\frac{1}{2}s_{ik}-\frac{1}{2}s_{kj}}\mu^{-\frac{1}{2}s_{ki}-\frac{1}{2}s_{il}} - \lambda^{-\frac{1}{2}s_{lj}-\frac{1}{2}s_{il}}\mu^{-\frac{1}{2}s_{jl}-\frac{1}{2}s_{kj}}}{\sqrt{\lambda/\mu}-\sqrt{\mu/\lambda}}\frac{\tau_j}{\tau_k}\frac{\tau_l}{\tau_i}(z_j^2+z_j^{-2})(z_l^2+z_l^{-2}) =$$

$$= \frac{\lambda^{-\frac{1}{2}s^j_{ik}}\mu^{-\frac{1}{2}s^l_{ki}} - \lambda^{-\frac{1}{2}s^i_{lj}}\mu^{-\frac{1}{2}s^k_{jl}}}{\sqrt{\lambda/\mu}-\sqrt{\mu/\lambda}}L_{ij}(\lambda)L_{kl}(\mu)$$

All possible relative positions of the indices i, j, k, l can be encoded in the table

$$\begin{array}{cccc|c} s^j_{ik} & s^l_{ki} & s^i_{lj} & s^k_{jl} & s^k_{ij}+s^l_{ji} \\ \hline +1 & +1 & +1 & +1 & 0 \\ +1 & -1 & +1 & -1 & 0 \\ +1 & -1 & -1 & +1 & -2 \\ -1 & +1 & -1 & +1 & 0 \\ -1 & +1 & +1 & -1 & +2 \\ -1 & -1 & -1 & -1 & 0 \end{array} \tag{2.168}$$

which shows that 6.a) and 6.b) from (2.163) are equal. For 7.b):

$$f_i L_{ij}(\lambda)L_{ia}(\mu) - g_{aj}L_{ia}(\lambda)L_{ij}(\mu) = \tag{2.169}$$

$$= \frac{1}{2}\frac{(\sqrt{\lambda/\mu}+\sqrt{\mu/\lambda})\lambda^{-\frac{1}{2}s_{ij}}\mu^{-\frac{1}{2}s_{ia}} - 2\lambda^{-\frac{1}{2}s_{aj}-\frac{1}{2}s_{ia}}\mu^{-\frac{1}{2}s_{ja}-\frac{1}{2}s_{ij}}}{\sqrt{\lambda/\mu}-\sqrt{\mu/\lambda}}\cdot$$

$$\cdot\frac{\tau_j}{\tau_i}\frac{\tau_a}{\tau_i}(z_j^2+z_j^{-2})(z_a^2+z_a^{-2}) =$$

$$= \frac{1}{2}\frac{\sqrt{\lambda/\mu}+\sqrt{\mu/\lambda}-2(\lambda/\mu)^{-\frac{1}{2}s^j_{ia}}}{\sqrt{\lambda/\mu}-\sqrt{\mu/\lambda}}L_{ij}(\lambda)L_{ia}(\mu) = -\frac{1}{2}s^a_{ij}L_{ij}(\lambda)L_{ia}(\mu)$$

which is equal to 7.a). Similarly for 8 a) and b). To show that (2.161) is equal to (1.32) multiplied by $\frac{1}{2}$, we have to note that

$$\sum_{k=1}^{M} E_{kk}\otimes E_{kk} = \mathbf{1}\otimes\mathbf{1} - \sum_{i\neq j} E_{ii}\otimes E_{jj} \tag{2.170}$$

and $\mathbf{1}\otimes\mathbf{1}$ is commuting with anything, so can be always added to the r-matrix with the arbitrary coefficient, without any change of the relations.

Chapter 3

Solution of tetrahedron equation and cluster algebras

3.1 Introduction

In the theory of integrable systems one usually starts with the RLL equation

$$R_{12}\mathcal{L}_{1,a}\mathcal{L}_{2,a} = \mathcal{L}_{2,a}\mathcal{L}_{1,a}R_{12} \tag{3.1}$$

which defines the relation between the R-matrix $R : \mathrm{V} \otimes \mathrm{V} \to \mathrm{V} \otimes \mathrm{V}$ intertwining a pair of "auxiliary spaces" V, and the Lax operator $\mathcal{L} : \mathrm{V} \otimes \mathrm{F} \to \mathrm{V} \otimes \mathrm{F}$, acting on the tensor product of the auxiliary space and the "quantum" space F of the integrable system. The RLL equation implies $[\mathrm{tr}_1\, \mathcal{L}_{1,a}, \mathrm{tr}_2\, \mathcal{L}_{2,a}] = 0$, i.e. that the integrals of motion of the system commute. The renowned Yang-Baxter equation

$$R_{12}R_{13}R_{23} = R_{23}R_{13}R_{12} \tag{3.2}$$

appears in this approach as the associativity condition for the braiding relations (3.1). This condition can be formulated as an equality between two different ways of permuting the product of three Lax operators:

$$\mathcal{L}_{3,a}\mathcal{L}_{2,a}\mathcal{L}_{1,a} = \mathcal{J}_{\pm}(\mathcal{L}_{1,a}\mathcal{L}_{2,a}\mathcal{L}_{3,a}), \tag{3.3}$$

$$\mathcal{J}_{+} = \mathrm{Ad}_{R_{12}}\mathrm{Ad}_{R_{13}}\mathrm{Ad}_{R_{23}}, \quad \mathcal{J}_{-} = \mathrm{Ad}_{R_{23}}\mathrm{Ad}_{R_{13}}\mathrm{Ad}_{R_{12}}.$$

A solution of the Yang-Baxter equation allows one to construct an integrable system, e.g. a spin chain. Equivalently, in a more abstract language one can use the solution to define a quasitriangular Hopf algebra, e.g. a quantum group.

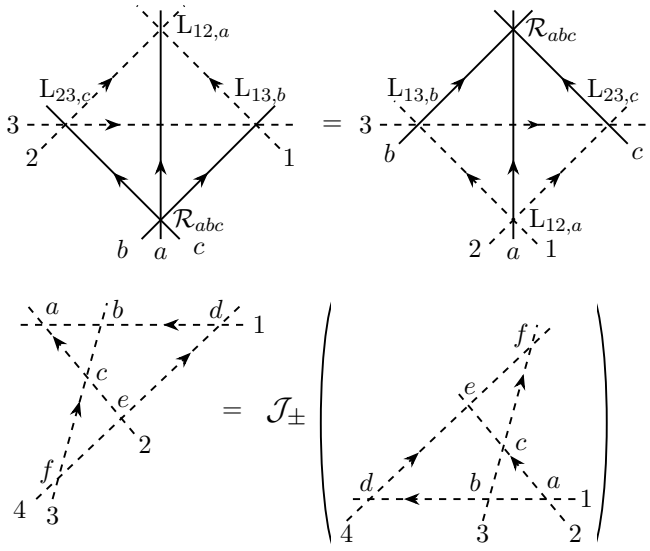

Figure 3.1. Top. The tetrahedron equation. To view it as a modification of the Yang-Baxter equation one has to look at the transformation of the dashed triangle. Bottom. The functional tetrahedron equation. The quantum spaces are located in the direction transverse to the plane of the figure.

Zamolodchikov tetrahedron equation [182, 184] is a natural generalization of the Yang-Baxter equation to three dimensions. While the Yang-Baxter equation is an equation on operators corresponding to crossings of lines in a plane, the tetrahedron equation describes triple crossings of planes in a $3d$ space. An analog of the RLL equation

$$\mathrm{L}_{12,a}\mathrm{L}_{13,b}\mathrm{L}_{23,c}\mathcal{R}_{abc} = \mathcal{R}_{abc}\mathrm{L}_{23,c}\mathrm{L}_{13,b}\mathrm{L}_{12,a}, \tag{3.4}$$

drawn in Fig. 3.1, left, involves two kinds of spaces, F and V, and two kinds of operators

$$\mathrm{L} : \mathrm{V}\otimes\mathrm{V}\otimes\mathrm{F} \to \mathrm{V}\otimes\mathrm{V}\otimes\mathrm{F}, \quad \mathcal{R} : \mathrm{F}\otimes\mathrm{F}\otimes\mathrm{F} \to \mathrm{F}\otimes\mathrm{F}\otimes\mathrm{F}. \tag{3.5}$$

The tetrahedron equation should lead to the structures which are no less profound and much more beautiful, compared to the Yang-Baxter equa-

tion. For example, in [122], the tetrahedral structure was related to higher algebra and category theory. Its interpretation as a "higher" analogue of the Yang-Baxter equation becomes clear, if one assumes invertibility of $\mathcal{R}_{abc}$ and multiplies both sides of the equation by $\mathcal{R}_{abc}^{-1}$ on the right[1]. This gives a version of Yang-Baxter equation "up to" conjugation, i.e. it is no longer an *equality* between two ways to permute the L-operators, but their *equivalence*. Considering $\mathrm{L}_{ij,x}$ as a matrix acting in $\mathrm{V}_i \otimes \mathrm{V}_j$, with coefficients in the algebra $\mathcal{A}_x = \mathrm{End}(\mathrm{F}_x)$, we can rewrite Eq. (3.4) as

$$\mathrm{L}_{12}(\{v_a\})\mathrm{L}_{13}(\{v_b\})\mathrm{L}_{23}(\{v_c\}) = \mathrm{L}_{23}(\{v'_c\})\mathrm{L}_{13}(\{v'_b\})\mathrm{L}_{12}(\{v'_a\}), \tag{3.6}$$

where by $\{v_x\}$ we denote the set of generators of $\mathcal{A}_x$,

$$\mathrm{L}_{ij,x} = \mathrm{L}_{ij}(\{v_x\}), \tag{3.7}$$

and

$$v'_x = \mathcal{R}_{abc}\, v_x\, \mathcal{R}_{abc}^{-1} \tag{3.8}$$

is the set of generators conjugated by $\mathcal{R}_{abc} \in \mathcal{A}_a \otimes \mathcal{A}_b \otimes \mathcal{A}_c$. Since conjugation is an inner automorphism of the algebra, generators v' satisfy the same relations as v, and all central functions remain unchanged.

We can apply four transformations (3.6) to rearrange six L-operators in a different way. Moreover, there are two different ways to perform this rearrangement (denoted by $\mathcal{J}_+$ and $\mathcal{J}_-$):

$$\begin{gathered}\mathrm{L}_{12,a}\mathrm{L}_{13,b}\mathrm{L}_{23,c}\mathrm{L}_{14,d}\mathrm{L}_{24,e}\mathrm{L}_{34,f} = \mathcal{J}_{\pm}(\mathrm{L}_{34,f}\mathrm{L}_{24,e}\mathrm{L}_{14,d}\mathrm{L}_{23,c}\mathrm{L}_{13,b}\mathrm{L}_{12,a}) \\ \mathcal{J}_+ = \mathrm{Ad}_{\mathcal{R}_{abc}}\mathrm{Ad}_{\mathcal{R}_{ade}}\mathrm{Ad}_{\mathcal{R}_{bdf}}\mathrm{Ad}_{\mathcal{R}_{cef}}, \quad \mathcal{J}_- = \mathrm{Ad}_{\mathcal{R}_{cef}}\mathrm{Ad}_{\mathcal{R}_{bdf}}\mathrm{Ad}_{\mathcal{R}_{ade}}\mathrm{Ad}_{\mathcal{R}_{abc}}.\end{gathered} \tag{3.9}$$

See the pictorial representation in Fig. 3.1, right. Statement that these two ways are equivalent gives under certain assumptions the functional tetrahedron equation [166, 112]

$$\mathcal{R}_{cef}\mathcal{R}_{bdf}\mathcal{R}_{ade}\mathcal{R}_{abc} = \mathcal{R}_{abc}\mathcal{R}_{ade}\mathcal{R}_{bdf}\mathcal{R}_{cef}. \tag{3.10}$$

The first assumption is that (3.6) fixes $\mathcal{R}$ uniquely up to constant, or in other words, that centralizer of $\mathrm{L}_{12,a}\mathrm{L}_{13,b}\mathrm{L}_{23,c}$ in $\mathcal{A}_a \otimes \mathcal{A}_b \otimes \mathcal{A}_c$ is trivial. The second assumption is that centralizer of $\mathrm{L}_{12,a}\mathrm{L}_{13,b}\mathrm{L}_{23,c}\mathrm{L}_{14,d}\mathrm{L}_{24,e}\mathrm{L}_{34,f}$ in $\mathcal{A}_a \otimes \mathcal{A}_b \otimes \mathcal{A}_c \otimes \mathcal{A}_d \otimes \mathcal{A}_e \otimes \mathcal{A}_f$ is trivial as well. It will become clear later

[1] We always assume that $\mathcal{R}$ is invertible.

that (classical limits of) these assumptions are actually satisfied for the L-operators that we consider in the present Chapter, once we identify these 3-fold and 6-fold products with elements in the largest double Bruhat cells in $PGL(3)$ and $PGL(4)$, respectively. These two assumptions are sufficient to derive (3.10) still up to some extra constant factor. To prove that this factor is identity one needs either to check some matrix element, or find some extra property (for example, that traces of l.h.s. and r.h.s. are defined and non-zero). We are not going into such details and refer to [19, 20] and references therein.

Forgetting about the space F, one can consider Eq. (3.6) as an equation on the L-matrix valued in some algebra $\mathcal{A}$, together with an automorphism of $\mathcal{A}_a \otimes \mathcal{A}_b \otimes \mathcal{A}_c$. Suppose that $\mathcal{A}$ has classical limit to commutative Poisson algebra. Then conjugation with $\mathcal{R}_{abc}$ has to be replaced by some canonical transformation of $\mathbb{C}[\mathcal{A}_a, \mathcal{A}_b, \mathcal{A}_c]$.

A solution of tetrahedron equation with $V = \mathbb{C}^2$ and the Lax operator valued in the q-oscillator algebra was found in [160, 23] and further studied in [120], [131], [117], [19], [162], [20], [17]. We do not give the quantum solution here as we will not need it here. The classical limit of the solution is an operator $\mathrm{L}_{\mathrm{BS}} : \mathbb{C}^2 \otimes \mathbb{C}^2 \to \mathbb{C}^2 \otimes \mathbb{C}^2$ acting as a matrix[2]

$$\mathrm{L}_{\mathrm{BS}}(x, y, \lambda, \mu) = \begin{pmatrix} 1 & & & \\ & \mu k & -\lambda\mu x & \\ & y & \lambda k & \\ & & & -\lambda\mu \end{pmatrix}, \tag{3.11}$$

where $k^2 = 1 - xy$ and the Poisson brackets are

$$\{x, y\} = k^2, \quad \{x, \lambda\} = \{x, \mu\} = \{y, \lambda\} = \{y, \mu\} = 0. \tag{3.12}$$

The Lax operator (3.11) satisfies the tetrahedron equation (3.6) with the

[2]Note that compared with [23] we use different notation for 4×4 matrices representing operators acting on $\mathbb{C}^2 \otimes \mathbb{C}^2$: indices of the first $\mathbb{C}^2$ encode the position of the 2×2 block while index of the second $\mathbb{C}^2$ encodes matrix elements inside the block.

transformed variables being

$$\begin{aligned}
x'_a &= k'^{-1}_b \frac{\lambda_b}{\lambda_c}\left(k_c x_a - \frac{1}{\lambda_a\mu_c} k_a x_b y_c\right), & y'_a &= k'^{-1}_b \frac{\lambda_c}{\lambda_b}\left(k_c y_a - \lambda_a\mu_c k_a y_b x_c\right),\\
x'_b &= x_a x_c + \frac{1}{\lambda_a\mu_c} k_a k_c x_b, & y'_b &= y_a y_c + \lambda_a\mu_c k_a k_c y_b,\\
x'_a &= k'^{-1}_b \frac{\mu_b}{\mu_a}\left(k_a x_c - \frac{1}{\lambda_a\mu_c} k_c y_a x_b\right), & y'_c &= k'^{-1}_b \frac{\mu_a}{\mu_b}\left(k_a y_c - \lambda_a\mu_c k_c x_a y_b\right),\\
k'_a &= k_a \frac{k_b}{k'_b}, & k'_c &= k_c \frac{k_b}{k'_b},\\
k'^2_b &= k^2_a k^2_b k^2_c - 2k^2_a k^2_c + k^2_a + k^2_c - \frac{k_a k_c y_a x_b y_c}{\lambda_a\mu_c} - \lambda_a\mu_c k_a k_c x_a y_b x_c,
\end{aligned} \tag{3.13}$$

The new variables (3.13) satisfy the same Poisson brackets, so the transformation is indeed canonical. Variables with different labels a, b, c Poisson commute, and λ's and μ's do not change under the transformation (the reason for this is that λ and μ are central functions, so after quantization they will not be changed by (3.8), and so we demand that they are do not change in the classical limit as well).

By contracting N Lax operators along one space, and taking the trace

$$\mathcal{L}_{2^N} = \mathrm{Tr}_0\left(\mathrm{L}_{01,a_1}\mathrm{L}_{02,a_2}...\mathrm{L}_{0N,a_N}\right) \tag{3.14}$$

one gets the Lax operator with auxiliary space $(\mathbb{C}^2)^N$. This solution is called the "quantum group-like" solution, as the Lax operator is block-diagonal and preserves the decomposition $\mathcal{L}_{\mathbb{C}^{2^N}} = \bigoplus_{k=1}^{N} \mathcal{L}_{\Lambda^k\mathbb{C}^N}$, where $\mathcal{L}_{\Lambda^k\mathbb{C}^N}$ is the Lax operator whose auxiliary space is k-th fundamental representation of $U_q(\mathfrak{gl}_k)$. In particular, the first non-trivial operator $\mathcal{L}_{\mathbb{C}^N}$ in the classical limit satisfies the r-matrix Poisson bracket

$$\{\mathcal{L}_{\mathbb{C}^N}(\lambda), \mathcal{L}_{\mathbb{C}^N}(\mu)\} = [r(\lambda/\mu), \mathcal{L}_{\mathbb{C}^N}(\lambda) \otimes \mathcal{L}_{\mathbb{C}^N}(\mu)] \tag{3.15}$$

with r being the classical trigonometric r-matrix. The quantum version of the Lax operator satisfies the RLL relation with the quantum trigonometric R-matrix [3]. This implies that by multiplying such Lax operators one obtains monodromy matrix of some integrable system. This system can be identified with the XXZ spin chain in the q-oscillatory representation, or its classical limit.

[3] We do not give here explicit expression for the classical r-matrix. Interested reader can find it e.g. in [84], [128] or [140].

Cluster algebras originally appeared in the theory of Lie groups and algebras (see e.g. [57]) and are now known to provide convenient language in the theory of integrable systems [82, 71, 39, 128, 80, **?**, 14]. In the present Chapter we try to make a small step towards fully integrating the tetrahedron equations into the general mathematical physics context, showing how Bazhanov-Sergeev solution naturally appears in the theory of cluster integrable systems. Namely, we show that the Lax operator (3.11) can be identified with the transfer matrix of paths on a four-gonal bi-coloured graph shown in Fig. 3.6. The tetrahedron equation for such Lax operators is then translated into the equality between the transfer matrix of a graph composed from three four-gonal blocks and the result of the action of four "spider moves" on it (see Fig. 3.7). This correspondence allows us to generalize the construction for the spectral curve of the XXZ chain given in [23] to systems with arbitrary symmetric Newton polygon. We shall note here that this block and the sequence of mutations leading to tetrahedron equation already appeared in the related contexts [109, 160, 23, 181, 4], however the full identification was missing.

We start our exposition in Section 3.2 where we give a brief recapitulation of planar networks, Poisson structure on the variables associated with paths on these networks and the transformations of the networks preserving the Poisson structure and partition function of paths. We give three-parametric family of mappings of Poisson variables corresponding to "corner" paths, shown in Fig. 3.3, all leading to the usual formulas for the transformations of the face variables.

Then in Section 3.3 we show that the Lax operator (3.11) coincides with the transfer matrix (3.30) of non-intersecting paths on the planar network from Fig. 3.6. We interperet the auxiliary space $\mathbb{C}^2$ in the Lax operator as a space on which the transfer matrix of paths acts. We realize the tetrahedron transformation (3.6) as a sequence of four spider-moves (and several two-moves) of the planar network shown in Fig. 3.7 and Fig. 3.11. Surprisingly, this sequence of transformations appears to be well known in cluster-algebraic literature [119, 181], however it was not identified before with the Bazhanov-Sergeev solution of the tetrahedron equation. We also show that the transformation of the "corner" variables (3.35) derived from the transformations of the network is consistent with those given by Eq. (3.13).

In Section 3.4 we extend the construction of the Lax operator (3.14) for

the XXZ spin chain (which has rectangular Newton polygon) made by contraction of the "tetrahedron" Lax operators (3.11), to integrable systems with arbitrary centrally symmetric Newton polygon. Finally, we discuss this construction from the point of view of the embedding of cluster integrable system into affine group $\widehat{\mathrm{PGL}}(N)$ and extend it to non-symmetric Newton polygons. We also prove a Lemma which shows the converse: it classifies conjugacy classes in double affine Weyl group of A-type by Newton polygons.

3.2 Perfect networks and flows on them

In this introductory section we recall notions of perfect networks and flows on them, construct Poisson structure on paths and discuss discrete transformations of networks preserving this structure. This will allow us to construct solution of the tetrahedron equation in Section 3.3 and Hamiltonians of cluster integrable system with arbitrary Newton polygon in Section 3.4. The way of exposition, which we follow here, is a mixture of approaches from [83], [175] and [71].

3.2.1 Flows on perfect networks

The main actor in considered approach to cluster integrable systems is a (planar) perfect network $N = (G, w)$ — (planar) perfectly oriented graph in disk, with edges weight function w. Orientation is called perfect if all vertices of a graph can be coloured in three colours: all boundary vertices are grey (×), all internal vertices are either white (○) (and have exactly one outgoing edge) or black (●) (and have exactly one incoming edge). We do not assume graph to be connected, however we assume that there are no 1-loops (edges going form the vertex to itself) and leaves (internal 1-valent vertices). All boundary vertices are assumed to be 1-valent. Boundary vertex with edges oriented away from it is called source. Vertex with edges oriented toward it is sink. We denote the set of sources by I, and the set of sinks — by J. It will be useful to put additional grey vertices in the middles of internal edges, and refer to edges connecting black and white vertices with grey vertices as half-edges. We say that the vertex v with the all adjacent half-edges is the fan of vertex v, number of half-edges in the fan is degree of the vertex and is denoted by $\deg(v)$. To each half-edge e oriented from black or white to grey vertex we as-

sign weight $w_e \in \mathbb{C}^*$, to half-edge with opposite orientation $-e$ we assign weight $w_{-e} = w_e^{-1}$. Weight of any set of oriented edges P is the product of weights of all half-edges in it $w_P = \prod_{e\in P} w_e$.

Flow p on the perfect network N is the set of such non-intersecting and non-self-intersecting paths (—) oriented by G that $\partial p = B - A$ with $A \subset I$, $B \subset J$, i.e. with all begin and end points belonging to the boundary. The set of all flows with starting points A and end points B is called $\mathcal{F}_A^B$. For example, the set of all closed non-intersecting oriented cycles on graph is $\mathcal{F}_\varnothing^\varnothing$. The sum of weights over all flows from A to B

$$\mathcal{Z}_N(A \to B) = \sum_{p\in\mathcal{F}_A^B} w_p \tag{3.16}$$

is called partition function of flows from A to B. One can find examples of perfect networks and sets of all flows on them in Fig. 3.6.

The partition function is naturally multiplicative with respect to the gluing of disks: take pair of planar networks $N' = (G_1, w_1)$ and $N_2 = (G_2, w_2)$ on disks D_1 and D_2. Take intervals $\ell_1 \subset \partial D_1$ containing $A_1 \subset I_1, B_1 \subset J_1$ at boundary of D_1, and $\ell_2 \subset \partial D_2$ containing $A_2 \subset I_2, B_2 \subset J_2$ at boundary of D_2. We say that perfect network N in disk D is the result of gluing of N_1 over ℓ_1 to N_2 over ℓ_2 if disks are glued $D = (D_1 \sqcup D_2)/_{\ell_1\sim\ell_2}$ in such a way that the grey vertices from A_1 are glued to B_2, and from B_1 — to A_2. Set of sources of N is $I = (I_1\backslash A_1) \cup (I_2\backslash A_2)$ and set of sinks is $J = (J_1\backslash B_1) \cup (J_2\backslash B_2)$. It is easy to see that partition function of flows from A to B on glued network N is given by

$$\mathcal{Z}_N(A \to B) = \sum_{C\subset A_1, E\subset B_1} \mathcal{Z}_{N_1}\left(C \cup (A \cap I_1) \to E \cup (B \cap J_1)\right) \cdot \tag{3.17}$$

$$\cdot \mathcal{Z}_{N_2}\left(E \cup (A \cap I_2) \to C \cup (B \cap J_2)\right),$$

where the sum goes over all subsets of $A_1 = B_2$ and $B_1 = A_2$.

Consider corresponding subsets in example of two planar networks glued together in Figure 3.2. Sets that depend on planar networks only are $I = \{1, 3, 8\}$ (all sources in ∂D), $J = \{2, 4, 5, 6, 7\}$ (all sinks in ∂D), $I_1 = \{1, 3, 13, 11\}$ (all sources in ∂D_1), $J_1 = \{2, 4, 5, 12, 10\}$ (all sinks in ∂D_1), $I_2 = \{8, 9, 10, 12\}$ (all sources in ∂D_2), $J_2 = \{11, 13, 6, 7\}$ (all sinks in ∂D_2), $A_1 = B_2 = \{11, 13\}$ (passages from D_2 to D_1), $A_2 = B_1 = \{10, 12\}$ (passages from D_1 to D_2). The particular flow (denoted by —) determines sets $A = \{1, 3\}$ (starting points of the flow), $B = \{5, 7\}$

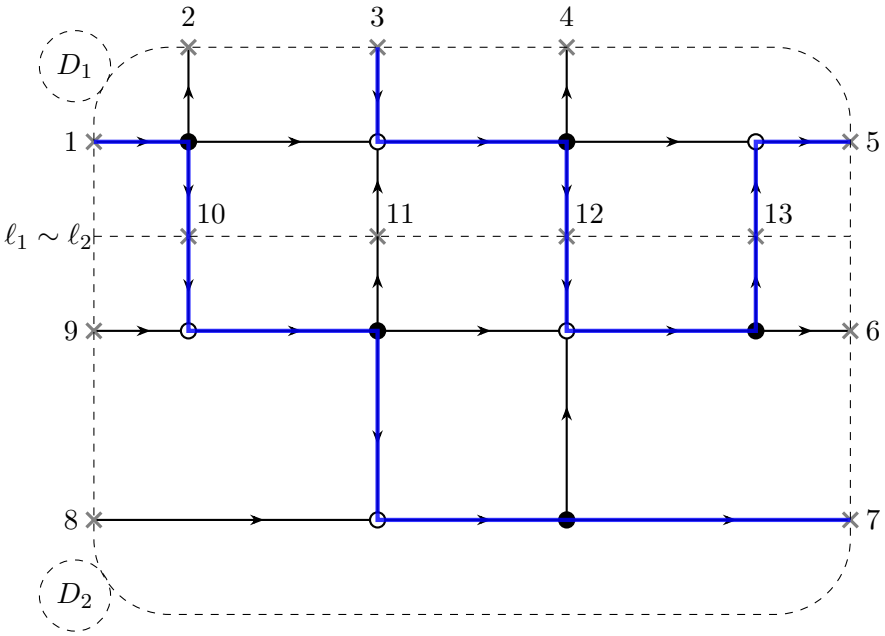

Figure 3.2. Gluing of two planar networks.

(endpoints of the flow), $C = \{13\}$ (passages where flow is allowed to go from D_2 to D_1), $E = \{10, 12\}$ (passages where flow is allowed to go form D_1 to D_2). This is a single term in summation which goes over all possible subsets $C \subset A_1 = B_2$ and $E \subset B_1 = A_2$, as we sum over all possible flows in disk D.

Formula (3.17) can be conveniently encoded using transfer matrix of flows T_N. This is an operator $T_N : (\mathbb{C}^2)^{\otimes |I|} \to (\mathbb{C}^2)^{\otimes |J|}$ given by

$$T_N = \sum_{A \subset I, B \subset J} \mathcal{Z}_N(A \to B) \cdot \bigotimes_{j \in J} e_{s(j,B),\, j} \otimes \bigotimes_{i \in I} e^*_{s(i,A),\, i}, \tag{3.18}$$

where $s(k, X) = +$ if $k \in X$ and $s(k, X) = -$ if $k \notin X$. The vectors $e_{\pm,\, j}$ are basis vectors in j-th component of $(\mathbb{C}^2)^{\otimes |J|}$, vectors $e^*_{\pm,\, i}$ are basis covectors in i-th component of $(\mathbb{C}^2)^{\otimes |I|}$. Using this operator (3.17) becomes simply

$$T_N = T_{N_1} \circ T_{N_2}, \tag{3.19}$$

where spaces with labels A_1 contract with corresponding spaces in B_1, and

the same for A_2 and B_2. Transfer matrices for perfect networks drawn in Fig. 3.6 are written in (3.30).

Remark. For the reader, familiar with combinatorics of dimers, we note that there is a bijection between bipartite graphs without two-valent vertices with selected perfect matching D_0, and perfect networks without neighbouring vertices of the same colour. The bijection can be established by choosing orientation on the bipartite graph from black to white for the edges not in D_0, and from white to black for those in D_0. There is also similar bijection between perfect matchings on bipartite graphs and flows on perfect networks.

3.2.2 Poisson structure on paths and $\mathcal{X}$-cluster variety

There is a two-parametric family of Poisson brackets on the weights of half-edges, see [83]. Here we will use, however, 1-parametric specialization of it restricted to the paths connecting middles of the edges[4] considered in [71]. Any path p on perfect network $N = (G, w)$ which begins and ends at the grey vertices (in the middles of edges or at boundary points) can be decomposed into sum of contributions associated with the fans of internal vertices

$$p = \sum_{v \in C_0(G)} n_{i,v} \gamma^*_{v,i} \tag{3.20}$$

where $C_0(G)$ is the set of internal vertices of G. Generators $\gamma^*_{v,i}$ are called simple corners and are associated with paths which go through v and connect middles of adjusted edges in the clockwise order, see Fig. 3.3 for example. They satisfy relation $\sum_{i=1}^{\deg v} \gamma^*_{v,i} = 0$ which means that by traversing all simple corners associated with one vertex we get trivial path. The logarithmically constant Poisson bracket on weights of paths is

$$\{w_{p_1}, w_{p_2}\} = \varepsilon(p_1, p_2) w_{p_1} w_{p_2}, \tag{3.21}$$

[4]The latter can be obtained from the former using procedure of the gauge symmetry reduction in black and white vertices.

where the skew-linear form ε is defined as sum of local contributions of each fan

$$\varepsilon(p_1,p_2)=\sum_{v\in C_0(G)}\operatorname{sgn}(v)\delta_v(p_1,p_2),$$
$$\delta_u(\gamma^*_{v,i},\gamma^*_{w,j})=\begin{cases}\pm\frac{1}{2}\delta_{u,v}\delta_{u,w} & \text{if } j=i\pm 1\\ 0 & \text{otherwise}\end{cases}, \tag{3.22}$$

where $\operatorname{sgn}(v)=1$ for the black vertices and $\operatorname{sgn}(v)=-1$ for the white. Example of pairing at three-valent black vertex is shown in Fig. 3.3. In fact, bracket can be defined by extending it from the bracket on weights of simple corners $\gamma_{v,i}=w_{\gamma^*_{v,i}}$. Thanks to the local structure of the bracket, the gluing of perfect networks is Poisson map, as it was shown in [83]. There is an opposite operation of splitting network $N=(G,w)$ on D to $N_1=(G_1,w_1)$ and $N_2=(G_2,w_2)$ by cutting D into D_1 and D_2 along some simple curve, which intersects G only at middles of edges and divide grey vertices into pairs of vertices belonging to different networks. It is not uniquely defined, if only weights of paths connecting boundary vertices of D are known, because of the gauge redundancy under transformations at internal grey vertices, which multiply weights of all paths ending at internal grey vertex v by $x_v\in\mathbb{C}^*$, and all paths starting at v by x_v^{-1}. We will face this problem again in Section 3.3.2.

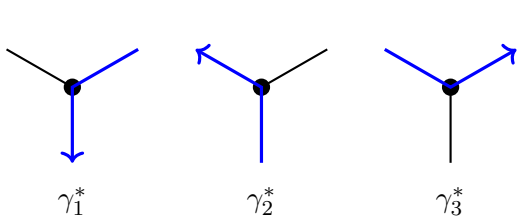

Figure 3.3. Definition of the local pairing on paths at the three-valent vertex, $\gamma_1^*+\gamma_2^*=-\gamma_3^*$. Simple corners are shown by blue.

The weight of any flow on planar network can be expressed using only the weights of oriented boundaries of faces $\mathbf{x}_i=w_{(\partial\bar{f}_i\cap G)}$. Faces are defined from decomposition $D\backslash G=\bigcup_i f_i$. Note that for unbounded disks (adjacent to ∂D) we take only parts belonging to G. The face variables $\mathbf{x}_i$ satisfy single relation $\prod_i\mathbf{x}_i=1$, as each edge of G belongs to the boundaries of exactly two faces with the opposite orientations.

Space of face weights admits structure of the toric chart in the $\mathcal{X}$-cluster variety. This means that it is algebraic torus with coordinate functions $\mathbf{x}_i$ satisfying log-constant Poisson bracket

$$\{\mathbf{x}_i, \mathbf{x}_j\} = \varepsilon_{ij}\, \mathbf{x}_i \mathbf{x}_j \tag{3.23}$$

with some skew-symmetric matrix ε called exchange matrix. We say that $\mathbf{x}_i$ are $\mathcal{X}$-cluster variables, and those $\mathbf{x}_i$ which come from faces adjacent to ∂D are frozen variables. Exchange matrix ε for perfect networks follows from (3.21). It is convenient to represent ε as oriented graph (quiver) with edges with multiplicities, whose oriented adjacency matrix is ε and vertices correspond to $\mathbf{x}_i$, see examples in Fig. 3.5 and 3.7. Toric charts are glued by transformations of mutations in directions of non-frozen variables $\mathbf{x}_i$. Mutation μ_i in direction of variable $\mathbf{x}_i$ is defined by the action

$$\mu_i(\mathbf{x}_j) = \begin{cases} \mathbf{x}_j^{-1}, & i = j \\ \mathbf{x}_j(1 + \mathbf{x}_i^{\operatorname{sgn}\varepsilon_{ji}})^{\varepsilon_{ji}}, & i \neq j \end{cases} \tag{3.24}$$

$$\mu_i(\varepsilon_{kl}) = \begin{cases} -\varepsilon_{kl}, & \text{if } i = k \text{ or } i = l \\ \varepsilon_{kl} + \dfrac{|\varepsilon_{ki}|\varepsilon_{il} + \varepsilon_{ki}|\varepsilon_{il}|}{2}, & \text{otherwise} \end{cases}$$

on cluster variables and exchange matrix. We will call $\mathcal{X}$-cluster variety of face variables of graph G by X_G. Realization of mutations as transformations of perfect network will be discussed in the next subsection.

Operation of gluing of the disks results in the product of $\mathcal{X}$-cluster varieties with amalgamation, for details see [49]. In simple words one has to replace pair of frozen variables corresponding to two unbounded faces, which are glued to one bounded, by the new unfrozen variable (which equals to the product of initial variables), and obtain new exchange matrix from the glued graph. From the point of view of quivers, product with amalgamation is gluing of quivers by vertices corresponding to frozen variables.

3.2.3 Plabic graph transformations

There are two well-known basic local transformations of perfect networks, which preserve both partition function of flows on them and Poisson structure: two-move shown in Fig. 3.4 and four-move (also known as spider

move or urban renewal or square move) shown in Fig. 3.5. The choosing of perfect orientation is inessential here. For the two-move either face variables and quiver stay the same, while under the four-move they change as under mutation [157, 71]. Here we present formulas for transformation of corner variables under this moves, which will be required in Section 3.3.

For both two- and four- moves we derive mapping of the corner variables from reasonable monomial ansätze using three requirements

1. Transfer matrix of flows has to be preserved

2. Poisson brackets of new corner variables have to be consistent with the transformed plabic graph

3. Mapping has to respect symmetries of plabic graph

It is easy to see that the unique monomial transformation rule under the black two-move for corner variables labelled in Fig. 3.4, left, satisfying this requirements is

$$l'_1 = t_3 b_2, \quad l'_2 = b_3 (t_1 b_1)^{\frac{1}{2}}, \quad l'_3 = t_2 (t_1 b_1)^{\frac{1}{2}}, \tag{3.25}$$

$$r'_1 = b_3 t_2, \quad r'_2 = t_3 (t_1 b_1)^{\frac{1}{2}}, \quad r'_3 = b_2 (t_1 b_1)^{\frac{1}{2}}.$$

Under white two-move variables labelled in Fig. 3.4, right, transform as

$$l'_1 = t_2 b_3, \quad l'_2 = t_3 (t_1 b_1)^{\frac{1}{2}}, \quad l'_3 = b_2 (t_1 b_1)^{\frac{1}{2}}, \tag{3.26}$$

$$r'_1 = b_2 t_3, \quad r'_2 = b_3 (t_1 b_1)^{\frac{1}{2}}, \quad r'_3 = t_2 (t_1 b_1)^{\frac{1}{2}}.$$

Exchange matrix ε does not change under these transformations.

For the four-move there is a family of transformations, parametrized

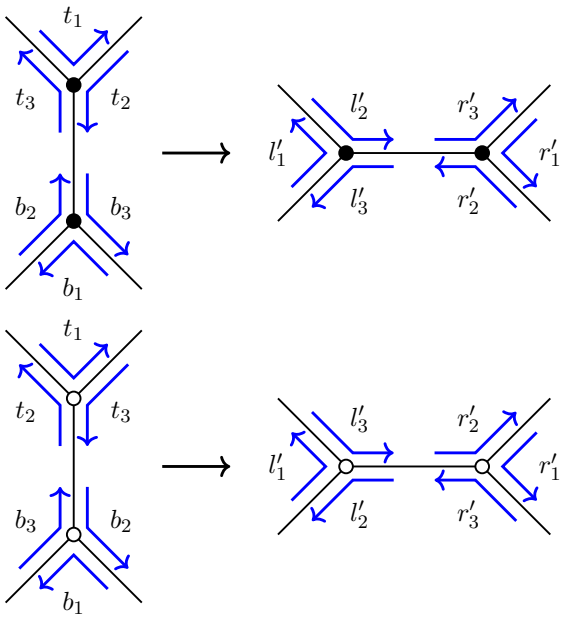

Figure 3.4. Transformations of the plabic graph under the two-moves at black and white vertices.

by $\alpha_1, \alpha_2, \alpha_3$, which acts on corner variables by

$$
\begin{gathered}
a'_1 = b_2 d_3 \cdot m_2^{-\alpha_3+\alpha_2} m_3^{-\alpha_3-\alpha_2}, \quad a'_2 = d_2 \cdot (1+\mathbf{x}^{-1})^{-\frac{1}{2}} m_1^{-\frac{1}{4}+\alpha_1} m_2^{-\alpha_2} m_3^{\alpha_3}, \\
a'_3 = b_3 \cdot (1+\mathbf{x})^{\frac{1}{2}} m_1^{-\frac{1}{4}-\alpha_1} m_2^{\alpha_3} m_3^{\alpha_2}, \\
b'_1 = a_2 c_3 \cdot m_2^{\alpha_3+\alpha_2} m_3^{-\alpha_3+\alpha_2}, \quad b'_2 = c_2 \cdot (1+\mathbf{x}^{-1})^{-\frac{1}{2}} m_1^{\frac{1}{4}-\alpha_1} m_2^{-\alpha_2} m_3^{\alpha_3}, \\
b'_3 = a_3 \cdot (1+\mathbf{x})^{\frac{1}{2}} m_1^{\frac{1}{4}+\alpha_1} m_2^{-\alpha_3} m_3^{-\alpha_2}, \\
c'_1 = d_2 b_3 \cdot m_2^{\alpha_3-\alpha_2} m_3^{\alpha_3+\alpha_2}, \quad c'_2 = b_2 \cdot (1+\mathbf{x}^{-1})^{-\frac{1}{2}} m_1^{-\frac{1}{4}+\alpha_1} m_2^{\alpha_2} m_3^{-\alpha_3}, \\
c'_3 = d_3 \cdot (1+\mathbf{x})^{\frac{1}{2}} m_1^{-\frac{1}{4}-\alpha_1} m_2^{-\alpha_3} m_3^{-\alpha_2}, \\
d'_1 = c_2 a_3 \cdot m_2^{-\alpha_3-\alpha_2} m_3^{\alpha_3-\alpha_2}, \quad d'_2 = a_2 \cdot (1+\mathbf{x}^{-1})^{-\frac{1}{2}} m_1^{\frac{1}{4}-\alpha_1} m_2^{\alpha_2} m_3^{-\alpha_3}, \\
d'_3 = c_3 \cdot (1+\mathbf{x})^{\frac{1}{2}} m_1^{\frac{1}{4}+\alpha_1} m_2^{\alpha_3} m_3^{\alpha_2},
\end{gathered}
\tag{3.27}
$$

where

$$\mathbf{x} = a_1b_1c_1d_1, \quad m_1 = \frac{a_1c_1}{b_1d_1}, \quad m_2 = \frac{a_2d_2}{b_2c_2}, \quad m_3 = \frac{a_3b_3}{c_3d_3}. \tag{3.28}$$

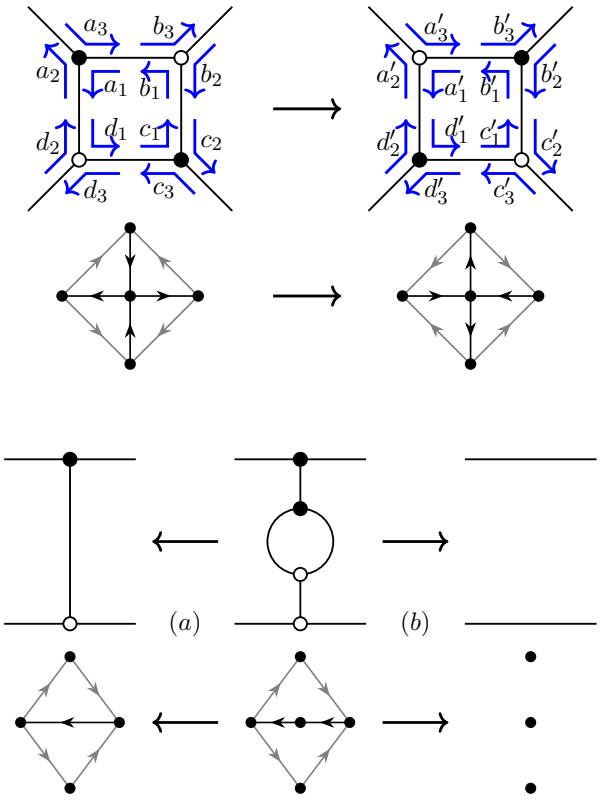

Figure 3.5. Top: change of bipartite graph under the spider-move and changes in the quiver. Grey arrows are for the entries $\pm 1/2$ of exchange matrix ε. Bottom: two ways for parallel bigon reduction and changes in the quiver.

Quivers encoding exchange matrix ε before and after transformation are drawn in Fig. 3.5, left, bottom. Whole family gives usual transformation rules for face variables, and are equivalent for our purposes, however choosing $\alpha_1 = \alpha_2 = 0$, $\alpha_3 = -\frac{1}{2}$ strangely makes formulas simpler.

The most subtle transformation is so-called parallel bigon reduction shown in Fig. 3.5, right. Recall that the zig-zags are paths, which turn right at each black vertex, and turn left on each white one. Parallel bigon

is a pairs of zig-zags which have such pair of intersection points, that disk(s) bounded by their segments between intersection points cannot be oriented in a way, consistent with orientation of segments.

The subtlety of parallel bigon reduction is that there are two different ways to perform it, both of which are bad. One of them, labelled by (a) in Fig. 3.5, change topology of zig-zag paths which will be unwanted for us in the following, but preserves transfer matrix of flows and acts as cluster transformation (mutation supplied by forgetting of one variable) on cluster variables. Another one, labelled by (b), does not change topology of zig-zags, however, its action on cluster variables is ill-defined and it changes partition function of flows on plabic network. In the following, we will either assume that the network does not contain parallel bigons, or reduce first all its parallel bigons with transformation (b), before considering any flows.

3.3 Tetrahedron equation from cluster algebra

The claim of this section is that transfer matrices for both plabic graphs shown in Fig. 3.6, left, coincide with Bazhanov-Sergeev solution of tetrahedron equation. Moreover, we will show that tetrahedron transformation is the result of sequence of four spider-moves.

3.3.1 Lax operators

As only paths which got both ends on the external edges of bipartite graph contribute to the transfer matrices of flows, we need only path variables γ_i shown in Fig. 3.6, left. For both graphs Poisson brackets of variables are

$$\begin{gathered}\{\gamma_1,\gamma_2\}=-\tfrac{1}{2}\gamma_1\gamma_2,\quad \{\gamma_2,\gamma_3\}=\tfrac{1}{2}\gamma_2\gamma_3,\quad \{\gamma_3,\gamma_4\}=-\tfrac{1}{2}\gamma_3\gamma_4,\\ \{\gamma_4,\gamma_1\}=\tfrac{1}{2}\gamma_4\gamma_1,\quad \{\gamma_1,\gamma_3\}=0,\quad \{\gamma_2,\gamma_4\}=0.\end{gathered}\tag{3.29}$$

All the paths contributing to the transfer matrices are drawn in Fig. 3.6, right. Note that the only difference between the cases is in non-equivalent perfect orientation. Two plabic graphs are related by one spider move.

The transfer matrices for upper and lower networks in the basis $\mathbb{C}^2\otimes$

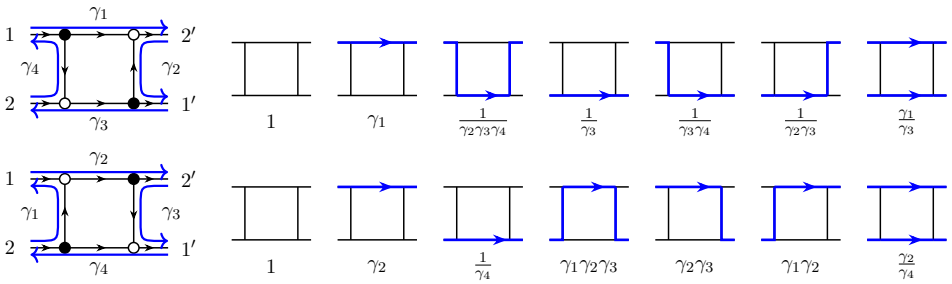

Figure 3.6. Left. Four-gonal pieces of bipartite graphs whose transfer matrices define Lax operators. Right. Paths contributing to transfer matrices.

$\mathbb{C}^2 = \langle e_+ \otimes e_+,\, e_+ \otimes e_-,\, e_- \otimes e_+,\, e_- \otimes e_- \rangle$ are respectively

$$\mathrm{L}_{\mathrm{CL}}(\gamma) = \begin{pmatrix} \gamma_1\gamma_3^{-1} & & & \\ & (\gamma_3\gamma_4)^{-1} & \gamma_3^{-1} & \\ & \gamma_1 + (\gamma_2\gamma_3\gamma_4)^{-1} & (\gamma_2\gamma_3)^{-1} & \\ & & & 1 \end{pmatrix}, \tag{3.30}$$

$$\overline{\mathrm{L}}_{\mathrm{CL}}(\gamma) = \begin{pmatrix} \gamma_2\gamma_4^{-1} & & & \\ & \gamma_2\gamma_3 & \gamma_4^{-1} + \gamma_1\gamma_2\gamma_3 & \\ & \gamma_2 & \gamma_1\gamma_2 & \\ & & & 1 \end{pmatrix}.$$

Matrix L_{CL} coincides with Bazhanov-Sergeev Lax operator (3.11) after conjugation

$$\mathrm{L}_{\mathrm{BS}} = (\sigma_1 \otimes \sigma_1 \circ \mathrm{P}) \circ \mathrm{L}_{\mathrm{CL}} \circ (\sigma_1 \otimes \sigma_1 \circ \mathrm{P}) \tag{3.31}$$

where P is a permutation matrix $\mathrm{P}(u \otimes v) = v \otimes u$, and after identification of variables

$$x = \gamma_1^{-1}, \quad y = \gamma_1 + (\gamma_2\gamma_3\gamma_4)^{-1}, \quad k = \frac{i}{\sqrt{\gamma_1\gamma_2\gamma_3\gamma_4}}, \tag{3.32}$$

$$\lambda = -i\sqrt{\frac{\gamma_1\gamma_4}{\gamma_2\gamma_3}}, \quad \mu = -i\sqrt{\frac{\gamma_1\gamma_2}{\gamma_3\gamma_4}},$$

The Poisson brackets (3.12) follow from (3.29). Matrix $\overline{\mathrm{L}}_{\mathrm{CL}}$ can be mapped to L_{CL} by conjugation with P and replacement

$$\gamma_1 \mapsto \gamma_4^{-1}, \quad \gamma_2 \mapsto \gamma_3^{-1}, \quad \gamma_3 \mapsto \gamma_2^{-1}, \quad \gamma_4 \mapsto \gamma_1^{-1}. \tag{3.33}$$

In the following we will be dealing with matrix L_{CL} only.

3.3.2 Tetrahedron transformation

Tetrahedron transformation (3.6) for the Lax operators L_{BS} itself recasts into the relation

$$\mathrm{L}^{23}_{\mathrm{CL}}(\gamma_a)\mathrm{L}^{13}_{\mathrm{CL}}(\gamma_b)\mathrm{L}^{12}_{\mathrm{CL}}(\gamma_c) = \mathrm{L}^{12}_{\mathrm{CL}}(\gamma'_c)\mathrm{L}^{13}_{\mathrm{CL}}(\gamma'_b)\mathrm{L}^{23}_{\mathrm{CL}}(\gamma'_a) \tag{3.34}$$

for the transfer matrices of perfect networks. Gluing left and right sides of this equation from the blocks shown in Fig. 3.6 gives equality for networks as drawn in Fig. 3.7. Note that as in Fig. 3.6, each Lax operator 'permutes' vector spaces. The networks are related by sequence of four spider-moves $\mu_{\mathcal{R}} = \mu_7\mu_4\mu_2\mu_3$ supported by two-moves, detailed sequence is shown in Fig. 3.11. Mapping (3.13) being rewritten in γ-variables using (3.32) results in

$$\begin{aligned}
\gamma'_{a,1} &= \frac{\gamma_{a,1}\gamma_{a,4}}{\gamma_{b,4}\gamma_{c,3}[\mathbf{x}_3^{-1},\mathbf{x}_2^{-1}]}\sqrt{\frac{\mathbf{x}_4}{\mathbf{x}_2\mathbf{x}_3}A}, & \gamma'_{a,2} &= \frac{\gamma_{a,2}\gamma_{b,4}\gamma_{c,3}}{\gamma_{a,4}}\mathbf{x}_2\mathbf{x}_3[\mathbf{x}_3^{-1},\mathbf{x}_2^{-1}],\\
\gamma'_{a,3} &= \frac{\gamma_{a,3}\gamma_{a,4}}{\gamma_{b,4}\gamma_{c,3}[\mathbf{x}_3^{-1},\mathbf{x}_2^{-1}]}\sqrt{\frac{\mathbf{x}_4}{\mathbf{x}_2\mathbf{x}_3}A}, & \gamma'_{a,4} &= \gamma_{b,4}\gamma_{c,3}\mathbf{x}_2\mathbf{x}_3[\mathbf{x}_3^{-1},\mathbf{x}_2^{-1}],\\
\gamma'_{b,1} &= \frac{\gamma_{a,1}\gamma_{c,1}}{[\mathbf{x}_3^{-1}]}, & \gamma'_{b,2} &= \frac{\gamma_{b,2}[\mathbf{x}_3^{-1}]}{\gamma_{a,1}\gamma_{a,4}\gamma_{c,1}\gamma_{c,2}}\sqrt{\frac{\mathbf{x}_3}{\mathbf{x}_2\mathbf{x}_4}\frac{1}{A}},\\
\gamma'_{b,3} &= \frac{\gamma_{b,3}\gamma_{a,1}\gamma_{a,4}\gamma_{c,1}\gamma_{c,2}}{\mathbf{x}_3[\mathbf{x}_3^{-1}]}, & \gamma'_{b,4} &= \frac{\gamma_{b,4}[\mathbf{x}_3^{-1}]}{\gamma_{a,1}\gamma_{a,4}\gamma_{c,1}\gamma_{c,2}}\sqrt{\frac{\mathbf{x}_3}{\mathbf{x}_2\mathbf{x}_4}\frac{1}{A}},\\
\gamma'_{c,1} &= \frac{\gamma_{c,1}\gamma_{c,2}}{\gamma_{a,3}\gamma_{b,2}[\mathbf{x}_3^{-1},\mathbf{x}_4^{-1}]}\sqrt{\frac{\mathbf{x}_2}{\mathbf{x}_4\mathbf{x}_3}A}, & \gamma'_{c,2} &= \gamma_{b,2}\gamma_{a,3}\mathbf{x}_4\mathbf{x}_3[\mathbf{x}_3^{-1},\mathbf{x}_4^{-1}],\\
\gamma'_{c,3} &= \frac{\gamma_{c,3}\gamma_{c,2}}{\gamma_{a,3}\gamma_{b,2}[\mathbf{x}_3^{-1},\mathbf{x}_4^{-1}]}\sqrt{\frac{\mathbf{x}_2}{\mathbf{x}_4\mathbf{x}_3}A}, & \gamma'_{c,4} &= \frac{\gamma_{a,3}\gamma_{b,2}\gamma_{c,4}}{\gamma_{c,2}}\mathbf{x}_4\mathbf{x}_3[\mathbf{x}_3^{-1},\mathbf{x}_4^{-1}]
\end{aligned} \tag{3.35}$$

where $A = 1 + \mathbf{x}_3^{-1} + \mathbf{x}_7^{-1}[\mathbf{x}_3^{-1},\mathbf{x}_2^{-1}][\mathbf{x}_3^{-1},\mathbf{x}_4^{-1}]$, $[x] = 1 + x$, $[x,y] = 1 + x(1+y)$ and locations of face variables $\mathbf{x}_i$ are shown in Fig. 3.7. Their

explicit expressions in terms of γ-variables are

$$\begin{aligned}
\mathbf{x}_2 &= \frac{1}{\gamma_{c,1}\gamma_{c,4}\gamma_{c,3}\gamma_{c,2}}, \quad \mathbf{x}_3 = \gamma_{b,1}\gamma_{a,4}\gamma_{c,2},\\
\mathbf{x}_4 &= \frac{1}{\gamma_{a,1}\gamma_{a,4}\gamma_{a,3}\gamma_{a,2}}, \quad \mathbf{x}_7 = \frac{1}{\gamma_{b,1}\gamma_{b,4}\gamma_{b,3}\gamma_{b,2}},\\
\mathbf{x}_1 &= \gamma_{c,4} \times (\text{weights of other boundaries}),\\
\mathbf{x}_5 &= \gamma_{a,2} \times (\text{weights of other boundaries}),\\
\mathbf{x}_6 &= \gamma_{b,4} \times (\text{weights of other boundaries}),\\
\mathbf{x}_8 &= \gamma_{b,2} \times (\text{weights of other boundaries}),
\end{aligned} \tag{3.36}$$

where by "weights of the other boundaries" we denote a product of the γ-variables that correspond to the other boundaries of the face corresponding to given $\mathbf{x}$-variable, which are unimportant as neither transform under four- and two-moves, nor contribute into the transfer matrices of flows.

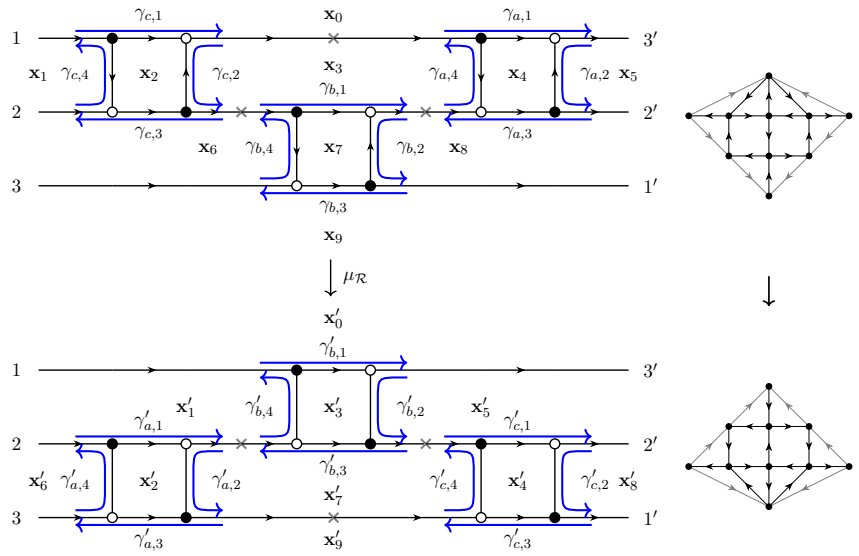

Figure 3.7. Left. Tetrahedron equation realized as equality of transfer matrices of perfect networks. Grey crosses are for the points of gluing of four-gonal building blocks. Graphs are related by sequence of four spider-moves $\mu_{\mathcal{R}} = \mu_7\mu_4\mu_2\mu_3$. Right. Corresponding quiver before and after mutation.

It is easy to check that formulas (3.35) are consistent with the mapping

of $\mathcal{X}$-cluster variables

$$\begin{aligned}
&\mathbf{x}'_0 = \mathbf{x}_0 \frac{1}{[\mathbf{x}_3^{-1}]}, \quad \mathbf{x}'_1 = \mathbf{x}_1 \frac{[\mathbf{x}_3^{-1}]}{[\mathbf{x}_3^{-1}, \mathbf{x}_2^{-1}]}, \quad \mathbf{x}'_2 = \frac{1}{\mathbf{x}_2\mathbf{x}_3}\frac{1}{A}, \\
&\mathbf{x}'_3 = \mathbf{x}_3\mathbf{x}_2\mathbf{x}_4\mathbf{x}_7 A, \quad \mathbf{x}'_4 = \frac{1}{\mathbf{x}_3\mathbf{x}_4}\frac{1}{A}, \quad \mathbf{x}'_5 = \mathbf{x}_5 \frac{[\mathbf{x}_3^{-1}]}{[\mathbf{x}_3^{-1}, \mathbf{x}_4^{-1}]}, \\
&\mathbf{x}'_6 = \mathbf{x}_6 \cdot \mathbf{x}_3\mathbf{x}_2[\mathbf{x}_3^{-1}, \mathbf{x}_2^{-1}], \quad \mathbf{x}'_7 = \frac{1}{\mathbf{x}_7}\frac{[\mathbf{x}_3^{-1}, \mathbf{x}_2^{-1}][\mathbf{x}_3^{-1}, \mathbf{x}_4^{-1}]}{[\mathbf{x}_3^{-1}]}, \\
&\mathbf{x}'_8 = \mathbf{x}_8 \cdot \mathbf{x}_3\mathbf{x}_4[\mathbf{x}_3^{-1}, \mathbf{x}_4^{-1}], \quad \mathbf{x}'_9 = \mathbf{x}_9 \frac{\mathbf{x}_7}{[\mathbf{x}_3^{-1}, \mathbf{x}_2^{-1}][\mathbf{x}_3^{-1}, \mathbf{x}_4^{-1}]} A,
\end{aligned} \tag{3.37}$$

under $\mu_{\mathcal{R}}$ which follows from (3.24). Trying to recover formulas (3.35) using 'refined' formulas (3.25) – (3.27) for transformation of corner variables one faces problems. In Appendix A we explain how these problems can be treated successfully.

3.4 Integrable system for arbitrary Newton polygon

In this section we give explicit construction for bi-coloured graph G defining integrable system with arbitrary Newton polygon. It will turn out that for symmetric Newton polygon Lax operator is 'patchworked' by contraction of 'XXZ spin chain' rectangular blocks (see Fig. 3.8), which are made from tetrahedron Lax operators (3.30). This extends results of [23] and [140] to the case of non-rectangular Newton polygons.

Then we will show, how our constructions come out in the approach to cluster integrable systems via double Bruhat cells in $\widehat{\mathrm{PGL}}(N)$. Tetrahedron Lax operator will be identified with generator $s_i\bar{s}_i$ of diagonal subgroup $W(A_{N-1}^{(1)}) \subset W(A_{N-1}^{(1)} \times A_{N-1}^{(1)})$, and tetrahedron transformation — with the Coxeter relation there. Embedding of commuting subgroups $\widehat{\mathrm{PGL}}(a_1) \times ... \times \widehat{\mathrm{PGL}}(a_n) \subset \widehat{\mathrm{PGL}}(N)$, $N = a_1 + ... + a_n$, will provide natural framework for the construction of Bruhat cell for arbitrary symmetric Newton polygon. Finally, we will construct double Bruhat cells for non-symmetric Newton polygons via triangular decomposition of Lax operators, discuss additional freedom, coming from Newton polygons with sides, containing internal integral points, and prove classification theorem for perfect networks on torus.

3.4.1 Spectral curve and perfect network on torus

To the moment we were considering bi-coloured graphs on disks only. Integrable system appears once we consider network on torus: due to [71], spectral curve, which is generating function of Hamiltonians of integrable system

$$S = \{(\lambda, \mu) \in \mathbb{C}^* \times \mathbb{C}^* \mid S(\lambda, \mu) = \sum_{(i,j)\in\mathbb{Z}^2} \lambda^i \mu^j H_{ij} = 0\}, \tag{3.38}$$

is equal to the partition function of flows on perfect network $N = (G, w)$ on torus $\mathbb{T}^2$. In this subsection we are going to explain how spectral parameters (λ, μ) and Hamiltonians of the system appear.

There are two major differences in structure of X_G for the network $N = (G, w)$ on torus $\mathbb{T}^2$ compared to the case of disk. First, there are no open faces, so $\mathrm{H}_1(G, \partial G) = \mathrm{H}_1(G)$, and second, not any path on G can be decomposed as a sum of paths along boundaries of faces, one has to take also representatives of $\mathrm{H}_1(\mathbb{T}^2)$. Bringing this together we can uniquely decompose any closed path $\gamma \in \mathrm{H}_1(G)$ into

$$\gamma = n_A(\gamma)\gamma_A + n_B(\gamma)\gamma_B + \sum_{f_i\in\mathrm{F}} n_i(\gamma)\partial f_i, \tag{3.39}$$

where F is the set of faces of graph G embedded into $\mathbb{T}^2$, and γ_A, γ_B is fixed pair of paths on G, which represent two classes in homologies of torus with non-trivial intersection. The best choices for $\gamma_{A,B}$ are zig-zag paths Z (those oriented paths which turn left at each white vertex and turn right at each black one) because, as it is easy to see, all face variables $\mathbf{x}_i$ and all zig-zag variables $\zeta_\alpha = w_{z_\alpha},\ z_\alpha \in \mathrm{Z}$ are Poisson-commuting

$$\{\mathbf{x}_i, \zeta_\alpha\} = 0, \quad \{\zeta_\alpha, \zeta_\beta\} = 0. \tag{3.40}$$

with respect to the bracket (3.21), so they are good candidates for the role of 'spectral parameters'. For further convenience, we fix trivialization $\mathrm{H}_1(\mathbb{T}^2) = \mathbb{Z}^2$ by choosing a pair of cycles on torus h_A, h_B with simple intersection $< h_A, h_B >= 1$, so one can assign a vector $\vec{u}_\alpha = (a_\alpha, b_\alpha) \in \mathrm{H}_1(\mathbb{T}^2)$ to each zig-zag $[z_\alpha] = a_\alpha[h_A] + b_\alpha[h_B]$. It often happens that the lattice [Z], generated by classes $\vec{u}_\alpha$ of all zig-zags, does not generate entire lattice $\mathbb{Z}^2 = \mathrm{H}_1(\mathbb{T}^2)$, but some sub-lattice of finite index $|\mathrm{H}_1(\mathbb{T}^2)/[\mathrm{Z}]| = d$ instead. In those cases there is no way to choose any pair of zig-zags

$z_\alpha, z_\beta \in \mathrm{Z}$ to be 'basic cycles' $\gamma_A = z_\alpha$ and $\gamma_B = z_\beta$, and express all classes in homologies as their integral combination. In such cases one has to make coefficients n_A, n_B, n_i in (3.39) rational numbers with denominators being divisors of d instead. So we get an embedding of finite index $\mathrm{H}_1(G) \subset \mathbb{Z}^2 \oplus \frac{1}{d}\mathbb{Z}^{|F|}$ which implies decomposition for the space of functions

$$\mathrm{X}_G = \mathbb{C}[(\mathrm{H}_1(G))^*] \subset \mathbb{C}[\lambda^{\pm 1}, \mu^{\pm 1}] \otimes \mathbb{C}[\mathbf{x}_i^{\pm 1/d}]_{i\in \mathrm{F}}, \tag{3.41}$$

where $\lambda = (\zeta_\alpha)^{k_{A,\alpha}}(\zeta_\beta)^{k_{A,\beta}}$, $\mu = (\zeta_\alpha)^{k_{B,\alpha}}(\zeta_\beta)^{k_{B,\beta}}$ will have powers chosen so that

$$k_{A,\alpha}\vec{u}_\alpha + k_{A,\beta}\vec{u}_\beta = (1,0), \quad k_{B,\alpha}\vec{u}_\alpha + k_{B,\beta}\vec{u}_\beta = (0,1), \tag{3.42}$$

so that λ, μ are variables corresponding to generators $(1,0)$ and $(0,1)$ of homologies, and will play the role of 'spectral parameters' in the following. Now, spectral curve of cluster integrable system defined by perfect network $N = (G, w)$ can be calculated as partition function of flows

$$S(\lambda, \mu) = \mathcal{Z}_{\mathbb{T}^2} = \sum_{p\in\mathcal{F}_{\mathbb{T}^2}} w_p = \tag{3.43}$$

$$= \sum_{p\in\mathcal{F}_{\mathbb{T}^2}} \lambda^{<[p],h_B>}\mu^{-<[p],h_A>} \prod_{f_i\in \mathrm{F}} \mathbf{x}_i^{n_i(p)} = \sum_{(i,j)\in\Delta} \lambda^i \mu^j H_{ij},$$

where $\mathcal{F}_{\mathbb{T}^2}$ is the set of flows on torus, Hamiltonians $H_{ij} = H_{ij}(\{\mathbf{x}_a\})$ depend only on face variables $\mathbf{x}_i$, which are $\mathcal{X}$-cluster coordinates, and set $\Delta \subset \mathbb{Z}^2$ is convex envelope of those $(i,j) \in \mathbb{Z}^2$ for which H_{ij} are non-zero, and is called Newton polygon of curve S. It was proved in [71] that for minimal bi-coloured graphs there exist special perfect orientations, called α-orientations (we will give both definitions in a moment)[5] for which following theorem holds.

Theorem ([71]). Let $N = (G, w)$ be α-orientated perfect network on torus with minimal bi-coloured graph and (3.43) be partition function of flows on it. Then:

1. Hamiltonians corresponding to boundary points of Δ are Casimir functions.[6]

[5] Actually, logic of [82] and [80] suggests that similar statement holds for any perfect orientation, however the understanding of this point is still missing in the literature.

[6] Spectral parameters (λ, μ) are obviously Casimirs as well, as they are expressible via zig-zag variables only.

2. Hamiltonians corresponding to internal points are algebraically independent and in involution

$$\{H_{ij}, H_{kl}\} = 0. \tag{3.44}$$

3. Number of Hamiltonians (which are not Casimirs) is exactly half of the dimension of symplectic leaf.

4. The Newton polygon Δ is the unique (up to permutation of collinear vectors) convex polygon whose set of primitive oriented boundary intervals is $\{\vec{u}_k\}_{k=1}^{|\mathrm{Z}|}$.[7]

Together statements 1-3 imply integrability of the system. Statement 4 gives simple way to predict shape of the Newton polygon without computation of entire spectral curve. We will use it intensively in the following. By deforming slightly zig-zag paths from the graph, so that they cross edges only at grey vertices, and erasing graph itself, one obtains so-called wiring diagram. This operation is invertible: it is easy to recover the graph from its wiring diagram [71].

Partition function of flows $\mathcal{Z}_{\mathbb{T}^2}$ on toric network $N = (G, w)$, $G \subset \mathbb{T}^2$ can be obtained by gluing of sides of the disk with network $\tilde{N} = (\tilde{G}, w)$. To do this, divide boundary of the disk into four clockwise oriented segments $\ell_a, \ell_b, \ell_c, \ell_d$ with no sources or sinks at the points of contact of segments. The gluing is possible if one can find such continuous monotonic map $j_1 : \ell_a \to \ell_c$ that puts beginning of ℓ_a to the end of ℓ_c, end of ℓ_a to the beginning of ℓ_c, sources to sinks and sinks to sources, and similar map for $j_2 : \ell_b \to \ell_d$. If one found $j_{1,2}$, then the partition function of flows on perfect network N on torus is related to $\tilde{N}$ on the disk, from which the torus is glued with $j_{1,2}$, by

$$\mathcal{Z}_{\mathbb{T}^2} = \sum_{A \subset I_a} \sum_{B \subset I_b} \sum_{C \subset I_c} \sum_{D \subset I_d} \cdot \tag{3.45}$$

$$\cdot \mathcal{Z}_{\tilde{N}}(A \cup B \cup C \cup D \to j_1(A) \cup j_2(B) \cup (j_1)^{-1}(C) \cup (j_2)^{-1}(D))$$

where I_k and J_k are sets of sinks and sources on ℓ_k for $k \in \{a, b, c, d\}$, and we use identifications $j_1(I_a) = J_c,\ j_2(I_b) = J_d,\ j_1^{-1}(I_c) = J_a,\ j_2^{-1}(I_d) = J_b$. Term with chosen subsets (A, B, C, D) contributes to Hamiltonian

[7] It might be so because there is a pair of zig-zags which travel in two opposite directions along each edge of graph, so $\sum_k [z_k] = \sum_k \vec{u}_k = 0$.

$H_{|C|-|A|,|D|-|B|}$, if generators of $\mathrm{H}_1(\mathbb{T}^2)$ are chosen to be $h_A = -\ell_b = \ell_d$ and $h_B = \ell_a = -\ell_c$ respectively. To obtain the same partition function using transfer matrix of flows, one can 'take trace' of transfer matrix by contraction of spaces whose boundary points are glued by $j_{1,2}$. With explicit dependence on λ and μ (which are not λ, μ from (3.41), but just generating parameters, keeping trace of classes in homologies) incorporated it looks

$$\mathcal{Z}_{\mathbb{T}^2} = \mathrm{Tr}_{j_1,j_2}\left(T_N \circ \lambda^{\hat{P}_{J_a}-\hat{P}_{J_c}}\mu^{\hat{P}_{J_b}-\hat{P}_{J_d}}\right), \quad \hat{P}_X = \sum_{i\in X}\frac{1}{2}(1+\hat{\sigma}_{z,i}), \quad (3.46)$$

where $\hat{\sigma}_{z,i} = 1 \otimes ... \otimes \sigma_z \otimes ... \otimes 1$ is operator acting by σ_z-matrix in space i, and by unity in all other spaces.

Now, it remains to construct special orientation for network on torus, for which Hamiltonians are involutive. We construct it using so-called dominant orientation for network on disk. In the following we will be considering only graphs called minimal graphs, for which zig-zags do not have self-intersections, there are no closed zig-zags (i.e. those isotopic to S^1) and no parallel bigons of zig-zags. For minimal planar graphs, we can label zig-zags by their staring points.

Take any linear order $\leqslant$ on the set of zig-zags, i.e. for any pair of zig-zags z_1 and z_2 set $z_1 \leqslant z_2$ or $z_2 \leqslant z_1$. For intersecting zig-zags order must be strict, those zig-zags which do not have intersection points could be equal in this order. Take any black or white vertex v, and let zig-zags which pass it are $z_a < z_{a-1} < ... < z_1$, where a is the degree of the vertex. We say that z_a is the lowest zig-zag at v and z_1 is the highest zig-zag at v. The order is said to be consistent at v if it satisfies the following requirements:

- If zig-zag z_1 is highest at v, then it is highest in the next vertex along z_1 if the next vertex is black, and in the previous vertex along z_1 if the previous vertex is white. Note, that the both cases could occur at the same vertex, as we do not demand graph to be bipartite.
- Any other zig-zags z_i, $i = 2, ..., a$ is not the highest in the next vertex along z_i if the next vertex is black, and in the previous vertex along z_i, if the previous vertex is white.

The order is consistent if it is consistent at all vertices. To construct perfect orientation on the graph by ordering on zig-zags, define first orientation on fans of all internal vertices. For any black vertex the only

incoming half-edge is those, along which the highest zig-zag come to the vertex, and all the other are outgoing. For any white vertex the only outgoing half-edge is those, along which the highest zig-zag leave the vertex, and all the other are incoming. It is easy to see that if the order on zig-zags is consistent, then orientations of halves of all the internal edges are consistent. We do not give explicit description of the set of all consistent orders on zig-zags, however make the following

Conjecture. All perfect orientations without oriented loops for graphs on disks are orientations constructed from some consistent orders on zig-zags.

If one glue pair of disks D_1 and D_2, each equipped with dominant orientation, the dominant orientation on $D_1 \cup_\ell D_2$ can also be obtained, once the orders on zig-zags are concerted, and consistency condition at boundary vertices holds (note that all the gluings in Section 3.3.2 was so). The same is true also for gluing disk into torus. Now, construct α-ordering by taking any zig-zag to be the highest among all, and other zig-zags to be ordered according to counter-clockwise order of their classes in $\mathrm{H}_1(\mathbb{T}^2, \mathbb{Z})$ considered as vectors in $\mathbb{Z}^2$. As it was claimed, for orientation built from such ordering, Hamiltonians H_{ij} are involutive.

3.4.2 Integrable system with symmetric Newton polygon

In this sub-section using four-gonal block from Fig. (3.6) we construct cluster integrable systems with arbitrary symmetric Newton polygon. As it was discussed in the previous sub-section, for this it is enough to construct such bi-coloured graph, that collection of homology classes of its zig-zags coincides with the set of oriented boundary intervals of the Newton polygon.

We say that Newton polygon is 'symmetric' if it is invariant under the central symmetry $(i, j) \mapsto (-i, -j)$, see e.g. Fig. 3.8. Due to the symmetry, it always has even number of vertices — it is $2n$-gonal. Let's select any point with the minimal i-coordinate. Starting from this point, we enumerate all oriented boundary intervals $\vec{u}_1 = (a_1, b_1), \vec{u}_2 = (a_2, b_2), ..., \vec{u}_n = (a_n, b_n)$ in counter-clockwise direction, until the point, which is symmetric to the initial one. Since we started from the left-most point, then all $a_i > 0$. We assume also that all intervals are primitive, i.e. $\gcd(a_i, b_i) = 1$.

Opposite half of polygon, which starts at rightmost point, and ends at leftmost, consists of vectors with coordinates $-\vec{u}_1, ..., -\vec{u}_n$.

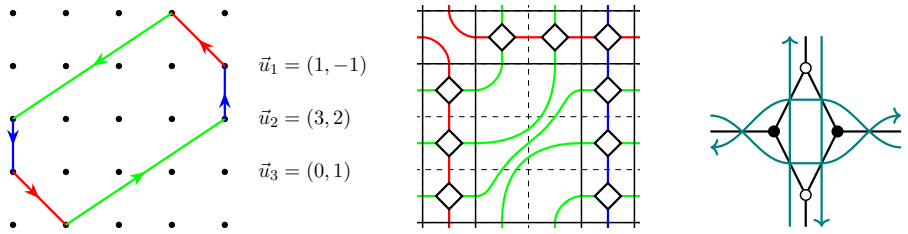

Figure 3.8. Left. Example of the Newton polygon. Center. Schematic drawing of the graph on torus. Four-gonal blocks are drawn in details on the right panel. Edges are coloured according to the colours of zig-zags going along them, by colours from the left panel. Right. Detailed view on graph and on wiring diagram of zig-zags at the intersection points.

Decompose fundamental domain of torus into grid of $n \times n$ rectangular blocks. Diagonal block at i-th position has a_i sources on its left side, a_i sinks on its right side, $|b_i|$ sinks and sources on upper and lower sides respectively if $b_i > 0$, or visa versa if $b_i < 0$. Edges are non-intersecting, and if $b_i > 0$, then graph is constructed by iterative connection of closest non-connected sources with sinks by edges starting from top-left corner, while if $b_i < 0$, the process of connection starts from bottom-left corner, see example in Fig. 3.8, center. Non-diagonal block at row i (counting from the top) and column j (counting from the left) is $a_i \times |b_j|$ 'fence net' bipartite graphs, which is rectangular grid glued from four-gonal blocks. As it is shown in Fig. 3.8, right, at each four-gonal block zig-zag paths are going without changing of direction, so it is easy to convince yourself that the classes of zig-zags in $\mathrm{H}_1(\mathbb{T}^2)$ are precisely $\vec{u}_1, ..., \vec{u}_n, -\vec{u}_1, ..., -\vec{u}_n$ as required.

Remark. Bi-coloured graphs on torus obtained in this way might be not simple because of parallel bigons. The evidence for this, is that the graph constructed by proposed recipe, for each pair of boundary intervals $\vec{u}_i$ and $\vec{u}_j$, has $|a_i b_j| + |a_j b_i|$ four-gonal blocks at their intersection points, which is not $\mathrm{SA}(2, \mathbb{Z})$-invariant quantity. Obtaining minimal graph, which is necessary for integrability theorem, requires additional spider-moves and parallel bigon reductions. As an illustration, interested reader can try to construct graph and reduce it for the Newton polygon obtained from the

one drawn in Fig. 3.8 by transformation $x \mapsto x + y, y \mapsto y$.

Transfer matrix of each four-gonal block is $\mathrm{L_{CL}}$ from (3.30), which we identified with the solution of tetrahedron equation. If all blocks are oriented as in Fig. 3.6, top, then the global orientation turns out to be the α-orientation, so does not have oriented cycles. It is known since [23], and redirived in the context of cluster integrable systems in [140], that 'fence net' $a \times b$ block being glued by pairs of opposite sides to cylinder defines either Lax operator of $\mathfrak{gl}_a$ classical XXZ spin chain on b sites or $\mathfrak{gl}_b$ chain on a sites, depending on pair of sides chosen to be glued. As we remarked in (3.14), it was noted in [23] that the result of contraction of tetrahedron Lax operators decomposes into direct sum of Lax operators for XXZ chain with auxiliary space being sum of all fundamental representations of $\mathfrak{gl}_a$

$$(\mathbb{C}^2)^{\otimes a} = \bigoplus_{i=0}^{a} \mathbb{C}^{\binom{i}{a}} \;\Rightarrow\; T(\mu) = \bigoplus_{i=0}^{a} \mathcal{L}_{\Lambda^i \mathbb{C}^a}(\mu). \tag{3.47}$$

In our approach this is the result of the natural grading by the number of paths which cross cylinder from the left to the right, and implication[8] of LGV lemma [86, 123]. Dependence on spectral parameter μ comes from the paths which cross horizontal boundary of fundamental domain, and formula (3.46).

Cylindric transfer matrix of the system with arbitrary Newton polygon can be obtained by cutting of graph drawn in Fig. 3.8 by vertical line between any pair of columns of four-gons. Due to the chosen orientation, all the sources are located on the left, and all sinks are located on the right side of cylinder. The transfer matrix by cylindric LGV lemma again provides Lax operator acting in direct sum $\bigoplus_{i=0}^{r} \Lambda^i \mathbb{C}^r$, $r = a_1 + ... + a_n$. The first fundamental Lax operator $\mathcal{L}_{\mathbb{C}^r}(\mu)$ satisfies r-matrix Poisson bracket (3.15), as it was proved in [84].

One can keep decomposing cylinder by vertical cuts, up to separating transfer matrix into product of n transfer matrices, each corresponding to flows passing one column in the array of fence-nets. We will clarify how this cylindric blocks are related to combinatorics of affine Weyl groups below. However, we want to stress here, that only the toroidal representation of the system makes $\mathrm{SA}(2, \mathbb{Z})$ covariance explicit.

[8] This is not LGV lemma itself, as we deal with cylinder. Some subtleties with spectral parameter and its signs appear because of the closed paths which go around cylinder. For discussions see [84] and [125].

3.4.3 Integrable systems on Poisson-Lie group

Another origin of cluster coordinates in integrable systems is factorization ansätze for elements of Poisson-Lie group $\widehat{\mathrm{PGL}}(N)$ [49], [82], [**?**], which appeared in theory of positive matrices [57]. In this approach phase spaces of systems are double Bruhat cells $B_w \subset \widehat{\mathrm{PGL}}(N)$, which are enumerated by elements w of extended double Weyl group $\widetilde{W}\left(A^{(1)}_{N-1} \times A^{(1)}_{N-1}\right)$, which has presentation

$$\widetilde{W}\left(A^{(1)}_{N-1} \times A^{(1)}_{N-1}\right) = \tag{3.48}$$

$$= \left\langle \begin{array}{c|l} s_i, \bar{s}_i, \Lambda & s_i s_{i+1} s_i = s_{i+1} s_i s_{i+1}, \quad \Lambda s_i = s_{i+1}\Lambda, \quad s_i^2 = 1, \quad \bar{s}_i s_j = s_j \bar{s}_i, \\ i \in \mathbb{Z}/N\mathbb{Z} & \bar{s}_i \bar{s}_{i+1} \bar{s}_i = \bar{s}_{i+1} \bar{s}_i \bar{s}_{i+1}, \quad \Lambda \bar{s}_i = \bar{s}_{i+1}\Lambda, \quad \bar{s}_i^2 = 1 \end{array} \right\rangle.$$

Each reduced decomposition of w into product of generators $s_i, \bar{s}_i, \Lambda$ provides open embedding of $\mathcal{X}$-cluster chart in B_w: to each generator one assigns certain matrix (namely, transfer matrix in one-path sector of blocks shown in Fig. 3.9), depending on $\mathcal{X}$-cluster variables. Product of these matrices in the same order, as letters in the word w are located, provide matrix $g(\lambda)$ parametrizing B_w. Cycle h_A is chosen to be interval lying on the 'back' side of cylinder and connecting its left and right boundaries, so the dependence on λ comes from generators $s_0, \bar{s}_0$ and Λ which contain edges crossing h_A, for details see [**?**].

The restriction of r-matrix bracket with trigonometric r-matrix

$$\{g(\lambda_1) \otimes g(\lambda_2)\} = [r(\lambda_1/\lambda_2), g(\lambda_1) \otimes g(\lambda_2)] \tag{3.49}$$

to double Bruhat cells, which are Poisson submanifolds, turns out to be compatible with logarithmically constant bracket (3.21). The simplest way to check this is by checking for each block drawn in Fig 3.9, and using co-product property of r-matrix bracket, that if g_1 and g_2 satisfy it, then $g_1 g_2$ also satisfies. Exchange matrix ε can be easily written from the word w by considering graphs, dual to those drawn in Fig. 3.9, as it was done in Fig. 3.5. Change of reduced decomposition via Coxeter relations $s_i s_{i+1} s_i = s_{i+1} s_i s_{i+1}$ and $\bar{s}_i \bar{s}_{i+1} \bar{s}_i = \bar{s}_{i+1} \bar{s}_i \bar{s}_{i+1}$ amounts in single four-move and pair of two-moves. Relation $\bar{s}_i s_j = s_j \bar{s}_i$ can be realized as single two-move and does not affect exchange matrix if $i = j \pm 1$, and is single four-move if $i = j$. The relations $s_i^2 = 1$ and $\bar{s}_i^2 = 1$ can be done by pair of two-moves followed by parallel bigon reduction of type (b), and therefore are not cluster transformations and do not preserve transfer

matrix, however preserves wiring of zig-zags. If one applies parallel bigon reduction of type (a) instead, one gets Weyl semi-group with relation $s_i^2 = s_i$. Below we will assume that we use reduction of type (b).

Spectral curve of integrable system is given by characteristic equation

$$S(\lambda, \mu) = \det(g(\lambda) - \mu). \tag{3.50}$$

Hamiltonians of the system are Ad-invariant functions on Bruhat cells, and so only conjugacy class of word w matters. Taking characteristic equation of $g(\lambda)$ is close relative of gluing torus into cylinder, so the spectral curve coincides with the one given by (3.43) up to transformations $S(\lambda, \mu) \mapsto f(\lambda)S(\lambda, \mu),\ \mu \mapsto g(\lambda)\mu$, where f, g are some rational functions with coefficients depending on Casimirs.

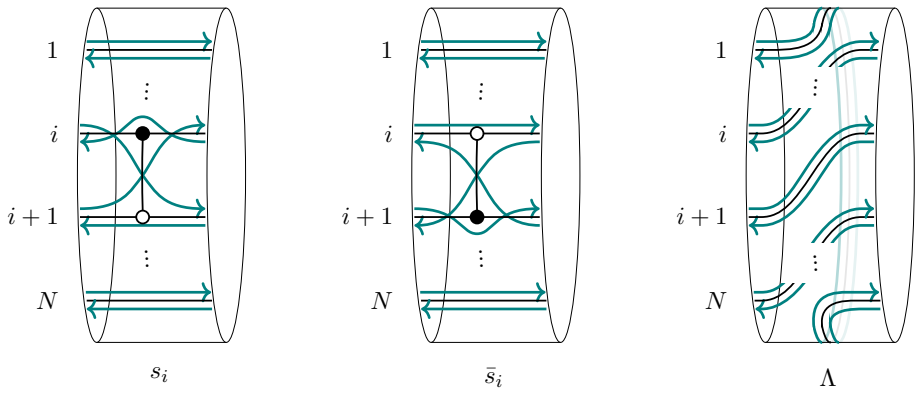

Figure 3.9. Basic graphs on cylinder corresponding to generators of Weyl group. Zig-zag paths are drawn by green lines, and generators act on their ends by permutation. Note that zig-zags are drawn so, that in-going and out-going ends of zig-zags alternate along the boundary.

Important observation, which we will need in the following, is that the building blocks for $s_i, \bar{s}_i, \Lambda$ indeed 'permute' zig-zag paths, which we will sometimes refer as strands. One can see in Fig. 3.9 that zig-zags going from the left to the right along lines i and $i+1$ are permuted after passing s_i, while $\bar{s}_i$ permutes those going from the right to the left along i and $i + 1$. Note, that the label i of generators s_i and $\bar{s}_i$ is given not by the number of zig-zag, but by the number of horizontal line of bi-coloured

graph. Generator Λ shifts by $+1$ all zig-zags going from the left to the right, and by -1 those going from the right to the left.

Weyl group interpretation of tetrahedron equation Double Weyl group of $\widehat{\mathrm{PGL}}(N)$ contains diagonal subgroup $W(A^{(1)}_{N-1}) \subset W(A^{(1)}_{N-1} \times A^{(1)}_{N-1})$ generated by $s_i\bar{s}_i$ and Λ. Comparing Fig. 3.6 and Fig. 3.9 one sees that plabic graphs corresponding to Lax operator of Bazhanov and Sergeev coincides with the one presenting word $s_i\bar{s}_i$ in double Weyl group! As we will see below, systems with symmetric Newton polygons can be constructed using diagonal subgroup only, so this again gives construction of integrable system with arbitrary symmetric Newton polygon from contraction of Lax operators (3.11). Tetrahedron transformation shown in Fig. 3.7, can be interpreted just as braiding relation

$$\mu_{\mathcal{R}}: \quad (s_i\bar{s}_i)(s_{i+1}\bar{s}_{i+1})(s_i\bar{s}_i) \mapsto (s_{i+1}\bar{s}_{i+1})(s_i\bar{s}_i)(s_{i+1}\bar{s}_{i+1}) \tag{3.51}$$

for diagonal subgroup of $\widetilde{W}(A^{(1)}_{N-1} \times A^{(1)}_{N-1})$. This is the same transformation, which relates two 'positive' parametrizations [57] for the largest Bruhat cell w_0 in PGL(3).

The functional tetrahedron equation (3.10) recasts into statement, that two ways to identify two different parametrizations for the largest Bruhat cell w_0 in PGL(4) are equivalent

$$w_0 = (s_1\bar{s}_1s_2\bar{s}_2s_3\bar{s}_3)(s_1\bar{s}_1s_2\bar{s}_2)(s_1\bar{s}_1) \cong (s_3\bar{s}_3s_2\bar{s}_2s_1\bar{s}_1)(s_3\bar{s}_3s_2\bar{s}_2)(s_3\bar{s}_3). \tag{3.52}$$

Symmetric Newton polygon Now, we are ready to show how construction from section 3.4.2 for integrable system with symmetric Newton polygon $(\vec{u}_1, ..., \vec{u}_r, -\vec{u}_1..., -\vec{u}_r)$ can be reproduced for double Bruhat cell of the group $\widehat{\mathrm{PGL}}(N)$, $N = a_1 + ... + a_n$. Construction comes from consideration of commuting subgroups $\widehat{\mathrm{PGL}}(a_1) \times \widehat{\mathrm{PGL}}(a_2) \times ... \times \widehat{\mathrm{PGL}}(a_n)$ in $\widehat{\mathrm{PGL}}(N)$, similar to those from [53], and observation that s_i and $\bar{s}_i$ act on zig-zag paths by permutations. Consider subgroup $\widetilde{W}_{i,j} = \widetilde{W}(A^{(1)}_{j-i} \times A^{(1)}_{j-i}) \subset \widetilde{W}(A^{(1)}_{N-1} \times A^{(1)}_{N-1})$ which permutes strands from i to j keeping

other strands intact. More precisely, generators s'_i, Λ' of this subgroup are

$$\begin{aligned}
&s'_a = s_{i+a-1}, \quad \bar{s}'_a = \bar{s}_{i+a-1}, \quad 1 \le a \le j-i,\\
&s'_0 = s_{i-1}s_{i-2}...s_1s_0s_{N-1}...s_{j+1}s_js_{j+1}...s_{N-1}s_0s_1...s_{i-2}s_{i-1},\\
&\bar{s}'_0 = \bar{s}_{i-1}\bar{s}_{i-2}...\bar{s}_1\bar{s}_0\bar{s}_{N-1}...\bar{s}_{j+1}\bar{s}_j\bar{s}_{j+1}...\bar{s}_{N-1}\bar{s}_0\bar{s}_1...\bar{s}_{i-2}\bar{s}_{i-1},\\
&\Lambda' = s_{i-1}\bar{s}_{i-1}s_{i-2}\bar{s}_{i-2}...s_1\bar{s}_1s_0\bar{s}_0s_{N-1}\bar{s}_{N-1}...s_{j+1}\bar{s}_{j+1}\Lambda,
\end{aligned} \tag{3.53}$$

so generators from s'_1 to s'_{j-i-1} act on strands $i, ..., j$ as usual, while the affine generators are 'skipping' other strands $1, ..., i-1, j+1, ..., N$. Generator Λ' of subgroup $W_{i,j}$ will be referred as $\Lambda_{i,j}$ in the following. Note, that bipartite graph defined by block Λ_{ij} is the same stripe of four-gons as a one, which appeared in Section 3.4.2.

It is always possible using $\mathrm{SA}(2,\mathbb{Z})$ transformation to place Newton polygon in such a way, that it does not have any vertical sides. It is straightforward to check that the Bruhat cell which gives Newton polygon $(\vec{u}_1, ..., \vec{u}_n, -\vec{u}_1..., -\vec{u}_n)$ is defined then by element

$$w = (\Lambda_{1,r_1})^{b_1}(\Lambda_{r_1+1,r_2})^{b_2}...(\Lambda_{r_{n-1}+1,r_n})^{b_n}, \quad r_k = a_1 + ... + a_k \tag{3.54}$$

in double Weyl group. Side (a_k, b_k) of the Newton polygon is generated by strands $a_{r_{k-1}+1}, ..., a_{r_k}$. Together they got projection a_k on the generator of homologies oriented along cylinder. Generator $\Lambda_{r_{k-1}+1,r_k}$ mixes only them, and each application of this 'twist' operator increases their common projection on generator of homologies, oriented across cylinder, by 1. By applying it b_k times and making torus from cylinder, they are gluing into longer strands representing class $(a_k, b_k) \in \mathrm{H}_1(\mathbb{T}^2, \mathbb{Z})$, so it presents side $\vec{u}_k$ of the Newton polygon. Strands going along the same lines but with the opposite orientations generate class $-\vec{u}_k$.

Non-symmetric Newton polygons For integrable system with non-symmetric Newton polygon it is convenient to present Lax operator in triangular decomposed form. This requires getting out of diagonal subgroup of $\widetilde{W}(A^{(1)}_{N-1} \times A^{(1)}_{N-1})$, and considering separately 'positive' and 'negative' commuting subgroups $\widetilde{W}(A^{(1)}_{a_1-1}) \times ... \times \widetilde{W}(A^{(1)}_{a_n-1})$ and $\widetilde{W}(A^{(1)}_{c_1-1}) \times ... \times \widetilde{W}(A^{(1)}_{c_m-1})$, where $\vec{u}_1 = (a_1, b_1), ..., \vec{u}_n = (a_n, b_n)$ are primitive oriented boundary intervals of polygon between the leftmost and rightmost points, $\vec{v}_1 = (-c_1, -d_1), ..., \vec{v}_m = (-c_m, -d_m)$ are intervals between the rightmost

and leftmost points in counter-clockwise direction. Introducing halves of 'twisting' operators

$$\Lambda^+_{ij} = s_{i-1}s_{i-2}...s_1 s_0 s_{N-1}...s_{j+1}\Lambda, \quad \Lambda^-_{ij} = \bar{s}_{i-1}\bar{s}_{i-2}...\bar{s}_1\bar{s}_0\bar{s}_{N-1}...\bar{s}_{j+1}\Lambda, \tag{3.55}$$

where $r_i = a_1 + ... + a_i$ and $l_i = c_1 + ... + c_i$, the word in double Weyl group which provides wiring diagram for non-symmetric Newton polygon is

$$w = w^+ w^- \Lambda^{-b_1-...-b_n}, \tag{3.56}$$
$$w^+ = (\Lambda^+_{1,r_1})^{b_1}...(\Lambda^+_{r_{n-1}+1,r_n})^{b_n}, \quad w^- = (\Lambda^-_{1,l_1})^{d_1}...(\Lambda^-_{l_{m-1}+1,l_m})^{d_m},$$

see example in Fig. 3.10, left. As far as the shifts $w^- \mapsto \Lambda^k w^- \Lambda^{-k}$ preserve Newton polygon, $b_1 + ... + b_n = d_1 + ... + d_m$ and only the conjugacy class of word matters, the same Newton polygon is provided by $w = w^- w^+ \Lambda^{-d_1-...-d_n}$. The upper- and lower- diagonal Lax operators defined by $w^\pm$ are constructed from hexagonal graph, in contrast to the symmetric case, where the basic building blocks were four-gonal 'fence-net' graph.

Wiring of parallel zig-zags It remains to discuss a wiring of parallel zig-zags. Take Newton polygon with integral points on the boundary, which are not at the corners, i.e. those having at least one 'non-simple' side $\vec{u}'_k = h_k \cdot (a_k, b_k)$, with $\gcd(a_k, b_k) = 1$ ($h_k > 0$, and let $a'_k > 0$ for certainty). Considering h_k simple boundary intervals (a_k, b_k) separately, one gets h_k commuting sub-groups $(\widetilde{W}(A^{(1)}_{a_k-1}))^{\times h_k}$, whose resulting contribution into word in double Weyl group by twists is

$$w_{k,k+h_k} = \left(\Lambda^+_{r_{k-1}+1,r_{k-1}+a_k}\right)^{b_k} ... \left(\Lambda^+_{r_{k-1}+(h_k-1)a_k+1,r_{k-1}+h_k a_k}\right)^{b_k}. \tag{3.57}$$

Alternatively, one can consider this intervals together, which gives group $\widetilde{W}(A^{(1)}_{h_k a_k-1})$ contributing by

$$w_{k,k+h_k} = \left(\Lambda^+_{r_{k-1}+1,r_{k-1}+h_k a_k}\right)^{b_k h_k}. \tag{3.58}$$

Two choices can be transformed one into another by local moves, however the second ansatz is more reduced compared to the first one, as it involves $(N - a_k h_k + 1)b_k h_k$ generators against $(N - a_k + 1)b_k h_k$ in the first case. Another benefit is that it can be easily extended to involve 'wiring' of parallel strands, by

$$w_{k,k+h_k} = \left(\Lambda^+_{r_{k-1}+1,r_{k-1}+h_k a_k}\right)^{h_k b_k} \tilde{w}_k, \quad \tilde{w}_k \in W(A_{h_k-1}), \tag{3.59}$$

where $W(A_{h_k-1})$ is group acting by permutations of strands $r_{k-1}+1, r_{k-1}+2, ..., r_{k-1}+h_k$, see example in Fig. 3.10, right. One can assign such 'non-affine' word to each non-simple boundary interval of Newton polygon, however it is more natural not to bring all parallel intervals together, but to join them according to decomposition of $\tilde{w}_k$ into a product of simple cycles.

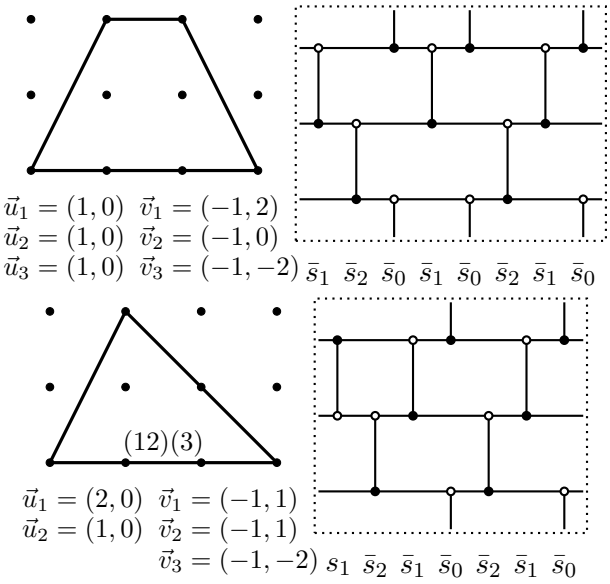

Figure 3.10. Top: Example of the double Bruhat cell in $\widehat{\mathrm{PGL}}(3)$ with non-symmetric Newton polygon. The corresponding element in the double Weyl group is $w = (\Lambda^-_{1,1})^{-2}(\Lambda^-_{3,3})^2 = (\bar{s}_0\bar{s}_2\Lambda)^{-2}(\bar{s}_2\bar{s}_1\Lambda)^2 = \bar{s}_1\bar{s}_2\bar{s}_0\bar{s}_1\bar{s}_0\bar{s}_2\bar{s}_1\bar{s}_0$, where we used commutation relations of $\bar{s}_i$ with Λ. The bipartite graphs are drawn on torus, i.e. one has to glue right side with the left one, and upper with the lower. Bottom: Example of the double Bruhat cell in $\widehat{\mathrm{PGL}}(3)$ with non-trivial wiring of parallel zig-zags, the corresponding element in double Weyl group is $w = s_1(\Lambda^-_{1,1})^{-1}(\Lambda^-_{2,2})^{-1}(\Lambda^-_{3,3})^2 = s_1(\bar{s}_0\bar{s}_2\Lambda)^{-1}(\bar{s}_1\bar{s}_0\Lambda)^{-1}(\bar{s}_2\bar{s}_1\Lambda)^2 = s_1\bar{s}_2\bar{s}_1\bar{s}_0\bar{s}_2\bar{s}_1\bar{s}_0$.

3.4.4 Classification of perfect networks on torus

Systematizing examples of previous subsection, we show now that all bi-coloured graphs on torus can be reduced by local moves to 'normal forms', which are enumerated by Newton polygons (containing information about

winding of zig-zags on torus), with the sides containing integral internal points partitioned according to the wiring of parallel zig-zags. Normal form attributed to graph is unique, up to $\mathrm{SA}(2,\mathbb{Z})$ transformation of Newton polygon. Similar combinatorics already appeared in [34] in the description of moduli spaces of monopole walls.

The statement is straightforward consequence of the fact, proved in [55], that one can always 'slice' bipartite graph on torus, and put into correspondence to it some conjugacy class in double Weyl group (3.48), and the following

Lemma. Any conjugacy class in double Weyl group (3.48) contains unique element of the form

$$w = w_1^+ \cdot ... \cdot w_n^+ \cdot w_1^- \cdot ... \cdot w_m^- \cdot \Lambda^{-b_1-...-b_n}, \tag{3.60}$$

$$w_k^+ = \left(\Lambda^+_{r_{k-1}+1,r_k}\right)^{b_k} (r_{k-1}+\gcd(a_k,b_k),...,r_{k-1}+1),$$

$$w_k^- = \left(\Lambda^-_{l_{k-1}+1,l_k}\right)^{d_k} \overline{(l_k+\gcd(c_k,d_k),...,l_k+1)},$$

where

- Numbers a_k, b_k, c_k, d_k define ordered set of counter-clockwise oriented, boundary intervals $\vec{u}_k = (a_k, b_k)$, $\vec{v}_k = (-c_k, -d_k)$ with $a_k, c_k > 0$, of some Newton polygon of width N. The order starts from the direction $(0,-1)$, 'parallel' vectors (i.e. proportional, with positive rational coefficient)[9] are ordered from the longest to shortest.

- Numbers r_k, l_k are defined by $r_k = a_1 + ... + a_k$, $l_k = c_1 + ... + c_k$ for $k > 0$, $r_0 = l_0 = 0$.

- Words $\Lambda^{\pm}_{ij}$ are 'subgroup twists' defined by formula (3.55).

- Words $(j,...,i) = s_i s_{i+1} ... s_{j-2} s_{j-1}$ and $\overline{(j,...,i)} = \bar{s}_i \bar{s}_{i+1} ... \bar{s}_{j-2} \bar{s}_{j-1}$ are simple cycles[10], $i < j$.

[9] Sides of the Newton polygon, containing internal integral points, can be split into pieces in various different ways.

[10] The name comes from its action as permutation $j \mapsto j-1, ..., i+1 \mapsto i, i \mapsto j$

Proof. Any element w of the group $\widetilde{W}(A^{(1)}_{N-1} \times A^{(1)}_{N-1})$ admits decomposition $w = w^+ w^- \Lambda^{-K}$, where w^+, w^- are words, which contain only generators s_i, Λ or $\bar{s}_i, \Lambda$ respectively, and total degree of Λ in either w^+ or w^- is K. Both $w^\pm$ belong to sub-groups of $\widetilde{W}(A^{(1)}_{N-1})$ - type, so we will classify conjugacy classes of its elements, and then show, how ambiguity with the distribution of Λ can be fixed. Choose for definiteness subgroup generated by s_i, Λ. There is a structure of semi-direct product

$$\widetilde{W}(A^{(1)}_{N-1}) = \mathbb{Z}^N \rtimes W(A_{N-1}), \tag{3.61}$$

which comes from presentation $w^+ = L \cdot g$, where g is element of non-affine Weyl group generated by s_i, and L is element of lattice generated by commuting elements $\Lambda^+_{i,i}$, as defined in (3.55), i.e. those which take strand, wind it up over cylinder, and bring back onto initial place. Writing this as pairs, and using additive notation for elements of lattice $e_i = \Lambda^+_{i,i}$, we get product rule

$$(L_1\,;\, g_1) \cdot (L_2\,;\, g_2) = (L_1 + R_{g_1}(L_2)\,;\, g_1 g_2), \tag{3.62}$$

where R_{g_1} acts on the basis elements of lattice by permutations

$$R_{s_i}(e_i) = e_{i+1},\ R_{s_i}(e_{i+1}) = e_i,\ R_{s_i}(e_j) = e_j \text{ if } i \neq j, j{+}1 \text{ and } R_{g_1} R_{g_2} = R_{g_1 g_2}. \tag{3.63}$$

The conjugacy classes in $\widetilde{W}(A^{(1)}_{N-1})$ are in bijection with the set of pairs $(\vec{q}, \lambda)$, where $\lambda = (\lambda_1 \geq ... \geq \lambda_{\ell(\lambda)} > 0)$ is the partition of number N, $\vec{q} \in \mathbb{Z}^{\ell(\lambda)}$ and $\ell(\lambda)$ is the number of parts in the partition λ. Indeed, conjugacy classes of permutations on N elements are enumerated by partitions λ of number N, each containing representative

$$(p_1, ..., 1)(p_2, ..., p_1 + 1) ... (p_{\ell(\lambda)}, ..., p_{\ell(\lambda)-1} + 1), \tag{3.64}$$

where $p_0 = 0$, $p_i = \lambda_1 + ... + \lambda_i$, and $(j, ..., i) = s_i ... s_{j-1}$ is cyclic permutation, acting on the lattice by

$$R_{(j,...,i)}: \quad e_i \mapsto e_{i+1} \quad , \quad ... \quad , \quad e_{j-1} \mapsto e_j \quad , \quad e_j \mapsto e_i \tag{3.65}$$

for $i < j$. As simple cycles $(p_k, ..., p_{k-1} + 1)$ commute for different k, and generators of the lattice can be shifted along the cycles

$$[(e_k\,;\, \mathrm{id}) \cdot (0\,;\, (j, ..., i))] = [(e_l\,;\, \mathrm{id}) \cdot (0\,;\, (j, ..., i))], \quad \forall\ i \leq k, l \leq j, \tag{3.66}$$

where [ ] is taking of conjugacy class, then by moving elements of the lattice to the 'first lines', one gets

$$[w^+] = [w_1^+ ... w_{\ell(\lambda)}^+], \quad w_k^+ = (q_k \cdot e_{p_{k-1}+1}\,;\,(p_k, \dots, p_{k-1}+1)), \qquad (3.67)$$

for some $q_k \in \mathbb{Z}$, so the vector $\vec{q} = (q_1, ..., q_{\ell(\lambda)})$ is the vector of the 'lengths' of lattice elements. To put conjugacy class in the form of the products of 'twists' Λ_{ij}, note that

$$\left(\Lambda_{p_{k-1}+1,\,p_k}\right)^{q_k} \cdot (p_{k-1}+\gcd(\lambda_k, q_k), \dots, p_{k-1}+1) = (V_k\,;\,\sigma_k\,(p_k, p_{k-1}+1)\,\sigma_k^{-1}), \qquad (3.68)$$

where the lattice element $V_k = t'_k(e_{p_{k-1}+1}+...+e_{p_k})+e_{p_{k-1}+1}+...+e_{p_{k-1}+t''_k}$ with $t'_k \in \mathbb{Z}_{\geq 0},\ 0 \leq t''_k < \lambda_k$ is defined by $q_k = t'_k\lambda_k + t''_k$, and comes from decomposition

$$\left(\Lambda_{p_{k-1}+1,\,p_k}\right)^{q_k} = (V_k\,;\,(p_k, ..., p_{k-1}+1)^{q_k}), \qquad (3.69)$$

which can be checked by direct computation, using that $\Lambda_{ij}^+ = (k, \dots, i) \cdot \Lambda_{kk}^+ \cdot (j, \dots, k)$ for any $i \leq k \leq j$, and non-affine permutation σ_k is defined from

$$(p_k, ..., p_{k-1}+1)^{q_k} \cdot (p_{k-1}+\gcd(\lambda_k, q_k), \dots, p_{k-1}+1) = \sigma_k \cdot (p_k, ..., p_{k-1}+1) \cdot \sigma_k^{-1} \qquad (3.70)$$

which holds, because all orbits of the action of $i \mapsto i + q_k$ on $\mathbb{Z}/\lambda_k\mathbb{Z}$ can be uniquely presented by one of the numbers $1, ..., \gcd(\lambda_k, q_k)$, so both sides of (3.70) got only one orbit. From (3.68), using (3.66), for conjugacy classes follows

$$\begin{aligned}[(\Lambda_{p_{k-1}+1,\,p_k})^{q_k} \cdot (p_{k-1}+\gcd(\lambda_k, q_k), \dots, p_{k-1}+1)] = \qquad (3.71)\\ = [(q_k \cdot e_{p_{k-1}+1}\,;\,(p_k, ..., p_{k-1}+1))] = [w_k^+],\end{aligned}$$

which is almost statement of the Lemma. The w^- part can be reduced to the normal form, encoded by $(\vec{\bar{q}}, \bar{\lambda})$, in the same way. The only element, which is common for words w^+ and w^- is Λ, which also do not commute with all generators s_i and $\bar{s}_i$. However, we initially distributed it in $w = w^+w^-\Lambda^{-K}$ in a such way, that the total degree of Λ inside $w^-\Lambda^{-K}$ or $\Lambda^{-K}w^+$ is zero, so the treatment of w^+ or w^- is not affected by another part. Finally, conjugating $w^\pm$ by suitable permutations from non-affine parts, we can rearrange indices of $s_i, \bar{s}_i$ inside $w_k^\pm$ by counter-clockwise order on the directions of vectors (λ_i, q_i), $(-\bar{\lambda}_i, -\bar{q}_i)$, starting from the

direction $(0,-1)$, and by decrease of lengths for the vectors of the same slope, obtaining numbers (a_i, b_i) and (c_i, d_i). The properties that the sum of vectors is zero, i.e. that they can be composed into the boundary of Newton polygon, and that the width of this polygon is N, are guaranteed by $\sum_i \lambda_i = \sum_i \bar{\lambda}_i = N$, $\sum_i q_i = \sum_i \bar{q}_i = K$.

3.5 Discussion

In this Chapter we have demonstrated that the Bazhanov-Sergeev solution of the tetrahedron equation appears naturally as the basic building block for the transfer matrix of paths in the theory of cluster integrable systems. We have also shown how the integrable system with arbitrary symmetric Newton polygon can be built using this building block. We have explained how this construction originates from the combinatorics of words in the double affine Weyl groups and used it to explicitly construct bi-coloured graph for the integrable system associated with any Newton polygon. We have also proven the classification Lemma stating that we have constructed all possible systems of such kind.

The following questions seem to be promising for future developments of this topic:

- As the Poisson brackets on weights of paths are bi-linearly constant, it can be quantized in a straightforward way by [48]

$$\{w_{\gamma_1}, w_{\gamma_2}\} = \varepsilon(\gamma_1,\gamma_2) w_{\gamma_1} w_{\gamma_2} \quad \longrightarrow \quad \hat{w}_{\gamma_1}\hat{w}_{\gamma_2} = t^{\frac{1}{2}\varepsilon(\gamma_1,\gamma_2)}\hat{w}_{\gamma_1+\gamma_2} \tag{3.72}$$

  The mutation, which was a canonical transformation classically, in the quantum world becomes a conjugation by quantum dilogarithm. Extension of the arguments presented in this Chapter to the quantum case will provide a closed formula for the tetrahedron $\mathcal{R}$-matrix $\mathcal{R}_{abc}$ in terms of four quantum dilogarithms. This can clarify the appearance of the product of four functions similar to quantum dilogarithms at the root of unity in the vertex weight of the 3d vertex model [10, 11, 107, 108], whose solution is known to be a solution of the tetrahedron equation [113, 170]. Such product (outside of the roots of unity) was also noted in [160]. Another promising direction of research is construction of new solution for the tetrahedron equation using cluster algebras with fermionic variables [152], as suggested by recent appearance of quivers with fermionic nodes in

representations theory of affine algebras [117, 126, 127, 12, 183] and approach of [162] to super-algebras using tetrahedron equation.

- Surprisingly, the same quiver and the same cluster transformation as those shown in Fig. 3.7 have already appeared in the context of the relation between cluster algebras and vertex integrable systems in [181]. The physical origin of these solutions was the 2d $\mathcal{N} = (2, 2)$ supersymmetric sigma-model, whose Kähler parameters were shown in [22] to transform as cluster variables under Seiberg dualities. From the other side, the approach to cluster integrable systems which we have used here is suspected to originate from $5d$ $\mathcal{N} = 1$ theories [39, 14, 140], where cluster variables play the role of Seiberg-Witten curve's moduli. This intriguing coincidence should have some unifying physical origins.

- The systems we have considered were mainly of "affine" type: they live on double Bruhat cells of the affine group $\widehat{\mathrm{PGL}}(N)$ and being rewritten in Darboux variables represent "closed" chains of interacting particles [39, 128, 55, 80]. The integrability theorem, proved in [71], assumes that the perfect network on torus is minimal, i.e. that its zig-zags do not have self-intersections, and that parallel zig-zags (those, whose classes in $\mathrm{H}_1(\mathbb{T}^2, \mathbb{Z})$ are proportional with positive coefficient) do not intersect. The cluster description of the "open" chains[11], which live on double Bruhat cells of the non-affine group $\mathrm{PGL}(N)$, involves networks drawn on a cylinder (or on a cut torus — this can be treated as a particular case of a "squashed" Newton polygon of zero area). So all the intersections of zig-zags are either self- or parallel-, and integrability of such systems is not guaranteed by [71]. However it can be proved by other methods.

  We have unified these classes of systems by considering the wiring of parallel zig-zags. As it was shown in [84], the Lax operator of any network on a cylinder has an r-matrix Poisson bracket with itself, however the general integrability criterion, which allows to compare the number of independent integrals of motion and the dimensions of the symplectic leaves still has to be developed.

- We have proven the classification theorem for bi-coloured graphs on

[11] Which were historically the first examples of the cluster description of integrable systems [82].

torus. Graphs which contain wiring of parallel zig-zags cannot be made minimal by local moves, i.e. self-intersections of zig-zags are protected by topology. However, they can always be made "locally minimal", which means that they become such networks on torus, that being cut by any curves into a disk, they become minimal network on the disk, as follows from the reduction theorem proved in [174]. In the language of double Weyl groups locally minimal diagrams are those defined by reduced words.

However, in our consideration we allowed to reduce parallel bigons by the use of $s_i^2 = 1$ which is not a cluster transformation. Classification of the normal forms of the locally minimal networks "up to cluster transformations" with the bigon reduction relation $s_i^2 = s_i$ seems to be a fruitful direction for further investigations, especially as it might exhibit interesting $\mathrm{SL}(2,\mathbb{Z})$ covariant behaviour [12]. The problem of parallel bigons itself is still poorly understood in cluster algebras, and also awaits its solution. We also expect, that the condition that the Newton polygon does not contain vertical sides might be removed and full $\mathrm{SL}(2,\mathbb{Z})$ covariance restored by the replacement of the double affine Weyl group with a certain generalization thereof, originating from toroidal algebras.

- In this Chapter we have been discussing continuous time integrability only. However, the cluster integrable systems are known to have rich discrete dynamics. In [65] the general structure of the group of discrete transformations generated by spider moves was given. However, it is known that even for quivers coming from bi-coloured graphs there is a much larger group of cluster transformations (sequences of mutations and permutations of quiver vertices) which bring quivers back into itself, which however cannot be represented by a sequence of bi-coloured graph transformations (see e.g. [99] for hexagonal lattice and [140] for the four-gonal one). These transformations are related to boundary intervals of Newton polygons with integral internal points, and realize permutations of "parallel" zig-zags (whose classes in torus homology coincide).

  We expect that using the results of this Chapter, a big piece of the cluster mapping class group containing the sub-group $W(A_N^{(1)})$

[12] However, we conjecture that the set of cyclically irreducible words will be the same for both relations, $s_i^2 = s_i$ and $s_i^2 = 1$.

for each boundary interval with N internal points, and a subgroup described in [65], can be explicitly constructed. The half Dehn-twists $\mathcal{R}$-matrix [87, 171] should also find their natural interpretation in this construction.

3.6 Appendix. Details on tetrahedron transformation.

As it was said in Section 3.3.2, it is easy to check that transformation of cluster variables (3.37) is agreed with tetrahedron transformation (3.13) via (3.32). However, it is not that easy to derive transformation rules for γ variables (3.35) directly from sequence of two- and four- moves. The major difficulty is that after sequence of moves shown in Fig. 3.11 new variables γ' defined in Fig. 3.7 can not be expressed using $\gamma_{x,i}$ with $x = a, b, c;\ i = 1, 2, 3, 4$ variables only, but more refined corner variables, $a_1, a_2, a_3, ..., l_1, l_2, l_3$, as indicated in Fig. 3.11, should be involved.

It turns out that this problem might be treated by choosing of appropriate gauge. After application of two- and four- moves one can still apply gauge transformations at points shown by grey crosses in Fig. 3.7, left, bottom, which transform γ' variables by

$$\begin{aligned}
&\gamma'_{a,1} \to X\gamma'_{a,1}, \quad && \gamma'_{a,2} \to X^{-1}Y\gamma'_{a,2}, && \gamma'_{a,3} \to Y^{-1}\gamma'_{a,3},\\
&\gamma'_{b,2} \to Z\gamma'_{b,2}, && \gamma'_{b,3} \to XZ^{-1}\gamma'_{b,3}, && \gamma'_{b,4} \to X^{-1}\gamma'_{b,4},\\
&\gamma'_{c,1} \to Z^{-1}\gamma'_{c,1}, && \gamma'_{c,4} \to Y^{-1}Z\gamma'_{c,4}, && \gamma'_{c,3} \to Y\gamma'_{c,3},
\end{aligned} \tag{3.73}$$

and change transfer matrix of each four-gonal block, but do not affect transfer matrix of whole network. Direct check shows[13] that once X, Y, Z are chosen to be

$$\begin{aligned}
X &= \sqrt{\frac{f_2\gamma_{a,4}}{e_3\gamma_{a,2}}}\left(\frac{\gamma_{a,1}\gamma_{a,4}\gamma_{b,3}^2\gamma_{c,1}\gamma_{c,2}}{\gamma_{a,2}\gamma_{a,3}\gamma_{b,1}^2\gamma_{c,3}\gamma_{c,4}}\right)^{1/8},\\
Y &= \sqrt{\frac{l_2b_2}{a_3k_3}}\left(\frac{d_3l_3}{i_2a_2}\right)^{3/8}\left(\frac{\gamma_{a,2}\gamma_{b,4}\gamma_{c,2}}{\gamma_{a,4}\gamma_{b,2}\gamma_{c,4}}\right)^{1/4},\\
Z &= \sqrt{\frac{h_2\gamma_{c,4}}{g_3\gamma_{c,2}}}\left(\frac{\gamma_{a,2}\gamma_{a,3}\gamma_{b,1}^2\gamma_{c,3}\gamma_{c,4}}{\gamma_{a,1}\gamma_{a,4}\gamma_{b,3}^2\gamma_{c,1}\gamma_{c,2}}\right)^{1/8},
\end{aligned} \tag{3.74}$$

[13] With four-move parameters chosen to be $\alpha_1 = \alpha_2 = 0,\ \alpha_3 = -\frac{1}{2}$ in (3.27)

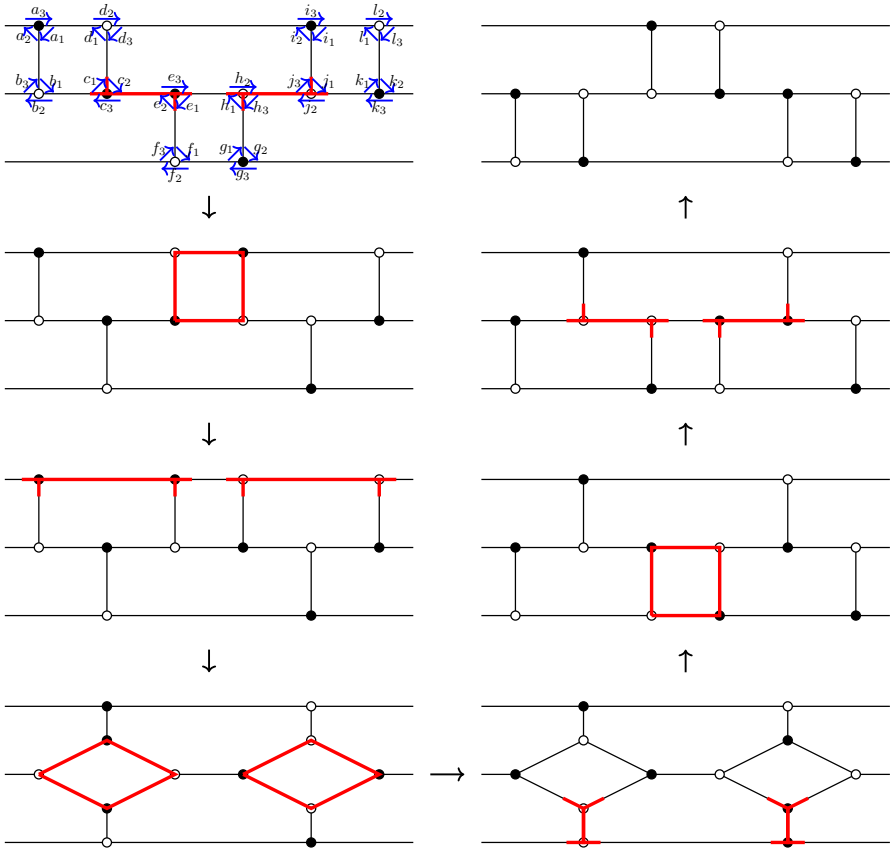

Figure 3.11. Tetrahedron transformation as sequence of eight two-moves and four spider-moves. Red colour highlights those parts of graph which being transformed by two- or four- moves.

transformed γ' variables match (3.35) obtained directly from (3.13) via (3.32).

Chapter 4

Topological strings amplitudes and Seiberg-Witten prepotentials from the counting of dimers in transverse flux

The proposal of this Paragraph is to show how the partition functions of topological strings can be obtained in purely cluster algebraic setting, building the missing red arrow on Fig. 1.1. We claim that in order to deautonomize the cluster integrable system, one has to uplift the Kasteleyn operator from torus to the plane, covering the torus. The deautonomization parameter q plays a role of the transverse flux of discrete $\mathbb{R}_{>0}$-connection. The partition function of dimers, which provided spectral curve in the autonomous case, becomes a partition function of dimers on the infinite plane. We claim, that being properly regularized and with certain scaling of parameters, this partition function reproduces the counting of topological vertices, which constitute topological string partition function.

This proposal is well agreed with the topological strings/spectral theory correspondence like in [16], since the partition function of dimers on a plane can be computed using the determinant of Kasteleyn operator,

which in this case is almost a quantization of spectral curve. Cluster algebraic interpretation of partition functions opens a room for proving bilinear relations among them as for A-cluster variables related by mutations of the cluster seed.

Structure of this Chapter In the Paragraph we illustrate all constructions using the single example of cluster integrable system isomorphic to relativistic Toda chain on two sites, which is shown on Fig. 1.1.

In Section 4.1 we introduce basic objects and recollect necessary facts on thermodynamic of dimer statistical models. Then we explain how the "deautonomization" of $\prod_f x_f = q \neq 1$ can be achieved by replacing spectral parameters λ, μ in the Kasteleyn operator of dimers on torus by the q-commuting operators of magnetic translations $\tilde{\mathrm{T}}_x$, $\tilde{\mathrm{T}}_y$. We also discuss degeneracy of their action on the space of functions on $\mathbb{Z}^2$ due to their commutativity with the dual magnetic translations.

In Section 4.2 we discuss $q \to 1$ limit. We show how the solution of "limit shape" problem can be derived from the WKB approximation for Kasteleyn operator. We show then that the free energy of the model, properly regularized in this limit, gives closed formula for the Seiberg-Witten prepotential of corresponding $5d$ $\mathcal{N} = 1$ gauge theory.

In Section 4.3 we show how all the necessary box-counting degrees of freedom arise from the counting of dimers, resulting in the main formula of equality of partition function of dimers (in the proper limit) to the dual partition function of topological strings

$$\mathcal{Z}(Q_0 = q, Q_B, Q_F, Q_2) = \tag{4.1}$$

$$= \sum_{n \in \mathbb{Z}} (Q_2)^{n-1} (Q_B Q_F)^{n(n-1)} q^{\frac{2}{3} n(n-1)(2n-1)} Z_{\text{boxes}}(q, q^{2n} Q_B, q^{2n} Q_F).$$

where Z_{boxes} is defined in 1.2. Then, we discuss some issues of inconsistency of the requirements of "infinite distance" between the walls of the room, and of "freezing out" of non-boxcounting degrees of freedom.

In Section 4.4 we outline results of the Paragraph, and propose some directions for the future developments.

4.1 Kasteleyn operator of dimers in transverse flux

In this section we will show, how making edge weights linearly dependent on the position of fundamental cell, one can relax condition $\prod_{f\in F_1} x_f = q = 1$, deautonomizing cluster integrable system.

4.1.1 Zero flux

Definition of the model. The dimer models are usually defined on bipartite graphs, such graphs Γ that the vertices V can be decomposed into black and white subsets $V = B \sqcup W$, and edges connect only vertices of the opposite colours, see example of Fig. 4.1. Throughout the Chapter we assume the graphs to be minimal in the sense of [71]. The edges $e \in E$ are weighted by the positive real statistical weights $w_e \in \mathbb{R}_{>0}$ for edges oriented from black to white vertex (which is assumed to be canonical in the following), and by weights $w_{-e} = w_e^{-1}$ for the edges taken with opposite orientations. We also extend multiplicatively w to any sets S of edges by $w_S = \prod_{e\in S} w_e$. It is often instructive to consider edge weights as discrete connections in $\mathbb{R}_{>0}$-bundle over Γ.

The possible microscopic states of the model are dimers configurations $D \in \mathcal{D}(\Gamma)$ (also called perfect matchings) on Γ, which are such collections of edges of Γ, that each vertex have exactly one adjacent edge from this collection and all edges are taken with the canonical black-to-white orientation. The partition function can be defined, as usual, as a sum of statistical weights over all configurations

$$\mathcal{Z}(\Gamma, w) = \sum_{D\in\mathcal{D}(\Gamma)} w_D. \tag{4.2}$$

It changes by simple common factor

$$\mathcal{Z}(\Gamma, w) \mapsto \left(\prod_{v\in B} g_v^{-1}\right)\left(\prod_{v\in W} g_v\right)\mathcal{Z}(\Gamma, w)$$

under $\mathbb{R}_{>0}$ gauge transformations of edge weights

$$w_e \mapsto g_{t(e)} w_e g_{s(e)}^{-1} \tag{4.3}$$

where g is $\mathbb{R}_{>0}$-valued function on vertices, and $s(e)$, $t(e)$ are starting and terminal vertices of edge e. So it is meaningful to consider the partition

function normalized by the weight of some fixed dimers configuration D_0

$$\mathcal{Z}(\Gamma, w; D_0) = \frac{\mathcal{Z}(\Gamma, w)}{w_{D_0}} = \sum_{D \in \mathcal{D}(\Gamma)} w_{D-D_0}. \tag{4.4}$$

which depends, for planar graphs, only on gauge invariant face weights $x_f = \prod_{e \in \partial f} w_e$, since for any dimers configurations D, D_0 holds $\partial(D - D_0) = 0$ and any cycle in a disk is contractible.

Kasteleyn operator. The dimer models are "free fermionic": it simply follows from the definition of determinant, that their partition functions can be effectively computed [105] as determinants

$$\mathcal{Z}(\Gamma, w) = \pm \det \mathrm{K}_\Gamma \tag{4.5}$$

where Kasteleyn matrix $\mathrm{K}_\Gamma : \mathbb{C}^{|B|} \to \mathbb{C}^{|W|}$ is twisted by additional signs weighted adjacency matrix of Γ

$$(\mathrm{K}_\Gamma)_{\alpha,\beta} = \sum_{\partial e = \alpha - \beta} (-1)^{\varkappa_e} w_e, \quad \alpha \in W,\ \beta \in B, \tag{4.6}$$

and signs $(-1)^{\varkappa_e}$, called Kasteleyn orientation, for every face f are required to satisfy condition

$$\prod_{e \in \partial f} (-1)^{\varkappa_e} = (-1)^{|\partial f|/2+1}. \tag{4.7}$$

For planar graph all Kasteleyn orientations are equivalent up to $\mathbb{Z}/2\mathbb{Z}$ gauge transformations

$$(-1)^{\varkappa_e} \mapsto (-1)^{\sigma_{s(e)} + \sigma_{t(e)}} (-1)^{\varkappa_e} \tag{4.8}$$

where $(-1)^{\sigma}$ is ± 1-valued function on vertices. The overall sign $\pm$ in (4.5) is gauge-dependent.

Fugacities of the translation invariant model on infinite lattice. The bipartite graph is called periodic and planar if it can be embedded into plane $\mathbb{R}^2$ without intersections of edges and in a way invariant under the action of a $\mathbb{Z}^2$ lattice generated by the pair of discrete translations $\mathrm{T}_x, \mathrm{T}_y$. The fundamental domains of this action are cells of rectangular grid, formed by infinite simple horizontal and vertical curves

$\gamma_{h,j} = (\mathrm{T}_y)^j \gamma_{h,0}$ and $\gamma_{v,i} = (\mathrm{T}_x)^i \gamma_{v,0}$ transversal to edges, cell (i,j) is bounded by the curves $\gamma_{v,i}, \gamma_{v,i+1}$ and $\gamma_{h,i}, \gamma_{h,i+1}$, see Fig. 4.1, left. We decompose set of vertices as $V = V_1 \times \mathbb{Z}^2$, where the first multiplier is finite and counts vertices inside of the cell, and the second denotes position of fundamental cell which a vertex belongs to. We assume that V_1 contains equal number of black and white vertices B_1 and W_1. Sets of edges and faces could be decomposed in a similar way $E = E_1 \times \mathbb{Z}^2$, $F = F_1 \times \mathbb{Z}^2$, where we attribute an edge to the fundamental cell according to the position of the black vertex adjacent to it, and a face intersecting few cells to one of the fundamental cells which it intersects.

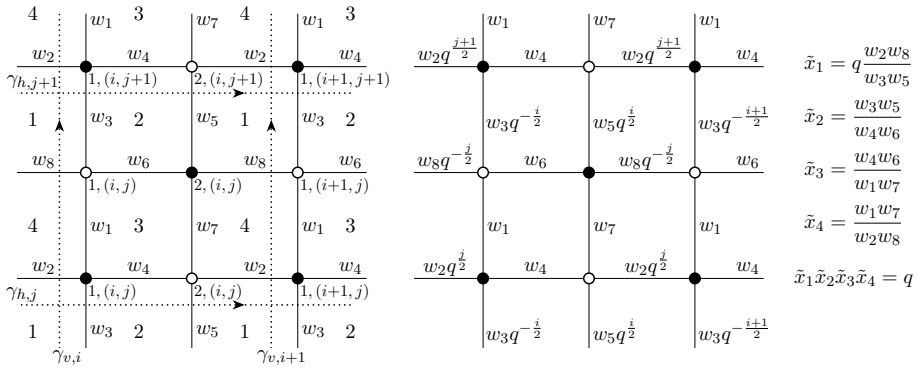

Figure 4.1. Example of bipartite graph, known to describe Toda integrable chain on two sites. Left: labelling of vertices, faces, and edge weights. Since we consider only periodic weightings of faces, we do not put labels of their fundamental domains on the plot. Right: edges weighting of finite flux $q = e^{-\varepsilon}$, according to (4.18) and face weights expressed in terms of edge weights.

If the weighting on periodic graph is also periodic $w_e = w_{\mathrm{T}_x e} = w_{\mathrm{T}_y e}$, then by factorization of plane by $\mathbb{Z}^2$ action we obtain associated model on graph Γ_1 embedded in torus $\mathbb{T}^2$, with the sets of vertices, edges and faces V_1, E_1 and F_1, and $\gamma_{h,i}$, $\gamma_{v,j}$ projected to cycles γ_h, γ_v generating $H_1(\mathbb{T}^2, \mathbb{Z})$. Since any closed cycle p on Γ_1 can be decomposed as

$$p = np_h + mp_v + \sum_{f \in F_1} n_f \partial f \tag{4.9}$$

where p_h, p_v are some cycles on Γ_1 homotopic to γ_h and γ_v, the set of gauge-invariant functions on the space of edge weights is generated by

face weights x_f and pair of "monodromies" $x_h = \prod_{e\in p_h} w_e$, $x_v = \prod_{e\in p_v} w_e$. The face weights of dimer model on torus are not independent, they always satisfy a "vanishing of total transverse flux" constraint

$$q = \prod_{f\in F_1} x_f = 1 \tag{4.10}$$

since $\sum_{f\in F_1} \partial f = 0$. We will construct the weighting for the model with non-vanishing flux q in the next subsection. Also, there is no canonical choosing for cycles p_h, p_v, however there is a "twist" of edge weights by $e^{B_x}, e^{B_y} \in \mathbb{R}_{>0}$

$$w_e \mapsto e^{\langle e,\gamma_v\rangle B_x + \langle \gamma_h, e\rangle B_y}\, w_e \tag{4.11}$$

where $\langle\ ,\ \rangle$ is a skew-symmetric intersection form with the orientation fixed by $\langle\gamma_h,\gamma_v\rangle = 1$, which do not change face weights, but shifts $x_h \mapsto e^{B_x} x_h$, $x_v \mapsto e^{B_y} x_v$. We will be using x_f, $f \in F_1$ and e^{B_x}, e^{B_y} as a full set of fugacities, determining model with the vanishing flux.

4.1.2 Non-vanishing flux

Below we will use the additive notations for gauge transformations, edge and face weights

$$g_v = e^{\mathrm{g}_v}, \quad w_e = e^{\mathrm{w}_e}, \quad x_f = e^{\mathrm{x}_f}, \tag{4.12}$$

where g, w and x are cochains from the discrete de Rham complex

$$0 \longrightarrow C^0(\Gamma,\mathbb{R}) \xrightarrow{d_0} C^1(\Gamma,\mathbb{R}) \xrightarrow{d_1} C^2(\Gamma,\mathbb{R}) \longrightarrow 0 \tag{4.13}$$

with the differentials

$$(d_0\mathrm{g})(e) = \mathrm{g}_{t(e)} - \mathrm{g}_{s(e)}, \quad (d_1\mathrm{w})(f) = \sum_{e\in\partial f} \mathrm{w}_e. \tag{4.14}$$

Using these differentials the gauge transformations and fluxes can be written as

$$\mathrm{w} \mapsto \mathrm{w} + d_0\mathrm{g} \quad \text{and} \quad \mathrm{x}_f = (d_1\mathrm{w})(f). \tag{4.15}$$

We will also refer to elements of $C^2(\Gamma,\mathbb{R})$ which are not necessary exact as to face weightings. The classification of discrete $\mathbb{R}_{>0}$-connections on V with arbitrary translation invariant fluxes is provided by the following:

Lemma. Choose any face weighting $\tilde{\mathrm{x}}$ on periodic graph, which is translation invariant $\mathrm{T}_{x,y}\tilde{\mathrm{x}} = \tilde{\mathrm{x}}$. Denote total flux through the fundamental cell by $-\varepsilon = \sum_{f\in F_1} \tilde{\mathrm{x}}_f$ and fix decomposition

$$\tilde{\mathrm{x}}_f = \mathrm{x}_f - \left(\chi_f + \sum_{(i,j)\in\mathbb{Z}^2} \delta_{f,f^{\times}_{(i,j)}}\right)\varepsilon \tag{4.16}$$

where x, χ are translation invariant face weightings of zero flux through the fundamental cell

$$\sum_{f\in F_1} \mathrm{x}_f = \sum_{f\in F_1} \chi_f = 0, \tag{4.17}$$

face $f^{\times}_{(i,j)}$ is the face, which the crossing $\gamma_{h,j}\cap\gamma_{v,i}$ belongs to, and $\delta_{f,f'} = 1$ if $f = f'$, and $\delta_{f,f'} = 0$ otherwise. Then there is a unique up to gauge transformation discrete connection $\tilde{\mathrm{w}}$ such that $d_1\tilde{\mathrm{w}} = \tilde{\mathrm{x}}$, and its gauge equivalence class is presented by edge weighting

$$\tilde{\mathrm{w}}_e = \mathrm{w}_e - \left(\omega_e + \frac{1}{2}\sum_{(i,j)\in\mathbb{Z}^2} i\langle\gamma^{[i,i+1]}_{h,j}, e\rangle + j\langle\gamma^{[j,j+1]}_{v,i}, e\rangle\right)\varepsilon \tag{4.18}$$

where w and ω are translation invariant edge weightings with fluxes $d_1\mathrm{w} = \mathrm{x}$, $d_1\omega = \chi$, $\gamma^{[i,i+1]}_{h,j}$ and $\gamma^{[j,j+1]}_{v,i}$ are intervals of $\gamma_{h,j}$ and $\gamma_{v,i}$ bounded by $\gamma_{v,i}, \gamma_{v,i+1}$ and $\gamma_{h,j}, \gamma_{h,j+1}$ respectively.

Remark. The illustrating example to this Lemma can be found in Fig. 4.1, right. Note, that we separated part of face weighting of zero total flux into x and χ, in order to fix fluxes in $\varepsilon \to 0$ limit by x and to control 'direction' along which the total flux vanishes by χ. We also put sign "$-$" at ε to have $q < 1$ for exponentiated flux $q = e^{-\varepsilon}$ at positive values of ε.

Proof. To prove existence of w and ω, push translation invariant fluxes x and χ down to Γ_1. The conditions that $\mathrm{x}, \chi \in \operatorname{Im} d_1$ are equivalent there to $\mathrm{x}, \chi \perp \operatorname{Ker}\delta_2$ where codifferential $\delta_2 : C^2(\Gamma_1, \mathbb{R}) \to C^1(\Gamma_1, \mathbb{R})$ is defined by

$$(d_1\mathrm{w}, \mathrm{x})_2 = (\mathrm{w}, \delta_2\mathrm{x})_1 \tag{4.19}$$

$$(\mathrm{w}', \mathrm{w}'')_1 = \sum_{e\in E_1} \mathrm{w}'_e\mathrm{w}''_e, \quad (\mathrm{x}', \mathrm{x}'')_2 = \sum_{f\in F_1} \mathrm{x}'_f\mathrm{x}''_f, \tag{4.20}$$

or explicitly by

$$(\delta_2\mathrm{x})(e) = \mathrm{x}_{t(e*)} - \mathrm{x}_{s(e*)}, \tag{4.21}$$

where e^* is the edge of dual graph, obtained from e by counter-clockwise rotation by 90°. Space $\operatorname{Ker}\delta_2$ is one-dimensional and generated by the constant function $\Omega:\ \Omega_f = 1\ \forall\ f \in F_1$, so orthogonalities $(\mathrm{x},\Omega)_2 = 0$ and $(\chi,\Omega)_2 = 0$ are guaranteed by (4.17).

The i and j depending terms in (4.18) contribute to (4.16) with $-\varepsilon\cdot\delta_{f,f^{\times}_{(i,j)}}$, and generate total flux $-\varepsilon$. This can be computed in any example, and then checked that upon adding vertices to $\partial f^{\times}_{(i,j)}$ and moving them in a way, which keeps $\gamma_{h,j}\cap\gamma_{v,i}$ inside of $f^{\times}_{(i,j)}$ and do not put other intersection points inside of it, flux remains the same. Intersections of boundaries of other faces with $\gamma_{h,\bullet}$ and $\gamma_{v,\bullet}$ come in pairs, whose contributions from these terms cancel each other.

To show uniqueness of the gauge orbit, take difference of any pair of discrete connections $\mathrm{w}_0 = \tilde{\mathrm{w}}' - \tilde{\mathrm{w}}''$ both having flux $\tilde{\mathrm{x}}$. It is closed $d_1\mathrm{w}_0 = 0$ and exact

$$\mathrm{w}_0 = d_0\mathrm{g},\quad \mathrm{g}_v = \sum_{e\in p_{v_0,v}} (\mathrm{w}_0)_e, \tag{4.22}$$

where $p_{v_0,v}$ is any path connecting some fixed vertex v_0 with v, and the sum is path independent as $\sum_{e\in p}(\mathrm{w}_0)_e = 0$ for any closed path p, so g is well defined. Thus, g provides desired gauge transformation $\tilde{\mathrm{w}}' = \tilde{\mathrm{w}}'' + d_0\mathrm{g}$. ■

The Kasteleyn operator $\tilde{\mathrm{K}}:\mathbb{C}^{|B_1|}\otimes\mathbb{C}^{|\mathbb{Z}^2|}\to\mathbb{C}^{|W_1|}\otimes\mathbb{C}^{|\mathbb{Z}^2|}$ constructed from weighting (4.18) can be compactly written in terms of Γ_1 as

$$\tilde{\mathrm{K}} = \tilde{\mathrm{K}}_1(\tilde{\mathrm{T}}_x,\tilde{\mathrm{T}}_y) = \sum_{e\in E_1}(-1)^{\varkappa_e} q^{\omega_e} w_e\cdot E_{t(e),s(e)}\otimes\overleftarrow{\mathrm{T}}(e) \tag{4.23}$$

where $q = e^{-\varepsilon}$ is exponentiated flux per fundamental cell, and the translation operator $\overleftarrow{\mathrm{T}}(e)$ is ordered along the edge e product over its intersections with γ_h, γ_v, which are images of $\gamma_{h,\bullet}$, $\gamma_{v,\bullet}$ under projection from $\mathbb{R}^2$ to $\mathbb{T}^2$

$$\overleftarrow{\mathrm{T}}(e) = \prod_{p\in e\cap\gamma_{h,v}}^{\leftarrow}\left(\tilde{\mathrm{T}}_x\right)^{\langle e,\gamma_v\rangle_p}\left(\tilde{\mathrm{T}}_y\right)^{\langle\gamma_h,e\rangle_p} \tag{4.24}$$

of the basic q-commuting "magnetic translations" $\tilde{\mathrm{T}}_{x,y}:\mathbb{C}^{|\mathbb{Z}^2|}\to\mathbb{C}^{|\mathbb{Z}^2|}$

$$\tilde{\mathrm{T}}_x = \sum_{(i,j)\in\mathbb{Z}^2} q^{-\frac{1}{2}j}\,\mathrm{E}_{i+1,i}\otimes\mathrm{E}_{j,j},\quad \tilde{\mathrm{T}}_y = \sum_{(i,j)\in\mathbb{Z}^2} q^{\frac{1}{2}i}\,\mathrm{E}_{i,i}\otimes\mathrm{E}_{j+1,j}, \tag{4.25}$$

$$\tilde{\mathrm{T}}_y\tilde{\mathrm{T}}_x = q\tilde{\mathrm{T}}_x\tilde{\mathrm{T}}_y. \tag{4.26}$$

The notation $\tilde{\mathrm{K}}_1(\tilde{\mathrm{T}}_x, \tilde{\mathrm{T}}_y)$ means that we can consider $\tilde{\mathrm{K}}$ as a finite matrix $\tilde{\mathrm{K}}_1 : \mathbb{C}^{B_1} \to \mathbb{C}^{W_1}$, with coefficients in the skew Laurent polynomials $\mathbb{C}[q, q^{-1}, \tilde{T}_x, \tilde{T}_x^{-1}, \tilde{T}_y, \tilde{T}_y^{-1}]$. For example, this matrix presentation for Kasteleyn operator of the network drawn in Fig. 4.1 is

$$\tilde{\mathrm{K}}_1 = \begin{pmatrix} w_1 + w_3\tilde{\mathrm{T}}_y^{-1} & -w_6 - w_8\tilde{\mathrm{T}}_x \\ w_4 + w_2\tilde{\mathrm{T}}_x^{-1} & w_7 + w_5\tilde{\mathrm{T}}_y \end{pmatrix}. \tag{4.27}$$

The space $\mathbb{C}^{|\mathbb{Z}^2|}$ as a representation of the algebra of q-difference operators by $\tilde{\mathrm{T}}_x$ and $\tilde{\mathrm{T}}_y$ is largely reducible. The degeneracy can be lifted utilizing the algebra of q^{-1}-difference operators, represented by "dual magnetic translations"

$$\tilde{\mathrm{T}}_x^\vee = \sum_{(i,j)\in\mathbb{Z}^2} q^{-\frac{1}{2}j}\, \mathrm{E}_{i-1,i} \otimes \mathrm{E}_{j,j}, \quad \tilde{\mathrm{T}}_y^\vee = \sum_{(i,j)\in\mathbb{Z}^2} q^{\frac{1}{2}i}\, \mathrm{E}_{i,i} \otimes \mathrm{E}_{j-1,j}, \tag{4.28}$$

$$\tilde{\mathrm{T}}_y^\vee \tilde{\mathrm{T}}_x^\vee = q^{-1} \tilde{\mathrm{T}}_x^\vee \tilde{\mathrm{T}}_y^\vee. \tag{4.29}$$

which commute with the former

$$[\tilde{\mathrm{T}}_s, \tilde{\mathrm{T}}_{s'}^\vee] = 0, \quad s, s' = x, y. \tag{4.30}$$

Therefore any operator, which is a skew Lauren polynomial $\tilde{\mathrm{Q}} = \tilde{\mathrm{Q}}(\tilde{\mathrm{T}}_x^\vee, \tilde{\mathrm{T}}_y^\vee)$ in $\tilde{\mathrm{T}}_x^\vee, \tilde{\mathrm{T}}_y^\vee$, commutes with $\tilde{\mathrm{K}}$ in the sense that

$$\left(\mathrm{Id}_{\mathbb{C}^{|W_1|}} \otimes \tilde{\mathrm{Q}}\right) \cdot \tilde{\mathrm{K}} = \tilde{\mathrm{K}} \cdot \left(\mathrm{Id}_{\mathbb{C}^{|B_1|}} \otimes \tilde{\mathrm{Q}}\right). \tag{4.31}$$

The form (4.23) of Kasteleyn operator survives under gauge transformations constant inside of fundamental cells, the universal condition determining operators of dual translations is

$$\tilde{\mathrm{T}}_x^\vee \tilde{\mathrm{T}}_x = q^{-\hat{y}}, \quad \tilde{\mathrm{T}}_y^\vee \tilde{\mathrm{T}}_y = q^{\hat{x}}, \tag{4.32}$$

$$q^{\hat{x}} = \sum_{(i,j)\in\mathbb{Z}^2} q^i\, \mathrm{E}_{i,i} \otimes \mathrm{E}_{j,j}, \quad q^{\hat{y}} = \sum_{(i,j)\in\mathbb{Z}^2} q^j\, \mathrm{E}_{i,i} \otimes \mathrm{E}_{j,j}. \tag{4.33}$$

The operator $\tilde{\mathrm{Q}}$ is hypostasis of eponymous Laurent polynomial from [116], which was shown there to label possible limit shapes of dimer model. In the next section we will show that the complex Burgers equation controlling limits shapes in [116] is simply the WKB approximation in $q \to 1$ limit to the spectral problem for the Kasteleyn operator (4.23).

4.2 Seiberg-Witten integrability in WKB approximation

In this Section we look at the "melting" $q \to 1$ limit of vanishing flux for dimer model. The usual arguments of quantum mechanical quasiclassics are applicable to Kasteleyn operator (4.27) in this limit. The main result of this Section is that the free energy (4.58), which is a regularized volume under the "limit shape" (4.52), satisfies Seiberg-Witten equations (4.59). We will use only the example (4.27) throughout the Section, but all arguments of it can be generalized in a straightforward way.

4.2.1 Quasiclassics of vanishing flux at $q \to 1$ and height function of limit shape

The main observable in dimer models is "height" function, which counts portions of dimers oriented "horizontally" and "vertically" in average configuration. Its meaning becomes more clear, once the configurations of dimer model are interpreted as stepped surfaces.

Let's choose some reference configuration D_0 as in (4.4). As for any $D \in \mathcal{D}(\Gamma)$ holds $\partial D = W - B$, the difference $D - D_0$ is a collection of closed and non-intersecting (having no common vertices) cycles on plane, which we interpret as boundaries of "steps". The orientation of cycle determines whether its step is upward or downward. Assuming each step to be of heights 1, the difference of heights between the pair of faces f_1, f_2 of Γ is $\langle p^*_{f_2,f_1}, D - D_0 \rangle$, where $p^*_{f_2,f_1}$ is any path on the dual graph Γ^* connecting f_1 and f_2 and $\langle \, , \rangle$ is an intersection pairing. Since $\partial(D - D_0) = 0$, the heights difference is independent on choosing of path $p^*_{f_2,f_1}$ for planar Γ. The averaged height function $h : F \times F \to \mathbb{R}$ computes the mean difference of heights over the ensemble of stepped surfaces

$$h_{f_2,f_1}(\Gamma, w; D_0) = h_{f_2,f_1} = \frac{1}{\mathcal{Z}(\Gamma, w; D_0)} \sum_{D \in \mathcal{D}(\Gamma)} \langle p^*_{f_2,f_1}, D - D_0 \rangle w_{D-D_0}. \tag{4.34}$$

It is clear from this definition, that the fugacity ε in $q = e^{-\varepsilon}$ controls the "volume" under the stepped surface made out of these loops, since each loop $l = \partial B$ contributes to the statistical weight of configuration in partition function by $\sim e^{-\varepsilon \cdot \mathrm{Area}(B)}$. The infinite volume limit corresponds to $\varepsilon \to 0$, and the problem of finding the height function and its fluctuations in this limit is called the limit shape problem.

Due to free-fermionic nature of the model, all correlating functions of any local observables in it can be computed by bare knowledge of two-point Green function G, defined by the equations[1]

$$\tilde{\mathrm{K}} \cdot \mathrm{G} = \mathrm{Id}\,, \quad [\tilde{\mathrm{Q}}, \mathrm{G}] = 0. \tag{4.35}$$

The problem (4.35) for generic q is fully solved only for hexagonal lattices with various boundary conditions using free fermionic vertex operators in [149, 150]. The knowledge of the solution of (4.35) in few leading orders in ε at $\varepsilon \to 0$ limit is enough for any purposes of the limit shape problem, but this is still a cumbersome problem. However, the information about height function itself can be heuristically extracted from the structure of $\operatorname{Ker}\tilde{\mathrm{K}} \cap \operatorname{Ker}\tilde{\mathrm{Q}}$, which is the solution of the simpler problem

$$\tilde{\mathrm{K}}\psi = 0, \quad \tilde{\mathrm{Q}}\psi = 0. \tag{4.36}$$

In coordinates $x = \varepsilon i,\ y = \varepsilon j$, considered as continuous coordinates on $\mathbb{R}^2$, these equations become

$$\begin{cases} \sum_{b\in B_1} (\tilde{\mathrm{K}}_1)_{v,b} \left(e^{\frac{1}{2}y - \varepsilon\partial_x}, e^{-\frac{1}{2}x - \varepsilon\partial_y} \right) \psi_b(x,y) = 0 \\ \tilde{\mathrm{Q}} \left(e^{\frac{1}{2}y + \varepsilon\partial_x}, e^{-\frac{1}{2}x + \varepsilon\partial_y} \right) \psi_b(x,y) = 0 \end{cases}, \quad b \in B_1,\ v \in W_1. \tag{4.37}$$

They can be solved order-by-order in ε using standard quasi-classical anzaets for wave-function

$$\psi_b(x,y) = \exp\left(\frac{\mathrm{i}}{\varepsilon} S_b^{(0)}(x,y) + S_b^{(1)} + \ldots \right),\ b \in B_1. \tag{4.38}$$

In the leading orders $e^{\frac{1}{\varepsilon}\#}$ and ε^0 the consistency conditions for the equations (4.36) become

$$\begin{cases} P(e^z, e^w) \equiv \det \mathrm{K}_1(e^z, e^w) = 0 \\ Q(e^{z^\vee}, e^{w^\vee}) = 0 \\ \sum\limits_{b\in B_1} (\mathrm{K}_1)_{v,b}\,(e^z, e^w)\, e^{S_b^{(1)}} = 0 \end{cases}, \tag{4.39}$$

[1] The equation $[\tilde{\mathrm{Q}}, \mathrm{G}] = 0$ has not-clear-yet physical nature, but should be related to the control over boundary conditions of the model, and the exact Green functions from [149, 150] satisfy it.

where $\mathrm{K}_1 = \tilde{\mathrm{K}}_1|_{\varepsilon=0}$, $Q = \tilde{\mathrm{Q}}|_{\varepsilon=0}$ and

$$z = \frac{1}{2}y - \mathrm{i}\partial_x S^{(0)}(x,y),\ w = -\frac{1}{2}x - \mathrm{i}\partial_y S^{(0)}(x,y), \tag{4.40}$$

$$z^\vee = \frac{1}{2}y + \mathrm{i}\partial_x S^{(0)}(x,y),\ w^\vee = -\frac{1}{2}x + \mathrm{i}\partial_y S^{(0)}(x,y). \tag{4.41}$$

Commutativity of $\tilde{\mathrm{K}}$ and $\tilde{\mathrm{Q}}$ implies in the quasiclassical limit that the differential

$$dS^{(0)} = \partial_x S^{(0)} dx + \partial_y S^{(0)} dy = \tag{4.42}$$
$$= \frac{\mathrm{i}}{2}(zdw - wdz) - \frac{\mathrm{i}}{2}(z^\vee dw^\vee - w^\vee dz^\vee) + \frac{\mathrm{i}}{2} d(w^\vee z - z^\vee w)$$

is closed, so the quasiclassical action $S^{(0)} = S^{(0)}(x,y)$ can be defined by its integration from. In the simplest case when $Q = P$, the conditions (4.39) and (4.40) can be solved by $z^\vee = \bar{z},\ w^\vee = \bar{w}$ and one can simplify (4.42) to

$$S^{(0)}_{Q=P}(x,y) = \mathrm{Im}\left(\int^{z(x,y)} (wdz - zdw) + \bar{z}w\right) = \tag{4.43}$$
$$= -2 \cdot \mathrm{Im}\left(\int^{z(x,y)} zdw\right) + 2 \cdot \mathrm{Re}\,(z)\mathrm{Im}\,(w),$$

which up to exact terms is (-2) times an imaginary part of integral of the meromorphic differential zdw, called Seiberg-Witten differential, over the complex curve

$$\mathcal{C}_P = \{P(e^z, e^w) = 0 \subset (\mathbb{C}^*)^2\}. \tag{4.44}$$

To compute the height function, let's assume now that the local behaviour of model with flux in $\varepsilon \to 0$ limit mimics those of the "homogeneous" model of zero flux on the torus. For homogenous model the height function can be easily computed using an expression for free energy density [118]

$$\mathcal{R}(B_x, B_y) = \int_0^{2\pi}\int_0^{2\pi} \frac{d\theta d\phi}{(2\pi)^2} \log P(e^{B_x + \mathrm{i}\theta}, e^{B_y + \mathrm{i}\phi}), \tag{4.45}$$

since the average number of "horizontal" and "vertical" dimers are dual to the "twist" parameters (B_x, B_y)

$$\begin{cases} h(x+\varepsilon, y) - h(x,y) \simeq -\partial_{B_y}\mathcal{R} = \frac{\theta_*}{\pi} \\ h(x, y+\varepsilon) - h(x,y) \simeq \partial_{B_x}\mathcal{R} = \frac{\phi_*}{\pi} \end{cases}, \tag{4.46}$$

where $P(e^{B_x+\mathrm{i}\theta_*}, e^{B_y+\mathrm{i}\phi_*}) = 0$. At the same time, the zero-mode of homogeneous model is

$$\psi_{\alpha,(a,b)} = e^{\mathrm{i}(a\theta_*+b\phi_*)}\xi_\alpha, \quad \alpha \in B_1,\ (a,b) \in \mathbb{Z}^2, \tag{4.47}$$

where $(\mathrm{K}_1)(e^{B_x+\mathrm{i}\theta_*}, e^{B_y+\mathrm{i}\phi_*}) \cdot \xi = 0$. Applying in (4.47) coordinates $a = x/\varepsilon,\ b = y/\varepsilon$ and comparing it with (4.38), one can guess the height function of the model with flux in $\varepsilon \to 0$ limit to be

$$h(x,y) = \int (\partial_x h\, dx + \partial_y h\, dy) \simeq \frac{S^{(0)}(x,y)}{\pi\varepsilon}. \tag{4.48}$$

The WKB quantization condition coming from single-valuedness of wavefunction becomes also the natural condition for height difference between frozen regions of the model [116] to be integral.

In the case of $Q = P$ comparing formulas (4.39), (4.40) with (4.46), one can deduce

$$h_{Q=P}(x,y) = -\frac{2}{\varepsilon}\mathcal{R}\left(\frac{y}{2}, -\frac{x}{2}\right). \tag{4.49}$$

In [116] similar results were obtained, but the logic (and notations) were different. Pair of equations (4.39) appeared there as a solution of variational problem, optimizing the total surface tension[2] to be minimal. The Euler-Lagrange equation of this problem results to equations

$$\partial_y z - \partial_x w = 1, \quad P(e^z, e^w) = 0, \tag{4.50}$$

called complex Burgers equation. The function Q appears then as a free function, parametrizing the space of solutions of this equation, and controlling the boundary conditions for solutions. So the equation, which in our setup is a consistency condition supporting Hamilton-Jacobi equation, appears also to be the stationary-action principle for $2d$ field theory. Expression for height function similar to (4.48) was also derived in [116].

4.2.2 Free energy density is Seiberg-Witten prepotential.

The WKB arguments can be also applied to computation of partition function in $\varepsilon \to 0$ limit. The usual heuristics

$$\mathrm{Tr}[A(T_x,T_y)] \ \to\ \iint \frac{dxdy}{\varepsilon^2} \iint \frac{d\theta d\phi}{(2\pi)^2} A(e^{\frac{y}{2}+\mathrm{i}\theta}, e^{-\frac{x}{2}+\mathrm{i}\phi}) \quad \text{as} \quad \varepsilon \to 0 \tag{4.51}$$

[2]The surface tension density is a Legandre dual to the free energy density $\mathcal{R}$. It computes the energy of the region with the known slope $(\partial_x h, \partial_y h)$ in opposite to $\mathcal{R}$, which computes energy of the region with fugacities (B_x, B_y).

gives the integral formula for the partition function of the model

$$\mathcal{Z} = \det \tilde{\mathrm{K}} = e^{\operatorname{tr}\log \tilde{\mathrm{K}}} \propto \exp\left(\frac{1}{\varepsilon^2}\iint dxdy\,\mathcal{R}\left(\frac{y}{2},-\frac{x}{2}\right)\right) = q^{\mathrm{Vol}(P,P)}, \tag{4.52}$$

$$\mathrm{Vol}(P,P) = \frac{1}{2}\iint \frac{dxdy}{\varepsilon^2} h_{Q=P}(x,y).$$

The proportionality of the free energy of the model to the volume[3] under the limit shape is a natural thing: in the leading order, the partition function is dominated by single configuration, and the free energy determined by it is proportional to the sum of areas of all contours which this configuration contains (which is basically volume). It is diverging, and proper regularization of determinant in (4.52) and extension of the formula to the case $Q \neq P$ requires careful consideration of the boundary conditions for the model and role of Q. We will instead define some regularization of Vol guided by its properties and natural equation satisfied by it. In order to to this we need first to make a closer look to the properties of spectral curve $P(e^z, e^w) = 0$ and function $\mathcal{R}$.

For the lattice drawn on Fig. 4.1, the Laurent polynomial P computed using (4.27) is

$$P(\lambda,\mu) = \det \mathrm{K}_1(\lambda,\mu) = \tag{4.53}$$
$$= \frac{w_2w_6}{\lambda} + w_4w_8\lambda + w_1w_5\mu + \frac{w_3w_7}{\mu} + (w_3w_5 + w_2w_8 + w_1w_7 + w_4w_6)\,.$$

For the purposes of this Section the rescalings $P(\lambda,\mu) \mapsto A\cdot P(B\lambda, C\mu)$ are immaterial, so we will be using here P in the equivalent form

$$P(\lambda,\mu) = \lambda + \frac{Z}{\lambda} + \mu + \frac{1}{\mu} - U, \tag{4.54}$$

$$Z = x_1x_3, \quad -U = \sqrt{x_1x_4} + \frac{1}{\sqrt{x_1x_4}} + \sqrt{Z}\left(\sqrt{x_3x_4} + \frac{1}{\sqrt{x_3x_4}}\right), \tag{4.55}$$

where x_i are face variables labelled following Fig. 4.1, left. Curves $\mathcal{C}_P$ appearing in planar dimer models are Harnak [115], which means that the logarithmic projection $(\lambda,\mu) \mapsto (\log|\lambda|, \log|\mu|)$ of spectral curve $\mathcal{C}_P$ to $\mathbb{R}^2$ is 2 to 1 mapping in the interior of amoeba[4]

$$\mathcal{A}(P) = \{(x,y) \in \mathbb{R}^2 \mid \exists\ (\theta,\phi) \in \mathbb{R}^2 : P(e^{x+\mathrm{i}\theta}, e^{y+\mathrm{i}\phi}) = 0\}, \tag{4.56}$$

[3] Up to 1/2, whose appearance in the definition of Vol is unclear.

[4] Starting from here and until the end of this Section we use coordinates (x,y) differently compared to the usage above.

and 1 to 1 at its boundary. The inverse is also true: any Harnak curve in $\mathbb{C}^* \times \mathbb{C}^*$ can be obtained from some planar dimer model. For Laurent polynomial (4.53) the curve is Harnak if $Z \in \mathbb{R}_{\geq 0}$, $U \geq U_0 = 2(\sqrt{Z}+1)$ which is satisfied because of $x_i \in \mathbb{R}_{\geq 0}$, following from positivity of edge weights. The corresponding amoeba is drawn on Fig. 4.2, left.

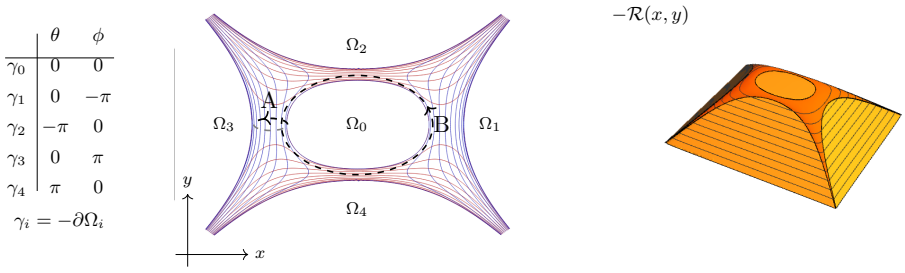

Figure 4.2. Left: Amoeba $\mathcal{A}(P)$ of the curve $P(e^{x+\mathrm{i}\theta}, e^{y+\mathrm{i}\phi}) = 0$. Red lines are for $\theta = \text{const}$, blue are for $\phi = \text{const}$, their values are taken for one of two sheets of $\mathcal{C}_P$ over $\mathcal{A}(P)$. Boundaries γ_i of ovals Ω_i are oriented counter-clockwise along $\partial\mathcal{A}$. The projections of $A-$ and $B-$ cycles are drawn by dashed lines. Right: minus Ronkin function $-\mathcal{R}(x,y)$ for the same P.

Complement of amoeba of Harnak curve consists of disjoint regions $\mathbb{R}^2 \backslash \mathcal{A}(P) = \cup_i \Omega_i$, which are bounded and unbounded ovals. Their combinatorics of ovals is captured by Newton polygon N_P of polynomial P - the convex hull of such $(i,j) \in \mathbb{Z}^2$, that $\lambda^i \mu^j$ is contained in $P(\lambda, \mu)$ with non-zero coefficient. Bounded ovals correspond to integral internal points of N_P, unbounded ovals to integral boundary points, so the amoeba can be contracted to the graph, dual to some triangulation of Newton polygon. The function $\mathcal{R}$, called Ronkin function of P in mathematical literature, in case of Harnak P is concave function on $\mathbb{R}^2$, linear of slope (i,j) on oval corresponding to point (i,j) of Newton polygon, and interpolating slopes of ovals in the interior of amoeba, as shown on Fig. 4.2, right.

Since the ovals have to be invariant under the complex involution $(\lambda, \mu) \mapsto (\bar{\lambda}, \bar{\mu})$, functions $\theta(x,y)$ and $\phi(x,y)$ can take only $\pi\mathbb{Z}$ values there. The parametrization of $\mathcal{C}_P$ by (z,w) is uniquely determined by the condition, that the single-valued smooth functions $\theta(x,y)$, $\phi(x,y)$ in the interior of $\mathcal{A}$ are such solution of

$$z = x + i\theta(x,y), \quad w = y + i\phi(x,y) : \quad P(e^z, e^w) = 0, \tag{4.57}$$

that $\theta = \phi = 0$ at γ_0 and $\phi(x, y)$ is increasing along the short paths from γ_0 to γ_3. We call part of $\mathcal{C}_P$ parametrized by this (z, w) to be upper sheet, and those, which is complex conjugated, to be lower. Both θ, ϕ considered as a functions on $\mathcal{C}_P$ are single valued in the interior of $\mathcal{A}$ and on γ_0, however they can have jumps at other γ_i.

Now we can define the regularization of free energy in (4.52) by

$$\mathcal{F}(U) = \tilde{\mathcal{F}}(U) - \tilde{\mathcal{F}}(U_0), \tag{4.58}$$

$$\tilde{\mathcal{F}}(U) = \frac{\mathrm{i}}{\pi}\left(\iint\limits_{\mathbb{R}^2} \mathcal{R}(x,y)dxdy - \left(\int\limits_{\gamma_1} - \int\limits_{\gamma_3}\right)\frac{x^2 dy}{8} - \left(\int\limits_{\gamma_4} - \int\limits_{\gamma_2}\right)\frac{y^2 dx}{8}\right).$$

It is finite, since at large x, y graphs or Ronkin functions for P with the same values of Z but different U are exponentially close. The overall normalization and presence of boundary terms is justified by the following Claim, which is natural due to the reasons explained in Introduction:

Claim. The prepotential $\mathcal{F}$ defined in (4.58) satisfies Seiberg-Witten equation

$$\frac{\partial \mathcal{F}}{\partial a} = a_D, \qquad a = \oint_A z\frac{dw}{2\pi\mathrm{i}}, \qquad a_D = \oint_B z\frac{dw}{2\pi\mathrm{i}}, \tag{4.59}$$

where A and $B = -\gamma_0$ are simple cycles on curve, which intersect with $A \cap B = 1$, as shown on Fig. 4.2, and orientation of A-cycle is such, that it is directed from γ_0 to γ_3 when goes along the upper sheet of $\mathcal{C}_P$.

Proof. Firstly, note that $a = a(U)$ is analytic function at a generic point, so (4.59) is equivalent to

$$\frac{\partial \mathcal{F}}{\partial U} = a_D \frac{\partial a}{\partial U}, \tag{4.60}$$

and that since $\mathcal{R}(x, y; U) - \mathcal{R}(x, y; U_0)$ is exponentially small at infinity, we can interchange integration and differentiation

$$\frac{\partial}{\partial U}\iint\limits_{\mathbb{R}^2}\left(\mathcal{R}(x,y;U) - \mathcal{R}(x,y;U_0)\right)\frac{dx\wedge dy}{2\pi\mathrm{i}} = \iint\limits_{\mathbb{R}^2}\frac{\partial \mathcal{R}(x,y)}{\partial U}\frac{dx\wedge dy}{2\pi\mathrm{i}}. \tag{4.61}$$

Decompose $\mathbb{R}^2 = \Omega_0 \cup \mathcal{A} \cup \Omega_1 \cup \Omega_2 \cup \Omega_3 \cup \Omega_4$, and consider integrals over the regions separately. For any of Ω_i or $\mathcal{A}$, their shapes depend on U, so change of the order of differentiation and integration over any single of them would change integral by additional contact term.

- Let $(x,y) \in \Omega_0$, then

$$\frac{\partial \mathcal{R}(x,y)}{\partial U} = \int\limits_0^{2\pi} \frac{d\phi}{2\pi} \oint\limits_{|z|=x} \frac{dz}{2\pi \mathrm{i}} \frac{\partial_U P(e^z, e^{y+\mathrm{i}\phi})}{P(e^z, e^{y+\mathrm{i}\phi})} = \tag{4.62}$$

$$= \int\limits_0^{2\pi} \frac{d\phi}{2\pi} \frac{\partial_U P(e^{z_*}, e^{y+\mathrm{i}\phi})}{\partial_z P(e^{z_*}, e^{y+\mathrm{i}\phi})} = -\oint_A \frac{\partial z(w)}{\partial U} \frac{dw}{2\pi \mathrm{i}} = -\frac{\partial a(U)}{\partial U}$$

where the contour of integration is deformed first from $\operatorname{Re} z = x$ to $\operatorname{Re} z = -\infty$, keeping $\operatorname{Re} w = y$, and picking pole at z_*, such that $P(e^{z_*}, e^{y+\mathrm{i}\phi}) = 0$, see Fig. 4.3. Then the remaining integration over $d\phi$ becomes integral of $-\mathrm{i}dw$ over A-cycle, and we use that $0 = dP/dU = \partial_U P + \partial_z P \partial_U z$, assuming that $z = z(U,w)$ [5]. As $\partial_U \mathcal{R}(x,y)$ does not depends on $(x,y) \in \Omega_0$, it remains to compute

$$\iint\limits_{\Omega_0} \frac{dx \wedge dy}{2\pi \mathrm{i}} = \oint\limits_{\partial\Omega_0} \frac{x dy}{2\pi \mathrm{i}} = \tag{4.63}$$

$$= \frac{1}{2\pi \mathrm{i}} \oint\limits_{-\gamma_0} (z dw - \mathrm{i}(\theta dy + x d\phi) + \theta d\phi) = \oint_B z \frac{dw}{2\pi \mathrm{i}} = a_D(U)$$

where we used that $\theta = \phi = 0$ at γ_0.

- Regions $\Omega_1, \Omega_2, \Omega_3, \Omega_4$ do not contribute to integral, as we can deform integration contour there to $\operatorname{Re} z \to +\infty$, $\operatorname{Re} w \to +\infty$, $\operatorname{Re} z \to -\infty$, $\operatorname{Re} w \to -\infty$ respectively, where integrand is exponentially suppressed, without picking any poles.

- For any $(x,y) \in \mathcal{A}$ we can shift integration contour to $x \to -\infty$, along any sequence of straight segments of rational slope. The poles are picked as in (4.62), because of $\mathrm{SL}(2,\mathbb{Z})$ invariance of integration measure

$$-\frac{\partial z(w)}{\partial U} \frac{dw}{2\pi \mathrm{i}} = \frac{\partial_U P}{\partial_z P} \frac{dw}{2\pi \mathrm{i}} = \tag{4.64}$$

$$= \frac{\partial_U P}{d\partial_{\tilde{z}} P - c\partial_{\tilde{w}} P} \left(d + c \frac{\partial \tilde{z}}{\partial \tilde{w}} \right) \frac{d\tilde{w}}{2\pi \mathrm{i}} = -\frac{\partial \tilde{z}(\tilde{w})}{\partial U} \frac{d\tilde{w}}{2\pi \mathrm{i}},$$

[5] These two steps are equivalent to deformation of $2d$ contour and picking Poincaré residue of $\frac{dz \wedge dw}{P}$ at $P = 0$

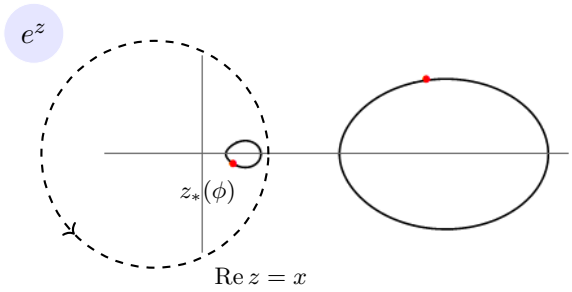

Figure 4.3. Slice of the curve $\mathcal{C}_P$ by $y = \text{const}$ section, plotted in e^z coordinate, shown by ovals. The y is such that the $y = \text{const}$ line crosses a hole of amoeba. Red dots are points with the same ϕ. Dashed circle is dz integration contour in (4.62), which has to be contracted to zero.

where $z = a\tilde{z} + b\tilde{w}$, $w = c\tilde{z} + d\tilde{w}$, with $a, b, c, d \in \mathbb{Z}$, $ad - bc = 1$. As the integrand is a holomorphic form, the integration contour might be deformed to any convenient smooth contour which goes from $w = w(x, y)$ to γ_3, and then to $\bar{w}$, on another sheet. Using that inside of $\mathcal{A}$ we can present area element $dx \wedge dy$ as

$$dx \wedge dy = \frac{1}{4}\left(dz \wedge d\bar{w} + d\bar{z} \wedge dw\right), \tag{4.65}$$

we apply integration by parts, to get

$$\begin{aligned}
&-\iint_{\mathcal{A}} \left(\int_w^{\bar{w}} \frac{\partial z(w)}{\partial U}\frac{dw}{2\pi \mathrm{i}}\right) \frac{dz \wedge d\bar{w} + d\bar{z} \wedge dw}{8\pi \mathrm{i}} = \\
&= \int_{\partial\mathcal{A}} \left(\int_w^{\bar{w}} \frac{\partial z(w)}{\partial U}\frac{dw}{2\pi \mathrm{i}}\right) \frac{\bar{w}dz + wd\bar{z}}{8\pi \mathrm{i}} + \\
&+ \iint_{\mathcal{A}} \left(\bar{w}\frac{\partial \bar{z}(\bar{w})}{\partial U}\frac{dz \wedge d\bar{w}}{(4\pi \mathrm{i})^2} - w\frac{\partial z(w)}{\partial U}\frac{d\bar{z} \wedge dw}{(4\pi \mathrm{i})^2}\right) = \\
&= \int_{\partial\mathcal{A}} \left(\int_w^{\bar{w}} \frac{\partial z(w)}{\partial U}\frac{dw}{2\pi \mathrm{i}}\right) \frac{\bar{w}dz + wd\bar{z}}{8\pi \mathrm{i}} + \\
&+ \int_{\partial\mathcal{A}} \left(\frac{\partial \bar{z}(\bar{w})}{\partial U}\frac{z\bar{w}d\bar{w}}{(4\pi \mathrm{i})^2} - \frac{\partial z(w)}{\partial U}\frac{\bar{z}wdw}{(4\pi \mathrm{i})^2}\right).
\end{aligned} \tag{4.66}$$

Using that the contours in $\int_w^{\bar{w}}(\partial z/\partial U)dw$ are now closed (since $w = \bar{w}$ at $\partial\mathcal{A}$), and some of them can be contracted to points at

infinity, where $\partial z(w)/\partial U$ is exponentially suppressed, the first integral reduces to

$$\sum_{i=0}^{4}\int\limits_{\gamma_i}\left(\int_w^{\bar w}\frac{\partial z(w)}{\partial U}\frac{dw}{2\pi\mathrm{i}}\right)\frac{\bar w dz+wd\bar z}{8\pi\mathrm{i}}=\frac{\partial a}{\partial U}\int\limits_{\gamma_0}\frac{ydx}{4\pi\mathrm{i}}=\frac{a_D}{2}\frac{\partial a}{\partial U}. \tag{4.67}$$

Using also the values of $\theta,\phi\in\pi\mathbb{Z}$ on γ_i at upper sheet of $\mathcal{C}_P$, which are indicated on Fig. 4.2, and $\mathrm{SL}(2,\mathbb{Z})$ invariance (4.64), we get for the remaining

$$\sum_{i=0}^{4}\int\limits_{\gamma_i}\left(\frac{\partial\bar z(\bar w)}{\partial U}\frac{z\bar w d\bar w}{(4\pi\mathrm{i})^2}-\frac{\partial z(w)}{\partial U}\frac{\bar z w dw}{(4\pi\mathrm{i})^2}\right)= \tag{4.68}$$

$$=\sum_{i=0}^{4}\int\limits_{\gamma_i}\frac{\partial z}{\partial U}\frac{(z\bar w-\bar z w)dw}{(4\pi\mathrm{i})^2}=\int\limits_{\gamma_1-\gamma_3}\frac{\partial x}{\partial U}\frac{xdy}{8\pi\mathrm{i}}+\int\limits_{\gamma_4-\gamma_2}\frac{\partial y}{\partial U}\frac{ydx}{8\pi\mathrm{i}}.$$

All contributions brought together give us identity (4.60). ■

Another interesting limit can be taken now. It is called perturbative or tropical or decompactification in different contexts. In it, the parameters scale as

$$U=e^{R_5 u},\quad Z=e^{R_5 z},\quad R_5\to+\infty. \tag{4.69}$$

The amoeba shrinks then to its spine, which is a union of intervals as shown on Fig. 4.4, and pre-image of projection $\mathcal{C}_P\to\mathcal{A}$ becomes S^1 over the internal points of intervals, and pairs of triangles, connecting these circles, over the joints of intervals. The Ronkin function in the leading in R_5 order become piecewise linear function of x,y, and integrations in (4.58) becomes trivial exercises in computations of polyhedron volumes. Taking $U_0=2(\sqrt{Z}+1)$ at which domain Ω_0 shrinks to point, one gets

$$\mathcal{F}\to-\frac{R_5^3}{24\pi\mathrm{i}}(2u-z)^2(4u+z), \tag{4.70}$$

$$a=\oint_A z\frac{dw}{2\pi\mathrm{i}}\to R_5\cdot(z-u),\quad a_D=\oint_B z\frac{dw}{2\pi\mathrm{i}}\to\frac{R_5^2}{2\pi\mathrm{i}}2u(2u-z).$$

This completely "frozen" by extreme values of parameters configuration will be the starting point in the next Section. However we will "unfroze" it in a different way, keeping finite q under extreme values of x_i.

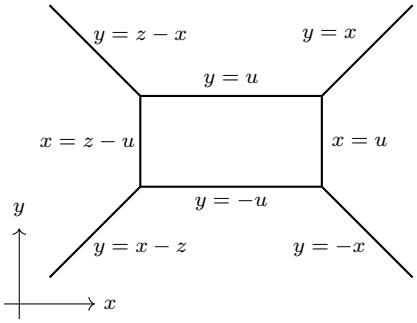

Figure 4.4. Amoeba of the curve $\mathcal{C}_P$ in tropical limit. Coordinates here are normalized by R_5

4.3 Boxcounting in tropical limit

In this Section we will show, how the Fourier-transformed topological string amplitude (4.1) comes combinatorially from the counting of dimers in the running example as on Fig. 4.1: we identify degrees of freedom corresponding to $0d$ boxes constituting $3d$ Young diagrams, $1d$ boxes constituting $2d$ Young diagrams and $2d$ boxes constituting $1d$ Young diagrams. We also suggest how the properly taken tropical limit for face weights $x_i = e^{R_5\xi_i + \mathrm{x}_i}$, $R_5 \to \infty$ might suppress all the other degrees of freedom, but it appears to be inconsistent with the thermodynamic limit.

4.3.1 Combinatorics of boxcounting

The starting point for the box counting combinatorics is the "empty room" dimers configuration, which is drawn on all four panels of Fig. 4.5 by coloured dimers. The structure of configuration is similar to the structure of amoeba drawn on Fig. 4.2: there are four unbounded domains corresponding to $\Omega_1, \Omega_2, \Omega_3, \Omega_4$, and one internal domain Ω_0. Dimers configurations in unbounded domains are just the tilings by configurations corresponding to four "external" monomials at $\lambda, \lambda^{-1}, \mu, \mu^{-1}$ in (4.53), and configuration in Ω_0 is one of those at $\lambda^0\mu^0$. Two parameters defining this configuration are width N and height M of central domain. For the configuration on Fig. 4.5 we have $N = 4$, $M = 5$ by the number of fundamental domains filled by purple dimers plus 1.

The "rotation in the set of faces" is a transition from one dimers con-

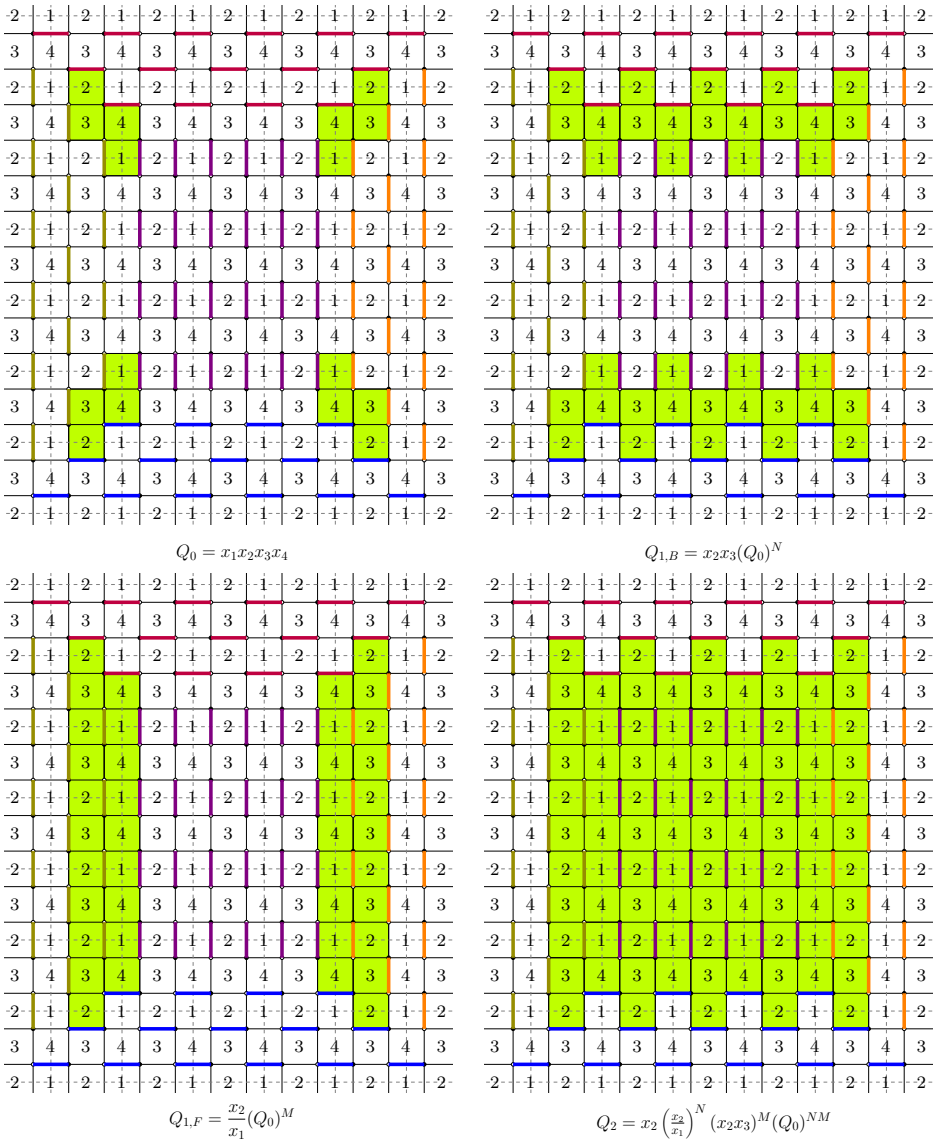

Figure 4.5. Toda bipartite lattices with "empty room" configuration D_0 drawn. Faces involved in the rotations corresponding to addition of boxes weighted by $Q_0, Q_{1,B}, Q_{1,F}, Q_2$ are highlighted by lime colour.

figuration to another by choosing such a set of faces that exactly half of edges on their common boundary (each second edge) is contained in

dimers configuration, and exchanging sets of occupied and non-occupied edges on this boundary. This changes the weight of the dimers configuration by the product of the corresponding face weights. There are four classes of transformations of the "empty room" configuration (and configurations obtained from it by these transformations), which correspond to adding of different types of boxes to the room:

- Four rotation in the sets of faces as on Fig. 4.5, left, top. Each rotation of this type is weighted by $q = Q_0 = x_1x_2x_3x_4$, and corresponds to the addition of $0d$ box to one of four $3d$ Young diagrams located in the corners of the room. First rotation of this type opens possibility for three more similar rotations in the adjacent locations, which is in agreement with the fact that there are three $3d$ Young diagrams containing two boxes. Similar matching works further, until the diagram growing in one corner touches diagram from another corner. This can be easily seen considering e.g. left top corner of the "room" and erasing edges between the faces 2 and 3, 3 and 4, 4 and 1, which are not covered by any dimers there and are not involved into transformations then. Making reduction of pairs of adjacent 2-valent vertices of bipartite graph after erasing, we get hexagonal lattices, which provides $3d$ box counting [151].

- Two rotations weighted by $Q_{1,B}$ as shown on a top right panel, and two ones weighted by $Q_{1,F}$ from a bottom left panel are corresponding to addition of $1d$ boxes constituting four $2d$ Young diagrams. These $2d$ Young diagrams can be considered as a so long lines of boxes added to the corners, that they meet each other. However, since the shapes corresponding to addition of boxes to different corners are different, there is a mismatch, because of which $Q_{1,B}$ and $Q_{1,F}$ are not simply degrees of q, but contain also other combinations of the weight of faces. So the $2d$ Young diagrams determine the initial shape, on the top of which $3d$ Young diagrams are built.

- Rotation shown on a bottom right panel is weighted by Q_2 and results in the change $(N, M) \mapsto (N + 2, M + 2)$. In terms of the boxes, this can be viewed as change of the level of "floor" in the room. Since you can repeatedly apply this transformations, they are enumerated by $\mathbb{N}$ or $1d$ Young diagrams.

- There are also two types of transformations of infinite weights, shown on Fig. 4.6, left. They change $(N, M) \mapsto (N + 1, M)$ and $(N, M) \mapsto$

$(N, M+1)$, and do not contribute to the partition, since we assume boundary conditions at infinity to be fixed. However, we will be back to them in the Discussion section, we expect them to play an important role in the context of solutions of q-difference equations with the partition functions of dimers. From the point of view of box counting, these transformations are corresponding to shifts of the "walls" of the room.

Summation of $3d$ and $2d$ boxes is given by $Z_{\text{boxes}}(q, Q_B, Q_F)$ in (4.1), Q_2, Q_B and Q_F in the formula are taken at some large fixed values of (N, M). The weight in front of $Z_{\text{boxes}}(q, Q_B, Q_F)$ originates from multiplication by Q_2 factors for (N, M), $(N+2, M+2)$,...,$(N+2n-2, M+2n-2)$. The growth rate $\frac{4}{3}\varepsilon n^3$ in the exponent is related to the volume of pyramid. It matches nicely with the leading in u term

$$\mathcal{F} \sim -\frac{4}{3}\frac{(R_5 u)^3}{2\pi \mathrm{i}} \tag{4.71}$$

in (4.70), where $2\pi\mathrm{i}$ comes from the different normalization of prepotential compared to the volume. The external summation over n is for the summation over the "heights" of the floor, or divergences of size of central domain from (N, M). It has to go in the limits $-\min(N, M) \leq n \leq +\infty$, but we can take it to be two-sided infinite, since we are working in approximation $N, M \to +\infty$, which is also important for $3d$ Young diagrams to not to touch each other.

4.3.2 Inconsistency of "freezing out" and thermodynamic limit

We are going to suggest now how to freeze all non-boxcounting "rotations" at once by the proper tuning of weights of faces, and show then why thermodynamically this is incompatible with $N, M \to +\infty$ limit.

First of all, there are no possible local rotations of size $\ll N, M$ in non-bounded domains $\Omega_1, \Omega_2, \Omega_3, \Omega_4$, since the dimers configurations which tile them are "extremal": the difference with any other configuration will be a collection of paths which go in one direction and can't go back. There are many possible local rotations in the central domain, as it is shown on Fig. 4.6, right. We are looking for such limit of faces' weights to zeroes or infinities (tropical limit), that weights of all rotations in this domain are suppressed. We also want to keep finite q, so we will assume now

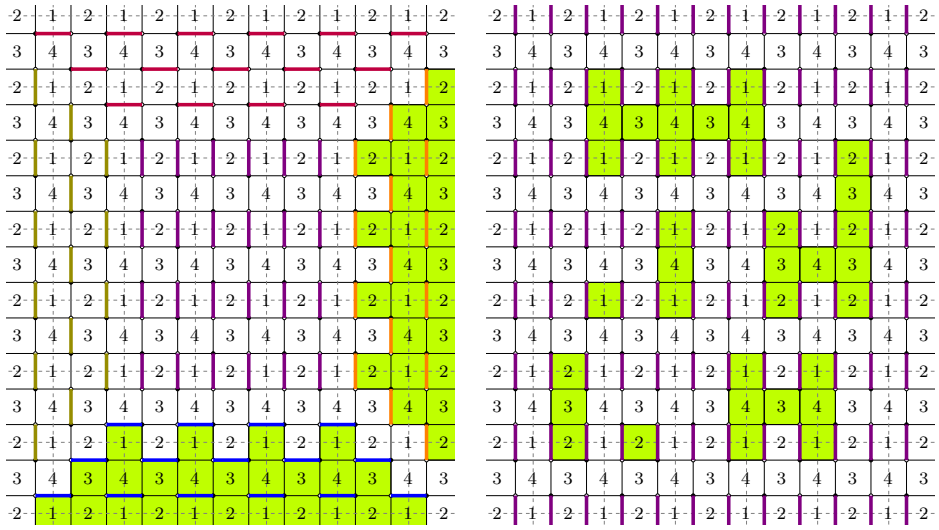

Figure 4.6. Left: "Unbounded" rotations, changing $(N, M) \mapsto (N+1, M+1)$ and $(N, M) \mapsto (N, M+1)$. Right: different types of rotation possible in the central region, which are freezing out in tropical limit. The weights of rotations shown on picture by lime color are $x_1, (x_1)^2 x_4, (x_2)^{-1}, (x_2)^{-2}(x_3)^{-1}, (x_1)^4 x_3 (x_4)^2, (x_1)^6 (x_3)^2 (x_4)^3, (x_2)^{-5}(x_3)^{-3}(x_4)^{-1}, ...$

$x_1 x_2 x_3 x_4 = 1$ in compare with the weights of individual faces. Then, the partition function of local rotations can be estimated, by selecting the term at $\lambda^0 \mu^0$ in the partition function on large torus of size $L \times L$ [118], which can be estimated as

$$\mathcal{Z}_{\mathbb{T}^2, L\times L}(\Gamma, w; D_0)|_{\lambda^0\mu^0} \leq \tag{4.72}$$

$$\leq (w_3 w_5)^{-L^2} \prod_{a=1}^{L} \prod_{b=1}^{L} \det \mathrm{K}_1(\lambda e^{\frac{2\pi i a}{L}}, \mu e^{\frac{2\pi i b}{L}})|_{\lambda^0\mu^0} \leq \left(\frac{\det \mathrm{K}_1(\lambda, \mu)}{w_3 w_5} \right)^{L^2} |_{\lambda^0\mu^0} =$$

$$= \sum_{2a+2b+c=L^2} \left(\frac{x_1}{x_2} \right)^a (x_1 x_4)^b \, (1 + x_1 + x_1 x_4 + x_1 x_3 x_4)^c$$

Using additive variables ξ_i in $x_i = e^{R_5 \xi_i + \mathrm{x}_i}$ at $R_5 \to +\infty$, all terms except 1 are vanishing if

$$\xi_1 < 0, \quad \xi_1 + \xi_4 < 0, \quad \xi_1 + \xi_3 + \xi_4 < 0, \quad \xi_1 + \xi_2 + \xi_3 + \xi_4 = 0. \tag{4.73}$$

As a check, one can see that all of the rotations shown on Fig. 4.6, right, are suppressed in this limit. It also has to be shown that these bounds

are enough to suppress all the local rotations in between of domain Ω_0 and other domains Ω_i. We do not know how to show this systematically though.

Unfortunately, constraints (4.73) are inconsistent with the thermodynamic limit $N, M \to +\infty$. We require that in thermodynamic limit all the weights $Q_0, Q_{1,B}, Q_{1,F}, Q_2$ should be finite, not becoming 0 or ∞. Inverting formulas for their weights on Fig. 4.5, one gets

$$x_1 = X_{N+1,M}, \quad x_2 = X_{N,M}, \quad x_3 = \frac{1}{X_{N,M+1}}, \quad x_4 = \frac{1}{X_{N+1,M-1}}, \tag{4.74}$$

where $X_{N,M} = \dfrac{Q_2 \cdot (Q_0)^{NM}}{(Q_{1,B})^M \cdot (Q_{1,F})^N}$. The leading terms are determined here by $Q_0 = q = e^{-\varepsilon}$ since $NM \gg N, M \gg 0$, so taking $R_5 = NM$, one gets

$$\xi_1 = -\varepsilon, \quad \xi_2 = -\varepsilon, \quad \xi_3 = \varepsilon, \quad \xi_4 = \varepsilon \quad \Rightarrow \quad \xi_1 + \xi_3 + \xi_4 = \varepsilon > 0, \tag{4.75}$$

which is inconsistent with (4.73).

Another issue with thermodynamic limit is the instability due to the multiplier $\sim q^{\frac{4}{3}n^3}$ in (4.1). Even if all Q are finite and non-boxcounting degrees of freedom are suppressed, the cubic term at $n \to -\infty$ dominates all the other contributions at fixed n, making small n preferable and breaking $N, M \gg n \gg 1$ assumptions.

4.4 Discussion

In the Chapter we made several steps towards understanding the role of cluster algebras in the theory of topological string. We have shown how starting from the "deautonomization" of cluster integrable system one naturally gets objects related to topological string: either Seiberg-Witten prepotential in the "melting" limit, or boxcounting of topological vertices in the "tropical" limit. Despite of inconsistencies, outlined in the Section 4.3.2, this consideration seems to provide proper framework for the construction of the arrow shown on Fig. 1.1 in the Introduction.

We want to sketch now how the missing arrow from Fig. 1.1 can be constructed, after resolving of inconsistencies of Section 4.3.2. First, it has

to be understood how the transformations of the weighted bipartite graph on torus, corresponding to the mutations in $\mathcal{X}$-cluster algebra, should be properly uplifted to the transformation of quasi-periodically bipartite graph on a plane. Then, in the theory of total positivity, many of A-cluster variables are come as minors of the transfer matrices of paths on the bipartite graphs [60], [13], [157], or equivalently to the different minors of the Kasteleyn operator of this graph. We can relate then the different minors of infinite-dimensional q-difference Kasteleyn operator to the different A-cluster variables in deautonomized case. These minors also correspond to the partition functions of dimers with the different boundary conditions. Those, which are related by the unbounded "rotations" from Fig. 4.6, left, in the boxcounting limit present the same partition functions, but with the slightly shifted parameters. In our example, one can produce four different partition functions in this way, corresponding to (Q_B, Q_F) and its shifts

$$(Q_{1,B}, Q_{1,F}) \mapsto (qQ_{1,B}, Q_{1,F}), \quad (Q_{1,B}, Q_{1,F}) \mapsto (Q_{1,B}, qQ_{1,F}), \quad (4.76)$$

$$(Q_{1,B}, Q_{1,F}) \mapsto (qQ_{1,B}, qQ_{1,F}),$$

which reproduces shifts of parameters in four τ-functions in [14]. Then, the q-difference equations, satisfied by the dual topological string amplitudes become a Plucker relations between the regularized infinite dimensional minors of Kasteleyn operator, or exchange relations in the corresponding A-cluster algebra. The evidences of proper combinatorics, underlying this problem, might be contained in [73], [161], [44].

There is also a number of other intriguing directions, in which the developments of this Chapter might be continued:

- It is conjectured that all the fluctuations of the height function above the limit shape at "infinite volume" $q \to 1$ limit can be described using the Gaussian free field in the properly chosen complex structure, see e.g. [104]. In Section 4.2.1 using the quasi-classical computation for the zero-mode of Kasteleyn operator we provided a heuristic derivation for the height function of the limit shape. Similar quasi-classical computation for the Green function (4.35) would provide a solution for a problem of uniformization of fluctuations in spirit of [116]: for any bipartite lattice and boundary conditions.

- The distinguishing property of prepotential $\mathcal{F}(U, Z)$ is that it satisfies the Seiberg-Witten equation (4.59). However, this equation does not fix Z-dependence completely. There are also the so-called residue formulas and WDVV equations, which are differential equations on prepotential, involving $\partial/\partial Z$ derivatives [130], [76]. These formulas would be important approbations for prepotential (4.58) as for the physical prepotential related to gauge theory.

  The formula (4.58) has to be extended also beyond the Harnak locus, since it essentially uses the property that the complex curve $P(e^z, e^w) = 0$ projects 2 to 1 inside its amoeba. Another promising direction of studies is their extension to the case $P \neq Q$. This is a completely novel direction with no known analogue of Seiberg-Witten equation.

- In [14] the quantization of cluster algebras [27], [48] was also applied, and the non-commutative q-difference bilinear equation on quantum τ-functions where derived there as a result of application of several mutations. The solutions of these equations were provided there in terms of $5d$ Nekrasov functions with the generic Ω-background, which generalizes the self-dual background of the commutative case. Our approach can be also generalized to this case in a straightforward way, promoting the face variables to be t-commutative, and performing the proper normal ordering. In this case, we expect the boxcounting formulas to be upgraded to the (q, t) counting of "refined topological vertices" [98]. Similar ideas were proposed in [142]. Also the property of refined topological amplitude to intertwine the action of quantum toroidal algebra [3] might find its "cluster" interpretation using two-parametric quantization of classical r-matrix of [83]. It would be also interesting to "refine" results of [37] in this setting.

- The dimer models are similar to the Hermitian matrix models, since both can be described as specifications of Schur processes [149], [132]. One of the most fundamental properties of matrix models is the genus expansion, when the diagrams of perturbation theory are interpreted as ribbon graphs, and the entire series is interpreted as a summation over all topologies. Similar expansion in q-case is more tricky and there is no final answer what to count as "expansion over genuses" in that case yet [138]. However, the dimer models might

shed some light on this.

By bipartite graph on surface one can construct bipartite graph on dual surface by twisting all of its ribbons [71]. This can be also done with the graph Γ on the plane $\mathbb{R}^2$, getting the graph $\tilde{\Gamma}$ on the infinite genus, but "regular", dual surface $\tilde{S}$. Uplifting the paths, which are contributions to the normalized partition function of dimers, to the dual surface, one gets the set of cycles of non-trivial topology on $\tilde{S}$. Shrinking all the cycles on $\tilde{S}$, which are not winded by these paths, one gets finite genus curve, so the entire partition function becomes a summation over the surfaces of different topologies.

Once the expansion is properly formulated, one can find the observables for q-deformed resolvent, cut and joint, and check operators to obtain the loop equations and formulate q-topological recursion. This topological recursion might be also useful for the enumerative problems of [103] and [37].

- The phase space of cluster integrable system, as $\mathcal{X}$-cluster variety, is equipped with the logarithmically quadratic Poisson bracket for the face variables. For our main example from Fig. 4.1 the quiver encoding this bracket is drawn on Fig. 2 from [14] under the name $A_7^{(1)'}$. The same quiver can be obtained[6] by computing the Euler form of sheaves from the exceptional collection

$$\mathcal{C} = (\mathcal{O}(0), \mathcal{O}(1,0), \mathcal{O}(1,1), \mathcal{O}(2,1)) \tag{4.77}$$

of coherent sheaves on Hirzebruch surface $\mathbb{F}_0 = \mathbb{P}^1 \times \mathbb{P}^1$ [18]. More striking coincidence is that the formula (4.22) from [18] for the Chern classes $[N; (c_{1,1}, c_{1,2}); c_2]$ of the dual objects

$$\gamma_1 = [1; (0,0); 0], \quad \gamma_2 = [-1; (1,0); 0], \tag{4.78}$$

$$\gamma_3 = [-1; (-1,1); 1], \quad \gamma_4 = [1; (0,-1); 0]$$

can be reproduced taking the "finite", not depending on N and M parts of degrees of Q_i variables in (4.74), and under identifications

$$\gamma_1 \leftrightarrow x_2, \quad \gamma_2 \leftrightarrow x_3, \quad \gamma_3 \leftrightarrow x_4, \quad \gamma_4 \leftrightarrow x_1, \tag{4.79}$$

[6] We are grateful to Fabrizio Del Monte for bringing our attention to this correspondence

$$N \leftrightarrow \deg Q_2, \quad c_{1,1} \leftrightarrow \deg Q_{1,B}, \quad c_{1,2} \leftrightarrow \deg Q_{1,F}, \quad c_2 \leftrightarrow \deg Q_0. \tag{4.80}$$

The correspondences above are precise to be just coincidence, so the dimer statistical model should have the deeper meaning in the counting of geometric objects, and there is a point to start. The local $3d$ Calabi-Yau, a mirror dual to the one defined by $uw = P(\lambda, \mu)$ with P from (4.54), is the total space of the canonical bundle over $\mathbb{F}_0$ [6], and D-branes on this total space are in correspondence with the exceptional collection of sheaves on the base [18]. And there is a straightforward way to produce more examples of this kind for check, since the both sides (either local $3d$ CY and cluster integrable system with the spectral curve P) can be conveniently constructed starting from the Newton polygon.

Chapter 5

Alternating currents and shear waves in viscous electronics

5.1 Introduction

Existence of strongly interacting carriers in high-mobility materials opens fascinating possibilities for "viscous electronics" where current flows like a viscous fluid rather than according to Ohm's law [9, 33, 137, 176, 124]. Here we describe a new phenomenon that could be observable in such materials - propagating shear waves. We show that, apart from intrinsic interest, observing such waves gives an independent way to measure the viscosity of the electronic fluid and establish what are the real boundary conditions satisfied by electronic flows.

Propagation of weak low-frequency currents in strongly interacting systems is described by classical viscous hydrodynamics. Viscous hydrodynamics has been mostly focused on the flows past the bodies. Viscous electronics makes it necessary to consider flows produced by sources and sinks. Studies of DC currents were started recently in [124, 54, 176, 66, 67] and brought several interesting effects (current flowing against electric field, super-ballistic conductance, electric field expulsion from a flow, etc), some of which were observed experimentally [9, 168].

In this Chapter we present a study of alternating current (AC) either flowing across the strip or past the obstacles like strongly disordered zones in the bulk. In the Ohmic case, time-dependent voltage on the electrodes

makes the current and potential distribution instantaneously adjust to it, as far as the flow is incompressible. In the viscous case, momentum propagates by diffusion, which leads to retardation and the possibility of running waves. We consider only charge neutral viscous modes, interaction of electromagnetic waves with viscous electron flows was considered in [41].

For weak currents we can neglect non-linearity in the Navier-Stokes equations and by incorporating Ohmic resistance get the following equation:

$$mn(\partial_t + \gamma_p(r))v_i - \eta\nabla^2 v_i = -ne\partial_i\varphi. \tag{5.1}$$

For AC case all quantities depend on time as $e^{-i\Omega t}$. For such dependence equation gets form:

$$(-i\Omega + \gamma_p(r))v_i - \nu\nabla^2 v_i = -em\partial_i\varphi\,, \tag{5.2}$$

where $\nu = \eta/mn$ is the kinematic viscosity.

We start by describing the simplest setting for generating a shear wave. During the process of placing a graphene sheet on an insulating substrate many impurities are accumulating between them. Due to Van-der-Waals forces, the impurities tend to concentrate in the localized regions, "bubbles" and "folds", where resistance is high. Running AC current through the sample with such regions will generate shear viscous waves transversal to the current. If impurities concentrate in a long fold, we suggest running AC current parallel to its boundary $\vec{v}_0(x,y) = v_0 e^{-i\Omega t}\vec{e}_x$. We assume that $\gamma_p \to \infty$ inside the fold and zero outside. Then the current must turn to zero at the boundary of the current-carrying region, which thus corresponds to the no-slip boundary condition. The solution of (5.10) then has a simple form

$$v_x(y,t) = v_0\,\mathrm{Re}\left(\exp[-i\Omega t](1-\exp[-|y|\sqrt{-i\Omega/\nu}])\right), \tag{5.3}$$

which describes a wave propagating with the speed $\sqrt{2\nu\Omega}$ while oscillating and exponentially decreasing in space with the same wavenumber $\kappa = \sqrt{\Omega/2\nu}$. Therefore, registering such a wave gives one an ability to directly measure the viscosity of the electronic fluid. The above consideration is valid at sufficiently low frequencies such that the speed of the viscous wave is much smaller then the speed of sound-plasmon mode: $\sqrt{2\nu\Omega} \ll v_F/\sqrt{2}$. On the other hand, the wavelength must be less than the sample size, which is realistically not much larger than Nl_{ee} with $N \simeq 5$.

One can estimate $\nu \simeq v_F l_{ee}$ where l_{ee} is the mean free path for momentum-conserving electron-electron collisions. That allows one to recast the applicability condition as $N^{-2} < \Omega l_{ee}/v_F < 1$. At $\Omega \simeq 10GHz$ the respective wavelength is several microns for graphene with $v_F \simeq 10^6\, m/sec$ and $\nu \simeq 10^3 cm^2/sec$ [9]. Due to small sizes of samples, the retardation effects for EM waves related to the finite light speed can be neglected up to THz frequencies, for which EM wave length is about 100 μm.

5.2 Half-plane geometry

In order of increasing complexity, we consider now the current injected into a half plane. The potential in the half-plane with a no-stress boundary can be computed exactly:

$$\phi = \frac{I_0 \nu}{\pi m e} \mathrm{Re}\, e^{-i\Omega t} \left(\frac{\gamma_p - i\Omega}{\nu} \log(r\lambda_{\mathrm{IR}}) - \frac{y^2 - x^2}{(x^2+y^2)^2} \right)$$

Note that finite frequency is equivalent to a finite imaginary resistivity, for the large r-s - we have logarithmic behavior at infinity as in the Ohmic case. And like in the usual electrical networks, "impedance" $z = \dfrac{\gamma_p - i\Omega}{\nu}$ defines the phase shift between I and ϕ. But in half-plane there are no real running waves of the potential - only zero-potential line which is oscillating between 0 and ∞ once each half-period. In the no-slip case we have the same asymptotic behaviour. However, running waves could be clearly seen on the vorticity map. For example, vorticity for the no-stress case is given by:

$$\omega = -\frac{I}{\pi} \mathrm{Re}\, e^{-i\Omega t} \int_0^{+\infty} e^{-qy} k \sin(kx) dk$$

where $q^2 = k^2 + \varkappa$, $\varkappa = (\gamma_p - i\Omega)/\nu = \rho e^{i\theta}$ so ρ describes overall intensity of resistance, and $\theta = -\arctan \Omega/\gamma_p$ - relative contributions of reactance and resistance. As $\Omega > 0$, $\gamma_p > 0$, thus $0 > \theta > -\pi/2$. Properties of the running wave can be extracted by considering the asymptotic $y \to +\infty$ in the vicinity of $x = 0$, where the integral oscillates and exponentially decreases with y. Vorticity in this limit is given by:

$$\omega = -Ix \sqrt{\frac{\rho^{3/2}}{2\pi y^3}} \cos\left(-y\sqrt{\rho} \sin\frac{\theta}{2} + \frac{3}{2}\theta - \Omega t \right) e^{-y\sqrt{\rho}\cos\theta/2}$$

The propagation speed of zero-vorticity lines and the amplitude decay rate are the same in both no-slip and no-stress cases and respectively given by

$$v = \frac{\Omega}{\sqrt{\rho}|\sin\theta/2|}, \quad \gamma = \sqrt{\rho}\cos\frac{\theta}{2}. \tag{5.4}$$

The main difference between no-slip and no-stress cases is in the behavior near the boundary. In the no-stress case zero vorticity lines are approaching edge in the transverse direction, while in the no-slip case they are oriented along the edge. Running waves and behaviour near the boundary can be see in Fig. 5.6 and Fig. 5.7 in Section 5.5). Similar difference in the behaviour near the boundary could be also observed in the strip geometry.

5.3 Strip geometry

Let us now describe in detail how AC current across the strip generates a shear wave running along the strip. It is instructive to comment on the DC case first. In this case, at the distance from the electrodes comparable to the strip width w, the pair of separatrices appears, dividing the inside streamlines connecting electrodes and closed lines outside, that belong to vortices [54]. The pattern of the vortical flow outside depends crucially on the boundary conditions [163]. If the boundary is stress-free then the streamlines close to the separatrices are able to go arbitrary far before turning back. If, however, boundary stress is non-zero (as, for instance, at a no-slip boundary) then the streamlines turn back at a finite distance and a chain of vortices appears (an infinite chain in an infinite strip). The properties of waves in the AC case are then also strongly dependent on the boundary conditions, as shown below.

Experimentally, it is most feasible to change the frequency Ω. Whether the frequency is large or small is determined by comparing the period with the viscous time of momentum diffusion across the strip, $\tau = w^2/\nu$. Therefore, the dimensionless parameter is $\Omega\tau = \Omega w^2/\nu$. We can also denote $D_v = \sqrt{\nu/\Omega}$, which is the characteristic vortex's length scale, as it can be seen e.g. from the formula (5.4). Since $\Omega\tau = (w/D_v)^2$ then low frequency (DC limit) corresponds to a narrow strip. When the frequency $\Omega \to 0$, we find very different phase velocities for different boundary conditions: no-slip boundary corresponds to the wave velocity going to zero while no-stress to a finite value.

Assuming translational symmetry along x and a uniform Ohmic resistance we write for the Fourier harmonics of the stream function defined by $\vec{v}(x,y) = \nabla \times \vec{e}_z \psi(x,y)$:

$$(\partial_{yy} - q^2)(\partial_{yy} - k^2)\psi = 0 \tag{5.5}$$

Considering dynamics of the fluid constrained by the two edges at $-w/2$ and $w/2$, we have to put also boundary conditions. The velocity component normal to the boundary is zero everywhere, except the source and the sink: $v_y(x, \pm w/2) = I_0 \delta(x)$. For the tangential component we generally impose mixed conditions $v_x = l\partial_y v_x$ at $y = -w/2$ and $v_x = -l\partial_y v_x$ at $y = w/2$, which transforms into no-slip in the limit $l \to 0$ and into no-stress in the limit $l \to \infty$. Dependence of the results on l could be analytically evaluated in the DC case (see Supplementary Materials): for a finite nonzero l the features are qualitatively similar to the no-slip limit. Influence of a finite Ohmic resistance is similar to that in the half-plane case, so from now on we neglect Ohmic resistance.

We start analysis of vortex dynamics in the strip from the vorticity distribution in the no-stress case:

$$\omega(x,y) = -\frac{I}{\pi} \mathrm{Re}\, e^{-i\Omega t} \int_0^{+\infty} k \sin kx \frac{\cosh yq}{\cosh \frac{wq}{2}} dk \tag{5.6}$$

For a wide strip, dynamics is almost width-independent: vortices are ejected from the electrodes and move toward the mid-line of the strip, where they meet, join, and move along the strip as a single big vortex which occupies entire strip. It can be seen, that far from the source they have regular form, distinct geometrical periodicity and on average - vorticity decays exactly exponentially.

When $w/D_\nu \to \infty$, the distance between vortices saturates to a constant, while if $w/D_\nu \to 0$, the wave length tends to infinity as D_ν/w. The results of numerical computation shown in the Fig. 5.2, left, are in a good agreement with the results of the "saddle point" estimation for the integral. To put it simply, vortices cannot be squeezed into too narrow strip.

Let us see how different is the no-slip case. Vorticity in this case is

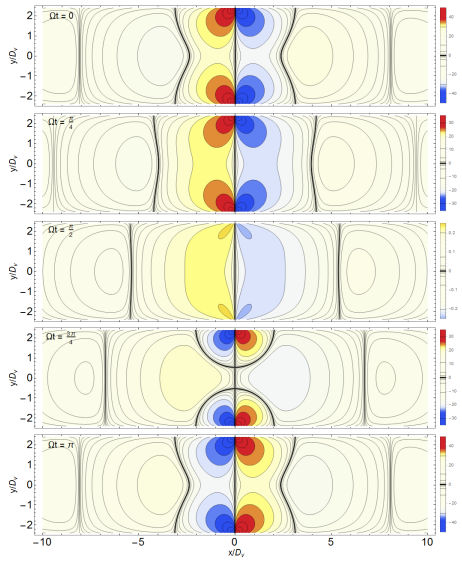

Figure 5.1. Contours of constant vorticity $\omega(x, y) = const$ for the no-stress boundary conditions for $w/D_\nu = 5$. Different pictures correspond to different moments of time. Places where lines condensate correspond to the isolines $\omega(x, y) = 0$. Videos with the dynamic here and below can be sent by authors on demand.

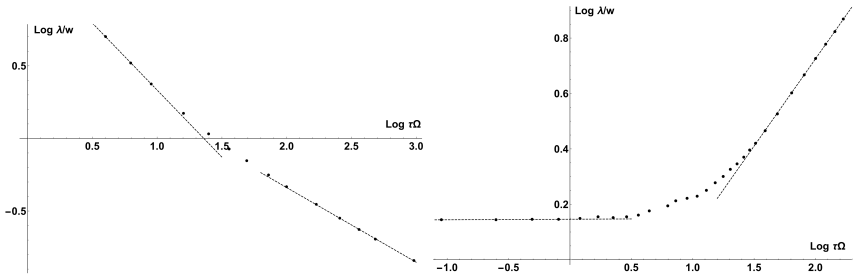

Figure 5.2. Dependence of the distances between zeroes of function $\omega(x, 0)$ (see Fig. 5.3) far from the source in log-log scale. Lines - linear fit, points - results of numerics. Upper panel: no-stress case. Asymptotic dependence on the frequency is $\lambda/w \sim (\tau\Omega)^{-1}$, $\Omega \to 0$ and $\lambda/w \sim (\tau\Omega)^{-1/2}$, $\Omega \to \infty$ $(x \gg w,\ D_\nu)$ Lower panel: no-slip case. Here $\lambda/w \sim const$, $\Omega \to 0$ and $\lambda/w \sim (\tau\Omega)^a$, $\Omega \to \infty$, $a \sim 0.6$. Characteristic time scale is $\tau = w^2/\nu$

given by:

$$\omega = \frac{I}{\pi} \operatorname{Re} e^{-i\Omega t} \int_0^{+\infty} \frac{dk \; \varkappa \cosh yq \sinh \frac{wk}{2} \sin kx}{k \cosh \frac{wq}{2} \sinh \frac{wk}{2} - q \cosh \frac{wk}{2} \sinh \frac{wq}{2}}$$

The major striking difference is that zero-vorticity lines at mid-strip move towards the source as seen in Fig. 5.3. The reason is that the wave of vorticity is emitted from the source not as a round vortices, as in the no-stress case, but rather as elongated ellipses oriented along the edge.

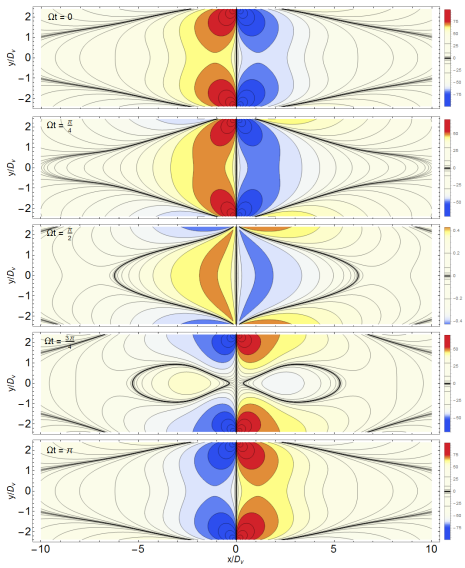

Figure 5.3. Contours of the constant vorticity $\omega(x, y) = const$ for the no-slip boundary conditions for $w/D_\nu = 5$.

The movement of the vortex line in mid-strip is the result of the meeting of 'waves', coming from the source and the sink. Frequency dependence of the distance between zero-vorticity points at $y = 0$, which in fact is the vortex size, is shown on the Fir. 5.2, right. This horizontal distance is different from the vertical distance between "layers" in the half-plane case, and thus doesn't tend to some constant in the limit $w \to \infty$ (in distinction from the distance between vortices in the no-stress case). DC limit $\Omega \to 0$ corresponds to $w/D_\nu \to 0$. As follows from the consideration of the DC

case, there must still exist vortices of finite length in this limit, as long as

$$\lambda/D_\nu \sim w/D_\nu \quad \Rightarrow \lambda \sim w, \tag{5.7}$$

that is the vortex size shouldn't depend on Ω. Another interesting novelty in comparison with the no-stress case is that for the narrow strip vortexes are moving by jumps, not smoothly. The less is w, the shorter is the duration of jump - major part of the period vortices are spending as a standing wave, and only when the amplitude is very little, $I(t) \to 0$, they are moving. In the limit $w \to \infty$, vortexes are moving smoothly. This phenomenon is due to the asymmetry between the real and imaginary parts of the function.

Formula for the voltage in the no-stress case has the form:

$$V_{l\to\infty}(x,y) = \phi(x,y) - \phi(+\infty,y) =$$

$$= -\frac{m\nu I_0}{e\pi}\ \mathrm{Re}\ e^{-i\Omega t} \int\limits_0^{+\infty} dk \frac{q^2 \sinh ky}{k \cosh \frac{kw}{2}} \cos kx \tag{5.8}$$

and, surprisingly, there are no vortices at all, as it can be seen, e.g. on the Fig. 5.4. This happening because of miraculous cancellation of the terms containing $\cosh qw/2$ in the numerator and in the denominator. However, this cancellation is absent for finite l length, and thus for general l we shall see vortices as in the no-slip case. Potential for the no-slip case has the form:

$$V_{l\to 0}(x,y) = \phi(x,y) - \phi(+\infty,y) = -\frac{m\nu I_0}{e\pi}\ \mathrm{Re}\ \varkappa e^{-i\Omega t} \times$$

$$\times \int\limits_0^{+\infty} \frac{qdk}{k} \frac{\sinh ky \sinh \frac{wq}{2} \cos kx}{k \cosh \frac{wq}{2} \sinh \frac{wk}{2} - q \cosh \frac{wk}{2} \sinh \frac{wq}{2}} \tag{5.9}$$

General behaviour is qualitatively similar to that of the vorticity, including freezing and inverted phase speed.

5.4 Conclusions

To conclude, vorticity and potential waves propagating along the strip are qualitatively different for no-stress and no-slip boundary conditions - waves could be observed on the vorticity map in the both cases, and on

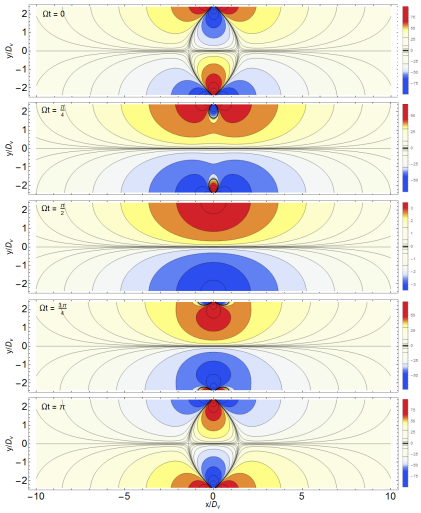

Figure 5.4. Distribution of the voltage for the no-stress case

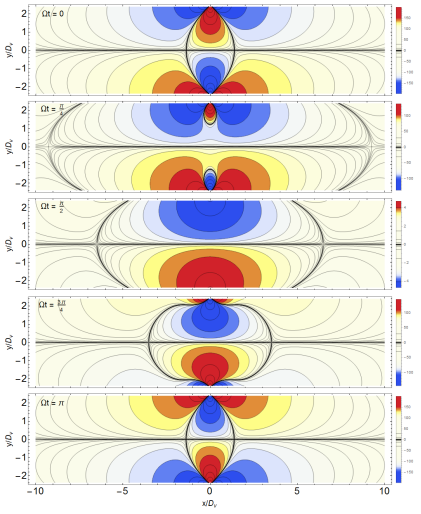

Figure 5.5. Distribution of the potential in the no-slip case.

the potential map in the no-slip case only. There is no running potential wave for no-stress case. Moreover, phase speed of the waves is directed in the opposite directions in the different cases. Wave-length of viscous

waves also depending on the frequency in a different ways for the no-stress and no-slip cases.

5.5 Appendix A. AC current in a half-plane

To find the velocity field of a Ohmic-viscous flow we need to solve the equation:

$$(-i\Omega + \gamma_p(r))v_i - \nu\nabla^2 v_i = -em\partial_i\varphi\,, \tag{5.10}$$

with the uniform Ohmic resistivity $\gamma_p(r) = const$. Acting by $\nabla\times$ on both sides and assuming translational invariance along x, we get the equation for the stream function:

$$(\partial_{yy} - q^2)(\partial_{yy} - k^2)\psi = 0. \tag{5.11}$$

Here the stream function is defined by $\vec{v}(x,y) = \nabla\times\vec{e}_z\psi(x,y)$, its Fourier image $\psi(x,y) = \int \frac{dk}{2\pi}e^{ikx}\psi(k,y)$, and

$$q^2 = k^2 + \varkappa, \quad \varkappa = (\gamma_p - i\Omega)/\nu = \rho e^{i\theta}.$$

This equation has 4 solutions $\psi(k,y) = c_1e^{-|k|y} + c_2e^{|k|y} + c_3e^{qy} + c_4e^{-qy}$. General boundary conditions $v_y(x,0) = I_0\delta(x)$ and $v_x(x,0) = l\partial_y v_x(x,0)$ give $\psi(k,0) = I/(ik)$ and $l\partial_{yy}\psi(k,0) = \partial_y\psi(k,0)$. Adding condition $v(x,y) \to 0, \quad y \to +\infty$ we completely define all the coefficients and find:

$$\psi(x,y) = \frac{I}{\pi}\int\limits_0^{+\infty} \frac{e^{-qy}k(1+kl) - e^{-ky}q(1+ql)}{k(k-q)(1+l(k+q))}\sin(kx)dk\ . \tag{5.12}$$

The solution for the non-resistive case corresponds to the limit $\varkappa \to 0$. The vorticity $\omega(x,y) = \Delta\psi(x,y)$ is plotted in Figure 6, where one can see two vortices appearing every half-period. A line of zero vorticity separates the two vortices from the next pair. In the lower panel of Fig. 5.6, the vorticity is shown for the case with strong ohmic resisitivity, $\theta = -\pi/6$. It can be seen that in this case vortices disappear much faster, yet there are no qualitative differences. Thus, for simplicity sake, further we will consider non-ohmic case only. In the no-slip case, zero-vorticity line is oriented along the edge of the bulk. On the contrary, the line comes in the transverse direction in the no-stress case. This difference gives

qualitatively different pictures for the strip case.
Most of the flow properties related to vortices are encoded in the vorticity:

$$\omega(x,y) = -\frac{I}{\pi}\int\limits_0^{+\infty} \frac{(1+kl)(k+q)}{1+l(k+q)} e^{-qy}\sin(kx)dk \tag{5.13}$$

In the no-stress case $l \to +\infty$ we have:

$$\omega(x,y) = -\frac{I}{\pi}\int\limits_0^{+\infty} e^{-qy} k\sin(kx)dk \tag{5.14}$$

It is vanishing at the $x = 0$. However, we can consider its behaviour at $x \sim 0$. As for $k \gg 1/y, k \gg 1/\sqrt{\rho}$ exponential suppresses other integrands, and for small x we can expand $\sin(kx) \sim kx$. At the first order we have:

$$\omega(x,y) = -\frac{Ix}{\pi}(\partial_{yy}^2 - \varkappa)\int\limits_0^{+\infty} e^{-qy}dk \tag{5.15}$$

Obtaining asymptotic at $y \to +\infty$, in the lowest order in $1/y$ we get:

$$\omega(x,y) = -Ix\sqrt{\frac{\varkappa\sqrt{\varkappa}}{2\pi y^3}} e^{-y\sqrt{\varkappa}}, \tag{5.16}$$

$$\omega(x,y,t) = \operatorname{Re}\omega(x,y)e^{-i\Omega t} =$$

$$= -Ix\sqrt{\frac{\rho^{3/2}}{2\pi y^3}}\cos\left(-y\sqrt{\rho}\sin\frac{\theta}{2} + \frac{3}{2}\theta - \Omega t\right) e^{-y\sqrt{\rho}\cos\theta/2}$$

Thus, zero-vorticity lines correspond to:

$$-y\sqrt{\rho}\sin\frac{\theta}{2} + \frac{3}{2}\theta - \Omega t = \pi\left(k + \frac{1}{2}\right), \quad k \in \mathbb{Z} \tag{5.17}$$

Or for the non-Ohmic case:

$$y\sqrt{\Omega/2\nu} - \Omega t = \pi\left(k + \frac{3}{4}\right), \quad k \in \mathbb{Z} \tag{5.18}$$

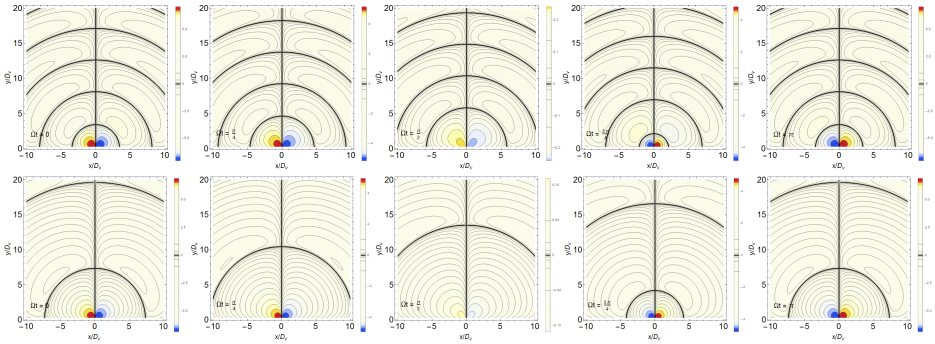

Figure 5.6. No-stress case. Upper row: vorticity for the half-plane for the pure AC case, $\theta = -\pi/2$. Lower row: partially ohmic case: $D_\nu = 1/\sqrt{\rho}$, $\theta = -\pi/6$

In the no-slip case $l \to 0$ we have:

$$\omega(x,y) = -\frac{I}{\pi}\int\limits_0^{+\infty} e^{-qy}(k+q)\sin(kx)dk \tag{5.19}$$

In the lowest degrees by $1/y$ and x it gives:

$$\omega = \omega_{l\to+\infty} - \frac{Ix\varkappa}{\pi y}e^{-y\sqrt{\varkappa}} = -Ix\left(\sqrt{\frac{\varkappa\sqrt{\varkappa}}{2\pi y^3}} + \frac{\varkappa}{\pi y}\right)e^{-y\sqrt{\varkappa}} \tag{5.20}$$

For large enough y we get:

$$\omega(x,y) \sim -\frac{Ix\varkappa}{\pi y}e^{-y\sqrt{\varkappa}}, \tag{5.21}$$

$$\omega(x,y,t) \sim -\frac{Ix\rho}{\pi y}e^{-y\sqrt{\rho}\cos\frac{\theta}{2}}\cos\left(y\sqrt{\rho}\sin\frac{\theta}{2} + \Omega t - \theta\right) \tag{5.22}$$

Thus, the coordinates of zero-vorticity lines are given by:

$$y\sqrt{\rho}\sin\frac{\theta}{2} + \Omega t - \theta = \pi\left(k+\frac{1}{2}\right) \quad k \in \mathbb{Z} \tag{5.23}$$

In the non-Ohmic case, it gives:

$$y\sqrt{\Omega/2\nu} - \Omega t = \pi k \quad k \in \mathbb{Z} \tag{5.24}$$

The speed of zero-vorticity line and the decay rate of excitations are the same in both cases:

$$v = \frac{\Omega}{\sqrt{\rho}|\sin\theta/2|}, \quad \gamma = \sqrt{\rho}\cos\frac{\theta}{2} \tag{5.25}$$

which shows robustness of the result with respect to appearance of small ($\gamma_p < \omega$) Ohmic contribution, which only slightly changes angle θ.

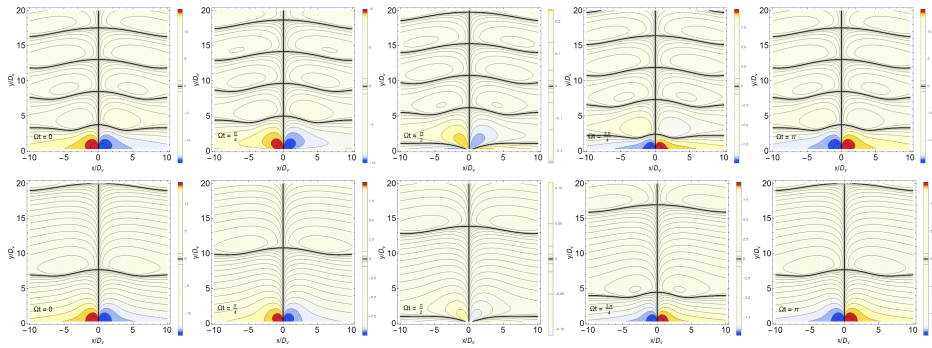

Figure 5.7. No-slip case. Upper: vorticity for the half-plane for the pure AC case, $\theta = -\pi/2$. Lower: partially ohmic case: $D_\nu = 1/\sqrt{\rho}$, $\theta = -\pi/6$

The potential is be obtained as follows:

$$\partial_i\varphi = -\frac{\nu}{em}(\varkappa - \nabla^2)v_i \tag{5.26}$$

which for general l gives

$$V(x,y) = \phi(x,y) - \phi(+\infty,y) = \frac{\varkappa I\nu}{\pi me}\int\limits_0^{+\infty} \frac{q(1+lq)e^{-ky}}{k(k-q)(1+l(k+q))}\cos(kx)dk\,. \tag{5.27}$$

That gives in the no-stress limit $l \to +\infty$

$$V_{l\to+\infty}(x,y) = -\frac{I\nu}{\pi me}\int\limits_0^{+\infty}\frac{q^2}{k}e^{-ky}\cos(kx)dk \tag{5.28}$$

which has singularity at $x, y \to 0$ given by

$$V_{l\to+\infty}(x,y) \sim -\frac{I\nu}{\pi me}\frac{y^2-x^2}{(y^2+x^2)^2}\,. \tag{5.29}$$

That coincides with the expression for the DC case. Asymptotic for large x is given by

$$V_{l\to+\infty}(x,y) \sim -\frac{I\nu\varkappa}{\pi me}\mathrm{Re}\int\limits_0^{+\infty}\frac{e^{-k(y+ix)}}{k}dk \sim -\frac{I\nu\varkappa}{\pi me}\log(r\lambda_{IR}) \qquad (5.30)$$

and has log-dependence on IR cutoff (assuming that $r \ll 1/\lambda_{IR}$). This assymptotic coincide up to a complex phase with the solution for the Ohmic case. No-slip limit $l \to 0$ is as follows:

$$V_{l\to 0}(x,y) = -\frac{I\nu}{\pi me}\int\limits_0^{+\infty}\frac{q(k+q)e^{-ky}}{k}\cos(kx)dk = \qquad (5.31)$$

$$= V_{l\to+\infty}(x,y) - \frac{I\nu}{\pi me}\int\limits_0^{+\infty} qe^{-ky}\cos(kx)dk,$$

and has similar asymptotic behaviour. In both cases there are no running waves, as far as there is no spatially oscillating mixing between real and imaginary parts.

5.6 Appendix B. General equations for the strip

Expression for ψ in the case of strip could be obtained from the general solution

$$\psi(k,y) = A\cosh ky + B\cosh qy + C\sinh ky + D\sinh qy \qquad (5.32)$$

of the equation

$$(\partial_{yy} - k^2)(\partial_{yy} - q^2)\psi = 0 \qquad (5.33)$$

with the boundary conditions

$$\psi(k,-w/2) = \frac{I}{ik},\ l\partial_{yy}\psi(k,-w/2) = \partial_y\psi(k,-w/2) \qquad (5.34)$$

$$\psi(k,w/2) = \frac{I}{ik},\ l\partial_{yy}\psi(k,w/2) = -\partial_y\psi(k,w/2) \qquad (5.35)$$

(for definitions of q and $\psi(k,y)$ see previous Section). General solution looks:

$$\psi(x,y) = -\frac{I}{\pi}\int\limits_0^{\infty}\frac{dk}{k}. \qquad (5.36)$$

$$\cdot\frac{q\cosh ky\left(lq\cosh\frac{qw}{2}+\sinh\frac{qw}{2}\right)-k\cosh qy\left(kl\cosh\frac{kw}{2}+\sinh\frac{kw}{2}\right)}{k\cosh\frac{qw}{2}\sinh\frac{kw}{2}-q\cosh\frac{kw}{2}\sinh\frac{qw}{2}-\varkappa l\cosh\frac{kw}{2}\cosh\frac{qw}{2}}\sin kx$$

where y - coordinate from the mid of the strip, and for vorticity:

$$\omega(x,y)=\frac{I}{\pi}\cdot \tag{5.37}$$

$$\cdot\int dk\frac{\varkappa\cosh qy\left(kl\cosh\frac{kw}{2}+\sinh\frac{kw}{2}\right)}{k\cosh\frac{qw}{2}\sinh\frac{kw}{2}-q\cosh\frac{kw}{2}\sinh\frac{qw}{2}-\varkappa l\cosh\frac{kw}{2}\cosh\frac{qw}{2}}\sin kx.$$

General expression for the potential

$$V(x,y)=\phi(x,y)-\phi(\infty,y)=-\frac{Im\nu}{e\pi}\cdot \tag{5.38}$$

$$\cdot\int_0^\infty\frac{dk}{k}\frac{\varkappa q\sinh ky\left(lq\cosh\frac{qw}{2}+\sinh\frac{qw}{2}\right)}{k\cosh\frac{qw}{2}\sinh\frac{kw}{2}-q\cosh\frac{kw}{2}\sinh\frac{qw}{2}-\varkappa l\cosh\frac{kw}{2}\cosh\frac{qw}{2}}\cos kx$$

is computed by integration of Stokes equation in x and differentiation on y.

5.7 Appendix C. Wavelength computations

Dependence $\lambda/D_\nu(w/D_\nu)$ can be found analytically in the various independent ways. First of all, we can apply saddle-point approximation, as far as we have large parameter $x\to+\infty$. If we find saddle-point value of the wave-number $k_0=k_0(w)$, we will be able to obtain distance between vortices as $\lambda_0=\pi/\mathrm{Re}\,k_0$. For integral

$$\omega(x,0)=-\frac{I}{2\pi i}\int_{-\infty}^{+\infty}ke^{ikx-\ln\cosh wq/2}dk \tag{5.39}$$

saddle-point equation can be written as:

$$\frac{kw}{qw}\tanh qw/2=i\frac{x}{w}\quad(\text{where }\ q=\sqrt{k^2-i/D_\nu^2}) \tag{5.40}$$

If we are interested in the behavior of the function for the large values of x, we should make l.h.s. of equation large. There are two ways to do so. If $w/D_\nu\gg1$, then we need $q\ll k$, and thus $k\to(1+i)/\sqrt{2}D_\nu$,

$\lambda_0 = \pi\sqrt{2}D_\nu$. In the opposite limit $w/D_\nu \ll 1$ we can make tanh large by choosing $q \sim k \sim i\pi/2w + O(w/D_\nu^2)$ - main contribution is purely imaginary. Sub-leading order:

$$k_0 \sim i\pi/2w + \sqrt{-i}/x + w/D_\nu^2\pi + O(w^3), \tag{5.41}$$

in the limit $x \to +\infty$ gives $\lambda_0 = \pi^2 D_\nu^2/w$. Both results agree with the results of the numerics presented in the main text.

For the no-slip case we can again try to find λ by finding the pole closest to the real axis. Equation for the pole has the form:

$$q \sinh\frac{qw}{2}\cosh\frac{kw}{2} - k\sinh\frac{kw}{2}\cosh\frac{qw}{2} = 0 \tag{5.42}$$

It can be symmetrized by using replacements:

$$k^2 = i/2(\sigma+1), \quad \gamma = w/2\sqrt{i/2} \tag{5.43}$$

and gets form

$$\sqrt{\sigma+1}\tanh\gamma\sqrt{\sigma+1} = \sqrt{\sigma-1}\tanh\gamma\sqrt{\sigma-1} \tag{5.44}$$

In the limit $\gamma \to 0$ (or equally $w \to 0$) it can be solved by direct expansion in σ. In the first order $\sigma = 3/(2\gamma^2)$, which gives $k_0 = \sqrt{6/w^2 + i/2D_\nu^2}$, $\lambda_0 = \pi w/\sqrt{6}$. Opposite limit $w \to +\infty$ is treated numerically in the main text.

5.8 Appendix D. Comment on DC case in the strip

The DC case in the strip was considered in the [124], where only one pair of vortices was shown both for no-slip and and no-stress case. Here we show that there could be multiple pairs of vortices. Consider, for instance, vorticity for the DC case:

$$\omega(x,y) = -\frac{4I_0}{\pi}\int\limits_0^{+\infty} \frac{k\cosh ky\left(kl\cosh\left(\frac{kw}{2}\right)+\sinh\left(\frac{kw}{2}\right)\right)}{2kl(1+\cosh kw)+kw+\sinh kw}\sin kx\, dk \tag{5.45}$$

At $x \gg w$ one can use the sadle-point approximatin with the following saddle point condition:

$$2kl(1+\cosh kw)+kw+\sinh kw = 0\,. \tag{5.46}$$

It gives in the two limits:

- $l \to 0$: $kw + \sinh kw = 0$ - lots of solutions, with non-zero imaginary part (minimal - with Re $k_0 \sim 2.25$).

- $l \to \infty$: $k_0 \sim i\pi(2k+1) + \dfrac{1}{\sqrt{lw}}$, i.e. $\lambda = \dfrac{\pi}{\mathrm{Re}\, k_0} \sim \pi\sqrt{lw}$

Results of numerical solving of this equation is given in the figure below, which coincides well with the analytic asymptotic.

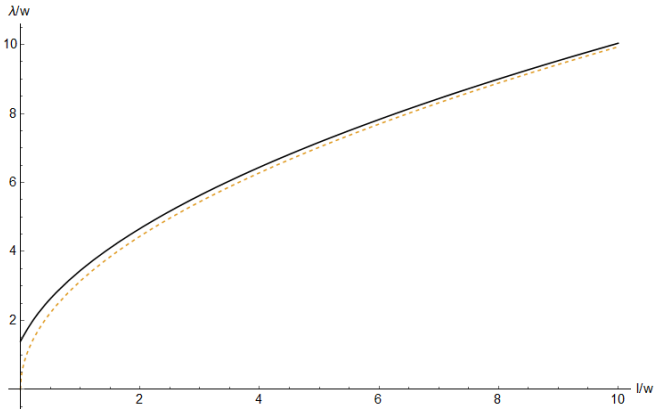

Figure 5.8. Dependence of the wavelength on the slippage parameter. In the limit $l \to +\infty$ the wavelength tends to infinity, while for all the other values it remains finite. Dashed line - analytical asymptotic for $l \to +\infty$.

Bibliography

[1] P.C.Argyres, M.R.Douglas, *New Phenomena in SU(3) Supersymmetric Gauge Theory*; Nucl. Phys. **B448** (1995) 93-126 [arXiv:9505062].

[2] H.Awata, B.Feigin, J.Shiraishi, *Quantum Algebraic Approach to Refined Topological Vertex*; J. High Energ. Phys. 2012, **41** (2012), [arXiv:1112.6074].

[3] H. Awata, B. Feigin, J. Shiraishi, *Quantum Algebraic Approach to Refined Topological Vertex*, J. High Energ. Phys. **2012**, 41 (2012) [arXiv:1112.6074].

[4] N. Affolter, M. Glick, P. Pylyavskyy, S. Ramassamy, *Vector-relation configurations and plabic graphs*, [arXiv:1908.06959].

[5] L.F.Alday, D.Gaiotto, Y.Tachikawa, *Liouville Correlation Functions from Four-dimensional Gauge Theories*; Lett. Math. Phys. **91**: 167-197, 2010, [arXiv:0906.3219].

[6] O. Aharony, A. Hanany, B. Kol, *Webs of (p,q) 5-branes, Five Dimensional Field Theories and Grid Diagrams*, J. High Energ. Phys. 01 (1998) [arXiv:hep-th/9710116].

[7] M. Aganagic, A. Klemm, M. Marino, C. Vafa, *The Topological Vertex*, Commun. Math. Phys. **254**, 425–478 (2005) [arXiv:hep-th/0305132].

[8] M. Aganagic, K. Schaeffer, *Wall Crossing, Quivers and Crystals*, J. High Energ. Phys. **2012**, 153 (2012) [arXiv:1006.2113].

[9] D. A. Bandurin, *et al.*, *Negative local resistance caused by viscous electron backflow in graphene*, Science **351**, 1055-1058 (2016). [arXiv:1509.04165].

[10] V. V. Bazhanov, R. J. Baxter, *New solvable lattice models in three dimensions*, J Stat Phys 69, 453–485 (1992);

[11] V. V. Bazhanov, R. J. Baxter, *Star-triangle relation for a three-dimensional model*, J Stat Phys 71, 839–864 (1993), [arXiv:hep-th/9212050].

[12] M. Bershtein, B. Feigin, G. Merzon, *Plane partitions with a "pit": generating functions and representation theory* , Sel. Math. New Ser. 24(1) (2018) 21-62, [arXiv:1512.08779].

[13] A. Berenstein, S. Fomin, A. Zelevinsky, *Cluster algebras III: Upper bounds and double Bruhat cells*, Duke Math. J. (2005) **126** 1, 1-52, [arXiv:math/0305434].

[14] M. Bershtein, P. Gavrylenko, A. Marshakov, *Cluster integrable systems, q-Painlevé equations and their quantization*, J. High Energ. Phys. **2018**, 77 (2018) [arXiv:1711.02063].

[15] M. Bershtein, P. Gavrylenko, A. Marshakov, *Cluster Toda chains and Nekrasov functions*, Theor Math Phys **198**, 157–188 (2019) [arXiv:1804.10145].

[16] G. Bonelli, A. Grassi, A. Tanzini, *Quantum curves and q–deformed Painlevé equations*, Lett. Math. Phys. **109**, 1961–2001 (2019), [arXiv:1710.11603].

[17] G. Bosnjak, V. Mangazeev, *Construction of R-matrices for symmetric tensor representations related to* $U_q(\widehat{sl}_n)$, J. Phys. A: Math. Theor. 49 (2016) 495204, [arXiv:1607.07968].

[18] G. Beaujard, J. Manschot, B. Pioline, *Vafa-Witten invariants from exceptional collections*, [arXiv:2004.14466].

[19] V. V. Bazhanov, V. V. Mangazeev, S. M. Sergeev, *Quantum geometry of 3-dimensional lattices*, J. Stat. Mech. (2008), P07006, [arXiv:0801.0129].

[20] V. V. Bazhanov, V. V. Mangazeev, S. M. Sergeev, *Quantum Geometry of 3-Dimensional Lattices and Tetrahedron Equation*, in Proc. XVIth International Congress on Mathematical Physics, pp. 23-44 (2010), Prague, Czech Republic, 3 - 8 August 2009, World Scientific:2010, [arXiv:0911.3693[math-ph]].

[21] L.Bao, E.Pomoni, M.Taki, F.Yagi *M5-branes, toric diagrams and gauge theory duality,* JHEP, **105** (2012); [arXiv:1112.5228].

[22] F. Benini, D. S. Park, P. Zhao, *Cluster algebras from dualities of 2d $\mathcal{N} = (2, 2)$ quiver gauge theories*, Commun. Math.Phys. 340 (2015) 1, 47-104, [arXiv:1406.2699].

[23] V. V. Bazhanov, S. Sergeev, *Zamolodchikov's tetrahedron equation and hidden structure of quantum groups*, Journal of Physics A 39 (2006) 13, [arXiv:hep-th/0509181].

[24] M. Bershtein, A. Shchechkin, *q-deformed Painlevé τ-function and q-deformed conformal blocks*, J. Phys. A: Math. Theor. **50** 085202 [arXiv:1608.02566].

[25] M. Bershtein and A. Shchechkin, *Painlevé equations from Nakajima-Yoshioka blow-up relations* [arXiv:1811.04050].

[26] M.Semenyakin, M.Bershtein, *To appear*

[27] A. Berenstein, A. Zelevinsky, *Quantum cluster algebras*, Advances in Mathematics (2005) **195** 2, 405–455 [arXiv:math/0404446].

[28] V. Chari, Integrable representations of affine Lie-algebras, Invent. math. 85 (1986), pp.317–335.

[29] W. Chuang, D.L. Jafferis, *Wall Crossing of BPS States on the Conifold from Seiberg Duality and Pyramid Partitions*, Commun. Math. Phys. **292**, 285-301 (2009), [arXiv:0810.5072].

[30] H. Cohn, R. Kenyon, J. Propp, *A variational principle for domino tilings*, J. Amer. Math. Soc. (2001), **14** 297-346, [arXiv:0008220].

[31] V. Chari, A. Pressley, A guide to quantum groups, Cambridge University Press, 1994.

[32] V. Chari, A. Pressley, Quantum affine algebras, Commun. Math. Phys. 142, 261—283 (1991).

[33] J. Crossno, *et al.*, *Observation of the Dirac fluid and the breakdown of the Wiedemann-Franz law in graphene*, Science **351** (6277), 1058-1061(2016) [arXiv:1509.04713].

[34] S. A. Cherkis, R. S. Ward, *Moduli of Monopole Walls and Amoebas*, J. High Energ. Phys. 2012, 90 (2012), [arXiv:1202.1294].

[35] J.T. Ding, I.B. Frenkel, *Isomorphism of two realizations of quantum affine algebra $U_q(\mathfrak{gl}(n))$*; Comm. Math. Phys. **156** 2 (1993), 277–300; [https://projecteuclid.org:443/euclid.cmp/1104253628].

[36] R. Dijkgraaf, D. Orlando, S. Reffert, *Dimer Models, Free Fermions and Super Quantum Mechanics*, Adv. Theor. Math. Phys. **13** 05, (2009) [arXiv:0705.1645].

[37] N. Do, B. Parker, *The tropological vertex*, Adv. Theor. Math. Phys. **13** 05, (2009) [arXiv:2205.02555].

[38] P. Etingof, I. Frenkel, A. Kirillov Jr., Lectures on representation theory and Knizhnik-Zamolodchikov equations, AMS, Providence, 1998.

[39] R. Eager, S. Franco, K. Schaeffer, *Dimer Models and Integrable Systems*, J. High Energ. Phys. 2012, 106 (2012), [arXiv:1107.1244].

[40] T. Eguchi, H. Kanno, *Topological Strings and Nekrasov's formulas*, J. High Energ. Phys. **2003**, 12 (2003) [arXiv:0310235].

[41] D. Forcella , J. Zaanen, D. Valentinis, D. van der Marel, *Electromagnetic properties of viscous charged fluids,* Phys. Rev. B **90**, 035143 (2014) [arXiv:1406.1356].

[42] P. Etingof, O. Schiffmann, Lectures on quantum groups, Second edition, International Press, 2010.

[43] G. Falkovich, *Fluid Mechanics, a short course for physicists*, Cambridge University Press 2011

[44] V. V. Fock, *Inverse spectral problem for GK integrable system*, [arXiv:1503.00289].

[45] A.Fayyazuddin, *Some comments on N=2 supersymmetric Yang-Mills*; Mod. Phys. Lett. A **10**: 2703-2708, 1995 [arXiv:hep-th/9504120v1].

[46] F.Ferrari,A.Bilal, *The Strong-Coupling Spectrum of the Seiberg-Witten Theory*; Nucl. Phys. **B469** (1996) 387-402 [arXiv:hep-th/9602082v3].

[47] V.V. Fock, A.B. Goncharov, *Moduli spaces of local systems and higher Teichmüller theory*, Publ. math. IHES **103**, 1–211 (2006) [arXiv:0311149].

[48] V.V. Fock, A.B. Goncharov, *Cluster ensembles, quantization and the dilogarithm*, Annales scientifiques de l'École Normale Supérieure, 4, **42** (2009) 6, 865-930. [arXiv:0311245].

[49] V.V. Fock, A. B. Goncharov, *Cluster X-varieties, amalgamation and Poisson-Lie groups*, In Algebraic Geometry Theory and Number Theory, pp. 27–68, Progr. Math., 253, Birkhäuser Boston, Boston, MA, 2006, [arXiv:math.RT/0508408].

[50] B. Feng, Y.-H. He, K.D. Kennaway, C. Vafa, *Dimer Models from Mirror Symmetry and Quivering Amoebae*, Adv. Theor. Math. Phys. **12** 03, (2008) [arXiv:hep-th/0511287].

[51] S. Franco, A. Hanany, K.D. Kennaway, D. Vegh, B. Wecht, *Brane Dimers and Quiver Gauge Theories*, J. High Energ. Phys. **2006** 01, (2006) [arXiv:hep-th/0504110].

[52] S. Franco, Y. Hatsuda, M. Marino, *Exact quantization conditions for cluster integrable systems*; Journal of Statistical Mechanics: Theory and Experiment, **6** 6 (2016) [arXiv:1512.03061].

[53] B. Feigin, M. Jimbo, T. Miwa, E. Mukhin, *Branching rules for quantum toroidal* $\mathfrak{gl}(n)$, [arXiv:1309.2147].

[54] G. Falkovich, L. Levitov, *Linking spatial distributions of potential and current in viscous electronics*, Phys. Rev. Lett. **119** (6), (2017). [arXiv:1607.00986].

[55] V.V. Fock, A. Marshakov, *Loop groups, Clusters, Dimers and Integrable systems*, [arXiv:1401.1606].

[56] V. V. Fock and A. Marshakov, *A Note on Quantum Groups and Relativistic Toda Theory*, Nucl.Phys. **56B** (Proc. Suppl.) (1997) 208-214.

[57] S. Fomin, A. Zelevinsky, *Total positivity: tests and parametrizations*, [arXiv:math/9912128].

[58] S. Fomin, A. Zelevinsky, *Cluster algebras I: Foundations*, Journal of the American Mathematical Society, **15**(2), 497–529. [arXiv:math/0104151].

[59] S.Fomin, A.Zelevinsky *Cluster algebras IV: Coefficients,* Compositio Mathematica, **143**(1) (2007), 112-164; [arXiv:0602259].

[60] S. Fomin, A. Zelevinsky, *Double Bruhat cells and total positivity*, [arXiv:math/9802056].

[61] P. Gavrylenko, *Isomonodromic τ-functions and W_N conformal blocks*, J. High Energ. Phys. **2015**, 167 (2015) [arXiv:1505.00259].

[62] D. Gaiotto, G. Moore, A. Neitzke *Wall-crossing, Hitchin Systems, and the WKB Approximation*, Adv in Math **234**, (2013), 239–403 [arXiv:0907.3987].

[63] I. Gelfand, S. Gelfand, V. Retakh, R. L. Wilson, Quasideterminants, Advances in Mathematics 193 (2005) 56–141.

[64] A.Grassi, Y.Hatsuda, M.Marino, *Topological Strings from Quantum Mechanics*; [arXiv:1410.3382].

[65] T. George, G. Inchiostro, *Cluster modular groups of dimer models and networks*, [arXiv:1909.12896].

[66] H. Guo, E. Ilseven, G. Falkovich, L. Levitov, *Stokes paradox, back reflections and interaction-enhanced conduction*, [arXiv:1612.09239].

[67] H. Guo, E. Ilseven, G. Falkovich, L. Levitov, *Higher-than-ballistic conduction of viscous electron flows*, PNAS **114** (12) 3068-3073 (2017) [arXiv:1607.07269].

[68] O. Gamayun, N. Iorgov, O. Lisovyy, *Conformal field theory of Painlevé VI*, J. High Energ. Phys. **2012**, 38 (2012) [arXiv:1207.0787].

[69] O. Gamayun, N. Iorgov, O. Lisovyy, *How instanton combinatorics solves Painlevé VI, V and III's*, J. Phys. A: Math. Theor. **46** (2013) 335203 [arXiv:1302.1832].

[70] P. Gavrylenko, N. Iorgov, O. Lisovyy, *Higher rank isomonodromic deformations and W-algebras*, Lett Math Phys **110**, 327–364 (2020) [arXiv:1801.09608].

[71] A. B. Goncharov, R. Kenyon, *Dimers and cluster integrable systems*, Ann. Sci. Ec. Norm. Sup **46** 5 (2013), 747–813, [arXiv:1107.5588].

[72] A.Gorsky, I.Krichever, A.Marshakov, A.Mironov, A.Morozov, *Integrability and Seiberg-Witten Exact Solution*; Phys. Lett. **B355** (1995) 466-474 [arXiv:2010.15871].

[73] I.M. Gelfand, M.M. Kapranov, A.V. Zelevinsky, *Generalized Euler integrals and A-hypergeometric functions*, Advances in Mathematics (1990) **64** 2, 255–271

[74] P. Gavrylenko, O. Lisovyy, *Fredholm determinant and Nekrasov sum representations of isomonodromic tau functions*, Commun. Math. Phys. **363**, 1–58 (2018) [arXiv:1608.00958].

[75] P.Gavrylenko, A.Lyashik, A.Marshakov, I.Motorin, M.Semenyakin, *To appear*

[76] P. Gavrylenko, A. Marshakov, *Residue Formulas for Prepotentials, Instanton Expansions and Conformal Blocks*, J. High Energ. Phys. **2014**, 97 (2014) [arXiv:1312.6382].

[77] P. Gavrylenko, A. Marshakov, *Free fermions, W-algebras and isomonodromic deformations*, Theor Math Phys **187**, 649–677 (2016) [arXiv:1605.04554].

[78] D.Gaiotto, G.W.Moore, A.Neitzke, *Four-dimensional wall-crossing via three-dimensional field theory*; Commun. Math. Phys. **299**:163-224, 2010 [arXiv:0807.4723].

[79] D.Gaiotto, G.W.Moore, A.Neitzke, *Wall-crossing, Hitchin Systems, and the WKB Approximation*; [arXiv:0907.3987].

[80] M. Gekhtman, M. Shapiro, S. Tabachnikov, A. Vainshtein, *Integrable cluster dynamics of directed networks and pentagram maps*, Adv. Math. 300 (2016), 390-450, [arXiv:1406.1883].

[81] M. Gekhtman, M. Shapiro, A. Vainshtein, *Cluster algebras and Poisson geometry*, Mosc. Math. J., **3**:3 (2003), 899–934 [arXiv:math/0208033].

[82] M. Gekhtman, M. Shapiro, A. Vainshtein, *Generalized Bäcklund–Darboux transformations for Coxeter–Toda flows from a cluster algebra perspective*, Acta Math. **206**(2), (2011) 245-310 [arXiv:0906.1364].

[83] M. Gekhtman, M. Shapiro, A. Vainshtein, *Poisson Geometry of Directed Networks in a Disk*, Selecta Math., (2009) 15, 61-103, [arXiv:0805.3541].

[84] M. Gekhtman, M. Shapiro, A. Vainshtein, *Poisson Geometry of Directed Networks in an Annulus*, Journal of the European Mathematical Society, (2012) 541–570, [arXiv:0901.0020].

[85] P.Gavrylenko, M.Semenyakin, Y.Zenkevich, *Solution of tetrahedron equation and cluster algebras*; J. High Energ. Phys. 2021, **103** (2021) [arXiv:2010.15871].

[86] I. Gessel, G. Viennot, *Binomial Determinants, Paths, and Hook Length Formulae*, Advances in Mathematics 58, 300-321 (1985)

[87] K. Hikami, R. Inoue, *Braids, Complex Volume, and Cluster Algebra*, Algebr. Geom. Topol. 15 (2015) 2175-2194, [arXiv:1304.4776].

[88] A. Hanany, K. D. Kennaway, *Dimer models and toric diagrams*, Acta Math. **206**(2), (2011) 245-310 [arXiv:hep-th/0503149].

[89] Y. Hatsuda, H. Katsura, Y. Tachikawa, *Hofstadter's Butterfly in Quantum Geometry*, New J. Phys. **18** 103023 (2016) [arXiv:1606.01894].

[90] A. Hone, R. Inoue *Discrete Painlevé equations from Y-systems*, J. Phys. A: Math. and Theor., **47 (47)** 2014; [arXiv:1405.5379].

[91] Y. Hatsuda, Y. Sugimoto, *Bloch electrons on honeycomb lattice and toric Calabi-Yau geometry*, J. High Energ. Phys. **2020**, 26 (2020) [arXiv:2003.05662].

[92] Y. Hatsuda, Y. Sugimoto, Z. Xu, *Calabi-Yau geometry and electrons on 2d lattices*, Phys. Rev. D **95**, 086004 (2017) [arXiv:1701.01561].

[93] A. Hanany, D. Vegh, *Quivers, Tilings, Branes and Rhombi*, J. High Energ. Phys. **2007** 10, (2007) [arXiv:hep-th/0511063].

[94] J. J. Heckman, C. Vafa *Crystal Melting and Black Holes*, J. High Energ. Phys. **2007** 09, (2007) [arXiv:hep-th/0610005].

[95] R. Inoue, T. Ishibashi, H. Oya *Cluster realizations of Weyl groups and higher Teichmüller theory*, [arXiv:1902.02716].

[96] A. Iqbal, A.-K. Kashani-Poor, *Instanton Counting and Chern-Simons Theory*, Adv.Theor.Math.Phys. **7** (2004) 457-497 [arXiv:hep-th/0212279].

[97] A. Iqbal, A.-K. Kashani-Poor, *$SU(N)$ Geometries and Topological String Amplitudes*, Adv.Theor.Math.Phys. **10** (2006) 1-32 [arXiv:hep-th/0306032].

[98] A. Iqbal, C. Kozcaz, C. Vafa, *The Refined Topological Vertex*, J. High Energ. Phys. **2009**, 10 (2009) [arXiv:hep-th/0701156].

[99] R. Inoue, T. Lam, P. Pylyavskyy, *On the cluster nature and quantization of geometric R-matrices*, [arXiv:1607.00722].

[100] N. Iorgov, O. Lisovyy, J. Teschner, *Isomonodromic tau-functions from Liouville conformal blocks*, Commun. Math. Phys. **336**, 671–694 (2015) [arXiv:1401.6104].

[101] A. Iqbal, N. Nekrasov, A. Okounkov, C. Vafa, *Quantum Foam and Topological Strings*, J. High Energ. Phys. **2008** 04, (2008) [arXiv:hep-th/0312022].

[102] M. Jimbo, H. Nagoya, H. Sakai, *CFT approach to the q-Painlevé VI equation*, Journal of Integrable Systems **2**, 1 (2017) [arXiv:1706.01940].

[103] H. Jenne, G. Webb, B. Young, *The combinatorial PT-DT correspondence*, [arXiv:2012.08484].

[104] R. Kenyon, *Height fluctuations in the honeycomb dimer model*, Commun. Math. Phys. **281**, 675 (2008), [arXiv:math-ph/0405052].

[105] P. Kasteleyn, *Graph theory and crystal physics*, in Graph Theory and Theoretical Physics, 43–110, Academic Press, London (1967)

[106] I.M. Krichever, *Two-dimensional periodic difference operators and algebraic geometry*, Sov. Math., Dokl. **32**, 623-627 (1985)

[107] I. G. Korepanov, *Tetrahedral Zamolodchikov Algebras Corresponding to Baxter's L-Operators*, Commun. Math. Phys. 154, 85–97 (1993).

[108] I. G. Korepanov, *A Dynamical System Connected with inhomogeneous 6-Vertex Model*, Zapiski Nauchn. Semin. POMI (S-Petersburg) 215 (1994) 178-196, [arXiv:hep-th/9402043].

[109] I. G. Korepanov, *Algebraic integrable dynamical systems, 2+1-dimensional models in wholly discrete space-time, and inhomogeneous models in 2-dimensional statistical physics*, [solv-int/9506003].

[110] V. Kac, Infinite dimensional Lie algebras, Cambridge University Press, 1990.

[111] S. Kharchev, *Unpublished.*

[112] R. M. Kashaev, I. G. Korepanov, S. M. Sergeev, *Functional tetrahedron equation*, Theor. Math. Phys. 117:3 (1998) 1402 - 1413, [arXiv:solv-int/9801015].

[113] R. M. Kashaev, V. V. Mangazeev, Yu. G. Stroganov, *Spatial symmetry, local integrability and tetrahedron equations in the Baxter-Bazhanov model*, International Journal of Modern Physics A, 8 (3) (1993) 587-601.

[114] R. Kenyon, A. Okounkov, *Low temperature limits of dimer models*, unpublished

[115] R. Kenyon, A. Okounkov, *Planar dimers and Harnack curves*, Duke Mathematical Journal **131** 3 (2006), [arXiv:math-ph/0311062].

[116] R. Kenyon, A. Okounkov, *Limit shapes and the complex burgers equation*, [arXiv:math-ph/0507007].

[117] A. Kuniba, M. Okado, S. Sergeev, *Tetrahedron equation and generalized quantum groups*, J. Phys. A: Math. Theor. 48 (2015) 304001 (38pp), [arXiv:1503.08536].

[118] R. Kenyon, A. Okounkov, S. Sheffield, *Dimers and Amoebae*, [arXiv:math-ph/0311005].

[119] R. Kenyon, R. Pemantle, *Double-dimers, the Ising model and the hexahedron recurrence*, [arXiv:1308.2998].

[120] A. Kuniba, S. Sergeev, *Tetrahedron Equation and Quantum R Matrices for Spin Representations of $B_n^{(1)}$, $D_n^{(1)}$ and $D_{n+1}^{(2)}$*, Commun. Math. Phys. 324, 695–713 (2013), [arXiv:1203.6436].

[121] M.Kontsevich, Y.Soibelman, *Stability structures, motivic Donaldson-Thomas invariants and cluster transformations*; [arXiv:0811.2435].

[122] M. Kapranov, V. Voevodsky, *2-categories and Zamolodchikov tetrahedra equations*, Proc. Sympos. Pure Math., 56 (2) 1994.

[123] B. Lindström, *On the Vector Representations of Induced Matroids*, Bulletin of the London Mathematical Society, 5: 85-90 (1973).

[124] L. Levitov, G. Falkovich, *Electron viscosity, current vortices and negative nonlocal resistance in graphene*, Nature Phys. **12**, 672-676 (2016). [arXiv:1508.00836].

[125] T. Lam, P. Pylyavskyy, *Total positivity in loop groups, I: Whirls and curls*, Advances in Mathematics, 230 (2012) 3: 1222 - 1271, [arXiv:0812.0840].

[126] A. Litvinov, L. Spodyneiko, *On W algebras commuting with a set of screenings*, J. High Energ. Phys. 2016, 138 (2016), [arXiv:1609.06271].

[127] A. Litvinov, L. Spodyneiko, *On dual description of the deformed $O(N)$ sigma model*, J. High Energ. Phys. 2018, 139 (2018), [arXiv:1804.07084].

[128] A. Marshakov, *Lie groups, cluster variables and integrable systems*, Journal of Geometry and Physics (2013) 67: 16-36, [arXiv:1207.1869].

[129] M. Marino, *Spectral Theory and Mirror Symmetry*, Proc. Symp. Pure Math. **98** (2018) 259 [arXiv:1506.07757].

[130] M. Matone, *Instantons and recursion relations in $\mathcal{N} = 2$ SUSY gauge theory*, J Phys.Lett. **B357** (1995) 342-348 [arXiv:hep-th/9506102].

[131] V. Mangazeev, V. Bazhanov, S. Sergeev, *An integrable 3D lattice model with positive Boltzmann weights*, J. Phys. A: Math. Theor., v. 46, 465206 (2013), [arXiv:1308.4773].

[132] A. Mironov, A. Morozov, *Superintegrability summary*, [arXiv:2201.12917].

[133] A.Marshakov, A.Mironov, *5d and 6d Supersymmetric Gauge Theories: Prepotentials from Integrable Systems*; Nucl.Phys. **B518** (1998) 59-91 [arXiv:hep-th/9711156v1].

[134] A. Mironov, A. Morozov, B. Runov, Y. Zenkevich, A. Zotov, *Spectral dualities in XXZ spin chains and five dimensional gauge theories*; JHEP **1312** (2013) 034 [arXiv:hep-th/1307.1502].

[135] T. Maeda, T. Nakatsu, *Amoebas and Instantons*, Int. J. Mod. Phys. **A22**: 937-984 (2007) [arXiv:hep-th/0601233].

[136] Y. Matsuhira, H. Nagoya, *Combinatorial expressions for the tau functions of q-Painlevé V and III equations*; [arXiv:1811.03285].

[137] P. J. W. Moll, P. Kushwaha, N. Nandi, B. Schmidt, A. P. Mackenzie, *Evidence for hydrodynamic electron flow in PdCoO2*, Science **351** (6277) 1061-1064 (2016) [arXiv:1509.05691].

[138] A. Morozov, A. Popolitov, S. Shakirov, *Quantization of Harer-Zagier formulas*, [arXiv:2008.09577].

[139] S. Mozgovoy, M. Reineke, *On the noncommutative Donaldson-Thomas invariants arising from brane tilings*, Advances in Mathematics **223**(5) [arXiv:0809.0117].

[140] A.Marshakov, M.Semenyakin, *Cluster integrable systems and spin chains*; J. High Energ. Phys. 2019, **100** (2019) [arXiv:1905.09921].

[141] N.Nekrasov, *Seiberg-Witten Prepotential From Instanton Counting*; Adv. Theor. Math. Phys. **7**:831-864, 2004 [arXiv:hep-th/0206161].

[142] N. Nekrasov, *Mathematical structures: On string theory applications in condensed matter physics. Topological string and two dimensional electron*, XXIII Solvay Conference, [PDF].

[143] N. Nekrasov, *Five Dimensional Gauge Theories and Relativistic Integrable Systems*, Nucl. Phys. B 531 **1-3** (1998) [arXiv:hep-th/9609219].

[144] N. Nekrasov, A. Okounkov, *Seiberg-Witten Theory and Random Partitions*, The Unity of Mathematics. Progress in Mathematics, **244**. Birkhäuser Boston [arXiv:hep-th/0306238].

[145] N.Nekrasov, S.L.Shatashvili *Quantization of Integrable Systems and Four Dimensional Gauge Theories*; [arXiv:0908.4052].

[146] N. Okubo, *Bilinear equations and q-discrete Painlevé equations satisfied by variables and coefficients in cluster algebras*, J. Phys. A: Math. Theor. **48** 355201; [arXiv:1505.03067].

[147] N. Okubo, *Co-primeness preserving higher dimensional extension of q-discrete Painlevé I, II equations*; [arXiv:1704.05403].

[148] A. Oskin, S. Pakuliak, A. Silantyev, *On the universal weight function for the quantum affine algebra* $U_q(\hat{\mathfrak{gl}}_N)$; Lett. Math. Phys. **91** (2010) 167; [arXiv:0711.2821].

[149] A. Okounkov, N. Reshetikhin, *Correlation function of Schur process with application to local geometry of a random 3-dimensional Young diagram*, [arXiv:math/0107056].

[150] A. Okounkov, N. Reshetikhin, *Random skew plane partitions and the Pearcey process*, [arXiv:math/0503508].

[151] A. Okounkov, N. Reshetikhin, C. Vafa, *Quantum Calabi-Yau and Classical Crystals*, In: Etingof, P., Retakh, V., Singer, I.M. (eds) The Unity of Mathematics. Progress in Mathematics, vol 244 [arXiv:hep-th/0309208].

[152] V. Ovsienko, M. Shapiro, *Cluster algebras with Grassmann variables*, to appear in Electron. Res. Announc. Math. Sci., [arXiv:1809.01860].

[153] N.Okubo, T.Suzuki *Generalized q-Painlevé VI systems of type* $(A_{2n+1}+A_1+A_1)^{(1)}$ *arising from cluster algebra* [arXiv:1810.03252].

[154] H. Ooguri, M. Yamazaki, *Crystal Melting and Toric Calabi-Yau Manifolds*, Commun. Math. Phys. **292**, 179-199 (2009) [arXiv:0811.2801].

[155] H. Ooguri, M. Yamazaki, *Emergent Calabi-Yau Geometry*, Phys. Rev. Lett. **102**: 161601 (2009) [arXiv:0902.3996].

[156] C. M. Ormerod, Y. Yamada, *From Polygons to Ultradiscrete Painlevé Equations*, SIGMA **11** (2015), 056, [arXiv:1408.5643].

[157] A. Postnikov, *Total positivity, Grassmannians, and networks*, [arXiv:math/0609764].

[158] L.D. Faddeev, N.Yu.Reshetikhin, L.A.Takhtajan, *Quantization of Lie groups and Lie algebras*; Algebra and Analysis (Russian) 1.1 (1989), 118-206

[159] S.N.M. Ruijsenaars, *"Relativistic Toda systems"*, Commun.Math. Phys., **133**:217 (1990), 753-760. [euclid.cmp/1104201396].

[160] S. M. Sergeev, *Quantum 2 + 1 evolution model*, Journal of Physics A: Mathematical and General, 32 (30), [arXiv:solv-int/9811003].

[161] J. Stienstra, *Hypergeometric Systems in two Variables, Quivers, Dimers and Dessins d'Enfants*, in "Modular Forms and String Duality", AMS, 2008, 125–161, [arXiv:0711.0464].

[162] S. M. Sergeev, *Supertetrahedra and superalgebras*, J. Math. Phys. 50, 083519 (2009), [arXiv:0805.4653].

[163] M. Semenyakin, *Comment on 'Linking Spatial Distributions of Potential and Current in Viscous Electronics'* [arXiv:1609.05316].

[164] N.Seiberg, *Five Dimensional SUSY Field Theories, Non-trivial Fixed Points and String Dynamics*; [arXiv:hep-th/9608111].

[165] N.Seiberg, *Non-trivial Fixed Points of The Renormalization Group in Six Dimensions*; [arXiv:hep-th/9609161].

[166] S. M. Sergeev, *Solutions of the functional tetrahedron equation connected with the local Yang – Baxter equation for the ferro-electric*, [arXiv:solv-int/9709006].

[167] S.Katz, A.Klemm, C.Vafa, *Geometric Engineering of Quantum Field Theories*; Nucl. Phys. **B497**: 173-195, 1997 [arXiv:hep-th/9609239].

[168] R. K. Kumar *et al.*, *Superballistic flow of viscous electron fluid through graphene constrictions*, Nature Phys **13**, 1182–1185 (2017). [arXiv:1703.06672].

[169] M. Sato, T. Miwa, M. Jimbo, *Holonomic quantum fields I–V*, Publ. RIMS Kyoto Univ. **14**, (1978), 223–267; **15**, (1979), 201–278; **15**, (1979), 577–629; **15**, (1979), 871–972; **16**, (1980), 531–584.

[170] S. Sergeev, V. V. Mangazeev, Yu. G. Stroganov, *The vertex formulation of the Bazhanov-Baxter Model*, J. Stat Phys 82, 31–49 (1996), [arXiv:hep-th/9504035].

[171] G. Schrader, A. Shapiro, *A cluster realization of $U_q(\mathfrak{sl}_n)$ from quantum character varieties*, [arXiv:1607.00271].

[172] N.Seiberg, E.Witten, *Monopole Condensation, And Confinement In N=2 Supersymmetric Yang-Mills Theory*; Nucl. Phys. **B426**: 19-52, 1994 [arXiv:hep-th/9407087].

[173] N.Seiberg, E.Witten, *Gauge Dynamics And Compactification To Three Dimensions*; [arXiv:hep-th/9607163].

[174] D. Thurston, *From Dominoes to Hexagons*, [arXiv:math/0405482].

[175] K. Talaska, *A formula for Plucker coordinates associated with a planar network*, Int Math Res Notices (2008), ID: rnn081, [arXiv:0801.4822].

[176] I. Torre, A. Tomadin, A. K. Geim, M. Polini, *Nonlocal transport and the hydrodynamic shear viscosity in graphene*, Phys. Rev. B **92**, 165433 (2015). [arXiv:1508.00363].

[177] A.P. Veselov, I.M. Krichever, S.P. Novikov, *Two-dimensional peroodic Schrödinger operator and Prym's θ-functions*, [PDF].

[178] E.Witten, *Solutions Of Four-Dimensional Field Theories Via M Theory*; Nucl. Phys. **B500**: 3-42, 1997 [arXiv:hep-th/9703166].

[179] B. Young, *Computing a pyramid partition generating function with dimer shuffling*, Journal of Combinatorial Theory Series A **116**(2), 334-350 [arXiv:0709.3079].

[180] M. Yamazaki, *Crystal Melting and Wall Crossing Phenomena*, Int. J. Mod. Phys. A26 (2011) 1097-1228, [arXiv:1002.1709v3].

[181] M. Yamazaki, *Cluster-Enriched Yang-Baxter Equation from SUSY Gauge Theories*, Lett Math Phys 108, 1137–1146 (2018), [arXiv:1611.07522].

[182] A. B. Zamolodchikov, *Tetrahedra equations and integrable systems in three-dimensional space*, JETP, Vol. 52, No 2, p. 325.

[183] Y. Zenkevich, *Higgsed network calculus*, [arXiv:1812.11961].

[184] A. B. Zamolodchikov, *Tetrahedron equations and the relativistic S-matrix of straight-strings in 2+1-Dimensions*, Commun. Math. Phys. 79, 489–505 (1981).

Summary

Partition functions in string theory and supersymmetric field theories can be often computed exactly and be shown to have rich symmetries. Often the symmetry can be presented in the form of the differential or difference equation, which the partition function solves. Among the first examples of this kind was the discovery of the relevance of classical integrable systems of particles in the context of Seiberg-Witten theory, describing low-energy dynamics of 4d $\mathcal{N} = 2$ supersymmetric gauge theories. Later it was independently observed that the Painlevé equations are solved by the instanton partition functions of those SUSY gauge theories in the self-dual Omega-background. From the point of view of integrable systems the pass from Seiberg-Witten theory to the full partition function is the"deautonomization" of them. The uplift of the story to 5d $\mathcal{N} = 1$ SUSY gauge theories compactified on a circle corresponds to the "relativisation" of integrable systems, i.e. making the momentum-dependence of Hamiltonians to be exponential. After the "deautonomization" these systems become the q-difference equations of q-Painlevé type.

The notions of cluster varieties and cluster algebras were invented in the early 2000th for the solution of the classical problem of the parametrization of the space of "totally positive" matrices, i.e. those matrices, all minors of which are strictly positive. The new notion was immediately and successively applied to the description of the moduli spaces of local systems on Riemann curves, to the theory of integrable systems, and to the description of stability conditions in algebraic geometry. The initial point for my work in this thesis was the observation that there is a natural structure of X-cluster variety on the phase space of the relativistic Toda chain, which corresponds to the 5d $\mathcal{N} = 1$ $SU(N)$ gauge theory without the matter multiplets. The discrete dynamics which appears as a result of the action of cluster mapping class group on the cluster variables, can be solved by the partition functions of these theories.

In Chapter 2 we construct the structure of the X-cluster variety on the phase space of the XXZ spin chain. This extends the class of the previously known examples of gauge theories/cluster integrable systems correspondences, since the XXZ spin chains are known to be corresponding to 5d $\mathcal{N} = 1$ quiver gauge theories, with the linear quivers of constant rank. The so-called spectral duality, interchanging the rank and the length of the spin chain, found its natural interpretation in the cluster description. We also described the structure of the large piece of the cluster mapping class group for those systems and derived the bilinear equation for the dynamic of A-cluster variables under the action of generators of cluster mapping class group.

In Chapter 3 we show that the "master" solution of Bazhanov-Sergeev to the tetrahedron equation has a clear cluster-algebraic origin. The action of tetrahedral R-matrix by conjugation appears to be equivalent to the application of four mutations; we also show how this interpretation fits into the context of application of cluster algebras to the parametrization of the double Bruhat cells in $GL(N)$. Using this interpretation of the Bashanov-Sergeev solution, we give a clear recipe how the cluster integrable system with the arbitrary symmetric Newton polygon can be constructed using it. We also prove there the combinatorial lemma, which allows us to generalize this consideration to the arbitrary Newton polygon.

In Chapter 4 we make a few steps toward understanding why it happens that the partition functions of topological string theory, generalizing the partition functions of the gauge theories, are solving the equations appearing from the discrete dynamics of the cluster variables. We claim that the box-counting of topological vertices, which is the major tool to compute the partition function of topological strings, can be obtained directly from the cluster algebras. In order to do this, one has to uplift the partition function of dimers on the bipartite graph on torus, which encodes the Hamiltonians of integrable system, to the periodic graph on the plane, and to "deautonomize" the discrete $U(1)$ connection on the graph, parametrizing the cluster variables, by applying non-zero transverse flux of purely imaginary magnetic field to it. This claim can be also viewed as a particular example of so-called Topological Strings/Spectral Theory correspondence, since the partition function of dimers on the plane can be computed as a determinant of the q-difference operator. We check the correspondence, by showing that the density of the free-energy of the model of dimers, being computed in the limit of vanishing flux, satisfies

the Seiberg-Witten equations, as it is expected from the string-theoretic perspective.

Chapter 5 is devoted to a project which is not directly related to the main lines of my research in the field of integrable systems. In this project we conduct the phenomenological study of the hydrodynamic regime of the flows of electrons in graphene. There we propose the principal scheme of the experiment, which would allow us to measure the viscosity of the electronic liquid, by applying the AC current of THz frequency to the sample of the Hall bar geometry.

Samenvatting

Partitiefuncties in snaartheorie en supersymmetrische veldentheorieën kunnen vaak exact worden berekend en er kan worden aangetoond dat zij rijke symmetrieën hebben. Vaak kan de symmetrie worden voorgesteld in de vorm van een differentiaalvergelijking, die door de partitiefunctie wordt opgelost. Een van de eerste voorbeelden van deze aard was de ontdekking van de relevantie van klassieke integreerbare systemen van deeltjes in de context van de Seiberg-Witten theorie, die de lage-energiedynamica van vier-dimensionale supersymmetrische ijkentheorieën beschrijft. Later werd ontdekt dat de Painlevé -vergelijkingen op een soortgelijke manier kunnen worden opgelost. In de theorie van integreerbare systemen is de overgang van Seiberg-Witten theorie naar de volledige partitiefunctie een voorbeeld van wat men "deautonomisatie" noemt.

De begrippen clustervariëteiten en clusteralgebra's zijn in het begin van de jaren 2000 uitgevonden voor de oplossing van het klassieke probleem van de parametrisatie van de ruimte van "totaal positieve" matrices, d.w.z. die matrices, waarvan alle minoren positief zijn. De theorie werd achtereenvolgens toegepast op de beschrijving van de moduliruimten van lokale stelsels op krommen in een Riemann-ruimte, op de theorie van integreerbare stelsels, en op de beschrijving van stabiliteitsvoorwaarden in de algebraïsche meetkunde. Het uitgangspunt van dit proefschrift was de waarneming dat er een natuurlijke structuur van clustervariëteiten bestaat in de faseruimte van de relativistische Toda-keten.

In hoofdstuk 2 construeren we de structuur van de clustervariëteit op de faseruimte van een XXZ-spin keten. De zogenaamde spectrale dualiteit, waarbij de rang en de lengte van de spinketen worden verwisseld, vindt zijn natuurlijke interpretatie in de clusterbeschrijving.

In hoofdstuk 3 laten we zien dat de bekende oplossing van Bazhanov-Sergeev voor de tetraëdervergelijking een duidelijke cluster-algebraïsche oorsprong heeft. We laten ook zien hoe deze interpretatie past in de

context van de toepassing van clusteralgebra's op de parametrisatie van Bruhatcellen. Met behulp van deze interpretatie van de Bashanov-Sergeev oplossing geven we een duidelijk recept hoe het clusterintegreerbare stelsel geconstrueerd kan worden.

In hoofdstuk 4 zetten we een paar stappen om te begrijpen waarom het gebeurt dat de partitiefuncties van de topologische snaartheorie, die de partitiefuncties van de ijktheorieën veralgemenen, de vergelijkingen oplossen die voortkomen uit de discrete dynamica van de clustervariabelen. Wij poneren dat het aantal topologische hoekpunten rechtstreeks uit de clusteralgebra's kan worden verkregen. Deze bewering kan ook worden gezien als een bijzonder voorbeeld van de zogenaamde Topologische Snaren/Spectrale Theorie correspondentie. We controleren de correspondentie door aan te tonen dat de dichtheid van de vrije-energie van het model van dimeren, berekend in de limiet van nul magnetische flux, voldoet aan de Seiberg-Witten vergelijkingen, zoals verwacht wordt vanuit het snaartheoretisch perspectief.

Hoofdstuk 5 is gewijd aan een project dat niet direct verband houdt met de hoofdlijnen van mijn onderzoek op het gebied van integreerbare systemen. In dit project verrichten wij de fenomenologische studie van het hydrodynamische regime van de elektrische stroom van elektronen in grafeen. Daar stellen wij een experiment voor, dat ons zou toelaten de viscositeit van de elektronische vloeistof te meten, door de wisselstroom van THz-frequentie toe te passen in de Hall-bar geometrie.

Curriculum Vitæ

I was born on 22th of May 1995 in Kryviy Rih, Ukraine. When I was five years old, our family moved to Kyiv, where I went to primary school. During my time in school we moved several times, so I have studied in the Kyiv, Moscow, Dnipro, and finished high school at the Kyiv Natural and Scientific Lyceum # 145, where I already started working on simple scientific projects under the supervision of my teachers D. Basov and O. Trylis.

Since the 10th grade of high school I have started attending extra curricular classes at the Bogolyubov Institute for Theoretical Physics organized by Dr. V. Shadura and Dr. N. Iorgov. When I finished high school in 2012, I entered the physics department of Taras Shevchenko National University of Kyiv. I did my bachelor project under the supervision of Dr. O. Gamayun, who was a postdoctoral scientist at Leiden University at that time. The project was related to the splitting of the solitons under a quench.

After finishing my bachelor's, in 2016, I entered the master program in theoretical physics at Taras Shevchenko National University of Kyiv and also the joint program in mathematical physics of Skoltech and Higher School of Economics at Moscow, Russia. I have done my master thesis in physics under the supervision of Prof. Dr. G. Falkovich from the Weizmann Institute, Israel. It was related to the phenomenology of hydrodynamic flows of electrons in graphene. My master thesis in mathematics was done under the supervision of Prof. Dr. A. Marshakov, who worked at Skoltech and HSE, and was related to cluster integrable systems.

In 2018 I successively finished both master programs, and continued working on the relations between cluster algebras, string theory, and integrable systems as a PhD student under the supervision of Prof. Dr. A. Marshakov. The core of this thesis is made from research done in this period. In February 2022 I left Moscow because of the war Russia forced on Ukraine. I moved to the Lorentz Institute at Leiden University, where

I finished my PhD thesis in the group of Prof. Dr. C. W. J. Beenakker.

Starting from the times of my bachelor studies I have been actively involved in the organization of outreach, scientific schools, competitions, and conducting formal and informal courses for both high school and university students.

After finishing my PhD I am invited to work at the Perimeter Institute in Canada for the next three years.

List of Publications

[1] *Topological string amplitudes and Seiberg-Witten prepotentials from the counting of dimers in transverse flux*,
M. Semenyakin, arXiv: 2206.02162 [Chapter 4].

[2] *A brief introduction to quantum groups*,
P. Etingof, M. Semenyakin, arXiv: 2106.05252.

[3] *Solution of tetrahedron equation and cluster algebras*,
P. Gavrylenko, M. Semenyakin, Y. Zenkevich, *J. High Energ. Phys.* 2021, **103** (2021) [Chapter 3].

[4] *Cluster integrable systems and spin chains*,
A. Marshakov, M. Semenyakin, *J. High Energ. Phys.* 2019, **100** (2019) [Chapter 2].

[5] *Alternating currents and shear waves in viscous electronics*,
M. Semenyakin, G. Falkovich, *Phys. Rev. B* **97**, 085127 (2018) [Chapter 5].

[6] *Comment on 'Linking Spatial Distributions of Potential and Current in Viscous Electronics'*,
M. Semenyakin, arXiv:1609.05316

[7] *Soliton splitting in quenched classical integrable systems*,
O. Gamayun, M. Semenyakin, *J. Phys. A: Math. Theor.* **49** 335201 (2016)

[8] *On diagrammatic technique for nonlinear dynamical systems*,
M. Semenyakin, *Mod. Phys. Lett. A*, Vol. **29**, No. **35**, (2014)

Stellingen

behorende bij het proefschrift

On cluster algebras and topological string theory

1. The XXZ spin chain is isomorphic to a cluster integrable system of rectangular Newton polygons [chapter 2].

2. The solution of the tetrahedron equation by Bazhanov and Sergeev has a cluster-algebraic origin. This observation greatly generalizes the class of integrable systems that can be constructed using this solution [chapter 3].

3. The counting of three-dimensional boxes by dimers on a hexagonal lattice can be generalized to general bipartite graphs [chapter 4].

4. The viscosity of electrons in graphene can be measured in AC electrical conduction [chapter 5].

5. Two-dimensional viscous flows of strongly interacting electrons in a channel create vortices. Depending on the boundary conditions, there appears either a vortex pair or an infinite vortex train.

6. The claim by Putzke *et al.* [Science **368**, 1234 (2020)] that the phase coherence length in their magnetoconductance experiment exceeds 10 μm is not supported by a semiclassical interpretation of their data.

7. Majorana zero-modes do not respond to electric or magnetic force fields, but they can be manipulated by means of the Magnus force.

8. Tangent fermions, massless fermions on a space-time lattice with a dispersion relation $\tan^2(E/2) = \sum_\alpha \tan(k_\alpha/2)$ in dimensionless units, solve all but one of the problems inherent with the discretization of the Dirac equation.

Mykola Semenyakin

15 september 2022